DEPARTMENT OF COMMERCE
R. P. LAMONT, Secretary
BUREAU OF STANDARDS
George K. Burgess, Director

BUREAU OF STANDARDS JOURNAL OF RESEARCH

July, 1929
Vol. 3, No. 1

UNITED STATES
GOVERNMENT PRINTING OFFICE
WASHINGTON : 1929

For a partial list of previous research papers appearing in Volumes 1 and 2, BUREAU OF STANDARDS JOURNAL OF RESEARCH, see pages 2 and 3 of the cover

SOLD ONLY BY THE SUPERINTENDENT OF DOCUMENTS
U. S. GOVERNMENT PRINTING OFFICE
WASHINGTON, D. C.
AT
$2.75 PER YEAR ON SUBSCRIPTION

A COURSE-SHIFT INDICATOR FOR THE DOUBLE-MODULATION TYPE RADIOBEACON

By H. Diamond and F. W. Dunmore

ABSTRACT

To further increase the reliability of the visual directive radiobeacon system developed by the Bureau of Standards, a course-shift indicating instrument primarily for station use has been developed which serves a twofold purpose—(1) to indicate to a station operator whether a given course as laid out in space remains unvarying during a given time of operation, and (2) to greatly facilitate a check of the beacon calibration.

The circuit arrangement used in applying this instrument at the beacon station comprises a rotatable pick-up coil inductively coupled to the two loop antennas of the beacon, a detector-amplifier unit, a suitable filter unit, and a differential ratio instrument. The ratio instrument consists of two fixed field coils and an armature or rotor coil. A pointer attached to the rotor coil moves over a suitable scale. The force actions of the two field coils upon the rotor coil are in opposition so that with equal currents in the field coils the pointer assumes a mid-scale position. The filter unit is so designed that with equal 65 and 85 cycle voltages impressed upon the instrument equal currents flow through the field coils. If the 65-cycle voltage becomes greater than the 85-cycle voltage, one field coil carries a greater current than the other and the net force action upon the rotor coil becomes greater than zero, the pointer attached to the rotor coil moving to the left of its mid-scale position. The reverse is true if the 85-cycle voltage becomes greater than the 65-cycle. The differential action of the two field coils upon the rotor coil, therefore, serves directly as a means for comparing the relative amount of 65 and 85 cycle modulation in the radio-frequency voltages induced in the pick-up coil coupled to the two-loop antennas.

Corresponding to each setting of the beacon course, there is a definite ratio of 65 to 85 cycle modulation in the two loop antennas of the beacon. For each course setting, then, there is a definite position of the rotatable pick-up coil at which the amounts of 65 and 85 cycle modulation in the voltage induced in the coil are equal, the instrument pointer being then at its mid-scale position.

The course-shift indicator has a twofold application at the beacon station.

1. For a given course setting the coupling coil is rotated so that the instrument pointer is at center scale or zero. A station attendant is then certain that the course marked out in space remains unvarying so long as the instrument pointer remains at zero. A change in course of 0.1° is readily detected. Easy adjustment is provided on the beacon transmitting set whereby a shift in the course once detected may be corrected.

2. If, during the original calibration of the beacon, the settings of the scale attached to the pick-up coil, when ratio instrument reads zero, corresponding to the various beacon course settings are recorded, the beacon is calibrated once and for all. A recalibration of the beacon may then be effected very rapidly and within the beacon station.

The instrument herein described may also be used as a visual course indicator on large aircraft. Its advantages and disadvantages as compared with the vibrating-reed course indicator are discussed.

CONTENTS

	Page
I. Introduction	2
II. Description of course-shift indicator	3
III. Application at the beacon station	6
IV. Use as a visual indicator for the double-modulation type of radio beacon	8

I. INTRODUCTION

To further increase the reliability of the visual directive radiobeacon system developed by the Bureau of Standards, an indicating instrument primarily for station use has been developed which serves a twofold purpose—(1) to indicate to a station operator whether a given course as laid out in space remains unvarying during a given time of operation, and (2) to serve as a check on the beacon calibration.

A brief description [1] of the directive radiobeacon is essential to a clear understanding of the operation of the course-shift indicator. The directive radiobeacon consists essentially of a master oscillator supplying power at 290 kc to two power amplifiers which, in turn, feed two loop antennas crossed at an angle of 90° with each other. Each power amplifier is modulated to a selected low-frequency note, the two modulating frequencies chosen being 65 and 85 cycles per second. One loop antenna, therefore, radiates a 290 kc wave modulated to 65 cycles while the other emits a 290 kc wave modulated to 85 cycles. Due to the directive properties of the loop antennas, these waves are a maximum in the directions of the planes of the antennas transmitting them and of zero value in the directions perpendicular to these planes. An airplane flying along a line bisecting the angle between the two antennas will, therefore, receive the two waves with equal intensity. If the airplane deviates in either direction from this line, the signal from one antenna becomes stronger and the other weaker. Equality of received signals thus indicates a fixed line or "course" in space and provides a means for guiding aircraft along that "course." For the purpose of orienting the course in any given direction a 4-coil goniometer, consisting of two stator coils crossed at an angle of 90° with each other and two rotor coils also crossed at 90°, is employed. The stator coils are connected to the plates of the power amplifiers while the rotor coils are connected each in series with one loop antenna.

The currents in these antennas, due to the driving voltage of one stator goniometer coil, create a resultant field corresponding to that

[1] A more detailed description may be found in a paper on Radio Aids to Air Navigation, by J. H. Dellinger and H. Pratt, Proc. I. R. E., **16**, pp. 890–920; July, 1928.

Other papers dealing with the details of the beacon system are: Receiving Sets for Aircraft Beacon and Telephony, by H. Pratt and H. Diamond, B. S. Jour. Research (RP19), October, 1928; and Design of Tuned-Reed Course Indicators for Aircraft Radiobeacon, by F. W. Dunmore, B. S. Jour. Research (RP28), November, 1928.

which would be produced by an imaginary or phantom loop rotating with the goniometer rotor and carrying only one modulation frequency. Since there are two primary or stator coils, two such phantom loops, one for each modulation frequency, rotating as the two movable goniometer coils rotate together, allow the equisignal zone or "course" in space to be oriented in any direction. For any given course setting, then, each loop antenna carries radio-frequency current modulated at both 65 and 85 cycles per second, the ratio of 65 to 85 cycle modulated radio-frequency power in each loop depending upon the position of the goniometer. A change in the proportion of 65 to 85 cycle modulation constitutes a change in course.

The course-shift indicator is a direct-reading switchboard type instrument designed to indicate a change in the relative amounts of 65 and 85 cycle modulation in the two antennas and, in consequence, a shifting of the course.

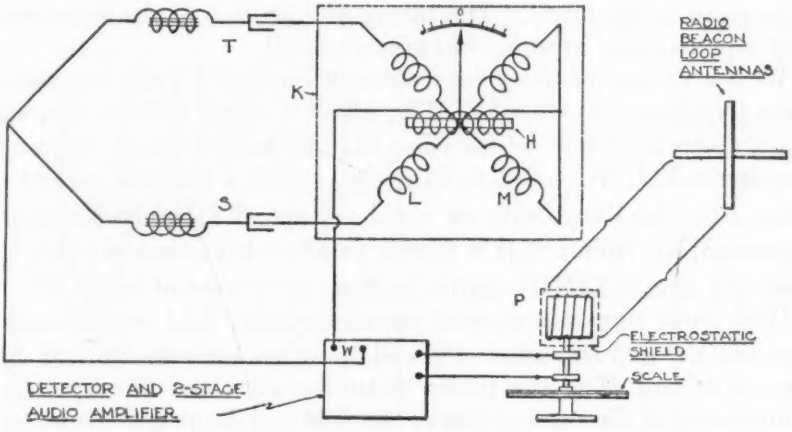

FIGURE 1.—*Circuit used with course-shift indicator*

II. DESCRIPTION OF COURSE-SHIFT INDICATOR

The circuit arrangement used in applying the course-shift indicating instrument at the beacon station is shown in Figure 1. A rotating inductance coil P is coupled magnetically to both loop antennas, electrostatic coupling being prevented by means of the electrostatic shield shown. Exact equality of magnetic coupling to the two antennas is not essential. The terminals of coil P are connected to the input terminals of a detector-amplifier unit consisting of a grid bias detector and two stages of amplification, the final stage comprising two 5-watt tubes in push pull in order to provide ample power output to the course-shift instrument.

The course-shift indicating instrument is a modification of a commercial horizontal-edge switchboard type of frequency meter having

an external reactor box. The meter consists of two field coils, L and M, and an armature or rotor coil, H. A pointer attached to the rotor coil moves over a suitable scale. The force actions of the two field coils upon the rotor coil are in opposition, so that with equal currents in the two field coils the pointer assumes a mid-scale position. The reactor box contains two filters, S and T, having constants such that with equal 65 and 85 cycle voltages impressed upon the instrument equal currents flow through the field coils L and M. If the 65-cycle voltage becomes greater than the 85-cycle voltage, the field coil L carries a greater current than M, while if the 65-cycle voltage is smaller, the reverse is true. The differential force action of the fields L and M upon the armature H, therefore, serves directly as a means for comparing the relative amount of 65 and 85 cycle modulation in the radio-frequency voltage induced in the coupling coil P. The resonance curves of the tuned circuits employed are given in Figure 2. The three curves shown are to be associated with the respective circuits given in the figure. The theory of operation of the instrument may now be given in somewhat greater detail.

With a voltage of 65 cycles frequency impressed upon the instrument terminals, the circuit SLHW, which is tuned to 68 cycles, carries a 65-cycle current whose value may be designated as $\overline{AC}$, while the circuit TMHW, tuned to 95 cycles, carries a 65-cycle current of value $\overline{BC}$. Similarly, with an equal voltage of 85 cycles frequency impressed, the circuit SLHW carries an 85-cycle current of value $\overline{DF}$ while the circuit TMHW carries an 85-cycle current of value $\overline{EF}$.

With both signals impressed simultaneously, field coil L carries currents $\overline{AC}$ and $\overline{DF}$, while field coil M carries currents $\overline{BC}$ and $\overline{EF}$. The rotor coil H is the return path for all these circuits. The components of the force action of the field coil L upon the rotor coil H are then proportional to

$$\overline{AC} \times \overline{AC} + \overline{AC} \times \overline{BC} + \overline{DF} \times \overline{DF} + \overline{DF} \times \overline{EF} \qquad (1)$$

while the components of the force action of the field coil M upon the rotor coil H are proportional to

$$\overline{BC} \times \overline{AC} + \overline{BC} \times \overline{BC} + \overline{EF} \times \overline{DF} + \overline{EF} \times \overline{EF} \qquad (2)$$

The net force action is then proportional to the difference between (1) and (2), or to

$$(\overline{AC} \times \overline{AC} + \overline{DF} \times \overline{DF}) - (\overline{BC} \times \overline{BC} + \overline{EF} \times \overline{EF}) \qquad (3)$$

Obviously, the first half of (3) should be made equal to the second half if the pointer is to be at mid scale when equal 65 and 85 cycle voltages are impressed.

Assume now that the 65-cycle voltage increases while the 85 cycle decreases. The currents $\overline{AC}$ and $\overline{BC}$ are proportionately increased

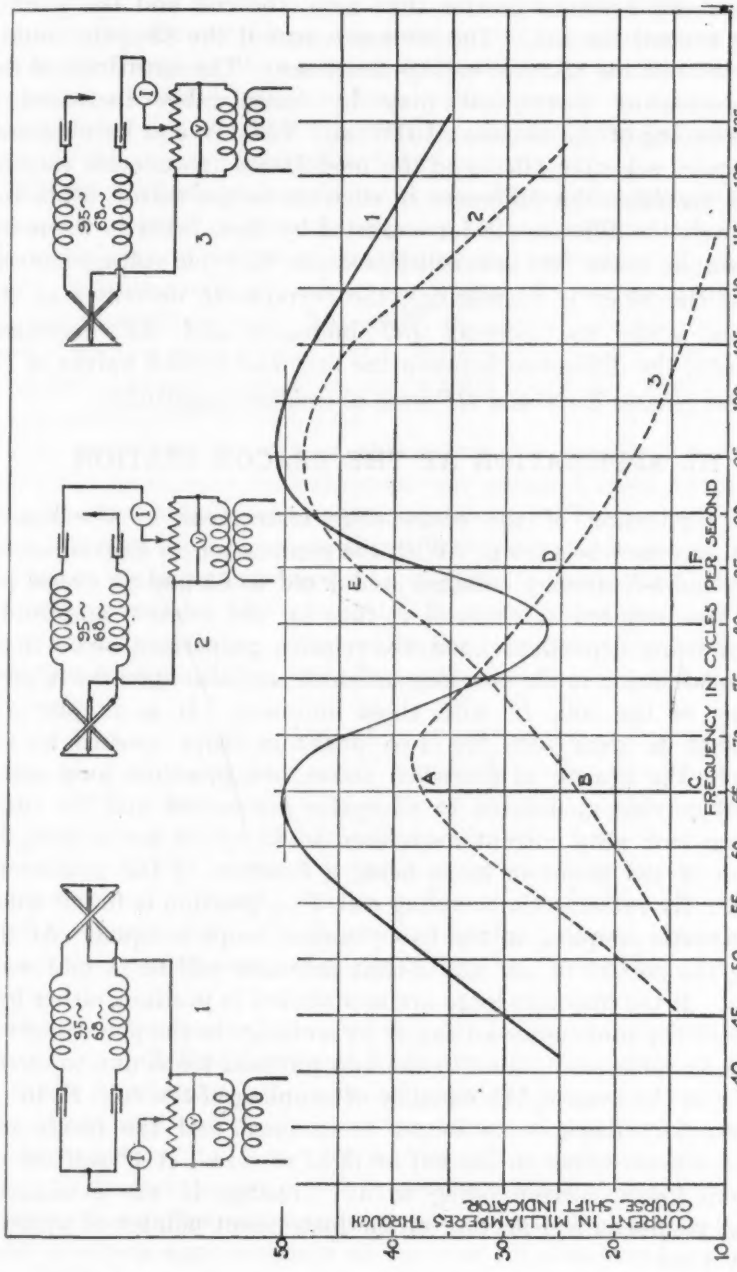

FIGURE 2.—*Resonance curves of course-shift indicator circuits*

and the currents $\overline{DF}$ and $\overline{EF}$ are reduced. The first half of (3) thus becomes greater than the second half and the net force action upon the rotor coil becomes greater than zero, the coil and the pointer moving toward the left. The reverse is true if the 85-cycle voltage increases while the 65-cycle voltage decreases. The sensitivity of the course-indicating instrument may be considerably increased if sharper tuning of the circuits SLHW and TMHW can be obtained. The greater selective effects on the modulation frequencies thereby secured amplifies the difference in currents in the stator fields and accordingly the difference in force exerted by these fields on the rotor. For example, in the first case considered (the 65-cycle voltage increasing and the 85 cycle decreasing), the current $\overline{DF}$ decreases as $\overline{AC}$ increases, while the current $\overline{BC}$ increases and $\overline{EF}$ decreases. Obviously, the difference between the first and second halves of (3) would be greater if $\overline{BC}$ and $\overline{DF}$ were of smaller magnitudes.

III. APPLICATION AT THE BEACON STATION

The application of the course-shift instrument at the beacon station may now be shown. With the goniometer on a given course setting, radio-frequency voltages modulated to 65 and 85 cycles per second are induced in the coil P (fig. 1), the relative amplitudes induced being dependent upon the relative proportion of 65 to 85 cycles modulation in the two loop antennas and also upon the relative coupling of the coil, P, with these antennas. It is simpler and equivalent to deal with the two phantom loops crossed at 90° set up by the beacon as described above, one phantom loop carrying only current modulated to 65 cycles per second and the other phantom loop only current modulated to 85 cycles per second, the position of the phantom loops being a function of the goniometer setting. By rotating the coupling coil, P, a position is found where the magnetic coupling to the two phantom loops is equal. At this setting the pointer of the course-shift indicator will be at mid scale, or zero. If the phantom loops are now shifted in position, either by a change of the goniometer setting or by a change in the percentages of 65 and 85 cycle modulation in the two physical loops due to circuit changes in the beacon, the equality of coupling of the coil, P, to the two phantom loops is no longer maintained and the instrument pointer deflects either to the left or right of zero. A 1° shift of the phantom loops, corresponding to a 1° change in the goniometer setting, results in a deflection of the instrument pointer of approximately 1 cm.

The twofold application of the course-shift indicator at the beacon station is now evident. Suppose that the goniometer is set on a given beacon course and the coupling coil rotated to adjust the course-

shift indicator pointer to zero. A station attendant is then certain that the course marked out in space remains unvarying so long as the instrument pointer remains at zero. As noted above, a 1° shift in the course will result in a 1 cm deflection of the instrument pointer, so that a change in the course of 0.1° may easily be detected. Easy adjustments of the radio-frequency voltage supply to the two amplifier trains of the beacon transmitting set are provided whereby a shift in the course once detected may be corrected.

To check the variations in the course during the operation of the beacon, a series of tests was made, each lasting from two to six hours. At no time was a deflection greater than 0.5 cm observed, the maximum deflections usually occurring during the warming up of the beacon transmitting set. Moreover, the shifts were as much on one side of zero as on the other. It is conceivable, however, that over a long period of operation difference in tube aging, etc., may introduce a permanent shift in the course.

The second application of the instrument described lies in the ability to recalibrate the beacon in very simple fashion with its aid, once the beacon has been properly calibrated. The usual procedure in calibrating the beacon consists of orienting the course on a given point and checking the course at a distance to insure that it has been properly oriented. This is repeated for a number of points of diverse geographical location. The calibration obviously involves a considerable amount of time and effort and should be repeated at definite intervals.

If, during the original calibration of the beacon, the settings of the scale attached to coupling coil P (at which the course-shift indicator reads zero), corresponding to the various goniometer settings are recorded, the beacon is calibrated once for all. A curve showing the calibration of the course-shift indicator-coil position in terms of the goniometer-rotor angles is given in Figure 3. So long as this calibration remains true, the beacon calibration is also correct. The points of the entire curve of Figure 3 may be checked in a very short time.

The peculiar shape of this curve is due to the unsymmetrical location of the coil P with respect to the two loop antennas. With a perfectly symmetrical arrangement, a straight line would be obtained. The figures on the curve indicate the degrees of rotation of the goniometer necessary to throw the course-shift indicator needle off scale either to the right or left and thus serve as a measure of the sharpness of indication of this instrument at each point. Since the instrument scale measures approximately 13 cm over all, the sensitivity of the instrument is seen to range from 0.7 to 1 cm per degree shift of the course, depending upon the setting of the coupling coil P.

Figure 4 shows the apparatus constituting the course-shift indicator installed at the Bureau of Standards beacon station at College Park, Md. The detector amplifier unit does not appear in the photograph.

IV. USE AS A VISUAL INDICATOR FOR THE DOUBLE-MODULATION TYPE OF RADIOBEACON

From the description of operation of the course-shift indicator it is evident that it may also be used as a course indicator on shipboard or on aircraft. To accomplish this it is only necessary to receive the double-modulation radio beacon signals with amplitude sufficient to properly operate the instrument. The operating voltage necessary

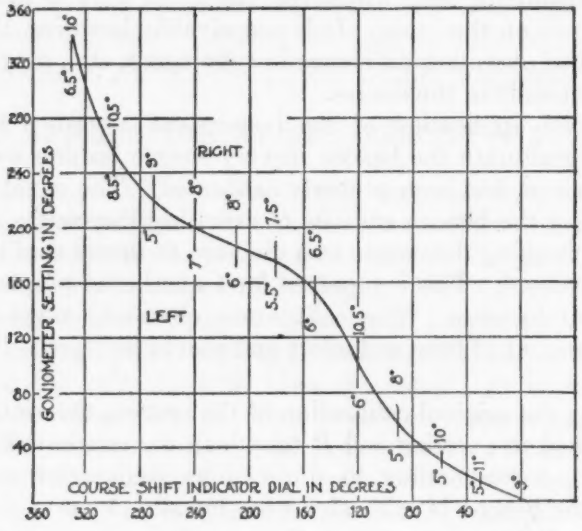

FIGURE 3.—*Calibration curve for course-shift indicator*

is of the order of magnitude which may be obtained from the output of a well-designed receiving set.

In order to prove the usefulness of this instrument as a visual course indicator, tests were made with it at a distance of 12 miles from the radiobeacon. The results obtained are given in the curve of Figure 5, which plots the deflections of the instrument pointer in centimeters to the right or left of zero, as the beacon course was oriented through 360°. The effect is identical with that obtained if an airplane carrying the instrument circled around the beacon maintaining a constant distance of 12 miles. The curve indicates that there are four courses, *A*, *B*, *C*, and *D*, which may be used, two of which, *A* and *C*, are sharper than the other two, *B* and *D*, as evidenced by the slope of the curve at these points. This is in accordance with

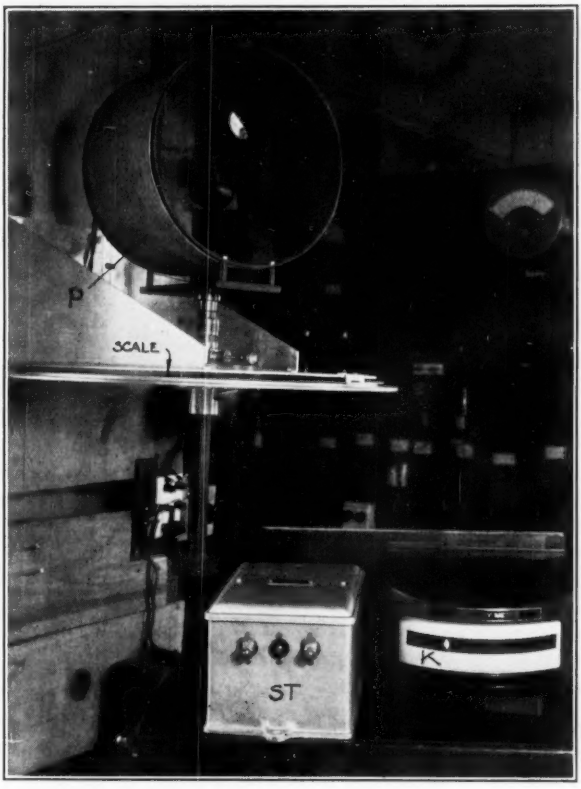

FIGURE 4.—*Course-shift indicator apparatus installed at College Park (Md.) double modulation beacon station*

UNIV. OF MICH.

results obtained with the vibrating-reed course indicator.[2] A course may here be defined as the locus of the positions in space at which the instrument receives equal signals from the phantom loops set up by

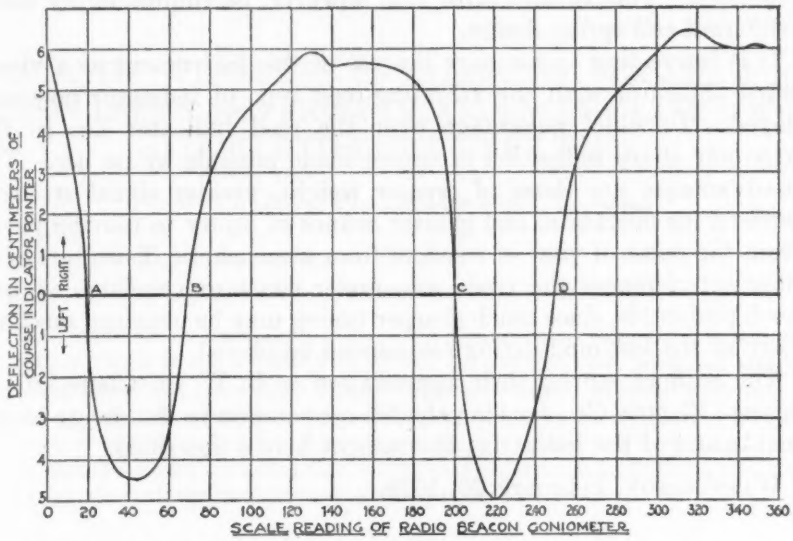

FIGURE 5.—*Scale reading of course-shift indicator installed on airplane as airplane circles 360° around the beacon*

the beacon, the instrument pointer being then at mid-scale or zero setting.

Figure 6 was prepared from the data of Figure 5, course *A*, and shows the instrument scale calibrated in degrees deviation from the

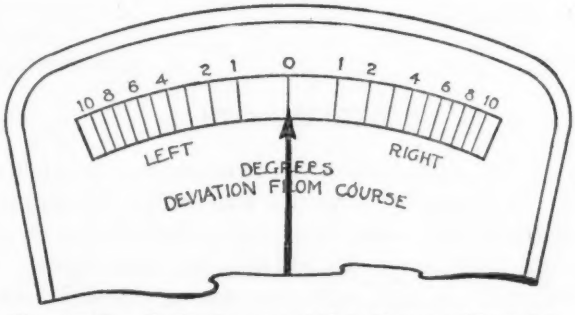

FIGURE 6.—*Scale of course-shift indicator calibrated in degrees deviation from course*

Calibration made 12 miles from beacon.

course. A deviation of 0.1° from the course may easily be detected. For the instrument used this calibration would not be practicable unless precautions were taken to keep the instrument operating

[2] See reference to third paper in footnote 1, p 3.

voltage of constant magnitude, since the type of coil spring used introduced a voltage error in the instrument, the degree of sharpness of indication being in part dependent upon the strength of signal impressed. This voltage error can, however, be eliminated by using a different coil-spring design.

It is interesting to compare the use of this instrument as a visual course indicator with the vibrating-reed type of indicator now employed. Its chief advantage over the reed indicator lies in the extremely sharp indication of course made possible by its use. The disadvantages are those of greater weight, greater signal strength required for operation, and greater chance of injury to moving parts. From the point of view of freedom from atmospheric disturbances or other interferences the reeds are, under constant condition of use, much preferable, since much sharper tuning may be obtained mechanically at the low modulating frequencies employed.

The authors express their appreciation to B. W. St. Claire, of the General Electric Co., for his valuable cooperation in the design of the final model of the indicating instrument herein described.

WASHINGTON, February 20, 1929.

RELATIVE VISIBILITY OF LUMINOUS FLASHES FROM NEON LAMPS AND FROM INCANDESCENT LAMPS WITH AND WITHOUT RED FILTERS

By F. Chapin Breckenridge and J. E. Nolan

ABSTRACT

The visibility of light derived from an incandescent lamp with a red filter has been tested in comparison with that of light from a neon lamp and also with that of a similar incandescent lamp without the filter. Especial attention was given to producing beams having similar candlepower distributions. The tests include a variety of clear, hazy, rainy, and foggy weathers and ranges up to 7 km. The results indicate no advantage in the case of the neon lamp and a loss of visibility in all weathers from the use of the filter.

CONTENTS

		Page
I.	Introduction	11
II.	The beacon	12
III.	Adjustments	14
IV.	The location and weather	17
V.	Procedure	17
VI.	Observations	18
VII.	Discussion	21
VIII.	Conclusions	24
IX.	Acknowledgments	25

I. INTRODUCTION

The development of commercial neon lamps led to experiments with such lamps as marine and aeronautical beacons. These experiments have been followed by frequent claims that the light from neon lamps has exceptional fog-penetrating properties, but no definite evidence was offered to support the claims. Contrary opinions followed in turn. Up to the present these service tests have led only to conflicting opinions regarding the fog-penetrating properties of the light from neon lamps.[1]

Very few tests definitely attempting comparison of the visibility of light from neon lamps with light from incandescent source lamps

[1] H. N. Green, Artificial Light as an Aid to Aerial Navigation, Ill. Eng. (London), **20**, pp. 101 and 133; 1927. Also discussion following.

with color filters have been reported. Porter [2] found that a neon induction lamp seemed at equal candlepowers to have slightly better fog penetration than a clear incandescent lamp or even an incandescent lamp with red color filter, but he also states that the advantage of the neon lamp, if there is any, is due more to color contrast, longer observation period, and greater beam spread than to any marked ability of the neon light to penetrate fog. On the other hand, Foulke concluded, apparently from the same and additional tests, that the neon beacon is superior to the incandescent lamp beacon.

Found and Forney [3] have reported that observations made in foggy weather have shown that it is possible to pick up the neon light before any of the other lights in the same vicinity are observed.

The experiments described in this paper were designed to determine definitely, under controlled conditions, whether the light from a neon lamp becomes visible at greater distances, or remains visible to greater distances, than light from an incandescent lamp with a color filter when the color, shape, and brightness of the source, the angular distributions of intensity in the beam, and the weather conditions are the same in both cases. As a matter of additional interest, the effect of the color filter upon the visibility of a clear beam was also determined. In general, the method was to observe flashing signals from an experimental beacon from various distances and under various weather conditions. Nearly all the observations were made at night, and a photometric wedge was used for most of them.

II. THE BEACON

The experimental beacon was designed to produce three rotating beams which will be referred to as the neon beam, the red beam, and the clear beam. The neon and red beams were made as closely alike as was possible with such different sources, in order that any characteristics peculiar to the light from neon lamps might be clearly differentiated from other effects. The clear beam was designed to duplicate the beam which was obtained if the filter was removed from the unit producing the red beam. The inclusion of the clear beam also made it possible to tell whether it was the neon or the red flash which was being seen when only one of them was visible.

Figure 1 shows diagrammatically the optical parts of the beacon designed to produce the three beams. T is a turntable on which the revolving parts are mounted. L is a plano-convex lens 140 mm in focal length and 110 mm in diameter. A is a circular aperture 15 mm in diameter in the plane of the principal focus of L. A piece of

[2] Discussion on The Present Status of Aeronautical Lighting in the United States, by L. C. Porter, Trans. I. E. S., **22**, p. 1003; 1927. See p. 1019 for discussion by T. E. Foulke and p. 1009 for statement by W. T. Harding.

[3] C. G. Found and J. D. Forney, Hot Cathode Neon Arcs, Trans. A. I. E. E., **47**, p. 747; 1928.

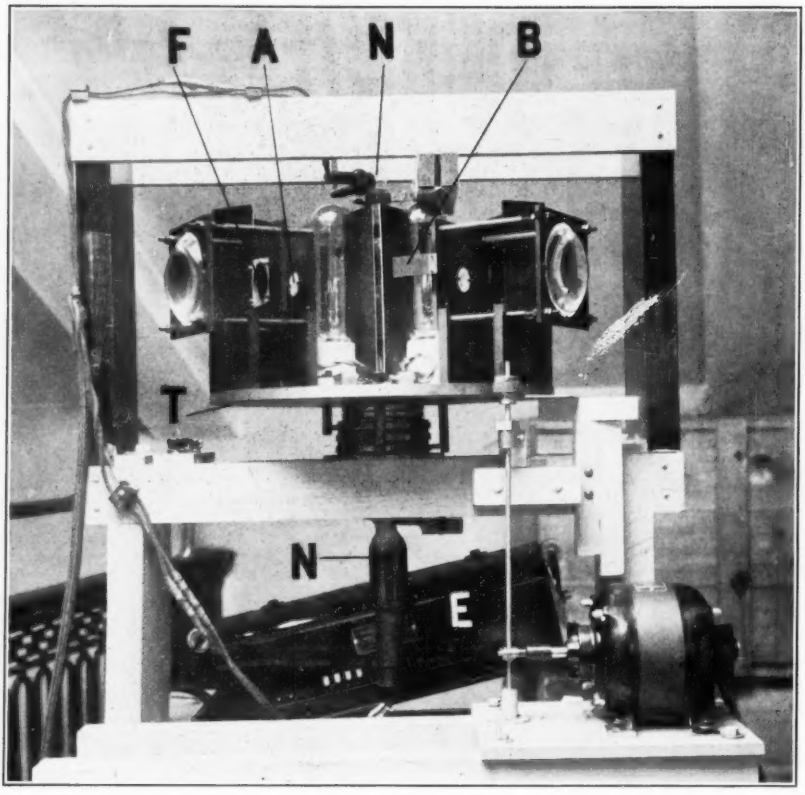

FIGURE 2.—*Beacon with some of the stray light shields removed*

A, aperature with ground glass in place; *B*, brass plate with fiducial lines for setting lamp at its correct position; *E*, equipment for starting the neon lamp; *F*, filter opening with filter removed; *N*, neon lamp; *T*, turntable.

FIGURE 3.—*Beacon house with photometer in place for measuring intensity distribution of beacon beams*

UNIV. OF MICH.

ground glass, *G*, covers this aperture in the red and clear units. *N* is the neon lamp which does not revolve but projects through the hole *H* at the center of the turntable. *I* is a 1,000-watt, 115-volt, incandescent lamp. *F* is the red glass filter.

Figure 2 is a photograph of the assembled beacon with some of the stray light shields removed. The parts are indicated as in Figure 1.

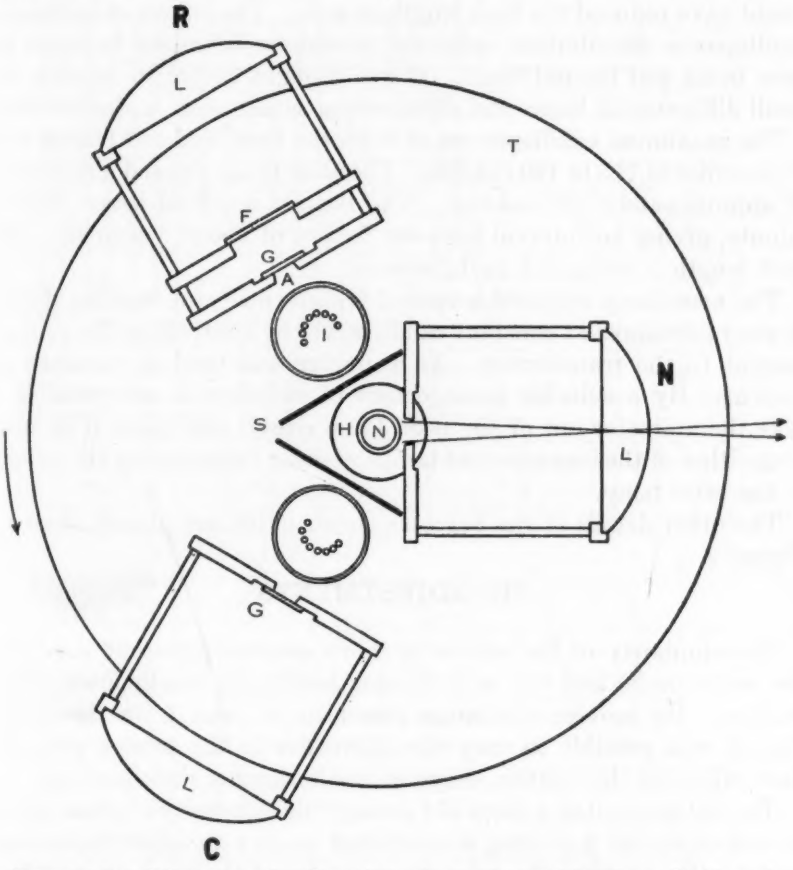

FIGURE 1.—*Diagrammatic plan view of experimental beacon. R, N, and C are red, neon, and clear units, respectively*

A, Aperture; *F*, filter of red glass; *G*, ground glass; *H*, hole in turntable; *I*, incandescent lamp; *L*, lens; *N*, neon lamp; *S*, shields for cutting off stray light, additional shields were used around the units and around the edge of the turntable; *T*, turntable. The arrow shows direction of rotation.

The clear unit is identical with the red unit except for the red filter and the metal plate to hold it. No ground glass was used in the neon unit, the aperture being placed as close to the neon lamp as practicable.

The neon lamp used is a hot-cathode, alternating-current lamp. The luminous part of the lamp is a tube 2.5 cm in diameter and 47 cm in length. Only the small portion of this length back of the aperture was used. The diameter of the tube was not large enough to make

the aperture uniformly luminous from all angles. When viewed from the center of the lens, the entire aperture appeared luminous. From the edge of the lens at either side a small part of the aperture appeared dark. As no larger neon tubes of sufficient brightness were available, and as the aperture was as close as practicable to the neon tube, this difficulty could be overcome only by making the aperture smaller, which would have reduced the flash length as well. The curves of horizontal candlepower distribution indicated no serious difference between the neon beam and the red beam. It was thought better to tolerate the small difference in horizontal distribution rather than a shorter flash.

The maximum candlepowers of both the neon and red beams were of the order of 175 to 190 candles. The clear beam showed a maximum of approximately 730 candles. The beacon revolved seven times a minute, giving an interval between flashes of about 3 seconds. The flash length is estimated as 0.2 second.

The neon lamp required a special transformer and starting device. It was maintained at constant candlepower by controlling the primary current to the transformer. An ammeter was used to measure the current. By a suitable arrangement of switches it was possible to take the ammeter out of the neon lamp circuit and place it in series with either of the incandescent lamps without interrupting the current in the neon lamp.

The other details of the beacon's construction are plainly shown in Figure 2.

III. ADJUSTMENTS

The similarity of the optical systems assured apparent sources of the same shape and size with similar horizontal candlepower distributions. By moving the lamps closer to or away from the ground glass it was possible to vary the intensities in the beams with very little effect on the relative shape of the horizontal distributions.

The red glass filter, a piece of Corning "lighthouse red" glass ground to a thickness of 2.15 mm, was selected to give an approximate color match. By varying the color temperature of the incandescent lamp in the red unit a very good color match was obtained at about 65 volts. The color temperature of the lamp in the clear unit was adjusted to match that of the lamp (filter removed) of the red unit. The adjustments for color-match were made before adjusting the position of the lamps back of the ground glass. The clear unit was adjusted to duplicate as closely as possible the beam given by the red unit when the red filter was removed.

The original adjustments for color match and equality of intensity were made at the bureau, using a Bechstein rotating sector photometer. A Sharp-Millar photometer was included in the field equipment, and a special stand was built in front of the beacon house to support

this photometer. The foundation for this stand was firmly set in the ground, but the stand itself was always removed when visibility observations were to be made, so that there was no possibility of obstructing the view of the beacon. Figure 3 shows the beacon house with the photometer on its stand. With this equipment satisfactory candlepower distribution curves were obtained during the test.

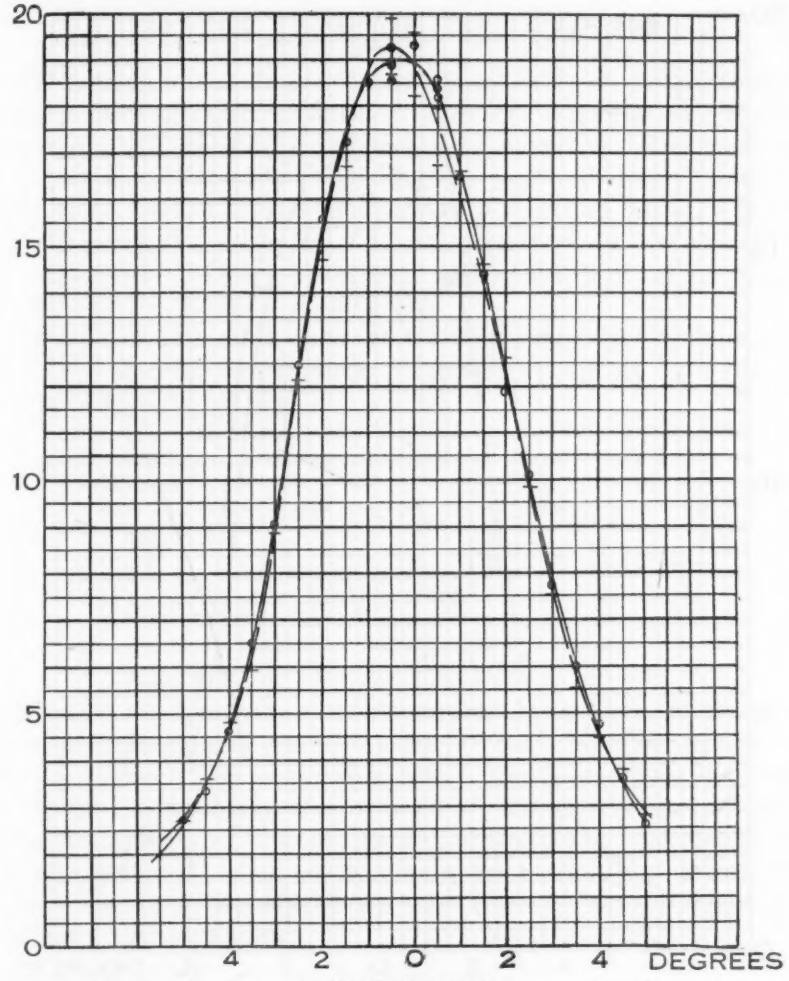

FIGURE 4.—*Intensity distribution of the neon and red beams*

Full line, with circles, red beam; broken line with crosses, neon beam. Ordinates show relative values in arbitrary units.

When first assembled in the field, the incandescent lamps were set by means of special lamp sights, the bulbs having fiducial lines etched upon them. One of these sights is shown at *B* in Figure 2. A gage was used to reset the neon lamp at the correct distance back of its aperture. This original set-up was later checked by taking distribu-

tion curves with the Sharp-Millar photometer and was found satisfactory. Twice the neon lamp failed and had to be replaced by a new one. Each time this was done the currents were readjusted to equalize the horizontal distributions. These changes amounted to less than 3.5 per cent and did not affect the color temperature seriously. After the readjustment a complete new set of distribution curves

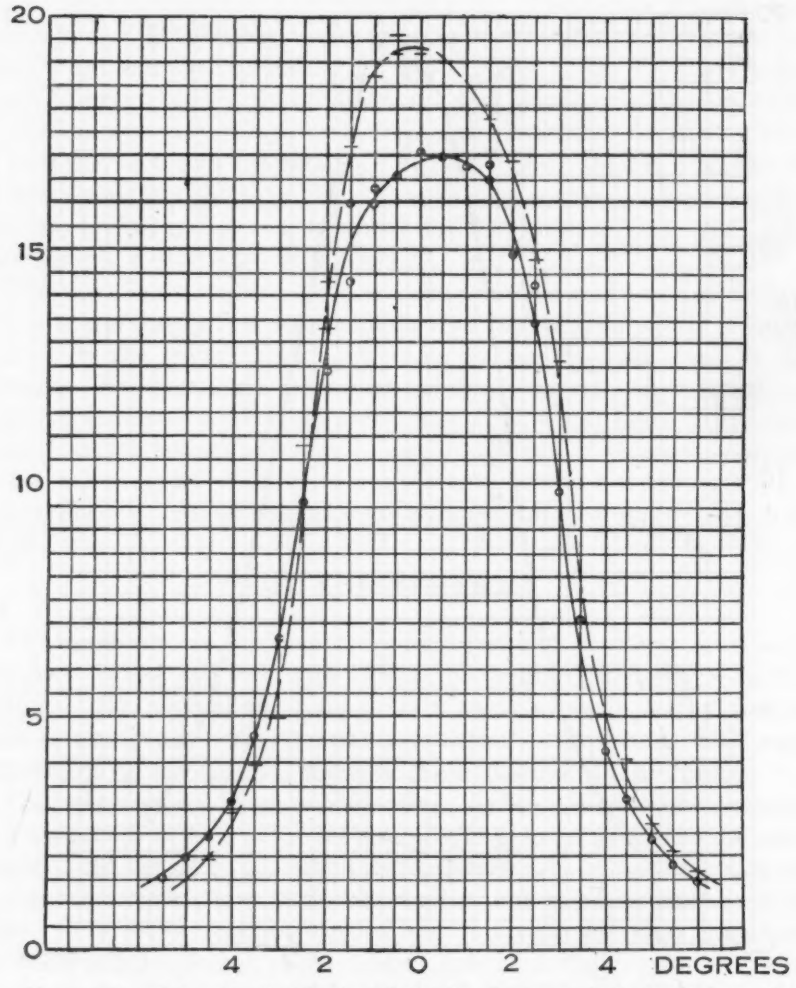

FIGURE 5.—*Intensity distribution of the clear beams and the beam from the red unit with the filter removed*

Full line with circles, beam from red unit; broken line with crosses, clear beam.

was made each time. A final set of distribution curves has been made since the apparatus was returned to the bureau, the lamps being again reset by lamp sights and gage.

Figures 4 and 5 reproduce the horizontal candlepower distribution curves taken September 22. The neon and red curves show one of

the closest agreements obtained on any of the calibrations of the red and neon units. The curves for the clear beam and the beam from the red unit with filter removed show one of the poorest agreements obtained on any of the runs for adjusting the clear beam. Taken together, they give a typical idea of the agreement obtained throughout the test.

IV. THE LOCATION AND WEATHER

The beacon was erected at Moody Point, Me., on the rocks immediately north of Ogunquit Beach. This location afforded a continuous view of the beacon along the beach for 4 km (2.5 miles) southward and frequent views of it along the coast eastward from Ogunquit to Bald Head Cliff, a maximum range of 7 km (4.35 miles). The fog signal records of the Bureau of Lighthouses indicate that this stretch of coast offers as high a probability of frequent fogs as any suitable location on the North Atlantic coast.

Thirty-three series of observations were made during the months of August and September, 1928. The weather during these runs has been classified as follows:

	Runs
Clear	15
Haze	6
Rain	5
Fog	9
Total	35
Counted twice	2
Total runs	33

Most of the fogs varied in intensity during the observations, and three of them cleared away so suddenly that the observations were not convincing. In these cases, before the observer was able to get to the limit of visibility, the fog suddenly lifted, allowing insufficient time for any satisfactory observations. There were other fogs which occurred on nights when no neon lamp was available or cleared away before observations could be started. One of the runs classified as fog was made in daylight.

V. PROCEDURE

The method of taking observations had to be varied somewhat with the weather. Generally, observations were made from five stations, designated by their distance from the beacon, as follows:

7,000 m (4.35 miles) station
5,700 m (3.54 miles) station
4,750 m (2.95 miles) station
4,000 m (2.49 miles) station
1,910 m (1.19 miles) station

The three more distant stations were located on the rocky shore between Ogunquit and Bald Head Cliff. The other two stations were located on the beach south of the beacon.

Except for some of the earlier observations, a photometric wedge was used in clear and hazy weather. This wedge, which was obtained from the Eastman Kodak Co., was of the gelatin filter type. It was mounted in a metal case having holes spaced 1 cm apart along the length of the wedge in such a manner that the observer could hold one of the holes in front of his eye while watching the beacon, thereby introducing a definite part of the wedge into the path of the light. The holes are designated by consecutive numbers, 1 being the hole having the highest transmission, about 86 per cent. The ratio of transmission from hole to hole was approximately 55 per cent. The procedure was to determine and record at each observation station the highest numbered hole on the wedge through which the observer could see each type of flash consistently. When the haze was heavy enough to reduce the maximum range of visibility to less than 4 km (2.5 miles), the observer sought to find the distance at which each type of flash was just visible. The transmission of a hazy atmosphere varies so rapidly, however, that this could not be done for all the flashes before conditions would change. It was, however, frequently possible to find a distance at which some of the flashes would be visible while others were not.

In taking the observations, the writers generally alternated from night to night, one man taking the observations, the other attending the beacon and controlling the currents.

VI. OBSERVATIONS

The observations taken with the photometric wedge are given in Tables 1 and 2. The larger the wedge reading the brighter the flash appeared. A plus sign indicates that the flash was quite readily visible through the hole corresponding to that number but was not consistently seen through the next hole. The symbol "V" means visible to the naked eye but not through hole 1 of the wedge. "N" means not visible but known to be operating. A blank space means no observation was taken. The observations have been grouped according to observers on account of the considerable difference in visual sensitivity between the observers, which causes the readings in Table 2 to average higher than those in Table 1.

TABLE 1.—*Wedge observations by F. C. B.*

Run No.	7,000 m			5,700 m			4,750 m			4,000 m			1,910 m			Weather
	Clear	Red	Neon	Clear	Red	Neon	Clear	Red	Neon	Clear	Red	Neon	Clear	Red	Neon	
12	3	2	2	4	3	3	4+	3+	3	5	4	4	9	5+	5	Clear.
14	3	2	2	3	2	2	4	3	3	5	3	3	7	4	4	Do.
14				3	2	2	5	3	3	4	3	3	5	3	3	Do.
16	1			1+	1	1	5	2	2	5	2	2	6	4	4	Light fog.
20	6	2	2	6	3	3	7	3	3	7	4+	4+				Clear.
22	3	2	2	4	2	2	6	2	2	7	3	3	7	4	4	Do.
24	5	1	1	3	2+	2	4	2	2	5	3+	3	9	5	5	Light haze.
26	4	2	2	6	2	2	7	3	3	6	3	2	9	5	5	Clear.
28				3	1		4	1		3	V					Rain and heavy haze.
30	4	1+	1	5	1	1	6	1	1	4	V	V	7	3	3	Hazy.

Larger numbers indicate higher apparent brightness.
V=visible to the naked eye but not through hole 1 of the wedge.
+=not reduced to the limit of visibility at the hole recorded, but not consistently visible through the next hole.
Blank space=no observations taken.

TABLE 2.—*Wedge observations by J. E. N.*

Run No.	7,000 m			5,700 m			4,750 m			4,000 m			1,910 m			Weather
	Clear	Red	Neon	Clear	Red	Neon	Clear	Red	Neon	Clear	Red	Neon	Clear	Red	Neon	
13	5	4	4	6	5	5	6	4+	4+	6+	5	5	9	7	7+	Clear.
15	4	3	3	5	4	4	6	4+	4+	5+	4	4	9	6	6	Slight haze.
19	2	2	2	4+	3	3	5	4	4	6	4	4	9	6	6	Slight haze, clearing.
21				6	5	5	5	4	4	6	5	5	8+	6	6	Clear.
23	5	4	4	5+	4+	4	8	5	5	8	6	6	10	7	7	Do.
25	4	3	3	5	4	4	6+	5	5	7	5+	5+	10	7	7	Slight haze.
27	6	3	3	7	4+	4	8	5	5	8+	5+	5+	9	6	6	Clear.
29				6	4	4	8	5+	5+	8	5	5	10	7	7	Do.
33	6	4	4	7+	5	5	8	5	5	8	5	5	10	7	7	Do.

Larger numbers indicate higher apparent brightness.
+=not reduced to the limit of visibility at the hole recorded but not consistently visible through the next hole.
Blank space=no observations taken.

Table 3 summarizes the observations taken on foggy nights when the wedge could be used at most only part of the time. These observations have been arranged in the order taken, so that progressive changes appear as successive observations. The movements of the observer toward and from the beacon can be followed by noting the changes in distance. The symbol "P" indicates that the flashes, previously invisible, are picked up. "L" indicates that the

flashes previously visible are lost from sight. "I" means intermittently visible. Additional details are given in the following notes:

TABLE 3.—*Observations through fog*

Run No.	Time	Distance	Clear	Red	Neon	Remarks	Observers
	p. m.	*m.*					
4	9.30	1,200	P	N	N	Fog cleared rapidly	F. C. B.
		1,200	V	P	P		
6	9.20	5,000	V	N	N	Fog getting heavier	Do.
	10.35	510	P	N	N		
		330	V	P	N		
		330	V	V	P	Slightly nearer beacon	
7		1,400		V	L	Fog getting heavier	J. E. N.
		1,427		L	N		
		700		P	N	Fog clearing	
		673		V	P		
		1,400		V	L	Fog clearing rapidly	Do.
		1,427		L	N		
11		3,000	N	N	P	In close succession	Do.
		3,000	P	P	V		
		1,900	P	P	P	do	
16		7,000	V	N	N	Light fog	F. C. B.
17	8.08	1,910	P	N	N	Heavy fog	J. E. N.
	8.18	1,240	V	P	N	Clearing rapidly	
	8.20	1,200	V	V	P	Red brighter than neon	
	9.29	500	5	4	4	Fog varying slowly	F. C. B.
	9.43	1,240	V	V	V		
	Later.	1,240	V	V	N		
	Later.	1,240	V	N	N		
	Later.	1,240	N	N	N		
	9.49	1,240	V	N	N		
	Later.	1,000	V	V	N		
	Later.	1,000	V	V	V		
	10.00	1,000	V	V	V		
	10.13	500	8	4	4		
18	8.16	7,000	I	N		Rain and haze	Do.
	8.38	5,700	V	N		Mist	
	8.56	4,750	I	N		Fog	
	9.15	4,000	N	N		do	
	9.37	1,910	V	V		Light haze	
	a. m.						
31	7.30	225	V	I	I	Fog varying	Do.
	p. m.						
32	6.40	1,000	7	4	4	do	Do.
	6.51	1,500	5	1	1		
	7.03	1,900	3	V	V		
	7.09	1,900	2	N	N		
	7.39	1,900	V	I	I	First flash count	
	Later.	1,100	V	N	N		
	Later.	1,100	V	I	I	Second flash count	
	8.02	1,000	7	4	4		

Larger numbers indicate higher apparent brightness.
I=intermittently visible.
L=lost from sight.
N=not visible.
P=picked up.
V=visible to naked eye but not through hole 1.
Blank space=no observations taken.

NOTES

Run No. 4.—The fog cleared so rapidly that about 45 seconds after the first gleam was detected all three flashes were clearly visible.

Run No. 6.—The increasing density of the fog obscured the beacon after the observations at 5,000 m (3.1 miles), so that no flashes were seen thereafter until the observer was only 510 m (560 yards) from the beacon. The neon flash was seen very soon after the red flash.

Run No. 7.—The line voltage dropped below normal during this run, making it impossible to operate all three units. The clear unit was not operated, and the neon unit frequently dropped to half its normal current. For this reason the results of this run are not conclusive.

Run No. 11—This is the only case in which the neon flash was picked up before the others. The fog cleared rapidly, and other flashes were seen immediately after the neon flash. The picking up of the neon flash first was probably a matter of chance.

Run No. 16.—At shorter distances the wedge was used; the observations are found in Table 1.

Run No. 17.—During the observations by J. E. N. the neon current was unsteady, dropping so low at times that the lamp went out. During the observations by F. C. B. the current was steadier.

Run No. 31.—The short range obtained was due to the daylight, which made it necessary to see the flashes against a background of illuminated fog. The red and neon flashes were each missed at times, apparently one as often as the other.

Run No. 32.—During the first flash count, which included about 40 cycles, 10 red flashes and 7 neon flashes were missed. The second flash count included 19 cycles; the only flash missed was the second red flash.

There were five runs made in rain or mist. None of these observations are significant in respect to the neon lamp. For the first three (2, 3, and 11) the wedge was not available, and during both the other runs (18 and 28) the neon lamp failed. Runs 2 and 3 are not included in the tables because none of the flashes were ever obscured. The observations furnish no definite proof that rain did not affect the clear and red flashes alike, but it was noted in the reports for runs 2, 3, and 11 that the clear flash did not appear as much brighter than the red flash as usual. Such observations are merely impressions and are not, of course, conclusive.

VII. DISCUSSION

The selectivity of the wedge used for the visibility observations has been determined for light of the three types used. For the red and neon lights the ratio of the transmission for the neon light to that for the red light remained between 0.98 and 1.04. This selectivity is not large enough to warrant a correction in view of the order of precision obtainable in making the observations.

The transmission of the wedge for the light of the clear and red beams has also been determined. These values showed an increasing selectivity for the higher readings on the wedge exceeding 15 per cent at hole 6. It was not feasible to measure the selectivity beyond hole 6 because the transmission was so low, but the transmission values have been extrapolated to cover all that portion of the wedge used in taking the visibility observations.

Having determined the transmission of the wedge for the light of the clear and red beams, respectively, it was possible to express the wedge observations given in Tables 1 and 2 for these beams as wedge transmission values and then in each case to form the ratio of the transmission value for the clear beam to that for the red beam. These ratios are given in Tables 4 and 5.

Since the clear beam was of higher intensity than the red beam, it is natural that lower wedge transmission could be used without obscuring the clear flashes. Had atmospheric effects offset the advantage of higher initial candlepower and conferred upon the red beam a greater visibility than that of the clear beam, then, under such conditions of weather and distance, the clear beam would require higher wedge transmissions than the red beam, and the ratios given in Tables 4 and 5 would exceed 1.00. We find, however, only one case in each table in which the ratio was equal to 1.00, while in all the other cases it is less than 1.00.

Figure 6 shows how the average wedge transmission ratio varied with distance for the visibility observations taken by each of the two

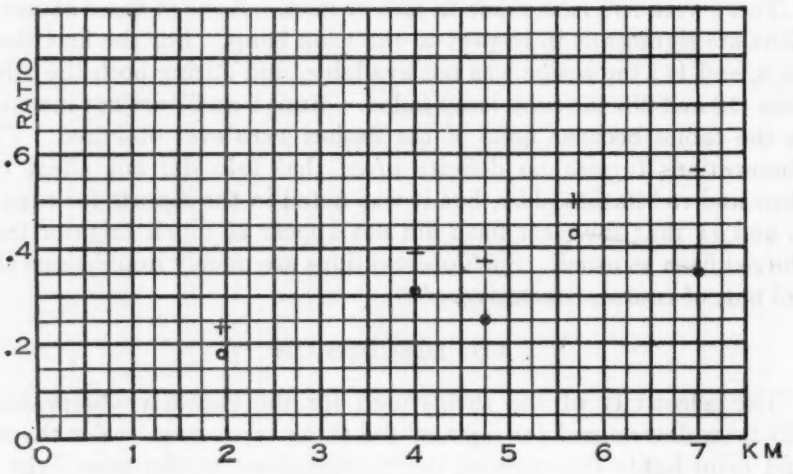

FIGURE 6.—*Variation of the wedge transmission ratio with distance*

The points plotted are the average of all those taken by each observer at each station; circles, observations by F. C. B.; crosses, observations by J. E. N.

observers. Since the results for each of the observers show the same systematic variation, it is assumed that this is not accidental. As the distance increases there is a tendency for the ratio to approach 1.00; that is, the visibility of the red beam approaches closer to that of the clear beam, a distance effect overcoming in part the advantage of the higher initial candlepower of the clear beam. In other words, there is a tendency for the energy in the clear beam to be reduced more rapidly than that in the red beam with increasing distance. Since the energy at the same wave length must be affected similarly in the two beams, this difference in transmission through the atmosphere must be due to the energy at the shorter wave lengths being lost from the clear beam more rapidly than that at the longer wave

lengths. This is presumably due to selective scattering. Such selective scattering must cause some reddening of the clear beam. That such a reddening was not generally observed was probably due to the impossibility of seeing the clear beam at short and long ranges simultaneously.

At the beacon the red beam had approximately 0.25 times the luminous intensity of the clear beam. At 1,910 m from the beacon one observer's values show a mean wedge transmission ratio of 0.18 and the other observer's values a ratio of 0.23. These low values may be due to Purkyne effect, the use of the wedge being virtually a comparison of brightnesses at a very low level with a consequent loss of sensitivity in the red region.

Turning to Tables 4 and 5, we do not find that there is any tendency for the values taken in foggy or hazy weather to rise above the means of all the values taken at their respective distances by the same observer, as should be the case if the red beam possesses superior fog-penetrating properties. This suggests that the shortening of the visible range of lights in fog is due to nonselective scattering, absorption, and the fact that the fog forms a luminous background affording less contrast to the light under observation. These effects are independent of the color of the light and are presumably due to particles of larger size than those which cause the selective absorption referred to above as a distance effect.

TABLE 4.—*Ratio of wedge transmission for clear beam to that for red beam (T_C/T_R), as indicated by observations in Table 1*

Run No.	7,000 m	5,700 m	4,750 m	4,000 m	1,910 m	Weather
12	0.58	0.60	0.60	0.61	0.10+	Clear.
14	.58	.58	.60	.33	.18	Do.
14		.58	.33	.60	.33	Do.
16		1.00−	.17	.17	.34	Light fog.
20	.10	.18	.10	.18+		Clear.
22	.58	.32	.10	.10	.18	Do.
24	.09	.58+	.32	.33+	.10	Light haze.
26	.32	.10	.10	.18	.10	Clear.
28		.31	.17			Rain and haze.
30	.17+	.09	.05		.10	Haze.
Mean	.35	.43	.25	.31	.18	

T_C and T_R-wedge transmission for clear and red beams, respectively.
+ indicates values given are somewhat too small.
− indicates values given are somewhat too large.
} See Note below.
Blank space=observations incomplete.

NOTE.—These symbols have been used because the corresponding observations in Table 1 indicate probable values in between two adjacent holes of the wedge.

TABLE 5.—*Ratio of wedge transmission for clear beam to that for red beam (T_C/T_R), as indicated by observations in Table 2*

Run No.	7,000 m	5,700 m	4,750 m	4,000 m	1,910 m	Weather
13	0.61	0.63	0.34+	0.63	0.36	Clear.
15	.60	.61	.34+	.61−	.19	Slight haze.
19	1.00	.60−	.61	.34	.19	Do.
21		.63	.61	.63	.35−	Clear.
23	.61	.61	.19	.35	.20	Do.
25	.60	.61	.63−	.34+	.20	Slight haze.
27	.18	.18+	.19	.19	.19	Clear.
29		.34	.19+	.19	.20	Do.
33	.34	.34−	.19	.19	.20	Do.
Mean	.56	.50	.37	.39	.23	

T_C and T_R-wedge transmission for clear and red beams, respectively.
+ indicates values given are somewhat too small. } See Note below.
− indicates values given are somewhat too large. }
Blank space=no observations taken.

NOTE.—These symbols have been used because the corresponding observations in Table 2 indicate probable values in between two adjacent holes of the wedge.

Of all the wedge observations taken only one can be interpreted as indicating greater visibility for the neon flash, and this is found in run 13 (Table 2) at the 1,910 m station. In this instance a plus sign was used for the neon flash but not for the red flash, indicating that the neon flash appeared brighter to the observer through the seventh hole of the wedge than did the red flash. Against this single case there are six instances in which the red flash seemed stronger than the neon flash in Table 1 and two instances in Table 2. The total comparisons of neon and red in Table 1 are 42 and 43 in Table 2. The wedge observations, therefore, indicate no advantage in visibility for the light from the neon lamp.

The observations made with the unaided eye, in general, show a slight advantage for the red beam. The only advantage indicated for the neon beam appears in run 32, in which the number of missed flashes was found to be about 50 per cent greater for the red beam than for the neon beam. As both sets of flashes were near the limit of visiblity so that only a small change in apparent brightness would cause a flash to be missed and as the number of observations is small so that an accidental variation is probable, this result does not indicate any marked difference in visibility.

VIII. CONCLUSION

We conclude that there is no difference, sufficiently great to be found by the methods of this test, between the visibility of light from a neon lamp and light of the same color and horizontal candlepower distribution from an incandescent lamp.

With regard to the comparison of the clear and red beams, the results of the test admit of no doubt. The addition of the red filter

does not increase the range of a clear beam under any weather conditions. It was, however, noticed that the red and neon flashes were generally easier to find among the shore lights, especially before the observers had learned just where to look for the beacon.

These conclusions applied to the problem of beacon design suggest that the neon lamp must be compared with the combination of incandescent lamp and color filter entirely on the basis of performance at the beacon. First of all, we must have a neon lamp which has a sufficiently high brightness to make possible a satisfactorily high intensity without using reflectors of impractical size. Second, the lamp and such auxiliary apparatus as is necessary must be reliable and inexpensive to maintain. If a neon lamp can be produced satisfying both these requirements, it will merit consideration upon the basis of efficiency alone, and in this respect it seems likely that the neon lamp will stand superior to the combination of incandescent lamp and filter.

In localities where competing lights are not common the use of incandescent lamps without filter makes possible longer distances between beacons. It seems probable that in regions where airway beacons must be seen against a backgound thickly set with other lights the loss of range which is caused by the use of a red filter is more than compensated by the greater facility with which the red flashes can be picked up.

IX. ACKNOWLEDGMENTS

It is a pleasure to acknowledge the many kindly and valuable suggestions received from Dr. J. Franklin Meyer both during the course of the experimental work and in connection with the preparation of this report. Thanks are also due to E. G. Anderson for determining transmission values for the wedge, to I. G. Priest and Dr. K. S. Gibson for the loan of calibrated filters and for helpful suggestions.

WASHINGTON, December, 1928.

A CRYSTALLINE DIFRUCTOSE ANHYDRIDE FROM HYDROLYZED INULIN

By Richard F. Jackson and Sylvia M. Goergen

ABSTRACT

The polysaccharide, inulin, has previously been shown to consist solely of fructose residues. Even if highly purified by recrystallization, however, inulin yielded upon hydrolysis with aqueous acids fructose solutions of but 92 per cent purity, regardless of the nature of the acid or the temperature at which the hydrolysis was carried out. The 8 per cent residue consisted of about 3 per cent aldose and 5 per cent nonreducing substance. The latter was isolated by removal of fructose by lime and fermentation of reducing sugars by yeast. The nonreducing residue showed a $[\alpha]_D^{20} = +55$ and yielded fructose by hydrolysis. The substance proved to be twenty-five times as resistant to hydrolysis as the remainder of the inulin molecule. Acetylation produced an oil from which 30 per cent crystallized in the form of prismatic needles. The latter after purification showed a $[\alpha]_D^{20} = +0.54$ in chloroform and contained but six acetyl groups. No modification of procedure produced a more highly substituted compound. Analysis and molecular-weight determination showed that the compound was the hexa-acetate of a disaccharide.

The hexa-acetate was deacetylated and the parent sugar obtained in crystalline form. It crystallized in minute plates from absolute alcohol and showed $[\alpha]_D^{20} = +27$ in water. Its formula, $C_{12}H_{20}O_{10}$, obtained from accumulated evidence, indicated that the substance was a difructose anhydride.

The mother liquors from the crystalline hexa-acetate showed a $[\alpha]_D^{20} = +31$ and a molecular weight corresponding to a disaccharide. There are, therefore, two or more isomeric disaccharides in the inulin residue.

Inasmuch as there is apparently a group of difructoses awaiting isolation, the sugar of $[\alpha]_D^{20} = +27$ is designated difructose anhydride I.

CONTENTS

	Page
I. Introductory	28
II. Purification and hydrolysis of inulin	28
III. Isolation of dextrorotatory constituent	29
IV. Acetylation of inulin residue	30
V. Difructose anhydride	30
VI. Experimental	32
1. Purification of inulin	32
2. Hydrolysis of inulin	32
3. Analysis of hydrolyzed inulin solutions	33
4. Isolation of nonreducing residue from hydrolyzed inulin	34
5. Hydrolysis of inulin residue	34
6. Difructose anhydride hexa-acetate	35
7. Difructose anhydride I	36
8. Hydrolysis of difructose anhydride I	37
9. Effect of H_2SO_4 on pure fructose	37
VII. Summary	38

I. INTRODUCTORY

The polysaccharide, inulin, was shown by Irvine and Steele[1] to consist solely of anhydro-γ-fructose residues. C. Tanret[2] had previously found that inulin in aqueous solution yielded upon hydrolysis with dilute acid sugar mixtures of specific rotation −81.3, very far short of the rotatory power of pure fructose. He concluded that the products of hydrolysis consisted of 12 parts fructose and 1 part glucose. Jackson, Silsbee, and Proffitt[3] studied the hydrolysis carefully and were able to obtain solutions of but 91 per cent purity[4] with respect to fructose. The anomaly exists, therefore, that, while inulin consists solely of fructose residues, hydrolysis fails signally to yield pure fructose solutions. The present paper is a study of the hydrolysis of inulin in aqueous solution and of the nature of the carbohydrates other than fructose produced by the hydrolysis.

II. PURIFICATION AND HYDROLYSIS OF INULIN

Since the possiblity existed that a persistent impurity, such as a hemicellulose, was responsible for the low purity of the hydrolyzed inulin, the purification was studied in detail. The inulin was repeatedly recrystallized from aqueous solution, and after each operation a portion was hydrolyzed and analyzed. It became evident that one recrystallization of the crude material produced a product indistinguishable by the analyses from one recrystallized repeatedly. Attention was then directed to the accumulated mother liquors, which were evaporated and fractionally crystallized. All products yielded solutions of about 92 per cent purity after hydrolysis.

The purity of the hydrolyzed inulin solution was found to be practically independent of the method of hydrolysis. Whether hydrolyzed with sulphuric acid at room temperature or with tartaric acid at boiling temperature or at intermediate temperatures and acidities, the purity was approximately the same, provided the hydrolysis was continued to apparent completion as indicated by the constancy of rotation.

In Table 1 are assembled the analytical data accumulated during the studies of purification and hydrolysis. While the variations are somewhat greater than the analytical uncertainties, the averaged values probably represent closely the composition of hydrolyzed inulin. The percentages are based upon 100 per cent dry substance, determined densimetrically in the hydrolyzed solution and, except in experiment No. 2, after removal of the hydrolytic agent. Experi-

[1] J. Chem. Soc., **117**, p. 1481; 1920.
[2] Bull. Soc. Chim., 3d series, **9**, p. 227; 1893.
[3] B. S. Sci. Paper No. 519, **20**, p. 604; 1926.
[4] The term "purity" is employed in the present paper in the quantitative sense customary in sugar analysis. It is the quotient of the amount of fructose divided by the total dissolved solids and is therefore independent of concentration.

ment No. 2 shows a somewhat lower purity than the others, owing to the partial destruction of fructose at the high temperature.

It will be observed that of the total carbohydrate but 91.8 per cent is fructose, that 94.8 per cent consists of reducing sugar estimated as fructose, and that there remains a nonreducing residue of 5.2 per cent. This residue is the main topic of the present paper. The nature of the 3 per cent nonfructose reducing sugar is still undetermined but will occupy our attention in a future investigation. That it is apparently an aldose sugar is indicated by its oxidizability by iodine.

TABLE 1.—*Summary of hydrolysis experiments*

Experiment No.	Fructose	Total reducing sugar	Aldose by iodine	Reducing sugar minus fructose	Ratio $\frac{\text{Fructose}}{\text{Reducing sugar}}$	Temperature of hydrolysis	Time of hydrolysis	Normality of H_2SO_4	Approximate concentration of inulin
	Per cent	*Per cent*	*Per cent*	*Per cent*		*°C.*	*Hours*	*N*	*Per cent*
1[1]	92.80	94.87	1.80	2.07	0.978	48.6	3.08	0.1224	13.2
2	90.21	92.36	2.41	2.15	.977	100.0	2.5	[2].005	13.5
3	92.15	94.84	1.82	2.69	.972	48.6	6.0	.0720	13.9
4	90.76	95.09	1.80	4.33	.955	48.6	8.2	.070	12.0
5	92.30	96.04	1.77	3.74	.961	20–30	[3] 13	.15	13.7
6	91.70	95.57	2.38	3.87	.960	20–60	[3] 6	.13	14.9
7a	92.32	94.84	2.23	2.52	.973	60.4	2.3	.08	16.7
7b	92.53	94.96	2.23	2.43	.974	60.4	3.2	.08	16.7
Average	91.85	94.82	2.06	2.98	.969				

[1] The method of preparation of the individual samples of inulin is described in the experimental part of this article.

[2] Tartaric acid normality with reference to first hydrogen. Arsem. United States Patent No. 1616169; Feb. 1, 1927.

[3] Days.

III. ISOLATION OF DEXTROROTATORY CONSTITUENT

From the hydrolyzed sirup the fructose was removed very nearly quantitatively by precipitation as calcium fructosate, and the filtrate after fermentation by yeast was found to be free from reducing sugars.

The substances in this solution were found to have a specific rotation of about +55. Although contaminated by impurities, a molecular-weight determination by the freezing-point method yielded the value 253, which suggested that the substance was mainly a disaccharide.

This material was extremely resistant to hydrolysis, but upon acidification to 0.4 *N* with H_2SO_4 partial hydrolysis was effected at boiling temperature. The dextrorotatory solution upon hydrolysis became strongly levorotatory. Careful analysis showed that the sole product of hydrolysis was fructose.

IV. ACETYLATION OF INULIN RESIDUE

From the dextrorotatory sirup no crystalline material could be obtained, but upon acetylation in the usual manner a portion, about 30 per cent, of the reaction mixture crystallized slowly in the form of prismatic needles. (Fig. 1.) This crystalline acetate was found to have a very low rotatory power and to contain but six acetyl groups. Consequently, in an effort to produce a more highly substituted compound, the acetylation of the original sirup was carried out repeatedly in the presence of the alternative catalysts, pyridine, zinc chloride, or sodium acetate, all of which catalyzed the reaction equally well. Polariscopic observation of the reaction mixture showed that, regardless of the nature of the catalyst, acetylation increased the rotatory power of the solution by about 10 per cent, and yet the same low rotating hexa-acetate in approximately the same yield was always recovered in crystalline form. The crystalline acetate itself was reacetylated but was recovered in unaltered form. It was, therefore, concluded that the original disaccharide contained but six hydroxyls and that the crystalline compound was the hexa-acetate of the disaccharide $C_{12}H_{20}O_{10}$. This conclusion was corroborated by a molecular-weight determination and by a combustion analysis.

The hexa-acetate recrystallized to a pure state showed a $[\alpha]_D^{20} = +0.54$ in chloroform. It has been indicated above that the reaction mixture at the completion of the acetylation possessed a high rotatory power, whereas the only acetate recovered was obtained in low yield and had a very low rotatory power. Furthermore, the mother liquors showed a specific rotation of +31 and a molecular weight of 573, the latter corresponding exactly to the hexa-acetate of a difructose anhydride. It is therefore evident that there were two or more acetates in the acetylation mixture, only one of which has been recovered in crystalline form. It will be shown below that this isomerism is not due to different modes of acetylation but is due to the presence of two or more different disaccharides in the original inulin residue.

V. DIFRUCTOSE ANHYDRIDE

The purified hexa-acetate was deacetylated by treatment with $Ba(OH)_2$ and the parent sugar obtained in crystalline form. The sugar crystallized in minute plates usually too small to permit a study of their form. When grown under favorable conditions they were seen to consist of rectangular plates (fig. 2), infrequently having one corner cut off at an angle of 45°. These plates were extremely thin and, if allowed to separate from a still solution, coalesced to form hard laminated clusters approximately spherical in shape.

The purified sugar exhibited an $[\alpha]_D^{20} = +27$ in water. The substances in the original crude-inulin residue, as we have indicated above, showed a specific rotation of +55. It is now evident that the latter

FIGURE 1.—*Difructose anhydride I hexaacetate*

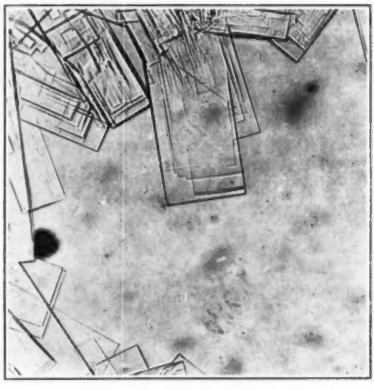

FIGURE 2.—*Difructose anhydride I*

UNIV OF MICH

value is merely the average rotatory power of at least two disaccharides and the one or ones which have not been isolated must have high rotations and yield acetates of high rotation.

The difructose in aqueous solution like the original crude mixture showed great resistance to hydrolysis. In sulphuric acid solution of pH = 0.965, $C_{H+} = 0.109$, it hydrolyzed at 100° C. with a velocity constant of about 0.009. In the work previously cited Jackson, Silsbee, and Proffitt found that inulin was hydrolyzed by 0.01 *N* HCl with a velocity constant of 0.020. The new difructose is therefore about twenty-five times as stable as the remainder of the inulin molecule, or about three hundred and twenty-five times as stable as cane sugar. An analysis showed that fructose was the sole product of the hydrolysis.

Previous work on the acetate had shown that the disaccharide was composed of two fructose residues condensed with a loss of two molecules of water. A combustion analysis of the sugar now proved definitely the formula $C_{12}H_{20}O_{10}$. It is therefore a difructose anhydride.

Inasmuch as there is apparently a group of difructoses awaiting isolation, we suggest the designation Difructose Anhydride I for the sugar $[\alpha]_D^{20} = +27$. It is our purpose to ascertain the structural formula of this sugar in continuation of the present work.

Evidence has been presented in recent literature [5] that inulin is constructed of difructose units either by association of difructose anhydride or by polymerization on classical principles of valence. The difructose anhydrides which we have described in the present paper can not serve for such units, for they are sharply distinct from the remainder of the inulin molecule in respect of their great resistance to hydrolysis.

The origin of these disaccharides is at present undetermined. Experiment showed that ordinary crystalline fructose is not condensed to difructose under the conditions of acidity and temperature which are suitable for the hydrolysis of inulin. The possibility that γ−fructose is condensed is also eliminated, for Jackson and Gillis [6] have shown that invert sugar produced from cane sugar by acid hydrolysis possesses a rotatory power equal to that of invert sugar produced by enzyme hydrolysis if corrected for the influence of the acid on the rotation. The rotation of invert sugar by enzyme hydrolysis has been shown by Zerban [7] to be exactly equal to the algebraic sum of the rotations of pure glucose and ordinary fructose.

The hypothesis that the difructoses were originally integral parts of the inulin molecule and on account of their high stability survived the hydrolysis was abandoned by the authors because as a logical

[5] For example, Bergmann and Knehe, Ann., **449**, p. 302; 1926; Schlubach and Elsner, Ber., **61**, p. 2358; 1928; Haworth and Learner, J. Chem. Soc., p. 621; 1928.

[6] B. S. Sci. Paper No. 375, **16**, p. 167; 1920.

[7] J. Am. Chem. Soc., **47**, p. 1104; 1925.

conclusion the inulin molecule would necessarily contain 40, 80, or 120 fructose residues if the 5 per cent of unhydrolyzed residue consisted of 1, 2, or 3 isomers, respectively.

It seems more probable that inulin, even when purified by many recrystallizations, may still consist of a number of closely related polysaccharides, some of which may contain the resistant difructose units and others aldose residues. Such a lack of homogeneity would account for the variable specific rotation which has been frequently observed and for the lack of precise agreement between the samples whose analyses are recorded in Table 1 of the present paper.

A remaining possibility is that the difructose anhydrides are formed by condensation of difructoses which may be intermediate products of the hydrolysis of inulin.

VI. EXPERIMENTAL

1. PURIFICATION OF INULIN

The expressed juice from dahlias was treated with kieselguhr and filtered while hot. The filtrate was allowed to stand either at room temperature or at 0° C. until the crystallization of inulin was complete. The separated inulin was collected on a filter and thoroughly washed. It was then redissolved in sufficient water to form an 18 to 20 per cent solution, treated with carbon if necessary, and recrystallized one or more times. In some instances the inulin was air-dried in order to preserve it for future experiments. On drying, the inulin shriveled and broke into hornlike fragments of a brownish-gray color. Before recrystallization or hydrolysis the dried inulin was suspended in water and kept in agitation for several hours. Under these conditions it formed a smooth paste free from lumps and indistinguishable from the undried material. No satisfactory criterion of purity was discovered. The specific rotations of samples which were deemed pure ranged from —38 to —40, in agreement with previous investigations.

The inulin samples upon which the data are recorded in Table 1 were prepared as follows: Nos. 1 and 2, crude inulin was once recrystallized; No. 3, twice recrystallized; No. 4, four times recrystallized; No. 5, the combined mother liquors from samples 1 to 4 were evaporated and recrystallized, and the resulting crystals recrystallized; No. 6, mother liquors from No. 5 precipitated by alcohol and crystals recrystallized from water; No. 7, a portion of No. 6 recrystallized from water.

2. HYDROLYSIS OF INULIN

A suspension containing from 12 to 17 per cent of inulin was agitated cold until free from lumps. It was then hydrolyzed under the variable specifications described in Table 1. In every instance the course of the reaction was followed by polariscopic observation of

samples taken at appropriate time intervals, and the reaction was considered complete when the rotation became constant. In some cases, as, for example, experiment No. 6, the inulin crystallized during hydrolysis. This made it necessary to heat the solution in order to redissolve the inulin, but it was at once cooled when this was accomplished. In one instance the sample was hydrolyzed until the reaction was apparently complete, and a portion, 7a, was analyzed. The remainder, 7b, was heated for an additional hour before analysis. Both samples showed the same properties within the limits of analytical precision.

3. ANALYSIS OF HYDROLYZED INULIN SOLUTIONS

The cooled solution was titrated to exact neutrality with a barium hydroxide solution and the barium sulphate removed by filtration. The density of the filtrate was determined to 5 decimals at 20.00° C. During the progress of the investigation a parallel research was conducted on the density of pure fructose solutions with the same degree of precision. This density table, which will be published in a later article, enabled us to determine with confidence the dry substance in the hydrolyzed inulin solutions. This procedure involved the assumption that the density of the unknown constituents was the same as that of fructose, but the deviations were for the present purpose unimportant. Total reducing sugars were determined by triplicate titrations by the method of Lane and Eynon,[8] control solutions of known concentration being titrated simultaneously.

Fructose was determined by its reducing action on copper carbonate at 49° C. according to a modification of the method proposed by Biourge [9] and Nyns.[10] The authors have examined this method in detail and have found it reliable, especially if fructose is the predominating substance present.

A portion of the hydrolyzed solution was tested for aldose sugars by iodine in the presence of sodium carbonate.[11] Although a blank analysis was made with pure fructose of the same concentration, the results are probably of little more than qualitative value. Nevertheless, the excess of total reducing sugar over the fructose and the invariably positive test with iodine indicates the presence of approximately 3 per cent of an aldose sugar in the hydrolyzed inulin.

[8] J. Soc. Chem. Ind., **42**, p. 32; 1923.
[9] Bull. Assoc. Ecole de Brasserie (Louvain); January, 1898.
[10] Ibid., January, 1925. C. A., **19**, p. 1236; 1925.
[11] Cajori, J. Biol. Chem., **54**, p. 622; 1922.

4. ISOLATION OF NONREDUCING RESIDUE FROM HYDROLYZED INULIN

From the hydrolyzed solution the fructose was removed as the calcium fructosate in the manner described by Jackson, Silsbee, and Proffitt.[12] The filtrate was caused to drain into a solution of oxalic acid in order to avoid the alkaline decomposition of the reducing sugars. It was then adjusted to neutrality with lime and filtered. The filtrate was evaporated to about 15 per cent solids, and residual reducing sugars were removed by fermentation with yeast. The resulting solution was clarified with carbon and evaporated nearly to dryness. Alcohol was added to precipitate yeast products. For analysis, a sample of this solution was evaporated under diminished pressure with addition of water to displace alcohol.

Rotation. $[\alpha]_D^{20}$ in water $= +55$ (12.68 in 100 ml, calculated from $d_4^{20} = 1.0474$, $\alpha = +40.68$, saccharimeter, 2 dm tube). *Mol. wt.* Subs., 12.68: water, 92.06; ΔT, 1.061. Mol. wt., 253.

5. HYDROLYSIS OF INULIN RESIDUE

A 25 ml portion of the residue in a 50 ml thin-walled flask was made 0.40 N with H_2SO_4, plunged into boiling water, and vigorously agitated for 8 minutes. It was then cooled rapidly and polarized and again heated in boiling water for 15 minutes. Its rotation was initially $+24.44$; after 8 minutes, $+5.42$; and after 23 minutes, -19.32. The solution was by this time too discolored for further polariscopic observation and was consequently analyzed to determine the products of hydrolysis. The following results are expressed in grams per 100 ml. Total reducing sugar, 5.49 g; fructose by Nyn's method, 5.58 g; fructose by temperature coefficient of polarization, 5.24 g; fructose by direct polarization, 5.21 g. The latter was calculated by subtracting from the observed polarization the polarization of the sugar unhydrolyzed. The remainder was the rotation of the products of hydrolysis. If fructose, the quantity was 5.21 g per 100 ml. During the period of 23 minutes heating 65 per cent of the original carbohydrate was hydrolyzed.

If any product but fructose were produced by hydrolysis, none of the three independent methods of calculation would approximate the total reducing sugar. It is thus evident that the sole product of hydrolysis was fructose. In further confirmation of this conclusion we may calculate roughly the velocity constant of hydrolysis. The initial rotation, $+24.44$, was directly observed. The rotatory power at complete hydrolysis may be calculated by multiplying the initial weight of substance by 1.11 (that is, the ratio, 2 $C_6H_{12}O_6$ to $C_{12}H_{20}O_{10}$) and converting to saccharimeter degrees on the assumption that fructose is the product of hydrolysis. The velocity constant for 8 minutes

[12] B. S. Sci. Paper No. 519, **20**, p. 609; 1926.

proved to be 0.018 and for 23 minutes, 0.020. If any substance other than fructose were produced, these values could not approach constancy.

6. DIFRUCTOSE ANHYDRIDE HEXA-ACETATE

The alcoholic solution containing 3.3 g of the disaccharide was evaporated in vacuo to a thick sirup and mixed with 40 ml of acetic anhydride, of which 25 ml was distilled off, carrying with it the remainder of the alcohol. To the residue 20 ml of acetic anhydride and 17 ml of pyridine were added and the mixture warmed for a short time to 60° to 70° and then left overnight at room temperature. The reaction mixture, poured into a large volume of ice water, separated as an oil which, after washing and neutralization with $NaHCO_3$, became a viscous wax, with no indications of complete hardening. Only after standing for five or six weeks did it harden sufficiently to indicate a partial crystallization. It was then dissolved in alcohol and a portion recovered in the form of prismatic needles; yield, about 30 per cent of the theoretical. Upon purification and analysis this substance proved to be the hexa-acetate of a disaccharide.

In an effort to produce a more highly substituted acetate, the acetylation was repeated with many modifications, of which the following are typical. Whenever possible the course of the reaction was followed by polariscopic observation.

A solution of 3.2 g of disaccharide in 16 g of acetic anhydride rotated +50.5 saccharimeter degrees in a 200 mm tube. One-tenth gram of zinc chloride was added and the mixture allowed to stand overnight at room temperature and then one and one-half hours at 50°. It was found that the rotation of the solution after cooling had risen to 56.4° and remained at this value after repeated heating and cooling. The reaction mixture was poured into iced water, neutralized with $NaHCO_3$, and extracted with chloroform. The chloroform solution was washed with water, dried with $CaCl_2$, and evaporated to a small volume. The crystalline substance which separated as prismatic needles was the same hexa-acetate as that obtained by catalysis with pyridine; yield, 30 per cent of the theoretical.

Similarly, an acetylation in the presence of sodium acetate produced a mixture of increased dextrorotatory power which yielded the same crystalline acetate.

The pure crystalline hexa-acetate was dissolved in acetic anhydride and an attempt made to acetylate further with zinc chloride as catalyst. The original substance was recovered in unaltered form.

Finally, 1.2 g of hexa-acetate was dissolved in 10 ml of chloroform and 1 g PCl_5 added in an effort to replace any unsubstituted hydroxyls by halogen. No product but the original hexa-acetate was recovered.

The acetylated sugar was recrystallized from alcohol to constant melting point and specific rotation. The purified substance in a capillary tube showed a visible sintering at 125° C. and melted sharply at 137° C. (uncorrected). *Anal.* Subs., 0.2569, 0.3242: CO_2, 0.4721, 0.5899; H_2O, 0.1298, 0.1623. Calcd. for $C_{12}H_{14}O_{10}$ $(OCCH_3)_6$: C, 50.00; H, 5.56. Found: C, 50.12, 49.63; H, 5.65, 5.60. *Rotation.* $[\alpha]_D^{20}$ in $CHCl_3 = +0.54$ (2.496 in 25 ml, $\alpha = +0.31°$, saccharimeter, 2-dm tube). $[\alpha]_{5780}^{20} = +0.65$ (2.674 in 25 ml, $\alpha = +0.138°$, circular), and $[\alpha]_{5461}^{20} = +0.69$ (2.674 in 25 ml, $\alpha = +0.147°$).

For the determination of acetyl groups the acetate was dissolved by heating gently in an excess of $Ba(OH)_2$ solution, and allowed to stand overnight. The excess alkali was titrated with acetic acid (Phenolphthalein). *Anal.* Subs., 0.2031, 0.2261 required 18.760 g, 20.934 g of 0.11296 *N* $Ba(OH)_2$ (weight burette). Calcd. for $C_{12}H_{14}O_{10}(OCCH_3)_6$: $OCCH_3$, 44.80. Found: 44.87, 44.97. *Mol. wt.* Subs., 1.0006, 0.8014: benzene, 23.488, 22.983; ΔT, 0.376, 0.317°. Calcd: 576. Found: 582, 566.

The mother liquors remaining from the hexa-acetate crystallization have even to the present writing continued to yield further quantities of the hexa-acetate by slow crystallization, but no isomeric acetate has yet crystallized. That they contain an acetylated disaccharide of high rotatory power is indicated by the following experimental data. The dry substance in the solution was determined by drying on sand at 85°. *Mol. wt.*, Subs., 3.102: benzene, 22.074; ΔT, 1.256°. Mol. wt., 573. *Rotation.* $[\alpha]_D^{21}$ in $CHCl_3 = +31$ (5.60 in 100 ml, $\alpha = +10.03°$, saccharimeter, 2-dm tube).

7. DIFRUCTOSE ANHYDRIDE I

Difructose anhydride hexa-acetate was suspended in an excess of $Ba(OH)_2$, warmed gently until completely dissolved and allowed to stand overnight. The calculated volume of H_2SO_4 sufficient to remove the barium quantitatively was added and the filtrate evaporated in a vacuum to nearly complete dryness. Absolute alcohol was added and the solution filtered with carbon. The filtered solution was evaporated on the steam bath to a relatively small volume and set aside to crystallize. By the following morning the crystalline sugar appeared in the form of spheres consisting of clusters of minute crystals. In all crystallizations subsequent to the first it was possible to seed the saturated solution and produce an unclustered crystal mass. Well-developed crystals on the microscope slide took the form of thin rectangular plates. The substance was readily purified by crystallization from hot absolute alcohol. *Anal.* Subs., 0.1540, 0.2232: CO_2, 0.2491, 0.3614; H_2O, 0.0856, 0.1227. Calcd. for $C_{12}H_{20}O_{10}$: C, 44.42; H, 6.22. Found: C, 44.12, 44.16; H, 6.22, 6.15. *Rotation.* $[\alpha]_D^{20}$ in $H_2O = +26.9$ (2.113 in 25 ml, $\alpha = +13.08°$, saccharimeter.

2-dm tube); a second solution gave $[\alpha]_D^{20} = +27.0$ (1.024 in 25 ml, $\alpha = +6.39°$, saccharimeter), and $[\alpha]_{5780}^{20} = +27.6$ ($\alpha = +2.257°$, circular), and $[\alpha]_{5461}^{20} = +30.7$ ($\alpha = 2.510$).

8. HYDROLYSIS OF DIFRUCTOSE ANHYDRIDE I

A 25.0 ml solution containing 78.8 mg difructose anhydride and sufficient H_2SO_4 to make 0.20 *N* was heated at 100° C. for 100 minutes. Upon analysis it was found to contain 2.95 mg of total reducing sugar and 2.80 mg of fructose per milliliter. The essential agreement indicates that fructose is the only product of hydrolysis.

The original disaccharide would yield, if hydrolysis were complete, 3.50 mg of reducing sugar per milliliter (that is, $78.8 \times 1.11 + 25$), while actually in a period of 100 minutes $\frac{2.95}{3.50} = 84.3$ per cent of the disaccharide was hydrolyzed. The velocity of reaction can be roughly calculated for the conditions specified.

$$k = \frac{1}{100} \log \frac{100}{100 - 84.3} = 0.008$$

in terms of minutes and common logarithms. (0.2 *N* H_2SO_4 and $T = 100°$ C.)

A 25 ml solution containing 7.8 mg of difructose anhydride and 0.2 *N* H_2SO_4 was heated at 100°. One-milliliter samples were withdrawn at various intervals of time and analyzed by the method of Folin and Wu.[13] The mean value of the velocity constant for three intervals of time was 0.0083. A quinhydrone electrode in the solution coupled with a saturated calomel half cell showed a potential of 0.395*v*, $t = 27°$; whence pH = 0.965 and $C_H = 0.109$.

In a previous section we have shown that the velocity of hydrolysis of the mixture of disaccharides in the presence of 0.4 *N* H_2SO_4 at 100° C. was 0.019. In 0.2 *N* acid this would be approximately 0.010.

The mean of these three estimates of the velocity constant is 0.009, which value is employed for the purpose of comparing the stability of difructose anhydride I with the remainder of the inulin molecule.

9. EFFECT OF H_2SO_4 ON PURE FRUCTOSE

An aqueous solution containing approximately 14 per cent of fructose was made 0.0732 *N* with H_2SO_4 and divided into two portions. One portion was retained for a standard of comparison; the other was heated at 48.6° C. for four hours. The rotations of the control and heated solutions were, respectively, −75.27° and −75.20° (saccharimeter). The apparent loss of purity was, therefore, 0.10 per cent. The oxidizability by iodine increased 0.08 per cent estimated

[13] J. Biol. Chem., **38**, p. 81; 1919; **41**, p. 367; 1920.

as glucose. There was, therefore, no condensation of fructose under these conditions.

An 11.5 per cent fructose solution 0.005 *N* with respect to the first hydrogen of tartaric acid was heated two and one-half hours at 100°. The sugar suffered a loss of 0.5 per cent in purity and an increase in 0.3 per cent reactivity with iodine.

VII. SUMMARY

Inulin upon hydrolysis with dilute acid yields solutions containing in 100 per cent solid matter 91.8 per cent fructose, 94.8 per cent reducing sugar, and a 5.2 per cent unfermentable residue.

The residue has a $[\alpha]_D^{20} = +55$ and is hydrolyzed by 0.4 *N* H_2SO_4 at 100° C. solely to fructose. It is twenty-five times as resistant to hydrolysis as the remainder of the inulin molecule.

Acetylation of the original residue yielded a mixture of acetates, one of which crystallized in 30 per cent yield in the form of prismatic needles of $[\alpha]_D^{20} = +0.54$. This was found to be the hexa-acetate of a disaccharide containing but six hydroxyl groups.

The mother liquors from the crystalline acetate contained one or more acetylated difructoses with a mean $[\alpha]_D^{20} = +31$.

The crystalline hexa-acetate upon deacetylation yielded a crystalline difructose anhydride of $[\alpha]_D^{20} = +27$. The latter was hydrolyzed to fructose by 0.2 *N* H_2SO_4 at 100° C. with a velocity constant of 0.009 (common logarithms, minutes).

The original residue of $[\alpha]_D^{20} = +55$ contains additional difructoses which have not as yet been isolated.

WASHINGTON, January 5, 1929.

FASTNESS OF DYED FABRICS TO DRY CLEANING

By A. S. Eichlin

ABSTRACT

Data on the behavior of dyes in actual dry cleaning have not been available. It is the purpose of this paper to supply this information.

A number of representative dyestuffs on wool, silk, cotton, rayon, and union fabrics were subjected to two tests. In the first a moisture-free solvent was used, and in the second the solvent contained 0.1 per cent free moisture and 0.01 per cent alkali. The apparatus used in making the tests was designed as a convenient substitute for a commercial dry-cleaning machine. The results are given in tabular form.

CONTENTS

		Page
I.	Introduction	39
II.	Purposes and scope	40
III.	Acknowledgments	40
IV.	Apparatus	40
V.	Testing procedure	41
VI.	Discussion of results	50
VII.	Conclusion	51

I. INTRODUCTION

The fastness of dyestuffs to most of the agencies and operations entering into the dry-cleaning process has already been established. The behavior of dyes on fabrics toward acids, alkalies, steaming, pressing, and ironing is known and can be ascertained from the catalogues of the dye manufacturers. The action of dry-cleaning solvents and soaps on dyed fabrics has not been systematically studied.

It is probable that any type of dyestuff will at one time or another be used on textile materials which will be subjected to the dry-cleaning process. The dye may occur on the principal fabric or on the linings, threads, or decorative effects on garments or household materials which are customarily dry-cleaned. A slight change in color resulting from dry cleaning would not be particularly serious in some instances, but any tendency to bleed is always a potential danger because of the liability of staining other materials in the same load.

This study of the action of dry-cleaning solvents and soaps on dyed fabrics was undertaken by the research associate at the bureau from the National Association of Dyers & Cleaners at the request of the association. It may well be stated here that, on account of the hundreds and even thousands of dyed materials handled every day in dry-cleaning plants, it was not considered practicable to study any

procedure whereby the dry cleaner would attempt to group the dyed materials into their respective fastness or dyestuff classes. In some plants it is customary in the prespotting operation to test for the presence of basic dyes on certain kinds of materials before applying spotting agents. It is believed that data obtained from this systematic study of the effects of dry cleaning on dyed fabrics will be useful not only to the dry cleaner, but also to the dyestuff manufacturer and to the fabric dyer.

II. PURPOSES AND SCOPE

The purpose of this study was to test the fastness of dyed fabrics (*a*) to dry-cleaning solvents and soaps, and (*b*) to dry-cleaning solvents and soaps to which small amounts of water and alkali were added.

Many dyestuffs are identical in composition but are sold under different trade names by the various companies. To test all dyes manufactured would thus have involved needless duplication and would have served no useful purpose. Accordingly, American manufacturers were requested to submit sample dyeings of the types of dyes in which they specialized, together with dyeings of the dyestuffs which they made exclusively. In a few instances, as will be noted in the tables, duplications occurred; but these served as check tests. It is to be noted that only American dyestuffs are included; an attempt to obtain dyeings from a large importer of foreign-made dyestuffs was not successful.

III. ACKNOWLEDGMENTS

An acknowledgment of appreciation for whole-hearted interest and cooperation is extended to the dye manufacturers [1] who provided the sample dyeings. Thanks are also due C. W. Schoffstall, formerly chief of the textile section, for his helpful suggestions.

IV. APPARATUS

The apparatus used in making these tests is pictured in Figure 1. The machine was designed as a convenient substitute for a commercial dry-cleaning machine. It has a capacity of six 1-liter bottles. The rotor is mounted on a shaft so geared to a motor that the rotor has a speed of 30 revolutions per minute. The bottles are corked and are held in position by a spring clamping lock. The bottles rest securely in holes countersunk in the base of the rotor.

---

[1] American Aniline Products Co.; Geigy Co. (Inc.); John Campbell & Co.; Celanese Corporation of America; E. I. Du Pont De Nemours & Co.; National Aniline & Chemical Co.; Newport Chemical Works (Inc.); Zinsser & Co.

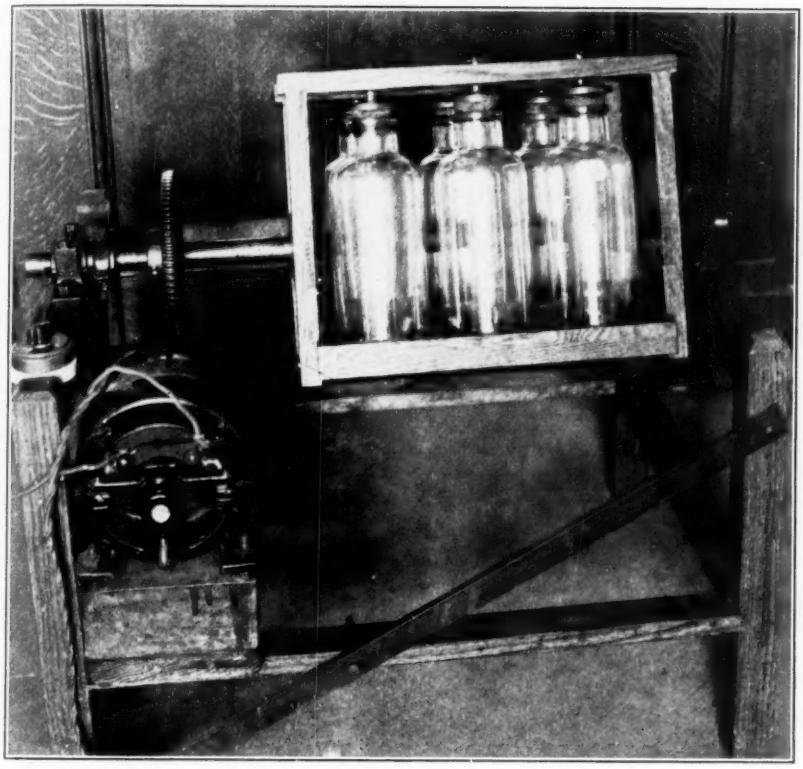

FIGURE 1.—*Machine for laboratory dry-cleaning tests*

V. TESTING PROCEDURE

Two series of tests were made. In the first the solvent was moisture free. The soap solutions prepared from this solvent contained only the small amount of moisture naturally present in the soaps. In the second series the solvent contained 0.1 per cent water and 0.01 per cent sodium hydroxide. The soaps were prepared with the solvent containing these amounts of water and alkali. Although this content of water and alkali may appear excessive, analyses of several samples of solvents received from various cleaners showed that the use of solvents containing the above percentages is not unusual in practice.

A sample of dyed fabric 10 square inches in area was placed in each bottle, together with small portions (about ¼ square inch) of cotton, wool, rayon, and weighted and unweighted silk to be used in judging staining. In order to simulate to a close degree the mechanical action encountered in a dry-cleaning machine, four small pieces of toweling were placed in each bottle. Enough dry-cleaning solvent to cover the cloth, about 50 ml, was then added and the bottles placed in the machine. The solvent employed in this investigation was in strict conformity with specifications for Stoddard solvent.[2] The machine was run for 15 minutes. The bottles were then removed, the solvent poured off, and a 0.5 per cent solution of benzene soap having a potassium oleate base added. The machine was again run for a 15-minute period, at the expiration of which the bottles were removed and the soap solution poured off. A 0.5 per cent solution of alcoholic benzene soap was next added and the machine run for an additional 15 minutes. The bottles were removed and this solution poured off. The samples were finally given a rinse in solvent for 10 minutes, extracted, and dried for 45 minutes at 120° F.

The test procedure was repeated with fresh portions of the dyeings, using the solvent and soaps containing water and alkali. After the completion of each test, the portions of undyed fabrics were examined to determine whether or not they had become stained. The treated dyed sample was compared with the original untreated sample in order to detect possible color changes. Any coloration of the clear solvent or the soap solutions was noted at the end of each operation.

In Table 1 are listed dyes which showed no change either in moisture and alkali-free solvent or in solvent containing 0.1 per cent water and 0.01 per cent caustic soda. The dyes are divided into eight classes, namely, direct, acid, basic, mordant, sulphur, vat, developed, and ice. The dyes in each class behave similarly toward the same fiber, and the method of their application is, in general, the same. Descriptions

[2] Stoddard Solvent (Dry Cleaning), Commercial Standard CS3-28. Obtainable from the Superintendent of Documents, Government Printing Office, Washington, D. C., for 10 cents.

of these classes and methods of application can be obtained from any standard book on dyeing.

In column 1 are listed the serial numbers assigned for reference purposes in this study.

Column 2 contains the Colour Index numbers of the dyes obtained from The Colour Index published by the Society of Dyers & Colourists (England, 1924).

This index should be consulted for data on chemical structure, methods of application, properties, uses, patent references, and trade names. The Year Book of the American Association of Textile Chemists & Colorists lists the American manufacturers of these dyes by Colour Index number. The annual census of dyes of the United States Tariff Commission gives similar data.

Dyes which have been assigned no numbers in the Colour Index are listed by name only. The manufacturers of these dyes can be found by consulting the Year Book of the American Association of Textile Chemists & Colorists.

Column 3 contains the names of the dyes which were tested.

In column 4 are listed the various fibers which were dyed with the dyes tabulated in column 3. The letters "C," "W," "S," "WtdS," and "R" denote cotton, wool, silk, weighted silk, and rayon, respectively.

TABLE 1.—*Dyes which showed no color change in either moisture-free and alkali-free solvent or in solvent containing 0.01 per cent caustic soda and 0.1 per cent water*

DIRECT COLORS

Serial No.	Colour Index No.	Name of dye tested	Fiber on which dyed
1	.....	Amanil brown GR	C-S.
2	653	Amanil fast orange PRZ	C-S.
3	448	Benzopurpine 4B Conc	C-S-WtdS-R.
4	495	Benzopurpine 10B	C-WtdS-R.
5	365	Chrysophenine Ex	C-WtdS-R.
6	401	Diazine black H Ex	R.
7	581	Direct black EG Ex	C-WtdS-R.
8	582	Direct black RB Ex	C-WtdS-R.
9	406	Direct blue 2B Conc	C-S-R.
10	447	Direct blue 3BX	C-S-R.
11	.....	Direct blue BXG	C-S-R.
12	401	Direct blue BH Ex Conc	C-R.
13	508	Direct brilliant blue G	C-S-R.
14	512	Direct fast blue RW	C-S-WtdS-R.
15	420	Direct fast brown M	C-S-WtdS-R.
16	130	Direct fast pink EBN	C-S-R.
17	419	Direct fast red F	C-WtdS-R.
18	326	Direct fast scarlet 4BS	C-S-WtdS-R.
19	326	Direct fast scarlet 8BA	C-S-R.
20	326	Direct fast scarlet G	C-S-R.
21	326	Direct fast scarlet 4BAN	C-S-R.
22	814	Direct fast yellow NN	C-S-WtdS-R.
23	552	Direct navy blue RS	C-R.
24	520	Direct sky blue Ex	C-S-R.
25	518	Direct sky blue 6B Ex green	C-S-R.
26	590	Direct steel blue G Conc	C-S-R.
27	394	Direct violet N	C-WtdS-R.
28	622	Direct yellow AFG	C-S.
29	581	Erie black BF	R.
30	581	Erie black GXOO	R.

C=cotton. S=silk. WtdS=weighted silk. R=rayon.

TABLE 1.—*Dyes which showed no color change in either moisture-free and alkali-free solvent or in solvent containing 0.01 per cent caustic soda and 0.1 per cent water*—Continued

DIRECT COLORS—Continued

Serial No.	Colour Index No.	Name of dye tested	Fiber on which dyed
31	539	Erie black NR Ext	R.
32	582	Erie black RF	R.
33	------	Erie blue green CN	R.
34	------	Erie bordeaux B	R.
35	596	Erie brown CN	R.
36	------	Erie brown GB	R.
37	495	Erie cardinal 7B	R.
38	420	Erie fast brown 3RB	R.
39	------	Erie fast gray M	R.
40	326	Erie fast orange A	R.
41	419	Erie fast red FD	R.
42	326	Erie fast scarlet 4BA	R.
43	326	Erie fast scarlet 8BA	R.
44	326	Erie fast scarlet YA	R.
45	814	Erie fast yellow WB	R.
46	128	Erie pink 2B	R.
47	448	Erie red 4B	R.
48	382	Erie scarlet B	W–R.
49	471	Erie violet 2B	R.
50	387	Erie violet BW	R.
51	394	Erie violet 3R	R.
52	365	Erie yellow Y	R.
53	873	Fast silk gray M Conc	C–S–R.
54	------	Light fast blue SFR	C–S–R.
55	------	Light fast blue SFF	C–S–R.
56	------	Light fast blue 4GL	C–S–R.
57	319	Light fast heliotrope 2BL	C–S–R.
58	278	Light fast red SBL	C–S–WtdS–R.
59	267	Neutral gray GG Spec	C–S–R.
60	406	Niagara blue 2B	R.
61	477	Niagara blue 3B	R.
62	552	Niagara blue DB	R.
63	405	Niagara blue HW	R.
64	468	Niagara blue 3RD	R.
65	512	Niagara blue RW	R.
66	------	Niagara fast blue RL	R.
67	520	Niagara sky blue	R.
68	518	Niagara sky blue 6B	R.
69	581	Pontamine black EBN	S.
70	------	Pontamine brilliant violet B	S.
71	598	Pontamine brown CG	S.
72	420	Pontamine brown R	S.
73	539	Pontamine fast black FF	S.
74	------	Pontamine fast black LN	S.
75	------	Pontamine fast blue 6GL	C.
76	------	Pontamine fast heliotrope BL	S.
77	------	Pontamine fast orange 2G Conc	C.
78	326	Pontamine fast orange S	S.
79	349	Pontamine fast yellow 4GL	S.
80	593	Pontamine green BX	S.
81	594	Pontamine green GY	S.
82	------	Pontamine light gray 2G	C.
83	------	Pontamine light gray BV	C.
84	------	Pontamine light orange 2G	C–S.
85	382	Pontamine scarlet B	S.
86	------	Pontamine scarlet 3B	S.
87	------	Solantine black L	R.
88	------	Solantine blue FF	R.
89	------	Solantine blue 2GL	R.
90	------	Solantine blue 4GL	R.
91	------	Solantine brown R	R.
92	------	Solantine orange G	R.
93	353	Solantine pink 4BL	R.
94	------	Solantine violet R	R.
95	------	Solantine yellow FF	R.
96	346	Solantine yellow 4GL	R.

C=cotton. S=silk. WtdS=weighted silk. R=rayon. W=wool.

TABLE 1.—*Dyes which showed no color change in either moisture-free and alkali-free solvent or in solvent containing 0.01 per cent caustic soda and 0.1 per cent water*—Continued

ACID COLORS

Serial No.	Colour Index No.	Name of dye tested	Fiber on which dyed
97	246	Acid blue-black Ex Conc	W.
98	699	Acid fast violet BG	W.
99	30	Acid fuchsine D	W.
100	666	Acid green L Ex	W.
101	57	Acid phloxine 6BX Conc	W.
102	29	Acid phloxine G	W.
103	------	Acid red OTH	W.
104	90	Acid violet 6R	W.
105	1054	Alizarine sapphire	W.
106	1054	Alizarine sapphire BN	W.
107	1054	Alizarine sapphire FS	W.
108	1053	Alizarine sapphire SE	W.
109	135	Alkali fast green 2G	W.
110	714	Alphazurine A	W.
111	671	Alphazurine FG	W.
112	712	Alphazurine 2G	W.
113	88	Azo bordeaux	W.
114	------	Azo dark green B	W.
115	------	Azo eosine 2B	W.
116	------	Azo fast blue G high Conc	W.
117	------	Azo fast blue B high Conc	W.
118	------	Azo fast blue 2R high Conc	W.
119	53	Azo wool violet 4B	W.
120	146	Azo yellow A5W	W.
121	185	Brilliant scarlet 3R	W.
122	------	Brilliant wool blue B	W.
123	------	Brilliant wool blue N	W.
124	------	Buffalo black AR	W.
125	246	Buffalo black NBR	W.
126	------	Buffalo black RB	W.
127	------	Buffalo black 3G	W.
128	------	Buffalo black 8B	W.
129	294	Buffalo black 10B	W.
130	253	Cloth red 2R	W.
131	26	Croceine orange Y Conc	W.
132	252	Croceine scarlet MOO	W.
133	307	Durol black B	W.
134	307	Durol black 2B	W.
135	304	Fast acid black N2B	W.
136	208	Fast acid blue SR Conc	W.
137	209	Fast acid blue SB	W.
138	667	Fast acid green B	W.
139	53	Fast acid violet RM Ex	W.
140	57	Fast crimson 6BL	W.
141	------	Fast crimson R	W.
142	289	Fast cyanine GB	W.
143	289	Fast cyanine 5R	W.
144	119	Fast light scarlet EG	W.
145	639	Fast light yellow 3G Ex Conc	W.
146	176	Fast red AN	W.
147	176	Fast red S Conc	W.
148	209	Fast wool blue B	W.
149	208	Fast wool blue R	W.
150	289	Fast wool cyanone R	W.
151	289	Fast wool cyanone 3R	W.
152	------	Fast wool violet 2R	W.
153	636	Fast wool yellow 3GL	W.
154	1180	Indigotine	W.
155	861	Induline B Ext	W.
156	79	Lake scarlet R	W.
157	------	Lanafuchsine B	W.
158	------	Light fast wool red BL Conc	W.
159	138	Metanil yellow 1955	W.
160	308	Naphthylamine black V	W.

W = wool.

TABLE 1.—*Dyes which showed no color change in either moisture-free and alkali-free solvent or in solvent containing 0.01 per cent caustic soda and 0.1 per cent water*—Continued

ACID COLORS—Continued

Serial No.	Colour Index No.	Name of dye tested	Fiber on which dyed
161	801	Quinoline yellow	W.
162	234	Resorcine brown R	W.
163	235	Resorcine brown RN	W.
164	------	Wool black B	W.
165	------	Wool black GRF	W.
166	------	Wool blue CG	W.
167	------	Wool green B	W.
168	737	Wool green S	W.
169	------	Wool navy B	W.
170	151	Wool orange A. Conc	W.
171	27	Wool orange 2G cryst	W.
172	184	Wool red 40F	W.
173	280	Wool scarlet BR	W.
174	------	Wool violet B	W.
175	698	Wool violet 4BN	W.
176	640	Wool yellow Ex Conc	W.

MORDANT AND ACID-MORDANT COLORS

177	------	Acid alizarine blue B	W.
178	------	Alizarine black powder	W.
179	1085	Alizarine blue-black 3B	W.
180	1035	Alizarine brown OR	W.
181	------	Alizarine brown 5R Ext	W.
182	1078	Alizarine cyanine green CG Ext	W.
183	------	Anthracene chrome brown 2BL	W.
184	------	Anthracene chrome brown RL	W.
185	1085	Anthraquinone blue black B	W.
186	180	Azo chrome blue B (chromed dyed)	W.
187	180	Azo chrome blue B (dyed acid)	W.
188	179	Azo rubine R (chrome dyed)	W.
189	179	Azo rubine R (dyed acid)	W.
190	179	Azo rubine Ex (dyed acid)	W.
191	------	Chromate brown R	W.
192	299	Chrome black F	W.
193	40	Chrome orange GG	W.
194	431	Chrome red A4B	W.
195	262	Cloth red B	W.
196	------	Cloth red R	W.
197	------	Fast chrome brown EB	W.
198	56	Fast fuchsine 6B	W.
199	29	Fast fuchsine G	W.
200	------	Fast fuchsine GR	W.
201	------	Hastings fast milling scarlet	W.

SULPHUR COLORS

202	------	Sulfogene dark brown GN Ex	C.
203	------	Sulfogene dark brown (a-t)	C.
204	948	Sulfogene yellow GA	C.
205	955	Sulfogene yellow CG	C.
206	955	Sulfogene yellow CG (a-t)	C.

W=wool. C=cotton.

TABLE 1.—*Dyes which showed no color change in either moisture-free and alkali-free solvent or in solvent containing 0.01 per cent caustic soda and 0.1 per cent water*—Continued

VAT COLORS

Serial No.	Colour Index No.	Name of dye tested	Fiber on which dyed
207	1102	Anthrene black B (double paste)	C.
208	1115	Anthrene blue GC (paste)	C.
209	1113	Anthrene blue GC (double paste)	C.
210	1114	Anthrene blue BCS (paste)	C.
211	.....	Anthrene blue RCX (paste)	C.
212	1106	Anthrene blue RS	C.
213	1109	Anthrene blue 3G	C.
214	1120	Anthrene brown BB	C.
215	.....	Anthrene brilliant blue R (paste)	C.
216	1099	Anthrene dark blue BO (paste)	C.
217	.....	Anthrene flavone GC (double paste)	C.
218	1096	Anthrene golden orange G (paste)	C.
219	.....	Anthrene golden orange RRT	C.
220	.....	Anthrene golden orange 4R	C.
221	1102	Anthrene green B (double paste)	C.
222	1101	Anthrene jade green	C.
223	1162	Anthrene red BN	C.
224	1161	Anthrene red violet RRN	C.
225	1163	Anthrene violet BNX (paste)	C.
226	1163	Anthrene violet RN (paste)	C.
227	1104	Anthrene violet 2R (paste)	C.
228	1118	Anthrene yellow G (paste)	C.
229	1102	Ponsol black B Conc (powder)	C.
230	1114	Ponsol blue BCS (powder)	C.
231	1113	Ponsol blue GD (double paste)	C.
232	1109	Ponsol blue 3G (paste)	C.
233	1106	Ponsol blue RS (paste)	C.
234	1106	Ponsol brilliant blue R (paste)	C.
235	1101	Ponsol brilliant green G	C.
236	.....	Ponsol brown AR (double paste)	C.
237	1099	Ponsol dark blue BR	C.
238	1096	Ponsol golden orange G (double paste)	C.
239	1097	Ponsol golden orange RRT (paste)	C.
240	.....	Ponsol golden orange 4R (paste)	C.
241	1102	Ponsol green BN (paste)	C.
242	.....	Ponsol pink B (double paste)	C.
243	1162	Ponsol red BN (double paste)	C.
244	1161	Ponsol red violet RRNX (paste)	C.
245	1104	Ponsol violet RR (double powder)	C.
246	.....	Ponsol yellow AR (double paste)	C.
247	1118	Ponsol yellow G (double paste)	C.
248	971	Sulfanthrene blue G (paste)	C.
249	971	Sulfanthrene blue GR (paste)	C.
250	.....	Sulfanthrene orange R (paste)	C.
251	.....	Sulfanthrene pink BG (paste)	C.
252	.....	Sulfanthrene pink FF	C.
253	.....	Sulfanthrene red 3B	C.
254	.....	Sulfanthrene scarlet 2B	C.
255	1222	Sulfanthrene violet B (double paste)	C.
256	.....	Thianthrene brilliant red 3B (paste)	C.
257	.....	Thianthrene orange R (paste)	C.
258	.....	Thianthrene pink FB (paste)	C.
259	.....	Thianthrene pink FF (paste)	C.

DEVELOPED COLORS

260	401	Diazo black BHSW	C.
261	401	Diazo black BHSW (DevTN)	C.
262	317	Diazo blue BR	C-S.
263	.....	Diazo blue 3G	C-S.
264	317	Diazo blue 2RL	C-S.
265	812	Primuline Ex Conc	C-R.
266	324A	Diazo scarlet A	C.
267	324A	Diazo scarlet R	C.

C=cotton. S=silk. R=rayon.

TABLE 1.—*Dyes which showed no color change in either moisture-free and alkali-free solvent or in solvent containing 0.01 per cent caustic soda and 0.1 per cent water*—Continued

ICE COLORS

Serial No.	Colour Index No.	Name of dye tested	Fiber on which dyed
268	69	Naphthanil AS red G base	C.
269	69	Naphthanil BS red G base	C.

C=Cotton.

In Table 2 are recorded those dyes which showed a slight color change only.

Columns 1, 2, and 3 are the same as in Table 1.

Columns 4 and 5 show the results obtained from the tests. A dash under a fiber heading denotes that that particular fiber was not dyed and consequently could not be tested.

TABLE 2.—*Dyes which showed only a slight color change*

DIRECT COLORS

Serial No.	Colour Index No.	Name of dye tested	Color change when treated with moisture-free and alkali-free solvent				Color change when treated with solvent containing 0.01 per cent caustic soda and 0.1 per cent water			
			C	S	WtdS	R	C	S	WtdS	R
270	415	Direct orange R	N	—	N	N	N	—	N	S
271	682	Direct yellow G	N	N	—	—	N	—	S	—
272	------	Erie catechine 3G	—	—	—	N	—	—	—	S
273	------	Erie catechine G Conc	—	—	—	N	—	—	—	S
274	487	Erie orange Y	—	—	—	N	—	—	—	S

SULPHUR COLORS

275	------	Sulfogene brilliant blue 2G Conc	N	—	—	S	—	—	—	—
276	------	Sulfogene brilliant blue 6BS	N	—	—	S	—	—	—	—
277	1006	Sulfogene brilliant green 2G	S	—	—	S	—	—	—	—
278	------	Sulfogene direct blue BRS	N	—	—	S	—	—	—	—
279	------	Sulfogene fast green B	N	—	—	S	—	—	—	—
280	------	Sulfogene fast green B (a-t)	S	—	—	S	—	—	—	—
281	940	Sulfogene golden brown G	N	—	—	S	—	—	—	—
282	940	Sulfogene golden brown G (a-t)	S	—	—	S	—	—	—	—
283	940	Sulfogene golden brown R	S	—	—	S	—	—	—	—
284	940	Sulfogene golden brown R (a-t)	S	—	—	S	—	—	—	—
285	------	Sulfogene indigo blue G Conc	N	—	—	S	—	—	—	—
286	------	Sulfogene navy blue GL Conc	N	—	—	S	—	—	—	—
287	------	Sulfogene navy blue RL Conc	N	—	—	S	—	—	—	—
288	------	Sulfogene ochre G	S	—	—	S	—	—	—	—
289	------	Sulfogene ochre G (a-t)	S	—	—	S	—	—	—	—
290	------	Sulfogene olive drab Y	S	—	—	S	—	—	—	—
291	948	Sulfogene yellow GA (a-t)	N	—	—	S	—	—	—	—

VAT COLORS

292	1133	Ponsol red AFF	N	—	—	S	—	—	—	—

N=no color change. S=slight color change.

TABLE 2.—*Dyes which showed only a slight color change*—Continued

DEVELOPED COLORS

Serial No.	Colour Index No.	Name of dye tested	Color change when treated with moisture-free and alkali-free solvent				Color change when treated with solvent containing 0.01 per cent caustic soda and 0.1 per cent water			
			C	S	WtdS	R	C	S	WtdS	R
293	401	Diazo black BH Ex Conc	N	N	—	N	N	S	—	N
294	.....	Diazo bordeaux 7B	N	N	—	—	S	N	—	—
295	.....	Diazo brown R	N	N	—	—	S	N	—	—
296	.....	Diazo green 2GL	N	N	—	—	S	N	—	—
297	.....	Diazo orange	N	N	—	—	S	N	—	—
298	.....	Diazo orange G	N	N	—	—	S	N	—	—
299	.....	Diazo red 5BL	N	N	—	—	S	N	—	—
300	.....	Diazo red 7BL	N	N	—	—	S	N	—	—
		ICE COLORS								
301	499	Naphthanil AS blue B base	N	—	—	—	S	—	—	—
302	82	Naphthanil AS garnet B base	N	—	—	—	S	—	—	—
303	82	Naphthanil BS garnet	N	—	—	—	S	—	—	—
304	38	Naphthanil AS orange R base	N	—	—	—	S	—	—	—
305	118	Naphthanil AS scarlet R base	N	—	—	—	S	—	—	—
306	118	Naphthanil BS scarlet	N	—	—	—	S	—	—	—

N=no color change. S=slight color change.

In Table 3 are listed those dyes which showed a decided color change. The letter "D" denotes a decided color change.

TABLE 3.—*Dyes which showed a decided color change*

DIRECT COLORS

Serial No.	Colour Index No.	Name of dye tested	Color change when treated with moisture-free and alkali-free solvent					Color change when treated with solvent containing 0.01 per cent caustic soda and 0.1 per cent water				
			C	W	S	WtdS	R	C	W	S	WtdS	R
307	.....	Amanil chrome brown GR	N	—	—	—	—	D	—	—	—	—
308	.....	Amanil chrome brown 2R	D	—	D	—	—	D	—	D	—	—
309	653	Amanil fast orange GLZ	N	—	N	—	—	D	—	D	—	—
310	.....	Amanil olive brown RL	N	—	N	—	—	D	—	D	—	—
311	502	Benzo axurine G Ex	N	—	—	N	N	S	—	—	N	D
312	596	Direct brown CR	S	—	N	N	N	D	—	N	N	S
313	608	Direct brown RG	D	—	—	N	N	D	—	—	N	D
314	598	Direct brown XR	D	—	N	N	N	D	—	N	N	D
315	.....	Direct fast black LR	N	—	N	N	N	N	—	N	N	D
316	561	Direct fast brown BT	D	—	—	N	N	D	—	—	N	D
317	.....	Direct fast orange RS	D	—	N	N	N	D	—	N	N	N
318	126	Direct fast pink E2GN	N	—	N	—	D	N	—	N	—	D
319	375	Direct garnet R	D	—	—	N	N	D	—	—	N	D
320	593	Direct green B	N	—	N	N	N	N	—	N	N	D
321	.....	Direct green 2GB Ex	D	—	N	—	N	D	—	N	—	S
322	589	Direct green 2Y	N	—	—	N	S	N	—	—	N	D
323	621	Direct orange 2R	N	—	N	—	N	N	—	D	—	N
324	621	Direct orange 2RG	D	—	N	—	—	D	—	D	—	—
325	225	Direct pink 2B	D	—	N	N	D	D	—	N	N	D

D=decided color changes. N=no color change. S=slight color change.

TABLE 3.—*Dyes which showed a decided color change*—Continued

DIRECT COLORS—Continued

Serial No.	Colour Index No.	Name of dye tested	Color change when treated with moisture-free and alkali-free solvent					Color change when treated with solvent containing 0.01 per cent caustic soda and 0.1 per cent water				
			C	W	S	WtdS	R	C	W	S	WtdS	R
326	596	Erie brown 3GN	—	—	—	—	N	—	—	—	—	D
326A	------	Erie catechine B	—	—	—	—	N	—	—	—	—	D
327	598	Erie fast brown GR	—	—	—	—	N	—	—	—	—	D
328	375	Erie garnet RB	—	—	—	—	N	—	—	—	—	D
329	593	Erie green MT	—	—	—	—	N	—	—	—	—	D
330	583	Erie green WT	—	—	—	—	N	—	—	—	—	D
331	------	Light fast brown R	D	—	N	—	N	D	—	D	—	D
332	------	Light fast brown 3YL	S	—	N	—	N	D	—	N	—	D
333	423	Light fast yellow 4GL	S	—	—	N	N	D	—	—	N	S
334	502	Niagara blue G Conc	—	—	—	—	N	—	—	—	—	D
335	------	Niagara blue NR	—	—	—	—	N	—	—	—	—	D
336	515	Niagara blue R	—	—	—	—	N	—	—	—	—	D
336A	------	Solantine red 8BLN	—	—	—	—	N	—	—	—	—	D

BASIC COLORS

337	655	Auramine O	N	—	—	—	—	D	—	—	—	—
338	332	Basic brown BR	D	—	—	—	—	D	—	—	—	—
339	21	Chrysoidine R	D	—	—	—	—	D	—	—	—	—
340	681	Crystal violet	N	—	N	—	—	D	—	D	—	—
341	680	Methyl violet NE	D	—	—	—	—	D	—	—	—	—
342	778	Phloxine B	—	N	N	—	—	—	N	D	—	—
343	749	Rhodamine B Ex	D	N	N	N	—	D	N	D	N	—
344	779	Rose bengal	—	N	N	—	—	—	D	D	—	—
345	841	Safranine T Ex	N	—	N	—	—	D	—	D	—	—
346	815	Thioflavine, T G Ex	—	N	N	N	D	—	N	D	N	D
347	729	Victorial blue BX	D	N	N	—	—	D	S	D	—	—
348	657	Victorial green	N	—	D	—	—	D	—	D	—	—

SULPHUR COLORS

349	1012	Sulfogene bordeaux BR	D	—	—	—	—	D	—	—	—	—
350	1012	Sulfogene bordeaux BR (a-t)	D	—	—	—	—	D	—	—	—	—
351	1012	Sulfogene bordeaux 5B	D	—	—	—	—	D	—	—	—	—
352	1012	Sulfogene bordeaux 5B (a-t)	D	—	—	—	—	D	—	—	—	—
353	------	Sulfogene brilliant green 4GX	S	—	—	—	—	D	—	—	—	—
354	988	Sulfogene carbon 2B Conc	N	—	—	—	—	D	—	—	—	—
355	978	Sulfogene carbon 8G Conc	N	—	—	—	—	D	—	—	—	—
356	------	Sulfogene carbon HXX	N	—	—	—	—	D	—	—	—	—
357	978	Sulfogene carbon M Conc	S	—	—	—	—	D	—	—	—	—
358	978	Sulfogene carbon supra	S	—	—	—	—	D	—	—	—	—
359	978	Sulfogene carbon R supra	S	—	—	—	—	D	—	—	—	—
360	------	Sulfogene cutch M Conc	S	—	—	—	—	D	—	—	—	—
361	------	Sulfogene cutch M Conc (a-t)	S	—	—	—	—	D	—	—	—	—
362	------	Sulfogene cutch O	S	—	—	—	—	D	—	—	—	—
363	------	Sulfogene cutch O (a-t)	S	—	—	—	—	D	—	—	—	—
364	1006	Sulfogene green 2B	N	—	—	—	—	D	—	—	—	—
365	1006	Sulfogene green 2B (a-t)	N	—	—	—	—	D	—	—	—	—
366	1006	Sulfogene green M Conc	N	—	—	—	—	D	—	—	—	—
367	------	Sulfogene olive G	N	—	—	—	—	D	—	—	—	—
368	------	Sulfogene olive G (a-t)	N	—	—	—	—	D	—	—	—	—
369	------	Sulfogene olive GN	N	—	—	—	—	D	—	—	—	—
370	------	Sulfogene olive GN (a-t)	N	—	—	—	—	D	—	—	—	—
371	------	Sulfogene olive drab Y (a-t)	S	—	—	—	—	D	—	—	—	—

D=decided color change. N=no color change. S=slight color change.

TABLE 3.—*Dyes which showed a decided color change*—Continued

DEVELOPED COLORS

Serial No.	Colour Index No.	Name of dye tested	Color change when treated with moisture-free and alkali-free solvent					Color change when treated with solvent containing 0.01 per cent caustic soda and 0.01 per cent water				
			C	W	S	WtdS	R	C	W	S	Wtds	R
372	552	Diazo black RS	N	—	N	—	N	N	—	N	—	D
373	------	Diazo brown 2G	N	—	N	—	—	D	—	N	—	—
374	------	Fast black V	N	—	N	—	N	S	—	S	—	D
375	------	Diazo orange 2R	N	—	N	—	—	S	—	D	—	—
376	------	Diazo scarlet 2BL	N	—	N	—	—	S	—	D	—	—
377	------	Diazo violet BL	N	—	N	—	—	N	—	D	—	—
378	654	Diazo yellow 2GL	N	—	N	—	—	D	—	N	—	—

ICE COLORS

379	499	Naphthanil BS-blue B base	N	—	—	—	—	D	—	—	—	—
380	38	Naphthanil orange R base	N	—	—	—	—	D	—	—	—	—
381	68	Naphthanil AS-scarlet G base	N	—	—	—	—	D	—	—	—	—
382	68	Naphthanil BS-scarlet	N	—	—	—	—	D	—	—	—	—

D=decided color change. N=no color change. S=slight color changes

VI. DISCUSSION OF RESULTS

The above results show that about 75 per cent of dyes of the direct class were unaffected by dry-cleaning solvents. No change was noted on dyeings made on weighted silks. Ninety per cent of the dyeings on silk, 72 per cent of the dyeings on rayon, 70 per cent of the dyeings on cotton showed no color change.

Dyeings on wool with acid, mordant, and acid-mordant colors were unaffected.

The basic colors offered poor resistance to dry cleaning. Samples Nos. 342, 343, and 346 on wool, and No. 343 on weighted silk, were unaffected. Sample No. 346, dyed on rayon and unweighted silk, was almost completely discharged. The majority of basic colors on cotton and silk stained other fabrics.

Practically all of the sulphur colors suffered an alteration in shade in both of the tests. The samples marked "(a–t)" were aftertreated with copper sulphate, sodium dichromate, and acetic acid. Dyeings made with the vat colors were unchanged. Several of these colors bled in the tests but did not stain white fabrics. This was particularly true of the red, pink, and red-violet colors. The bleeding of these colors is to be expected, since the majority of the dyes of this group are somewhat soluble in the solvent.

The ice and developed colors showed no change in shade in moisture-free solvent, but in the solvent containing alkali about 65 per cent of these dyeings suffered an alteration in shade. The majority of the

ice colors bled considerably in the tests but did not stain white materials.

In addition to the tests made above, other tests were conducted on the following dyed fabrics: Cellulose acetate rayon; weighted silk dyed with Setamine colors; mixed fabrics dyed with union colors; draperies, couch coverings, and cotton, linen, jute casement fabrics; silk velvet; and transparent velvets.

Of the 60 samples of cellulose acetate rayon tested, four samples showed a color change. One of the samples which was dyed a seasonal shade showed a slight color change in the solvent containing alkali. Two samples of printed material showed a decided color change in the solvent containing alkali. The fourth sample, a printed voile, showed a decided color change in both tests.

Weighted silk fabrics dyed with Setamine colors showed no color change in either test.

No change in shade was detected in testing 60 samples of union-dyed fabrics.

Of the 26 samples of draperies, couch coverings, and cotton, linen, and jute casement fabrics, three showed a decided color change in both tests. Two of these were cotton cretonnes and the other a cotton and rayon casement cloth.

A sample of silk velvet dyed with a basic color showed a decided color change in both tests. The color bled and tinted white silk, cotton, and rayon.

Six samples of transparent velvet showed no color change in either test.

Dyeings of acid colors on wool, sulphur colors on cotton, developed and vat colors, and direct colors on rayon were made in two strengths—the one a light shade, the other a dark shade. This was done in order to ascertain whether or not light dyeings behaved differently than deep shades. No difference in results was noted between dyeings made in two strengths.

VII. CONCLUSION

From the results obtained it is apparent that, although basic dyes offer poor resistance to dry cleaning, the majority of dyes which are most likely to be encountered in dry cleaning are unaffected by it. In order to minimize the danger of any change in color during dry cleaning, it is advisable to keep the solvent as free as practicable from moisture and alkali.

WASHINGTON, February 19, 1929.

NOTE ON A MERCURY SPARK GAP FOR INSTANTANEOUS PHOTOGRAPHY

By L. F. Curtiss

ABSTRACT

The improved form of high voltage mercury spark gap for instantaneous photography here described eliminates dangers from mercury poisoning. By including a bulb of cooler mercury vapor, through which the discharge does not pass, the shock caused by the sudden rise of pressure in the inclosing tube is partially absorbed. This greatly prolongs the life of the inclosing tube. It has been found that pyrex glass is quite suitable as a container.

The type of mercury spark gap used by C. T. R. Wilson [1] for photographing α-ray and β-ray tracks is a convenient source of illumination of great intensity for instantaneous photography. In the open form, as described by Wilson, it is not suitable for continuous use, particularly in a poorly ventilated room, since there is great danger of mercury vapor poisoning. Another annoying circumstance attendant on its use is the frequent shattering of the luminous portion of the tube containing the spark gap. This note gives a brief description of a design of the spark gap which eliminates both of these difficulties.

The spark gap in its usual form consists of a pyrex or quartz U-shaped open tube filled with mercury. The horizontal portion is of small cross section. It is operated by heating the mercury in the horizontal part until the hot mercury vapor separates the mercury into two columns. A condenser charged to 20,000 to 50,000 volts is then discharged through the hot mercury vapor, which is, of course, at a pressure slightly higher than atmospheric. The shattering of the tubes is a result of the sudden rise in pressure caused by the discharge, repeated shocks finally splitting the tube. The writer has tried both quartz and pyrex as containers, and as regards durability there is little to choose between them. Since the extreme ultraviolet is not utilized in ordinary photography and pyrex is much cheaper, it has been used in the spark gap to be described. Pyrex offers the further advantage that tungsten leads can be sealed into it easily to prevent the escape of the hot mercury vapor.

Figure 1 is a diagram of the spark gap filled with mercury before final sealing. It consists of a horizontal capillary C, of 0.5 to 3.0 mm diameter, terminating at one end in a bulb B, and at the other in the reservoir R, which carries a short, vertical stem. The spark gap is prepared by expelling all air by repeated boiling. The wire W_2 is then inserted, extending into the capillary, and sealed in, as shown

[1] C. T. R. Wilson, Proc. Roy. Soc., 87, p. 288; 1912.

in Figure 2. To operate, the mercury in B and C is heated by a coil H, of resistance wire wound throughout the horizontal length of the tube until the mercury has taken the position shown in Figure 2. The current through the coil is adjusted to maintain this position. The capillary and bulb B are now filled with hot mercury vapor which is held against a cushion of compressed air in the tube above

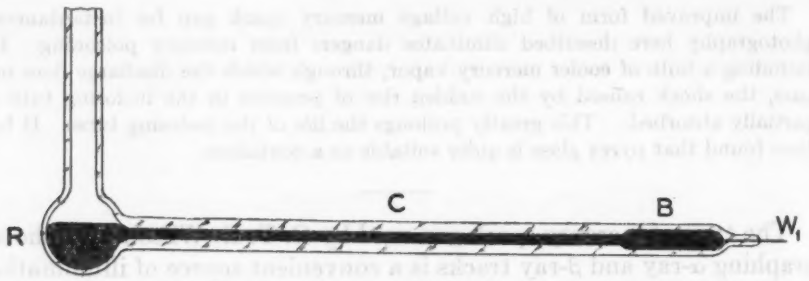

FIGURE 1.—*Showing spark gap filled with mercury before sealing*

the mercury reservoir R. When the condenser is discharged between the wires W_1 and W_2 the mercury vapor in C is heated suddenly while that in B remains at the same temperature as before, since the discharge does not pass through it. This cooler volume of mercury vapor serves to reduce the shock of the sudden rise in pressure in the capillary during the instant of flashing of the spark. It has been

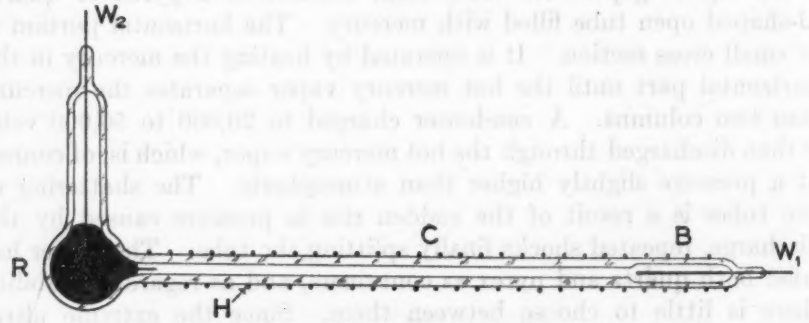

FIGURE 2.—*Spark gap after sealing, heated ready for operation*

found that under normal conditions this arrangement practically eliminates splitting of the capillary.

It should be noted in Figure 2 that the wire W_2 projects through the mercury into the capillary so that the discharge passes from one tungsten wire to the other. This arrangement is important for pyrex tubes. If the discharge is allowed to pass from the mercury in the reservoir to the wire W_1, a slight oscillation in the position of the mercury in the capillary is produced which repeatedly chills the pyrex until it cracks at the point where the reservoir is sealed to the capillary.

When it is desirable to use a spark gap of this kind as an instantaneous source of ultra-violet this design may also be made in quartz by using graded seals to pyrex and sealing the tungsten through the pyrex as before.

It may also be well to mention that if air is present with the hot mercury vapor in the luminous portion of the arc the glass or quartz soon discolors badly, cutting down the intensity considerably. This trouble may be avoided by carefully boiling the mercury when filling the tube so that all air is expelled from the capillary.

WASHINGTON, February 13, 1929.

RP82

IMPROVEMENTS IN THE PREPARATION OF ALDONIC ACIDS

By C. S. Hudson and H. S. Isbell

ABSTRACT

Nearly quantitative yields of aldonic acids are obtained by the use of a buffering salt of an organic acid, such as barium benzoate, during the oxidation of aldoses by bromine water. The buffer greatly increases the speed of the reaction by maintaining a relatively low hydrogen-ion concentration and permits the oxidation of disaccharides or other compound reducing aldoses without complications from hydrolysis. As examples, the preparation of calcium gluconate, the cadmium xylonate-cadmium bromide double salt, and calcium lactobionate are given.

CONTENTS

		Page
I.	Introduction	57
II.	Preparation of calcium gluconate	58
III.	Preparation of the cadmium xylonate-cadmium bromide double salt	59
IV.	Preparation of calcium lactobionate	59
V.	Hydrolysis of lactobionic acid to galactose and gluconic acid	60
VI.	Summary	61

I. INTRODUCTION

It is customary to prepare an aldonic acid by the oxidation of the corresponding aldose with bromine water. The reaction is a slow one because of the retarding influence of the hydrobromic acid that is produced during its course.[1] If the aldose is not a monosaccharide it may be partly hydrolyzed by the hydrobromic acid, with a resulting poor yield of the desired acid. Thus Fischer and Meyer's [2] oxidations of lactose and maltose to their respective aldobionic acids by bromine water gave yields of only about 30 per cent, and Kunz and Hudson [3] obtained similar yields in oxidizing neolactose. In these cases the isolation of the aldobionic acid was rendered difficult by the presence of gluconic and galactonic acids resulting from hydrolysis. Recently Goebel [4] has used the iodine oxidation in alkaline solution to produce

[1] Bunzel and Mathews, J. Am. Chem. Soc., 31, p. 464; 1909. Bunzel, J. Biol. Chem., 7, p. 157; 1910.
[2] Fischer and Meyer, Ber., 22, pp. 361, 1941; 1889.
[3] Kunz and Hudson, J. Am. Chem. Soc., 48, p. 2435; 1926.
[4] Goebel, J. Biol. Chem., 72, p. 801; 1927.

aldobionic acids in nearly quantitative yield. The method obviously avoids any hydrolysis by acids and should be very suitable in researches where small quantities of sugars are to be oxidized. In larger scale preparations,[5] however, the cost of the iodine and barium iodide becomes important, and for this reason we have sought to modify the plan of the bromine oxidation with the aim of making it a nearly quantitative reaction suitable for large-scale preparations. The modification which has brought success is a simple one, namely, the addition of a salt of a weak acid to the sugar solution. This acts as a buffer and keeps the hydrogen-ion concentration at a low acidity because the hydrobromic acid is neutralized by the salt and is replaced by the weak acid. The maintaining of the acidity of the solution at a low value results in the reduction of the acid hydrolysis of compound sugars to a negligible amount and in an important increase in the speed of the oxidation. The choice of a suitable buffering salt was made on the basis that its acid and basic constituents would not interfere with the isolation of the aldonic acid. The benzoates of barium and calcium have met these requirements very well. The details of the recommended procedure will be shown by the following examples of typical preparations.

II. PREPARATION OF CALCIUM GLUCONATE

Six milliliters of bromine (0.12 mole.) were added to an ice-cold solution of 18 g (0.1 mole.) of anhydrous glucose and 60 g (0.15 mole.) of barium benzoate in 750 ml of water. The bromine rapidly dissolved when the solution was shaken and crystals of benzoic acid soon formed. Although a faint, but definite, Fehling's test for reducing substances was obtained when light was not excluded a Fehling's test of the mixture after it had stood 36 hours at room temperature (20° to 25° C.) in darkness was negative, indicating the oxidation of all the sugar. The excess bromine was removed by a stream of air and the barium was precipitated quantitatively with sulphuric acid, about 60 ml of 5 N.H_2SO_4 being required. The barium sulphate was filtered off by suction, after the addition of about 10 g active carbon. The hydrobromic acid was removed quantitatively by the use of lead carbonate (27 g) followed by silver benzoate (5 g). A more rapid removal is obtained if silver carbonate (28 g) is used in place of lead carbonate. Soluble silver and lead salts were then removed as sulphides and the filtrate was concentrated to 200 ml under reduced pressure. The slight quantity of dissolved benzoic acid was largely removed by several extractions with chloroform. The resulting

[5] Stoll and Kussmal, U. S. Patent 1648368, Nov. 8, 1927, describe a method for the preparation of aldonic acids in good yields from the corresponding sugars by chlorine oxidation in the presence of a bromide or iodide. The method is excellent for the commercial preparation of the acids, but the conditions must be carefully controlled; consequently the method is not particularly desirable for general laboratory preparations.

aqueous solution of gluconic acid was colorless and did not reduce Fehling's solution. It was neutralized with calcium carbonate and concentrated to about 75 ml. The addition of 10 volumes of 95 per cent alcohol precipitated granular calcium gluconate, which weighed 21.5 g after drying at 80° C. The crude product was recrystallized by solution in 100 ml boiling water, addition of 2 g active carbon, filtration, concentration of the filtrate to 50 ml, and the addition of a small quantity of alcohol. After standing overnight in an ice box the crystals were separated, washed with 50 per cent alcohol, and dried. Yield, 20.2 g. The mother liquor yielded only 0.25 g. The total yield of the recrystallized product was thus 96 per cent of theory. The specific rotation of the calcium gluconate in about 3 per cent aqueous solution was $[\alpha]_D^{20} = +8.5$.

III. PREPARATION OF THE CADMIUM XYLONATE—CADMIUM BROMIDE DOUBLE SALT[6]

Six milliliters of bromine (0.12 mole.) were added to an ice-cold solution of 15 g *d*-xylose (0.1 mole.) and 60 g barium benzoate in 1,500 ml water, and the oxidation conducted in the dark at 20° to 25° C. The solution gave a negative Fehling test after 36 hours. The excess bromine and the barium were removed as described for the gluconate preparation, and the dissolved benzoic acid was extracted with chloroform. The solution was then boiled with 28.5 g cadmium carbonate to neutral reaction, filtered, and concentrated to a thin sirup under reduced pressure. Addition of a little alcohol and crystallization overnight in the ice box yielded 29.1 g of the double salt after washing with alcohol and drying at 80°. The mother liquor yielded 3.2 g of crystals and the total yield was 90 per cent of theory. The specific rotation of the double salt in 1.5 per cent aqueous solution was $[\alpha]_D^{20} = +8.8$. The only previous record seems to be that by C. A. Browne,[7] who found +7.4.

IV. PREPARATION OF CALCIUM LACTOBIONATE

Six milliliters of bromine (0.12 mole.) were added to an ice-cold solution of 36 g α-lactose monohydrate (0.1 mole.) and 60 g barium benzoate (0.15 mole.) in 1,500 ml water and the oxidation conducted in the dark at 20° to 25° C. The solution gave a negative Fehling test in from 36 to 48 hours. Free bromine and barium were removed as described for the gluconate preparation and the hydrobromic acid was removed by stirring the solution with lead carbonate (27 g), filtering off the lead bromide and removing the last traces of dissolved bromide

[6] Bertrand, Bull. Soc. Chim., 5, p. 554; 1891.
[7] C. A. Browne, Inaugural Dissertation, Gottingen, p. 21; 1901.

with silver benzoate (5 g).[8] The filtrate then showed no reaction with silver nitrate. Lead and silver were then removed as sulphides and benzoic acid was largely removed by several extractions with chloroform, finally blowing out the dissolved chloroform with air. The resulting solution contains no sugar by Fehling test, is colorless, and represents a nearly pure solution of lactobionic acid.

The substance may be further purified through its basic calcium salt. The addition of 37 g calcium hydroxide to the hot solution of lactobionic acid results in the slow formation of a fine white precipitate. After 18 hours standing at room temperature the precipitate was filtered off and washed three times with cold water saturated with calcium hydroxide. This precipitate was then suspended in 100 ml water, neutralized with carbon dioxide, and the bicarbonate decomposed by passing air through the warmed solution. The filtrate was concentrated to 50 ml on the water bath by a current of air transferred to a mortar and rubbed with 250 ml of 95 per cent alcohol. The precipitated gummy mass of neutral calcium lactobionate soon became granular on further rubbing. It was triturated successively with 50 ml portions of 80 per cent, 95 per cent, and absolute alcohol, collected on a filter and dried at 80° C. Yield, 34.5 g. The precipitation of lactobionic acid as its basic calcium salt by calcium hydroxide is not quite quantitative, and it was possible by concentrating the mother liquor and adding alcohol to obtain about 3 g more of an impure salt which reduced Fehling's solution slightly. Redissolving this in a little water and reprecipitating with alcohol purifies it. Three such purifications yielded 2.1 g which contained no sugars. The total yield of neutral calcium lactobionate was thus 36.6 g, or 95.7 per cent of theory. The result shows that the procedure of bromine oxidation can be applied to compound reducing aldoses in a way that avoids hydrolysis and gives nearly a quantitative yield of the corresponding compound aldonic acid or its salts.

V. HYDROLYSIS OF LACTOBIONIC ACID TO GALACTOSE AND GLUCONIC ACID

It will be recalled that Fischer and Meyer[9] first carried out this hydrolysis and by it proved that lactose is a galactosido-glucose rather than a glucoside-galactose. So far as we are aware, the preparation has never been repeated, though the beautiful reasoning from which the conclusion is deduced should appeal so strongly to students that the preparation might well be included in laboratory instruction. Doubtless the difficulties which Fischer records in preparing pure

[8] The hydrobromic acid may be more rapidly removed by using litharge in place of lead carbonate or by omitting lead entirely and using 28 g silver carbonate.

[9] See footnote 2, p 57.

lactobionic acid have deterred others from repeating the work. It is believed that the directions which are now supplied improve the method to such an extent that it may be used generally by students.

A solution of 9 g calcium lactobionate in 100 ml of 7.5 per cent sulphuric acid was heated three hours on the steam bath and then neutralized with calcium carbonate (8 g). The yellow solution was decolorized with carbon, filtered, and concentrated under reduced pressure to 30 ml. The gradual addition of 70 ml hot methyl alcohol precipitated most of the calcium gluconate as a heavy sirup, the galactose remaining in solution. The liquid was decanted and the sirup was extracted thrice with 50 ml hot methyl alcohol. The alcoholic solutions were combined, purified with 1 g of active carbon, filtered and evaporated to a sirup on a hot plate by a current of air. Galactose crystallized from this sirup on standing overnight. It may be preferable to start crystallization by nucleation. The crystals were washed with 50 per cent cold alcohol and dried at 65° C. Yield, 2.5 g. The mother liquor was concentrated to a sirup which was dissolved in 50 ml hot methyl alcohol. A small quantity of insoluble material was filtered off and added to the calcium gluconate fraction. The alcoholic solution was concentrated as before and from it was obtained, after nucleation, 0.95 g crystalline galactose. The total yield of galactose was 3.45 g, or 80 per cent of theory. After one recrystallization from 10 ml of hot water the sugar showed m. p. 165° and $[\alpha]_D^{20} = 79.7$ in aqueous solution.

The amorphous calcium gluconate was dissolved in 15 ml hot water and crystallized from the cooled solution by the addition of alcohol just short of cloudiness (about 5 ml) and scratching the container. After standing overnight in an ice box the crystals were filtered off, washed with a little cold water, and dried at 65°. Yield, 4.8 g. The mother liquor yielded only 0.1 g crystals. Total yield, about 95 per cent of theory. After one recrystallization and drying at 65° the salt showed $[\alpha]_D^{20} = +8.2$ in aqueous solution.

VI. SUMMARY

It is found that the use of a buffering salt of an organic acid such as barium or calcium benzoate, during the oxidation of aldoses by bromine water greatly increases the speed of the reaction, due to the maintaining of a relatively low hydrogen-ion concentration, and permits the oxidation of compound reducing aldoses, such as lactose, without complications from hydrolysis. The reaction mixture should be kept in the dark for best results. The yields of aldonic acid are nearly quantitative. In the case of lactose it is possible to oxidize it to nearly pure lactobionic acid which can then be hydrolyzed to galactose and gluconic acid, both of which can be obtained in high

yield. It is believed that the new directions make the method of bromine oxidation of aldoses much more precise and suitable for a wide range of preparations. Examples of the oxidation of glucose, xylose, and lactose are given. It is suggested that the improved directions may be found suitable for laboratory instruction in sugar chemistry as well as for research.

WASHINGTON, March 5, 1929.

NOTE ON THE RATIO OF THE ELECTROMAGNETIC TO THE ELECTROSTATIC UNIT OF ELECTRICITY AS COMPARED TO THE VELOCITY OF LIGHT

By Harvey L. Curtis

ABSTRACT

The value of the ratio of the electrical units has been revised to meet the new values of the absolute determination of the ohm. This revised value is compared with the latest value of the velocity of light.

In 1907, Rosa and Dorsey,[1] of the Bureau of Standards, published an article entitled "A New Determination of the Ratio of the Electromagnetic to the Electrostatic Unit of Electricity." Since that date no other determination of this ratio has been made, but there have been new determinations of the international ohm in terms of which Rosa and Dorsey expressed their result, and new determinations of the velocity of light to which they compared their result. This note is to discuss these new determinations.

In 1916 Rosa and Dorsey prepared an addendum which was to appear in later editions of their paper. However, as no such edition has been published, the addendum is given below:

ADDENDUM

In 1913 an absolute measurement of the international ohm was made by F. E. Smith at the National Physical Laboratory, London. Mr. Smith found that the international ohm is equal to 1.00052 ± 0.00004 absolute ohms (Phil. Mag., 214 A, p. 106). Consequently a value of v experimentally determined in terms of the international ohm and other units will be 2.6 ± 0.2 parts in 10,000 less than its value in terms of the absolute ohm, all else being as before. It is gratifying to note that this correction is substantially equal to the unexplained discrepancy (3 in 10,000) between the velocity of light and the value of v given in this paper. In 1907 (see above) we suggested that this discrepancy might be due to a difference between the values of the international and of the absolute ohm.

On applying this correction the value of v reduced to vacuo (p. 601) and in terms of the absolute ohm becomes

$$v_o = 2.9979 \times 10^{10} \left[\frac{\text{cm Abs } \Omega}{\text{sec.}}\right]^{\frac{1}{2}}$$

The velocity of light in vacuo (p. 603) is

$$v = 2.9986 \times 10^{10} \frac{\text{cm}}{\text{sec.}}$$

[1] Bul. Bureau of Standards, 3, p. 433; 1907.

Each of these values is subject to an estimated uncertainty [2] of 1 part in 10,000; the two values, therefore, may be considered as agreeing within the limits of experimental error.

THE AUTHORS.

NOVEMBER 21, 1916.

Since the above addendum was prepared, Grueneisen and Giebe [3] have published another determination of the ohm which differs from that of F. E. Smith by only 1 part in 100,000, and hence would not change the above result. Unpublished results obtained at this bureau show that Smith's result is not in error by as much as 1 part in 10,000, hence the best value to date of the ratio of the electromagnetic to the electrostatic unit of electricity is

$$299{,}790 \text{ km/sec.}$$

No improvement in this value can be expected until an entirely new determination is made.

The velocity of light has recently been determined by Michelson.[4] The value which he obtained for the velocity in vacuum is

$$299{,}796 \pm 4 \text{ km/sec.}$$

A preliminary determination by Karolus and Mittelstaedt [5] gave the value

$$299{,}778 \pm 20 \text{ km/sec.}$$

This agrees with Michelson's value within the limit of error.

The above results show that, within the limits of present measurements, the ratio of the electrical units agrees with the velocity of light. This is an important confirmation of Maxwell's electromagnetic theory of light.

WASHINGTON, March 19, 1929.

---

[2] Note that this is estimated uncertainty and not probable error. The authors did not compute the probable error of their result, but an inspection shows that it is considerably less than 1 in 10,000. No statement is made of the reasoning used in arriving at this estimated uncertainty of their result. However, for the velocity of light, the estimated uncertainty which they give agrees with the probable error as computed by Weinberg. (H. L. C.)

[3] Grueneisen and Giebe, Ber. Phys. Tech. Reich., **5**, p. 5; 1921. Also Ann. d. Phys., **368**, p. 179; 1920.

[4] Michelson, Astrophys. J., **65**, p. 1; 1927.

[5] Karolus and Mittelstaedt, Phys. Zeit., **29**, p. 698; 1928.

BUNSEN FLAMES OF UNUSUAL STRUCTURE

By Francis A. Smith and S. F. Pickering

ABSTRACT

A mixture of air or oxygen with a combustible gas is forced through a cylindrical burner tube, and the flame is observed as it burns in secondary air.

Complex structures observed in acetylene-air flames include the intersection of two zones, four distinct zones of light, and a hollow dark core extending upward from the tip of the primary zone.

When secondary air is excluded, the primary zones of some hydrocarbon-air flames become polyhedral. Flames having 3, 4, 5, 6, and 7 sides have been observed, which will rotate under some conditions and remain stationary under others. The number of sides is a function of the size of the burner tube and of the composition of the gas mixture.

Burning in secondary air under some conditions, the primary zone of a propane-oxygen flame becomes polyhedral, and yellow streamers rise from the tip and corners of the figure, which can be made to rotate slowly, or rapidly, or to remain stationary, by slight changes of the composition and velocity of the mixture of gas and oxygen supplied to the burner.

Accurate and reproducible control of the composition and rate of flow of the gas mixtures and very steady streamline flow in the burner tubes have been attained.

Twenty photographs of the above flames are presented and discussed.

CONTENTS

	Page
I. Introduction	65
II. Description of the flames	67
1. Polyhedral primary zone	67
2. Acetylene-air flame	68
3. Some interesting propane-oxygen flames	70
III. Discussion	71
1. Variables which affect the polyhedral primary zone	71
2. A possible cause of rotation of the polyhedral figure	73
3. Points of similarity and of contrast between the flames	73

I. INTRODUCTION

Certain phases of the physics and chemistry of flames are being studied for quite different purposes in more than one laboratory at the Bureau of Standards. The work of the present authors has for its primary object the improvement of combustion in gas burners.

In order to determine the conditions governing flash back and blow-off in burners, and to obtain a better understanding of the mechanism of flame propagation and of the relative importance of

the many factors involved, measurements of the flame velocities in a number of gas mixtures have been made.

The method employed was essentially that described by Bunsen,[1] Gouy,[2] Michelson,[3] Hofsäss,[4] Mache,[5] and others, modified in certain respects by F. W. Stevens,[6] and also by the authors.[7]

In the present connection it will be sufficient to say that accurate and reproducible control of the velocity and composition of the gas mixtures was attained by means of needle valves and flow meters, one set of which controlled the gas supply, and the other set the supply of primary air or oxygen. The homogeneous mixture flowed out through a vertical burner tube, the inner surface of which was made as smooth and as nearly cylindrical as possible, and burned in the presence of the surrounding secondary air. The flame which usually results is the ordinary Bunsen flame which has been described essentially as follows:

A Bunsen flame has three chemically distinct parts. The inner cone is a very thin greenish blue zone where the oxygen of the air supplied to the burner is consumed and the combustible components of the fuel gas are oxidized to a mixture of CO, CO_2, H_2, and H_2O. Combustion is completed to CO_2 and H_2O by outside air in a thin reaction zone surrounding the flame, and called the outer cone. The space between the two cones (called the water-gas space) is practically free from chemical processes.

In the course of this work several phenomena of a rather unusual nature have been encountered. Many of them have not been previously reported, and are sufficiently interesting to justify publication on their own account, even though their causes have not yet been determined.

It has been found necessary to alter the significance of some of the terms used to describe some parts of the flame, and in some cases to substitute a different term for one frequently used to avoid ambiguity when discussing the flames to be described. For instance, the word "zone" is substituted for "cone" because none of the zones is really a true cone, especially when the base is a regular polygon. The term "primary zone" refers to that part of a flame usually called the "inner cone" and is used because it is the seat of the initial or primary combustion, and because it is no longer necessarily the only inner zone. The term "mantle" designates the part or parts of a flame which are outside the primary zone. The term "envelope" is

[1] Bunsen, Pogg. Ann., **131**, p. 161; 1866.
[2] Gouy, Ann. Chim. Phys. (5), **18**, p. 27; 1879.
[3] Michelson, Ann. Phys. (3), **37**, p. 1; 1889.
[4] Hofsäss, Chem. Ztg., **39**, p. 64; 1915.
[5] Mache, Die Physik der Verbrennungserscheinungen, Leipzig; 1918.
[6] F. W. Stevens, National Advisory Committee on Aeronautics, Rept. No. 305; 1929.
[7] Investigation still in progress.

substituted for the terms "outer cone" or "mantle" as commonly used and designates that very thin outer portion of the mantle in which combustion is completed by means of outside or secondary air.

II. DESCRIPTION OF THE FLAMES

1. POLYHEDRAL PRIMARY ZONE

At one stage of the work on measurements of flame velocity it became necessary to determine whether or not the primary zone was affected in any way by the zone of secondary combustion which ordinarily surrounds it. A Smithells' flame separator [8] was, therefore, used to exclude secondary air. Under the conditions of the original experiment, using propane and air, when secondary air is excluded the primary zone or combustion surface presents the appearance shown in Figure 1.

In form it is very much like a tent supported by five ropes loosely draped from a center pole to pegs located at the corners of a regular pentagon. It is perfectly stable and reproducible. The phenomenon appeared so interesting that some other gas mixtures and burners of several sizes were tried in an effort to determine its cause. Several combinations were found which gave polyhedral flames of the same general character as those photographed. The length of a side at the base seems to be a characteristic of the gas mixture used. In the case of propane and air it averages about 6 mm, and by using larger or smaller burners figures having a larger or smaller number of sides are obtained. In this way, flames having 3, 4, 5, 6, and 7 sides have been observed. If the circumference of the burner is about the mean of the dimensions which give stable four-sided or five-sided figures, either may be obtained on the same burner by varying the composition of the mixture slightly. The figure can be made to rotate rapidly or slowly, or to remain stationary, by changing very slightly the composition and velocity of the gas mixture.

For example, in the case of a burner tube made of glass and having a diameter of 7.3 mm, a mixture containing 5.06 per cent of propane in air produced the usual circular "cone." An increase in the proportion of propane caused the figure to change to a rounded, steady, four-sided figure which became sharper, then somewhat unsteady, then changed to an unsteady five-sided figure, and finally broke into rapid rotation, at which time the mixture contained 5.47 per cent of propane, an increase of only 0.41 per cent.

This polyhedral primary zone, while unusual, is not new. Smithells and Ingle [9] briefly described a flame which must have been very similar to this one.

---

[8] Smithells and Ingle, J. Chem. Soc., **61,** p. 207; 1892. A glass tube of larger diameter than the burner tube is attached air-tight to the latter a little below the tip. It extends upward above the tip of the burner tube and completely excludes outside air from the primary zone. The gases from the primary zone then burn at the tip of the larger tube.

[9] See footnote 8.

2. ACETYLENE-AIR FLAME

When work was begun with acetylene-air mixtures, with the flame burning in secondary air in the usual manner, it was immediately evident that the structure of some acetylene flames is much more complex than that of Bunsen flames is ordinarily supposed to be.

The following figures show some of this structure in successive stages of development as the proportion of acetylene is increased:

Figure 2 shows the primary zone with very little mantle. The mixture (5.1 per cent C_2H_2) is almost as lean as it can be without the flame blowing off. This mixture contains 56 per cent more primary air than that required for the complete combustion of the acetylene. The excess of air either furnishes a sufficient concentration of oxygen to enable the reactions to go to completion in the primary zone, or by diluting with nitrogen so reduces the temperature of the gases leaving the primary combustion zone that no further reaction is apparent.

Figure 3 (11.7 per cent C_2H_2) shows much more mantle. This mantle is not a hollow shell as is usually the case, but extends inward all the way to the primary zone.

While a consideration of the greater depth through which the center of the flame is viewed, as compared with the edges, shows that the region near the outer boundary produces much more light than that toward the center, it is obvious that in this flame the emission of light is not confined to the envelope. Furthermore, flames having fairly large mantles result from mixtures approaching that used to obtain Figure 2, and in these flames the intensity of the light appears to the eye actually to increase from the boundary toward the center. In view of this fact, it seemed probable that the exclusion of secondary air by means of a Smithells' flame separator would not result in removing this mantle from about the primary zone. The experiment was tried and no difference in the appearance of the flame could be detected as a result of the exclusion of secondary air from the flame last described.

These facts indicate that some reaction is in progress, after the gases have passed the primary zone, which does not depend upon the presence of secondary air. The sharp outer boundary of the primary zone indicates that the reactions in the two regions are not of the same character, otherwise the primary zone would blend gradually into the region above.

Figure 4 shows the mantle with its usual hollow appearance (more clearly shown in fig. 5) only partly developed. This mixture (13.2 per cent C_2H_2) contains as primary air 55 per cent of the air required for the complete combustion of the acetylene and the remainder must come from the secondary air which surrounds the flame. Most of the light from this mantle comes from its envelope.

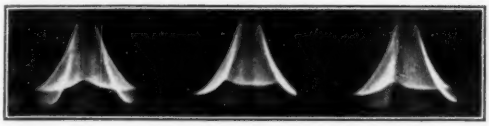

FIGURE 1

Pentahedral propane-air flames

FIGURE 2

FIGURE 3

FIGURE 4

Acetylene-air flames

UNIV. OF MICH.

FIGURE 5

FIGURE 6

FIGURE 7

FIGURE 8

Acetylene-air flames

FIGURE 9

FIGURE 10

FIGURE 11

Acetylene-air flames

UNIV. OF MICH.

Figure 5 (15.6 per cent C_2H_2) shows a second inner zone which emits light containing more yellow than that from the pale blue-green primary zone. This zone is shaped like a thimble and has no sharply defined boundary except near its base which extends to a somewhat lower level than the base of the primary zone and is considerably larger in diameter than the latter. The base of the primary zone is itself much larger in diameter than the tip of the burner tube and begins some distance above it.

In Figure 6 (16.3 per cent C_2H_2) the upper portion of the second zone is much larger, its base remaining about the same. A third inner zone has appeared, the base of which is located on the surface of the primary zone at or slightly above its base. It extends outward and upward until it crosses the boundary of the second inner zone, and that portion of it which is inside zone 2 begins to show the yellow color characteristic of flames commonly called "luminous." This color makes the outer boundary of zone 2 much more distinct. That portion of zone 3 which is outside of zone 2 is as yet scarcely visible.

In Figure 7 (16.6 per cent C_2H_2) the yellow third zone is entirely distinct. Starting at the base of the primary zone it occupies most of the second zone, intersects it, and extends outside it. The primary zone and the second and third inner zones are each surrounded by a thin space which appears dark. These dark spaces join at their tips in a continuous dark streak which extends from the tip of the primary zone upward through the center of the flame. Viewed from above, as shown in Figure 8, the streak is obviously a hollow, dark central core, and the spaces appear as rings of darkness surrounding and separating the zones of light.

In Figure 9 (17.7 per cent C_2H_2) the brilliance of the second and third inner zones has increased and the line of separation between them is no longer visible except at the base where that portion of zone 2 not occupied by zone 3 is still green. The dark core is still perceptible near the tip and the dark space separating zone 3 from the blue envelope is still clearly visible.

Zones 2 and 3 in Figure 10 (24.0 per cent C_2H_2) have increased in size and brilliance until they occupy nearly the entire volume of the flame. Although it is invisible until the eye has been shielded from the brilliance of the central portion of the flame a continuous blue envelope may then be seen which incloses the rest of the flame completely.

Figure 11 (44.8 per cent C_2H_2) shows the brilliance of all parts of the flame greatly reduced for lack of primary air. That which was the primary zone now appears merely as a brighter region in the yellow portion of the flame. The boundary of the yellow portion of this flame is exceedingly sharp. Above the primary zone at least it is a very thin and brilliant sheath, the edge of which appears on the

photograph as a sharply drawn white line shading toward the center. Just outside this line is a thin dark space which distinctly separates the yellow zone from the thin blue envelope which now can be seen plainly at the sides. This blue envelope no longer incloses the tip of the flame and unburned carbon is escaping freely at the top.

3. SOME INTERESTING PROPANE-OXYGEN FLAMES

Figures 12 to 17 show some of the flame structures which occur with mixtures of propane and oxygen as the proportion of oxygen is increased. These flames have a brilliant yellow stream rising from the tip of the primary zone instead of the hollow dark core of the acetylene flames.

In some of the photographs, such as Figures 12, 14, 16, 18, and 19, a departure was made from usual photographic practice in order to show structure which would otherwise have been obscured on account of the great differences in the intensity of the light from different parts of the flame. In these cases the plate was reversed so that the light passed through the glass before striking the emulsion, permitting the "denser" portions of the negative (in which the silver was reduced in the emulsion through its entire thickness to the outer surface) to be bleached considerably without affecting the "thinner" portions of the negative appreciably.[10]

Figure 12 shows a flame which results from a primary mixture containing 33.7 per cent propane in oxygen. It has a fairly well-defined primary zone surrounded by a diffuse yellow zone and the brilliant stream rising from the tip. The entire flame is surrounded by a blue envelope.

In Figure 13 (33.4 per cent C_3H_8) the "cone" has become a four-sided figure, and the diffuse yellow zone has separated and concentrated into four streams which rise along the dark ridges of the blue-green primary zone. This view, facing one side of the primary figure, shows the dark ridges from which little or no light is coming, the figure consisting of four apparently disconnected sides. The envelope, which is invisible because of the relatively small intensity of its light, is shown clearly in Figure 14, which is a photograph of the same flame taken with the plate reversed.

Figure 15 is a diagonal view of the same flame, in which faint yellow zones resembling zones 2 and 3 of the acetylene flame are visible. The envelope, which is almost invisible, is shown clearly in Figure 16, which, however, does not show the zones just referred to very distinctly.

---

[10] The authors are indebted to W. S. Rice, of the photographic section of this bureau, who made the photographs reproduced in this paper as well as an excellent set of autochrome photographs of the same flames.

FIGURE 12

FIGURE 13

FIGURE 14

FIGURE 15

FIGURE 16

Propane-oxygen flames

UNIV. OF MICH.

FIGURE 18

FIGURE 17

FIGURE 20

FIGURE 19

Propane-oxygen flames

Figure 17 (33.0 per cent C_3H_8) shows the four-sided figure changed into one having five sides. The yellow streams are smaller and rise from the corners of the base instead of all along the ridges. This view shows the yellow streams and the primary figure with reasonable clarity, but the envelope is very indistinct. Figure 18 shows the various parts of the flame in their proper relative proportions, but the details are less distinct.

Figure 19 is a view of the same flame from above. The line of vision departs slightly from the vertical allowing two of the dark ridges of the primary zone to be seen at one side of the brilliant yellow stream which rises from the tip. The primary zone and the yellow streams are enveloped in a region of darkness which in turn is surrounded by the usual blue envelope.

A little more oxygen causes the figure to begin rotating slowly and still more causes very rapid rotation, shown in Figure 20 (32.2 per cent C_3H_8), with the yellow streams, which are now much smaller, forming an apparently continuous ring at the base and extending upward like the sides of a cup.

III. DISCUSSION

1. VARIABLES WHICH AFFECT THE POLYHEDRAL PRIMARY ZONE

There are several factors which affect the formation or behavior of the polyhedral primary zone, but apparently changes in such variables as the length and material of the burner tube, length and diameter of the separator tube which excludes secondary air, and the position of the burner and separator tube assembly have little or no effect. In the case of the latter variable the assembly was connected flexibly to the supply of primary mixture, and gradually inverted with no apparent effect upon the flame.

On the other hand, such variables as the velocity of the primary mixture through the burner tube, the diameter and shape of the tip of the burner tube, the composition of the primary mixture, the identity of the combustible gas, and the presence or absence of nitrogen in the primary mixture, affect the polyhedral figure in various ways.

Of these variables, the last three affect the velocity of propagation of the flame, and this in relation to the first two, determines in a general way the size and shape of the primary zone.

One may consider the primary zone as the resultant of two opposing tendencies. In the normal operation of a burner the velocity of the primary mixture prevents the flame from entering the burner tube and "flashing back," and at the same time the velocity of propagation of the flame enables the latter to maintain its continuity and position at the tip of the burner against the tendency of the primary mixture to "blow it off."

Ordinarily the resulting figure approximates a right circular cone whose dimensions depend upon the relative values of the flame velocity, mixture velocity, and burner diameter.

The polyhedral figures presented in this paper and their observed behavior would seem to indicate that there are limiting values of the ratio of flame velocity to mixture velocity, and of each of those two variables, between which a figure with a circular section is less stable than one having concave sides separated by ridges spaced symmetrically around the circumference.

The distance between ridges measured along a side at the base varies with either the mixture velocity, flame velocity (or one or more of the factors which affect flame velocity), or with some combination of these variables.

The statement, previously made, that the length of a side is a characteristic of the gas mixture, is based upon the following facts. A small change in the composition of a mixture of propane and air, or of propane and oxygen suffices to change the number of sides of the figure from four to five or vice versa. The length of a side with propane-air mixtures is about 6.0 mm, with propane-oxygen mixtures it is from 2.4 to 3.0 mm, and with pentane-air mixtures it is about 3.6 mm.

If all the variables except the size of the burner tube are kept constant, the length of a side of the primary figure remains nearly constant while a smaller circumference results in a smaller number of sides, and vice versa.

Rotation of the polyhedral figure about its vertical axis is influenced by changes in either the composition or velocity of the mixture, or both. Rotation of the figure resulting from propane-air mixtures may be produced by changing the composition of the mixture toward the rich side, irrespective of whether a simultaneous change in the mixture velocity is an increase or a decrease. On the other hand, the direction of rotation of the five-sided figure obtained with propane-oxygen mixtures could be reversed by changing the velocity of the mixture, the composition remaining substantially constant. It was by this means that it was finally possible to maintain the figure stationary during the several minutes necessary for the exposure of autochrome plates.

Earlier in this paper a description has been given of a series of changes in the form of the primary figure (from a "cone" through a four-sided and a five-sided stage to a figure in rapid rotation), resulting from propane-*air* mixtures, which accompanied increases in the proportion of propane in the mixture. These increases in propane content were brought about by *decreasing* the air, with consequent *decreases* in the velocity of the mixture.

The same changes in form may be produced in the same order with propane-*oxygen* mixtures burning on a burner of appropriate size, but contrary to expectation the changes are accomplished by *increases* in the oxygen content, with consequent *increases* in the velocity of the mixture.

2. A POSSIBLE CAUSE OF ROTATION OF THE POLYHEDRAL FIGURE [11]

Little or nothing is known about the rotation of the polyhedral figure, but it is suspected that its cause may be traced to instability in the relation between the length of a side and the circumference of the burner tip.

On a given burner, the primary figure may have four sides with a given mixture composition and velocity. With some other composition and velocity the number of sides may change to five. This change in the number of sides must be the result of a decreased length of side, since the circumference of the burner tip is unchanged. With any intermediate condition the circumference divided by the length of a side is not a whole number, and the tendency toward symmetry in the polyhedral figure results in either a tendency for a ridge to flatten out and to stretch an inadequate number of sides over the whole circumference, or a tendency for a ridge to intrude itself into a side and distribute a larger number of sides over an inadequate circumference.

In either case the other ridges are displaced somewhat from their former positions, the figure reverts to the more stable of the two forms, and the process is rapidly repeated. If displacement of the ridges always occurs in the same direction, continuous rotation results in one direction or the other. If the displacement is not always in the same direction the rotation may be in either direction in a very haphazard manner, resulting in what has been described as an unsteady figure.

It must be borne in mind that if symmetrical polyhedral figures and figures which will rotate smoothly are to be obtained the burner tip must be circular and free from irregularities.

3. POINTS OF SIMILARITY AND OF CONTRAST BETWEEN THE FLAMES

There are some interesting and possibly significant points of general similarity and of difference to be noted between the various flames which have been described in this paper.

With propane-air mixtures the polyhedral primary figure can be obtained either with or without the exclusion of secondary air.

[11] This rotation about a vertical axis is a rotation of the figure only, and does not involve any rotation of the gas stream.

The hollow dark central core seems to be peculiar to acetylene, since it appears with acetylene-oxygen mixtures as well as with those of acetylene and air. In contrast with this, all oxygen-deficient flames of other hydrocarbons so far observed have shown the yellow stream of greater or less intensity rising from the tip of the primary figure, as in the case of the propane-oxygen flames.

The significance of the details of structure in these flames with respect to the various intermediate reactions taking place during combustion can be discussed intelligently only after the composition of the gases in the various parts of the flames has been determined.

WASHINGTON, February 6, 1929.

A STUDY OF SHEATHING PAPERS

By F. T. Carson and F. V. Worthington

ABSTRACT

In order to obtain data which might be used in the formulation of standard specifications for sheathing paper a study was made of some of the important properties of 36 samples of building papers made by 14 different manufacturers. These samples consisted of asphalt-saturated, paraffin-saturated, laminated and asphalt-treated, and machine-finished papers. The papers were tested for weight, thickness, tensile breaking strength, bursting strength, tearing resistance, water resistance, and air permeability.

The papers differ considerably in weight and thickness and also in density. Only in the case of papers of like structure does there appear to be any definite relation between weight and thickness or between either of these and other properties. A fair degree of parallelism exists between the tensile breaking strength and the bursting strength. In each of these two properties there were found differences amounting to about fourfold between extremes. Some of the strongest papers are among the thinner ones, and some of the heavier papers are comparatively weak. The papers differ greatly in strength retention after wetting. The time required for water to penetrate through the sheet differs between wide limits, from less than a minute to several days. In the rate of flow of air through the papers there are relatively large differences, although most of the papers are fairly resistant to air, a few being air-tight within the ability of the testing method to detect permeability.

It is concluded from the test data and supplementary information about sheathing paper that the thickness of building papers is relatively unimportant; that strength is of significance chiefly in handling the paper during erection; that water resistance and impermeability to air are of prime importance in making a wall weatherproof; but that most commercial sheathing papers are capable of performing this function sufficiently well.

CONTENTS

	Page
I. Introduction	76
II. Description of samples	76
1. Means of procuring samples	76
2. Group A, asphalt-saturated papers	77
3. Group P, paraffin-saturated papers	77
4. Group L, laminated papers of heterogeneous structure	77
5. Group M, machine-finished papers	78
III. Laboratory tests made and methods employed	81
1. Properties considered important	81
2. Testing methods used	81
(*a*) Official methods	81
(*b*) Water resistance	81
(*c*) Air permeability	82

Page
IV. Experimental results 83
1. Weight and thickness 83
2. Strength 84
3. Water resistance 84
4. Air permeability 85
V. Relation of laboratory tests to service demands 86
1. Uses made of sheathing paper 86
2. Cost of sheathing paper 86
3. Some probable relations between properties and service demands 86
(*a*) Thickness 86
(*b*) Strength 87
(*c*) Water resistance 87
(*d*) Air permeability 87
(*e*) Character of surface 88
(*f*) Permanence 88
VI. Summary 89

I. INTRODUCTION

Sheathing paper, although it is a relatively insignificant cost item in building construction, has some very important functions to perform in helping to make a weatherproof wall. In addition to its use in wall construction, the material has other uses, chiefly of a protective nature, which are very important. The wise choice of a building paper suited to a given purpose would obviously be greatly facilitated by a knowledge of the more important properties possessed by such materials and by the correlation of these properties with service demands. Practically no information of a definite character is available with reference to the properties of the many kinds of sheathing papers on the market.

In order to obtain some definite data which might be used in the formulation of standard specifications for sheathing paper, the National Bureau of Standards has made a study of some of the more important physical and mechanical properties of as representative a lot of samples as could be obtained. This work was done at the request of the National Lumber Manufacturers' Association, which desired the information to use as a part of its service to members. This association contemplates conducting field experiments to correlate the laboratory data with service results, which is a necessary sequel to the investigation reported in this publication.

II. DESCRIPTION OF SAMPLES

1. MEANS OF PROCURING SAMPLES

A preliminary survey was made of the products being used as building papers, and laboratory tests were made on a number of representative samples. A preliminary report was then prepared

and sent out with a form letter to 34 concerns scattered over the United States, inviting them to cooperate and to submit samples, together with such information as might be useful in formulating specifications. Compliance was made by 14 concerns, as a result of which 36 samples, consisting of 4 distinct groups and many types and weights, were included in the investigation.

2. GROUP A, ASPHALT-SATURATED PAPERS

A group of eight samples, designated as 1A, 2A, 3A, etc., was made up of papers which had been impregnated with asphalt to make them more resistant to permeation by air and water. The base papers ranged in composition from strong wrapping paper to rather weak paper containing a considerable amount of low-grade fiber, such as ground wood and fibers from waste materials of sundry sorts. The base paper of sample 1A was made of kraft pulp, such as is used in making strong wrapping papers; of 2A, 3A, and 5A to 8A, mixed fibers; of 4A, chemically prepared wood fiber similar to that used in medium-grade wrapping papers.

3. GROUP P, PARAFFIN-SATURATED PAPERS

A second, small group, designated as 1P, 2P, and 3P, consisted of three different weights of kraft paper impregnated with paraffin so as to make the sheathing paper weather resistant.

4. GROUP L, LAMINATED PAPERS OF HETEROGENEOUS STRUCTURE

A third group, designated as 1L, 2L, 3L, etc., consisted of laminated building papers made up of two or more layers of paper cemented together with one or more layers of asphalt, the asphalt layers constituting the weather-resisting medium and the paper imparting strength to the material. The base papers of most of these were kraft (strong wrapping paper stock), either plain or previously impregnated with oil or asphalt. The base paper of a few was made of reclaimed waste paper. The paper base of sample 1L consisted of one layer of plain kraft paper and one of kraft previously saturated with asphalt; of 2L, three layers of oiled kraft; of 7L, two layers of oiled kraft; of 3L, 6L, and 8L, two layers of plain kraft; of 4L, two layers of asphalt-saturated kraft; of 5L, 9L, 10L, and 11L, two layers of paper made from reclaimed waste paper. Sample 3L, in addition to the layers of paper and asphalt, had a layer of crossed fibers or threads embedded in the asphalt layer in order to impart additional strength to the material. Sample 8L also, in addition to the layers of paper and asphalt, had a layer of metal foil embedded in the asphalt layer in order to increase the weather-resisting properties.

5. GROUP M, MACHINE-FINISHED PAPERS

A fourth group, designated as 1M, 2M, 3M, etc., consisted of machine-finished papers which had not been subsequently treated or processed to enhance those properties desirable in building papers. Samples 1M, 6M, 11M, and 12M were composed of chemically-prepared wood fibers and were of the general nature of heavy wrapping papers. Sample 13M was made of reclaimed waste papers. Sample 14M was made of various kinds of fibers apparently derived from waste materials of the textile and paper industries. All the other samples in this group were composed of mixed wood fibers. Sample 14M was not strictly a sheathing paper in the same sense as the others, but was a heavy felt intended for use in deadening sound.

Other characteristics of these four groups of sheathing papers are shown in Table 1. Practically all the sheathing papers examined are furnished in rolls 36 inches wide. A few types are furnished also in the additional widths of 20, 40, 48, and 60 inches.

TABLE 1.—*Physical and mechanical properties of sheathing papers*

Identification No.	Weight of 1,000 square feet	Thickness	Tensile breaking strength						Bursting strength	Tearing resistance		Transudation of water	Air permeability	Price index per unit of area
			Dry paper		Wet paper		Ratio of wet to dry			Machine direction	Cross direction			
			Machine direction	Cross direction	Machine direction	Cross direction	Machine direction	Cross direction						
	Pounds	*Thousandths inch*	*Lbs./in.*	*Lbs./in.*	*Lbs./in.*	*Lbs./in.*			*Points*	*g*	*g*	*Minutes*	*Ft.³/ft.²/min.*	
Group A:														
1A	48	7.8	76.3	36.2	57.8	31.0	0.76	0.86	97	171	140	150		
2A	101	23.4	57.2	32.0	59.6	34.0	1.04	1.06	76	319	253	2,500		
3A	100	22.5	42.3	28.2	45.4	29.7	1.07	1.05	59	214	182	1,700		180
4A	44	13.3	61.0	18.9	9.5	3.4	.16	.18	76	244	154	18	0.003	89
5A	148	28.5	32.4	18.8	34.9	21.4	1.08	1.14	38	250	186	∞		
6A	163	35.5	30.1	15.0	27.6	10.0	.92	.67	51	726	573	900	.007	
7A	79	14.7	27.4	13.0	12.1	5.3	.44	.41	30	212	176	90		
8A	66	14.1	31.2	11.5	12.5	5.6	.40	.49	31	181	147	60	.006	
Group P:														
1P	35	6.5	60.8	32.0	24.6	11.3	.40	.35	75	146	114	35		137
2P	26	5.3	36.4	24.6	8.8	5.0	.24	.20	45	99	99	17		94
3P	18	3.9	29.6	13.0	6.7	2.8	.23	.22	38	58	55	7		80
Group L:														
1L	63	13.0	97.2	46.8	24.0	11.0	.25	.24	117	362	312	2,500		155
2L	70	13.8	79.3	40.9	38.6	20.5	.49	.50	93	255	250	3,200		124
3L	54	17.8	83.8	38.2	38.4	20.6	.46	.54	116			1,100		294
4L	41	7.8	58.7	31.1	18.2	8.6	.31	.28	78	157	157	25		97
5L	84	25.7	60.8	27.2	10.2	4.4	.17	.16	52	256	163	41	.002	77
6L	30	7.8	46.9	26.9	5.4	2.8	.11	.10	64	162	153	50		70
7L	47	9.4	60.9	22.4	18.4	7.3	.30	.33	73	245	201	1,100		81
8L	50	8.4	43.8	21.6	9.6	7.7	.22	.36	49	177	140	∞		291
9L	66	20.4	46.9	21.2	0.7	4.2	.21	.20	45	186	124	14	.004	61
10L	54	16.6	39.4	15.5	8.7	3.7	.22	.24	42	153	103	16	.002	50
11L	44	13.7	34.8	13.8	6.6	2.9	.19	.21	36	102	77	13	.004	41

TABLE 1.—*Physical and mechanical properties of sheathing papers*—Continued

Identification No.	Weight of 1,000 square feet	Thickness	Tensile breaking strength						Bursting strength	Tearing resistance		Transudation of water	Air permeability	Price index per unit of area
			Dry paper		Wet paper		Ratio of wet to dry							
			Machine direction	Cross direction	Machine direction	Cross direction	Machine direction	Cross direction		Machine direction	Cross direction			
Group M:	*Pounds*	*Thousandths inch*	*Lbs./in.*	*Lbs./in.*	*Lbs./in.*	*Lbs./in.*			*Points*	*g*	*g*	*Minutes*	*Ft.³/ft.²/min.*	
1M	40	13.1	63.8	40.5	7.3	5.1	0.11	0.13	85	393	360	2	0.039	77
2M	111	24.4	65.2	39.9	19.1	3.7	.29	.09	82	637	613	30	.022	129
3M	85	41.4	49.0	31.8	5.8	3.6	.12	.11	53	430	342	1	.233	85
4M	83	19.9	64.5	29.8	22.3	8.9	.35	.30	71	496	443	16	.024	96
5M	94	28.1	61.8	29.2	8.1	3.4	.13	.12	46	313	196	7	.008	----------
6M	22	6.8	41.5	25.7	5.8	3.4	.14	.13	61	202	174	1	.111	68
7M	62	15.5	43.2	23.1	10.6	6.3	.25	.27	48	421	379	10	.061	72
8M	60	17.6	39.8	22.0	4.4	2.3	.11	.10	41	171	124	3	.008	----------
9M	40	8.6	37.5	20.2	7.8	4.4	.21	.22	43	222	217	6	.022	50
10M	51	12.1	37.6	18.2	9.5	9.5	.25	.52	41	257	233	7	.037	59
11M	26	9.3	36.4	16.4	2.6	1.2	.07	.07	39	129	101	1	.034	37
12M	32	14.2	48.0	15.6	5.1	1.8	.11	.12	49	188	167	1	.132	74
13M	40	13.5	28.0	11.9	3.6	1.6	.13	.13	27	111	80	3	.013	29
14M	188	85.5	22.4	14.7	3.0	1.7	.13	.12	47	528	478	4	.365	----------

NOTE.—Tensile breaking strength recorded in pounds per inch of width. Machine direction is direction of travel of paper on paper-making machine. It is, in general, the stronger direction. Cross direction is transverse to the machine direction and is, in general, the weaker direction. Points = Bursting pressure in pounds per square inch of a 1.13-in.² circular area of paper under hydraulic pressure. Air permeability measured under pressure equivalent to that of a 20-mile wind.

III. LABORATORY TESTS MADE AND METHODS EMPLOYED

1. PROPERTIES CONSIDERED IMPORTANT

In view of the function of sheathing paper as a relatively impermeable membrane whose integrity within the wall must be maintained during and after erection, the important properties of the material appear to be strength and impermeability to air and water. Other characteristics, such as aging properties and repellence or passivity toward ravaging insects, are of considerable interest but are difficult of evaluation.

Thermal conductivity was suggested as an important property of sheathing paper. In fact, some sheathing papers are made thick in order to increase their insulating value. It was the opinion of members of the staff of the heat transfer section of the Bureau of Standards, however, that it would not be worth while to measure thermal conductivities of sheathing papers. Such measurements would give information of little or no value in this connection. Irrespective of the thermal conductivity or of the thickness of the paper (within practical limits), the resistance to heat flow by conduction through the paper itself is negligibly small compared to the total thermal resistance of the complete wall. A thin layer of paper would not have a significant thermal resistance from surface to surface unless its conductivity were much less than that of any known solid substance. It is true that sheathing paper might be so installed in a wall as to divide air spaces, and thus increase the insulating value of the wall by a significant amount. For the reasons given above, however, this effect is practically independent of the thermal conductivities and thicknesses of commercial building papers.

2. TESTING METHODS USED

The following properties were determined by laboratory tests: Weight, thickness, tensile breaking strength (of both dry paper and wet paper), bursting strength, tearing resistance, water resistance, and air permeability.

(*a*) Official Methods.—With the exception of the last two of these properties listed, for which no standard methods are available, the measurements were made according to the official paper-testing methods of the Technical Association of Pulp and Paper Industry.[1]

(*b*) Water Resistance.—Water resistance was measured by an adaptation of the dry indicator method.[2] A specimen about 2 inches square was sealed to a cover glass with a powdered indicator between

[1] Paper Testing Methods, 1928, Lockwood Trade Journal Co., New York, N. Y.

[2] Carson, Testing Paper for Permeability to Liquids, Tech. Assoc. Papers, 8, pp. 91-94, 1925; and Paper Trade J., March 5, 1925; Tech. Papers B. S., No. 326.

the specimen and the cover glass. The indicator was a mixture of a very soluble dye with a much larger amount of powdered sugar. The seal was made by turning the edges of the specimen over the edges of the cover glass and dipping these edges to a depth of a quarter of an inch in molten paraffin. No moisture could reach the indicator except by going through the paper. The specimens thus prepared were floated on water at a temperature of 20° to 25° C. The time required for water to penetrate through the paper and produce a decided coloration in the indicator powder was taken as a measure of the relative water resistance of the paper.

(*c*) Air Permeability.—Air permeability was measured with the apparatus pictured in Figure 1, which, in its original form, was developed by Weaver and Pickering, of the gas chemistry section of the Bureau of Standards. This apparatus consists of a permeability cell, a water manometer, a gas meter, and a rotary vacuum pump.

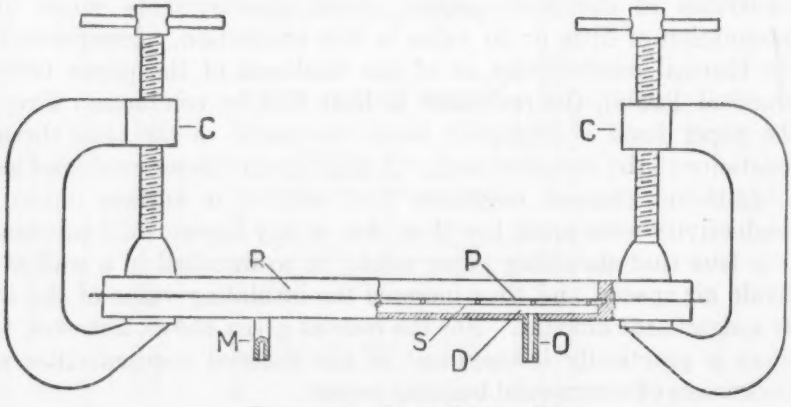

Figure 2.—*Permeability cell*

The permeability cell was designed to test a fairly large area of paper. This feature is particularly important in testing sheathing papers, since some of them lack uniformity, and hence a large area is necessary in order to obtain a test truly representative of the material. Furthermore, many of the sheathing papers tested were only slightly permeable to air, and a large area was desirable in order that a sufficient amount of air might be forced through these to give an adequate reading on the gas meter. The types of apparatus ordinarily used to test the porosity of paper present too small an area of paper to the air stream to be satisfactory for the testing of sheathing papers.

The details of the construction of the permeability cell are shown in Figure 2, which is drawn in partial section. This shallow cell consists of a steel plate having a circular depression, *D*, 7 inches in diameter and ¼ of an inch deep, covered by a very coarse wire screen, *S*, to support the paper. The paper *P*, the permeability of which is to be

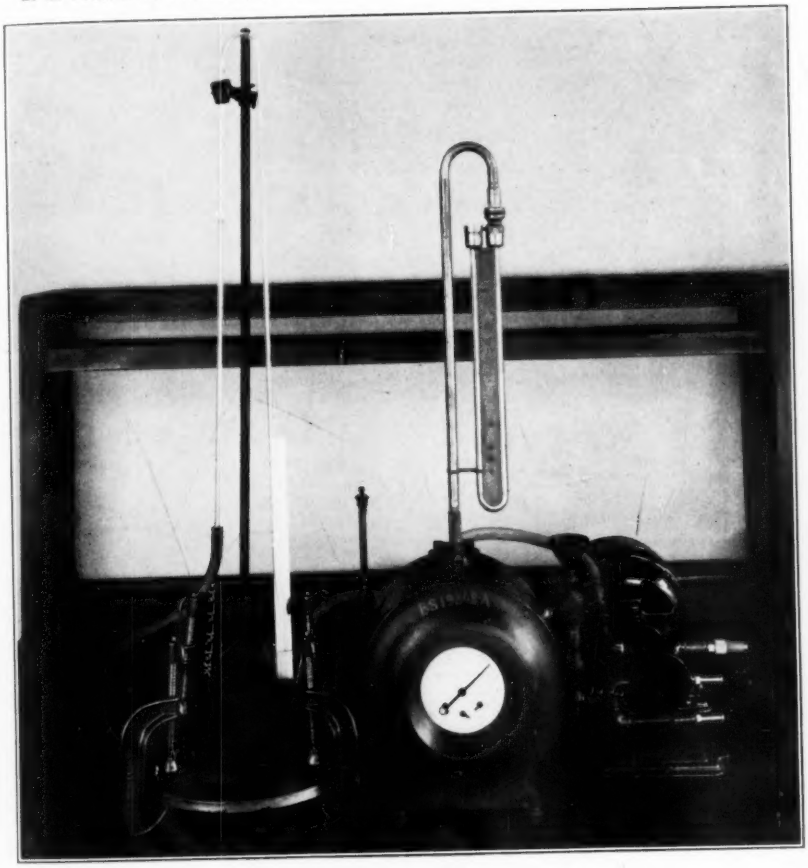

FIGURE 1.—*Permeability apparatus*

UNIV OF MICH.

measured, is clamped over the cell chamber by means of the ring *R*, which registers with the annular surface of the cell proper. An air-tight joint is obtained by smearing the annular clamping surface with a heavy grease before laying the paper over it.

As shown in Figure 1, the vacuum pump is connected to the gas meter, which in turn is connected to the permeability cell at the outlet, *O*. (See fig. 2.) The water manometer is connected at the outlet *M* of the permeability cell. In making the air-permeability tests, conditioned air having a temperature of 70° F. and a relative humidity of 65 per cent was drawn through the paper and the gas meter by means of the vacuum pump. A constant pressure difference corresponding to that which would be produced on the two sides of a wall in a 20-mile wind was maintained. This pressure difference corresponds to a difference in head in the water manometer of 6¼ mm. The volume of air which was drawn through the paper under these conditions in 10 minutes was measured by means of the gas meter. Six determinations were made on each sample, and the average value was used in calculating the volume of air in cubic feet which would pass through each square foot of freely exposed sheathing paper in one minute under a pressure difference corresponding to that produced by a 20-mile wind. Determinations were also made at double and triple this pressure difference.

IV. EXPERIMENTAL RESULTS

The results of the laboratory tests are given in Table 1. The samples are tabulated in four groups, as previously indicated. In each group the samples are arranged in the order of the tensile breaking strength in the cross direction, since this is probably the most important of the strength properties measured.

1. WEIGHT AND THICKNESS

The weight of 1,000 square feet of the material is recorded in pounds and the thickness in thousandths of an inch. It is seen that the papers differ considerably in weight and thickness. The two properties are not strictly proportional. In fact, there are some rather striking differences in apparent densities. These apparent differences are in some cases not very real, however, for some of the papers have corrugated or uneven surfaces, as a result of which the measured thickness would be that of the high spots and not an average thickness. Weight and thickness do not appear to be correlated with any other measured property except in papers which are alike but for differences in thickness and weight, such as the second group of three papers in which there is a regular gradation of nearly all properties corresponding with the thickness.

2. STRENGTH

The tensile breaking strength, especially the strength in the cross direction or weaker direction, is probably the most important indication of the ability of the material to stand the required handling during erection without injury. The tensile breaking strength in the two principal directions, and the bursting strength as well, show a certain parallelism within each group, although there are a few rather outstanding exceptions. The so-called tearing resistance, although of some interest, probably does not give as good an indication of the tendency of the paper to tear as does the tensile breaking strength. In this tearing test the paper is torn from the apex of a previously made slit in the paper, a state of things which apparently has very little relation to the tendency of a tear to start at the edge. The sort of stress which ordinarily starts a tear at the edge is somewhat like an eccentrically applied tensile stress. Hence, it is probable that the tensile breaking strength is the most important of the strength measurements made. The tensile breaking strength of the papers after they had been immersed in water for 30 minutes was also determined. Such data were thought to be of some value in predicting the behavior of paper that becomes wet in the rain or is applied in damp weather. The test is admittedly very severe and is probably unfair to some of the papers, especially those of the laminated type containing a water resistant inner layer which would prevent the papers from becoming wet through when only one side is exposed. However, the test brought out some rather striking results. Most of the impregnated papers of the first group, the asphalt-saturated papers, retained a relatively large portion of their strength after this severe wetting treatment. A few of them, indeed, were stronger after wetting than before. The last group, the machine-finished papers, became rather weak after the wetting treatment, as might have been expected. That the test is not fair to the laminated papers is emphasized by the relatively high strength retention of samples 2L and 3L, which have a third inner layer of paper or of textile fibers protected on both sides by a layer of asphalt.

3. WATER RESISTANCE

The resistance to the transudation of water, which is recorded as the number of minutes required for an appreciable amount of water to penetrate from one side of the sheet to the other, roughly parallels the strength retention of the wet paper, which is itself a form of water-resistance test. However, the two are not strictly comparable. The transudation test more nearly simulates the likelihood of water

seeping through the building paper to cause damage. The papers differ greatly in this respect even in the same group. Only the papers which contain asphalt as the water-resisting medium show any unusual degree of water resistance. In the case of two of the papers, 5A and 8L, no transudation of water could be detected by the method employed, which is the most sensitive method known to the writers. However, there were papers in all four groups which had comparatively little water resistance.

4. AIR PERMEABILITY

The susceptibility of sheathing paper to infiltration of air is recorded in Table 1 in cubic feet of air per square foot of paper per minute forced through sheathing paper under a pressure difference corresponding to that on the two sides of a wall exposed in a 20-mile wind. Most of the papers of the first three groups (all of the second) allowed no infiltration of air under conditions simulating wind pressures ordinarily encountered. The infiltration which was shown by a few of the samples in these three groups was very small, probably negligible for all practical purposes. A few of the machine-finished papers had good resistance to permeation of air, but most of them were only moderately resistant. It was only in this last group that relatively large differences in air permeability were observed.

Some of the papers showed considerable lack of uniformity in that the deviations of individual results from the average for each sample were in some cases large. The mean deviations ranged from 5 to 80 per cent for the different samples. A part of such deviations, perhaps 5 per cent or so, resulted from the inability to prevent slight fluctuations in the small pressure difference maintained. When the individual results for the three pressures at which determinations were made were plotted, pressure against air permeation, curves were obtained, some of which were convex upward, some convex downward, others practically straight lines. The curvatures were such as to lead to the conclusion that the experimental errors presumably responsible for the differences in curvature amounted to some 5 per cent. The mean deviations in excess of this amount were, therefore, presumed to be due to lack of uniformity in the structure of the paper. Taking into account the probable magnitude of the experimental error, it appeared that within the small pressure range at which experiments were made the air permeation was substantially proportional to the pressure.

V. RELATION OF LABORATORY TESTS TO SERVICE DEMANDS

1. USES MADE OF SHEATHING PAPER

Besides the chief application of sheathing papers as weatherproofing media in the walls and floors of buildings there are many other uses of such materials which are of considerable importance. Among the other uses suggested by manufacturers and dealers are: Protective covering for materials on the job; protective covering for fresh cement and concrete work, especially sidewalks, to prevent too rapid loss of moisture; any use where a moisture proof or waterproof covering or medium is required; lining of shipping cases; insulating material; lining in refrigerator-wall construction; weatherproofing medium in the walls of street cars and similar passenger cars; temporary shelters, especially for livestock on farms. Builders use large amounts of sheathing paper as protection for finished floors during the finishing stages of dwelling construction and during the exhibit period of such buildings.

2. COST OF SHEATHING PAPER

Although the cost of sheathing paper is a relatively small item in the cost of a building, the price paid for such materials may be of interest in connection with certain uses of the paper as well as of academic interest. In Table 1 are given price index values per unit area of all the sheathing papers for which such information was available. The price indexes are based on the average price as 100. There is apparently no very definite relation between the price of building paper and the properties of the material which determine its value as sheathing paper.

3. SOME PROBABLE RELATIONS BETWEEN PROPERTIES AND SERVICE DEMANDS

The relation of measurable properties of sheathing paper to the service demands and conditions is a matter for future determination requiring extensive field experiments, but at this time a few observations may not be amiss by way of suggesting some of the probable relations and possibilities which may be encountered. The relative importance of these measurable properties is, of course, dependent upon the specific use which is to be made of the paper. For some applications strength may be of paramount importance, for others water resistance may overshadow all other properties, while for still others the air permeability may be the chief consideration.

(*a*) THICKNESS.—In view of the fact previously mentioned that the insulating effect of sheathing paper in a wall is practically independent of the thickness of the paper, there does not appear to be

any particular advantage in using a thick sheathing paper if the other desirable properties of the material are satisfactory. For use under flooring, where the paper serves also in the capacity of deadening felt, thickness is doubtless an advantage.

(*b*) Strength.—The strength of sheathing paper, both dry and wet, is of importance in handling the paper and in getting it in place whole in any kind of weather. The strength of such materials, particularly when wet, is of considerable importance when the paper is used as a protective covering out of doors, for a flurry of wind and rain would rip to pieces a paper of inferior strength, particularly if the strength is largely destroyed by wetting.

(*c*) Water Resistance.—The water resistance of sheathing paper is of considerable importance, in that serious damage to plastering may be prevented in severe storms by a waterproof sheathing paper properly put in place. In some of the other suggested uses this property is obviously of great importance. It is also possible that paper which will remain moist in damp weather may promote mold or similar cause of deterioration. It is an interesting fact in connection with water resistance that waterproof sheathing paper put in floors laid over concrete in order to prevent moisture from coming through and warping the flooring has sometimes been observed to do more harm than good. In warm, humid weather the cool concrete causes condensation of water between the finished flooring and the sheathing paper. Since the paper is waterproof, the water remains in puddles on the paper until it is absorbed by the flooring and produces very serious warping. An interesting possibility in such a case lies in the use of paper of the type represented by the second group of Table 1. A paper well saturated with paraffin can be made air proof, but it is not very water resistant. This is a fairly well established characteristic of paraffin-saturated paper. In spite of the presence of the paraffin, when water comes in contact with the surface of such paper, capillary phenomena come into play, the paper swells, and the water finds its way through. Such a paper might effectually prevent moisture in the vapor phase from reaching the flooring from underneath and yet might alleviate the trouble somewhat by allowing water condensed on the paper to seep through to the concrete where it can do no harm.

(*d*) Air Permeability.—Although the primary function of sheathing paper is to prevent infiltration of cold air as a result of wind pressure, it does not follow that the differences ordinarily found in the air permeability of sheathing papers have very much significance. Only some 15 to 30 per cent of all the heat losses from buildings are ordinarily ascribed to infiltration of air from all sources. The infiltration of air through the joints of overlapping pieces of sheathing paper, around window casings and door frames, and especially through

doors and windows frequently opened and closed during the day, is very considerable, so that the differences in air leakage through different kinds of building paper are probably not very significant, except, possibly, in the case of a few of the more permeable papers of the fourth group. Much of the surface of the sheathing paper is covered by boards, usually on both sides. The paper serves chiefly to prevent the wind from entering through the cracks between boards. The use of any kind of sheathing paper is so far superior to no paper at all that the differences between papers, in respect to air permeability, are, perhaps, largely negligible for all practical purposes. Some idea of the magnitude of the infiltration of air through the sheathing paper itself may be had by assuming a room of moderate size, the walls of which are made of the most permeable sheathing paper of the first three groups of Table 1, exposed on two sides to a 20-mile wind. Under these conditions about half a day would be required to change the air in the room once. In view of the fact that much of the surface of the sheathing paper is covered by boards and that infiltration is not a large factor in heat loss in good construction, it is apparent that a sheathing paper would have to be unusually permeable to air in order for its relative permeability to be of much consequence.

(*e*) CHARACTER OF SURFACE.—The character of the surface of the paper is of importance for certain uses. This may be true if the sheathing paper is to be wholly or partially exposed. One of the sheathing papers tested was intended primarily for such purposes and was finished with a pleasing colored surface. Attention to character of surface is important in paper used as a temporary protection to finished floors. Paper coated with a material which would stick to the floor and mar its appearance is obviously unsuitable for the purpose.

(*f*) PERMANENCE.—The question of permanence is important, but very little is known in this regard. Papers containing ground wood are known to increase in degree of sizing, or water resistance, with age and to decrease in strength and elastic properties. The asphalt in some asphalt-saturated papers is known to undergo a slow process of polymerization resulting finally in a friable or powdered material which would probably retain little of its original ability to impart air and water resisting properties to the paper; but it is not known how many years would be required for such influences to become serious. Possibly most papers of this type would be substantially as permanent as the wooden walls with which the papers are usually used. Doubtless the paraffin-saturated papers would be the most permanent type, since paraffin is relatively inert chemically.

The above comments are offered as suggestions as to the possible behavior of building papers under certain conditions. Field tests are contemplated by the National Lumber Manufacturers' Association to obtain information which can not be had in the laboratory.

VI. SUMMARY

As a result of a study of a considerable number of sheathing papers, representing the various types which are being used in the building trade, and the measurement of such properties as weight, thickness, tensile breaking strength, bursting strength, tearing resistance, water resistance, and air permeability, the following observations appear to be justified:

1. Sheathing papers differ considerably in weight, thickness, and density. These properties are, in general, not definitely related to other important characteristics of building papers.

2. A range of about fourfold is found between extremes in both the tensile breaking strength and the bursting strength of such papers. The tensile breaking strength in the cross direction of the paper is probably the best criterion of mechanical serviceability. The papers differ greatly in their retention of strength after wetting, most of the papers losing more than half their strength as a result of immersion in water for 30 minutes.

3. The time required for water to penetrate through the papers differs within wide limits—from less than a minute to several days. Only sheathing papers containing asphalt as the waterproofing medium have any unusual degree of water resistance.

4. Sheathing papers, except some of the machine-finished variety, are relatively impermeable to air under conditions simulating wind pressures ordinarily encountered.

5. The price range of sheathing papers is about tenfold between the cheapest and the most expensive. There is no very definite relation between the price of such papers and their value as building papers.

6. There is no advantage in using a relatively thick sheathing paper if the strength and impermeability to air and water are satisfactory, except, perhaps, where sound deadening is a factor.

7. Strength sufficient to insure getting the material in place whole, water resistance sufficient to insure against the damage to plastering and inside finish which sometimes occurs in severe storms, and impermeability to air are apparently the requisite elements in a good sheathing paper.

8. Most sheathing papers, with the possible exception of some of the more permeable of the machine-finished type, appear to be sufficiently air-tight for all practical purposes.

WASHINGTON, January 18, 1929.

USE OF 8-HYDROXYQUINOLINE IN SEPARATIONS OF ALUMINUM

By G. E. F. Lundell and H. B. Knowles

ABSTRACT

Many analytical operations leave aluminum associated with elements, such as phosphorus, vanadium, arsenic, molybdenum, uranium, fluorine, boron, columbium, tantalum, and beryllium. The data presented show that aluminum can be quantitatively precipitated and separated from these elements by the use of the reagent 8-hydroxyquinoline, provided proper conditions are established.

CONTENTS

	Page
I. General considerations	91
II. Separations	92
1. Separation of aluminum from phosphorus	92
2. Separation of aluminum from vanadium	93
3. Separation of aluminum from tantalum, columbium, titanium, molybdenum, arsenic, fluorine, and boron	94
4. Separation of aluminum from beryllium	94
5. Separation of aluminum from uranium	95
III. Applications	95
IV. Summary	96

I. GENERAL CONSIDERATIONS

In analyses of material containing aluminum, preliminary separations, such as filtration after precipitation with an excess of sodium hydroxide or extraction of alkali carbonate or hydroxide melts with water, often leave aluminum still associated with elements, such as phosphorous, vanadium, arsenic, molybdenum, uranium, fluorine, boron, columbium, tantalum, and beryllium. A method that will yield a precipitate containing aluminum alone when applied to such mixtures is much needed. The experimental work that is to be described goes to show that precipitation with 8-hydroxyquinoline can be made to fulfill this requirement, provided proper conditions are established.

The use of 8-hydroxyquinoline (C_9H_6NOH, and variously called o-oxychinoline, 8-oxychinolin, oxin) for the determination of certain elements has been described by Berg,[1] Hahn and Vieweg,[2] and Robitshek.[3] These researches deal primarily with the determination of

[1] R. Berg, Z. anal. Chem., **70**, p. 341; 1927; **71**, pp. 23, 171, 321, 369; 1927; **72**, p. 177; 1928; **76**, p. 191; 1929.
[2] F. L. Hahn and K. Vieweg, Z. anal. Chem., **71**, p. 122; 1927.
[3] J. Robitshek, J. Am. Cer. Soc., **11**, p. 587; 1928.

elements such as copper, aluminum, cadmium, bismuth, zinc, and magnesium in pure solutions. As regards aluminum, it has been shown that it can be completely precipitated by 8-hydroxyquinoline in either ammoniacal or feebly acid solutions. The precipitate that is obtained has the composition expressed by the formula $Al(C_9H_6ON)_3$ and can be weighed as such after drying at 110° C.[4] It is also stated that the precipitate can be converted to aluminum oxide by igniting it under a cover of anhydrous oxalic acid [5] or dissolved in acid and titrated with a standard solution of potassium bromate-potassium bromide.[5] In such a titration 12 atoms of bromine represent 1 atom of aluminum.

Of the various methods that have been recommended for the treatment of the precipitate the authors have tried only direct ignition to the oxide. In such tests as were made difficulty apparently due to volatilization of the salt was experienced. As a result, in the experiments to be described, the actual determination of aluminum was made by decomposing the filter and precipitate with nitric and sulphuric acids, precipitating the aluminum as hydroxide, igniting to the oxide, and correcting for silica. This procedure was all the more attractive in that the effect of contaminating compounds was not minimized, as might be the case if calculations were based on the small factor (0.1110 for Al_2O_3) used for the dried salt, or hidden, as might be the case if titration were employed.

Tests of the ignited alumina generally showed complete removal of the other constituent or its presence in such minute quantities as to be wholly without effect on the determination.

II. SEPARATIONS

1. SEPARATION OF ALUMINUM FROM PHOSPHORUS

The separation of aluminum from phosphorus is satisfactorily accomplished by precipitating with 8-hydroxyquinoline in ammoniacal solution, as follows: To the solution slightly acid with sulphuric or hydrochloric acid and containing not more than 0.1 g of aluminum oxide in 100 ml of solution, add an excess of a 2.5 per cent solution of 8-hydroxyquinoline in diluted acetic acid,[6] then dilute ammonium hydroxide until alkaline, and finally an excess of 5 ml of strong ammonium hydroxide in 100 ml of solution. Warm to 60° to 70° C. and digest at this temperature until the precipitate becomes dense and crystalline. Cool, preferably in ice water, filter through a tight paper

[4] R. Berg, loc. cit.; I. M. Kolthoff and E. B. Sandell (J. Am. Chem. Soc., 50, p. 1900; 1928) obtained satisfactory results by drying at 120° to 140° C

[5] See footnote 1, p. 91.

[6] Prepared by triturating 2.5 g of 8-hydroxyquinoline and 5 ml of glacial acetic acid and pouring the resulting solution into 100 ml of water at 60° C. After cooling the solution is filtered. 1 ml of this solution suffices to precipitate 2.9 mg of alumina in pure solution. An excess of the reagent does no harm; in any case enough should be used to color the solution yellow.

and wash the precipitate thoroughly with a cold dilute solution of ammonium hydroxide (1:40) containing 25 ml of the reagent, previously neutralized with ammonium hydroxide, in 1 liter. Treat the precipitate and paper with nitric and sulphuric acids to destroy organic matter and precipitate the aluminum with ammonium hydroxide as usual. The results that can be obtained with the method are indicated by the data shown in Table 1.

TABLE 1.—*Separation of aluminum from phosphorus*

[Final volume of solution 200 ml]

Al_2O_3 taken	P_2O_5 taken	Al_2O_3 found	Difference	Remarks
g	*g*	*g*	*g*	
0.0945	0.05	0.0942	−0.0003	Single precipitation.[1]
.0945	.05	.0940	−.0005	Do.
.0945	.05	.0946	+.0001	Do.
.0945	.05	.0945	.0000	Double precipitation.
.0945	.05	.0944	−.0001	Do.
.0947	1.000	.0948	+.0001	Single precipitation in presence of P_2O_5.
.0947	1.000	.0948	+.0001	Do.

[1] After single precipitations in a solution containing 0.05 g of Al and in another containing 0.05 g of Al and 1 g of P_2O_5, no aluminum could be found in the filtrates and the precipitate obtained in the second solution contained less than 0.2 mg of P_2O_5.

2. SEPARATION OF ALUMINUM FROM VANADIUM

Complete separation of aluminum from vanadium can not be obtained by the preceding method, even by repeated precipitation, regardless of whether the vanadium is quadrivalent or quinquevalent. However, complete separation is easily obtained if vanadium is oxidized to a still higher valency; as, for example, by precipitating in a solution containing hydrogen peroxide. The only modification that is needed in the method as described in 1 is the addition of 10 to 15 ml of a 3 per cent solution of hydrogen peroxide before the 8-hydroxyquinoline is added. The results which can be obtained with the method are shown in Table 2.

TABLE 2.—*Separation of aluminum from vanadium*

[Final volume of solution 200 ml]

Al_2O_3 taken	V_2O_5 taken	Al_2O_3 found	Difference	Remarks
g	*g*	*g*	*g*	
0.0945	0.05	0.0947	+0.0002	Single precipitation.[1]
.0945	.05	.0945	.0000	Do.
.0945	.05	.0944	−.0001	Double precipitation.
.0945	.05	.0944	−.0001	Do.

[1] After single precipitation in a solution containing 0.05 g of Al and in another containing 0.05 g of Al and 0.5 g of V_2O_5, no aluminum could be found in the filtrates and the precipitate obtained in the second solution contained less than 0.2 mg of V_2O_5.

3. SEPARATION OF ALUMINUM FROM TANTALUM, COLUMBIUM, TITANIUM, MOLYBDENUM, ARSENIC, FLUORINE, AND BORON

The separation of aluminum from arsenic, fluorine, or boron can be satisfactorily carried out in ammoniacal solution as described under 1. For separations from tantalum, columbium, titanium, and molybdenum, hydrogen peroxide to form peroxidized compounds must be added as described in section 2.

Results are shown in Table 3.

TABLE 3.—*Separation of aluminum from boron, fluorine, arsenic, columbium, tantalum, titanium, and molybdenum*

[Final volume of solution 200 ml]

Contaminant	Al_2O_3 taken	Al_2O_3 found	Difference	Confirmatory experiments
	g	g	g	
[1] 1 H_3BO_3	0.0945	0.0941	−0.0004	No aluminum was found in the filtrate and no boron in the precipitate after a single precipitation of 0.05 g of aluminum in the presence of 0.5 g of B_2O_3.
[1] 0.20NaF	.0945	.0942	−.0003	No aluminum was found in the filtrate and no fluorine in the precipitate after a single precipitation of 0.05 g of Al in the presence of 5.0 g of NaF.
[1] 0.05As_2O_5	.0945	.0940	−.0005	No aluminum was found in the filtrate and less than 0.5 mg of arsenic was found in the precipitate after a single precipitation of 0.05 g of aluminum in the presence of 0.2 g of As_2O_5. No aluminum was found in the filtrates and no arsenic in the precipitate after a double precipitation of 0.05 g Al in the presence of 1 g of As_2O_5.
[2] 0.05Cb_2O_5	.0945	.0941	−.0004	The precipitate contained no Cb_2O_5 after double and less than 1 mg of Cb_2O_5 after single precipitation in a solution containing 0.05 g of Al and 0.2 g of Cb_2O_5.
[2] 0.05Ta_2O_5	.0945	.0945	.0000	The precipitate contained no Ta_2O_5 after double and less than 1.5 mg of Ta_2O_5 after single precipitation in a solution containing 0.05 g of Al and 0.2 g of Ta_2O_5.
[2] 0.05TiO_2	.0945	.0943	−.0002	The precipitate contained less than 0.1 mg of TiO_2 after double and less than 1 mg of TiO_2 after single precipitation in a solution containing 0.05 g of Al and 0.2 g of TiO_2.
[2] 0.05MoO_3	.0945	.0938	−.0007	No aluminum was found in the filtrates and less than 0.3 mg of MoO_3 in the precipitate after a double precipitation of 0.05 g of Al in the presence of 0.05 g of MoO_3.

[1] Single precipitation. [2] Double precipitation.

4. SEPARATION OF ALUMINUM FROM BERYLLIUM

It has already been shown by Kolthoff and Sandell [7] that a satisfactory separation of aluminum from beryllium can be had by precipitating with 8-hydroxyquinoline in dilute acetic acid solution, as follows: Warm a slightly acid solution of aluminum and beryllium to 50° to 60° C. and treat with an excess of an acetic acid solution of the precipitant. Add 2 *N* ammonium acetate until a permanent precipitate is obtained and then 20 to 25 ml in excess. Let settle, filter through a Jena glass or a porous porcelain crucible, wash with cold water, and dry at 120° to 140° C. The beryllium in the filtrate may be determined by precipitating with ammonia and igniting to the oxide.

[7] See footnote 4, p. 92.

5. SEPARATION OF ALUMINUM FROM URANIUM

Successful separations of aluminum from uranium can not be obtained by the methods given for phosphorus or vanadium. However, satisfactory results follow if ammonium carbonate is substituted for ammonia in the method outlined for the separation of aluminum from phosphorus. In such case prepare a faintly acid solution containing the aluminum, uranium, and 8-hydroxyquinoline, cautiously neutralize with a saturated solution of ammonium carbonate, add an excess of 25 ml per 100 ml of solution, and heat to about 50° C., taking care to avoid excessive effervescence caused by too rapid heating. The performance of the method is shown in Table 4.

TABLE 4.—*Separation of aluminum from uranium*

[Final volume of solution 200 ml]

Al_2O_3 taken	UO_3 taken	Al_2O_3 found	Difference	Remarks
g 0.0945	*g* 0.05	*g* 0.0946	*g* +0.0001	Double precipitation.[1]

[1] After single precipitations in a solution containing 0.05 g of Al and in another containing 0.05 g of Al and 0.2 g of UO_3, no aluminum could be found in the filtrates, and the precipitate obtained in the second solution contained no uranium.

III. APPLICATIONS

In tests on the Bureau of Standards standard sample of ferrovanadium No. 60 and ingot iron No. 55, in which speed rather than accuracy was sought, the results in Table 5 were obtained.

TABLE 5.—*Determination of aluminum in ferrous materials*

Material	Weight of sample	Al present	Al found
	g	*Per cent*	*Per cent*
Ferrovanadium No. 60 [1]	1.000	12.5	12.10
Ingot iron [1]	2.000	[2] 1.0	.96
Do. [2]	2.000	[2] 1.0	.95
Do. [3]	2.000	[2] .05	.03
Do. [3]	2.000	[2] .05	.04

[1] Single precipitation. [2] Added as pure aluminum. [3] Double precipitation.

In these analyses the acid solution of the material was partially neutralized with sodium hydroxide and poured slowly and with stirring into enough of a 5 per cent solution of the latter to make the final volume exactly 500 ml. A 250 ml aliquot portion was then filtered, acidified with sulphuric acid, and the aluminum precipitated with 8-hydroxyquinoline as in (1) in the case of ingot iron and as in in (2) with the ferrovanadium. Low results in such tests are to be expected, as there is always some retention of aluminum by the sodium hydroxide precipitate.

Another interesting application of 8-hydroxyquinoline is for the detection of impurities, such as iron and aluminum, in phosphoric acid or alkali phosphates. In such tests the reagent will give precipitates in solutions that remain absolutely clear when treated with ammonia alone. For example, ammonium hydroxide gave no precipitate whatever in a 25 ml portion of phosphoric acid (specific gravity 1.71) which had been diluted to 500 ml and treated with aluminum chloride equivalent to 0.001 g of Al_2O_3; while a similarly prepared portion gave a precipitate with 8-hydroxyquinoline which weighed 0.0025 g when ignited. A third 25 ml portion of the acid to which no aluminum was added gave a precipitate weighing 0.0015 g, exactly 0.001 g less than was obtained from the portion that was adulterated with 0.001 g of Al_2O_3, and representing 0.0035 per cent of "matter precipitable by 8-hydroxyquinoline" in the phosphoric acid. The precipitate produced by the reagent in an ammoniacal solution contains, in addition to the aluminum, all of the iron and no doubt other elements, such as magnesium, that may be present in the phosphoric acid and are normally precipitated in ammoniacal solution by 8-hydroxyquinoline.

IV. SUMMARY

The data presented show that precipitations with 8-hydroxyquinoline serve to separate aluminum from phosphorus, arsenic, fluorine, and boron if made in ammoniacal solutions, from tantalum, columbium, titanium, and molybdenum if made in ammoniacal solutions containing hydrogen peroxide, and from uranium if made in ammonium carbonate solutions. Others have shown that aluminum can also be separated from beryllium if precipitation is made in acetic acid solution.

These separations are of especial interest in that many of the preliminary separations that are usually made for aluminum leave it still associated with the most of these elements.

WASHINGTON, April 6, 1929.

REMOVAL OF DISSOLVED GASES FROM LIQUIDS BY VACUUM SUBLIMATION

By James H. Hibben

ABSTRACT

A method of removing and collecting dissolved gases from liquids is described. It is possible, through the application of the principle of vacuum sublimation, to prepare gas-free liquids for use in the determination of physical constants without appreciable loss of either liquid or dissolved gas. Experimental results are presented which demonstrate the practicability of the method as well as its theoretical limitations.

CONTENTS

	Page
I. Introduction	97
II. Theory	98
III. Description of apparatus	99
IV. Method of operation	100
V. Experimental results	101
1. Purification of water, Part I, HN_3 as the impurity	101
2. Purification of water, Part II, HCl as the impurity	102
3. Purification of water, Part III, O_2 as the impurity	103
4. Purification of water, Part IV, CO_2 as the impurity	103
VI. Summary	104

I. INTRODUCTION

The complete removal of dissolved gas from a liquid is usually the final step in the purification of the liquid for the purpose of determining certain of its physical properties. Removal by chemical means is often impracticable, particularly in the case of the gases of the atmosphere. The collection of the dissolved gas for analytical purposes is also of importance, for example, in determinations of gas solubilities. The general physical method of purification described below not only permits the complete removal of the dissolved gas, in most cases, but also allows an approximately complete recovery of both the gas and liquid.

The various methods described in the literature fall into four categories—those employing vacuum,[1] those employing heat,[2] those

[1] Frankland, J. Chem. Soc., **6**, p. 109; 1854. Meyer, Z. anal. Chem., **2**, p. 237; 1863. Swanson and Hulett J. Am. Chem. Soc., **37**, p. 2490; 1915. Jones, Yant, and Buston, Bureau of Mines Reports of Investigations No. 2553; December, 1923. McClendon, J. Biol. Chem., **30**, p. 259; 1927. Van Slyke, J. Biol. Chem., **30**, p. 347; 1917; **49**, p. 44; 1921. Austin and others, J. Biol. Chem., **54**, p. 129; 1922. Hall, J. Biol. Chem., **55**, p. 751; 1923.

[2] Reichardt, Z. anal. Chem., **11**, p. 271; 1872. Jacobsen, Ann., **167**, p. 12; 1873. Petterson, Ber., **22**, p. 1434; 1889.

employing both vacuum and heat,[3] and those employing freezing.[4]

Unfortunately little information is available as to the relative effectiveness of these processes. Heating alone does not prevent the resolution of the atmospheric gases on cooling, unless special precautions are taken, and it results in a partial loss of the liquid. Evacuation alone involves a similar loss of liquid, and only a partial removal of the total gas content if a constant boiling mixture is formed. Heating combined with evacuation is more effective, although the manipulation is generally inconvenient. The vacuum attainable is limited by the vapor pressure of the liquid at the temperature of condensation, so that the rate of removal is low. There is some loss of liquid, and a constant boiling mixture can not be completely freed from gas. Freezing, alone, is somewhat effective only in the removal of the permanent gases.

The vacuum sublimation process, to be described, includes all the processes named above, since it employs heat, vacuum, and freezing.

The liquids to be freed from gas are vaporized and frozen in vacuo. While the use of vacuum sublimation [5] as a possible means of purification is not new,[6] there are certain experimental requirements which must be met, otherwise little purification will result. These have not been heretofore discussed.

II. THEORY

The conditions essential to the best operation of the process of purification by vacuum sublimation are as follows: (*a*) The temperature at the condensing surface must be considerably below the freezing point of the pure liquid so that its vapor condenses directly to a solid, otherwise a resolution of the gas impurity may occur if a liquid phase is present at the condensing surface during condensation. (*b*) The sublimate must have a negligible vapor pressure at the temperature of condensation or a loss of the pure material will result. (*c*) The third condition can be stated in the following general form: The vapor pressure of the impurity from any system containing it which can exist on the condenser must be greater than the partial

[3] McLeod, J. Chem. Soc., **7**, p. 313; 1855. Hamberg, J. prakt. Chem., **141**, p. 433, 1885. Hoppe-Seyler, Z. anal. Chem., **31**, p. 367; 1892. Thresh, Trans. Chem. Soc., **39**, p. 399; 1881. Thomas, Chem. News, **36**, p. 37; 1877. Thorner, Chem. Zentr., **16**, p. 129; 1877. Richardson, J. Soc. Chem. Ind., **29**, p. 198T; 1910; **38**, p. 32T; 1919. Lorah, Williams, and Thompson, J. Am. Chem. Soc., **49**, p. 2991; 1927. Many patents have been granted for commercial degassing processes, utilizing one or more of these methods.

[4] Faraday, Researches in Chemistry and Physics, Taylor and Francis, p. 373; 1859. It is interesting to note that Mark Twain in "Life on the Mississippi," Author's National Edition, Harper & Bros., p. 303, mentions the removal of dissolved air by stirring during the freezing process in the manufacture of ice at New Orleans.

[5] The term sublimation as used in this article may be defined as the process of passing directly from the vapor to the solid state of aggregation, and is therefore independent of whether the substance sublimed was originally in the liquid or solid state.

[6] McKelvy and Taylor, B. S. Sci. Papers, **18**, p. 679; 1923. Gray, J. Chem. Soc., **87**, p. 1606; 1905.

pressure of the impurity in the gas phase. The following are possible systems of this kind: (1) A liquid phase in equilibrium with the sublimate. Such a system can form only above the eutectic temperature and for a given condenser temperature only if the partial pressure of the impurity in the gas phase exceeds a certain fixed value characteristic of the system. (2) The solid impurity. (3) Mixed crystals containing both sublimate and impurity. (4) Adsorbed impurity.

Condition ($c(4)$) can never be realized since for every pressure of the impurity in the gas phase some adsorption on the condensate is possible. This difficulty is usually of secondary importance, however, and its effect can be made as small as desired by repeated sublimations. The contamination resulting from ($c(3)$) is likewise reduced by successive sublimations.

The partial pressure of the impurity in the gas phase may be reduced by continuous pumping. The limiting total pressure thus obtainable is the vapor pressure of the sublimate. For example, with water as the liquid to be purified, NH_3 as the impurity, and a condensation temperature of $-78°$ C., the minimum total pressure obtainable is 0.001 mm Hg. The partial pressure of NH_3 from its aqueous solution in equilibrium with ice at this temperature is of the order of a millimeter. Condition ($c(1)$), therefore, can not occur and purification results. Similarly with CO_2 and O_2 as impurities, the water may be completely freed from gas.

A different circumstance is met, however, if HCl is the impurity. The partial vapor pressure of HCl from its aqueous solution in equilibrium with ice at $-78°$ C., is much less than 0.001 mm Hg, and condition ($c(1)$) may occur. Part of the ice melts and a resolution of HCl occurs.

In the experiments to be described, NH_3, HCl, CO_2, and O_2 were chosen as gas impurities. For the most part water could, of course, be conveniently freed from these particular impurities by chemical means. They represent, however, types of gas impurities, the complete elimination of which has been heretofore, difficult by physical means.

III. DESCRIPTION OF APPARATUS

The final form [7] of the apparatus employed is shown in Figure 1.

The apparatus consisted essentially of sublimation vessel *A*, liquid air trap *E*, McLeod gage *F*, mercury vapor pump *G*, P_2O_5 drying tubes *H*, and an oil pump. The sublimation vessel *A* was a modified Dewar tube. While the exact dimensions are not essential, it is necessary that the inside tube *C* be of sufficient length, and the space between the two tubes sufficiently small, to condense all the vapor. The distance between the surface of the sample at *D* and the bottom

[7] Other forms were tried and rejected on account of inadequate cooling or too slow a sublimation.

of the tube *C* must be sufficient to prevent small particles of the sample being carried to *C* when evaporation is rapid, but not so great as to materially retard the sublimation. For larger quantities of liquid the dimensions may be suitably increased.

The apparatus may be easily modified so that the purified liquid may be distilled in vacuo directly into a conductivity cell or other apparatus. If it is desired to collect the dissolved gases, a Töpler pump may be employed.

IV. METHOD OF OPERATION

From 10 to 25 ml of the liquid to be freed from gas is introduced into the sublimation tube by means of a pipette lowered through the

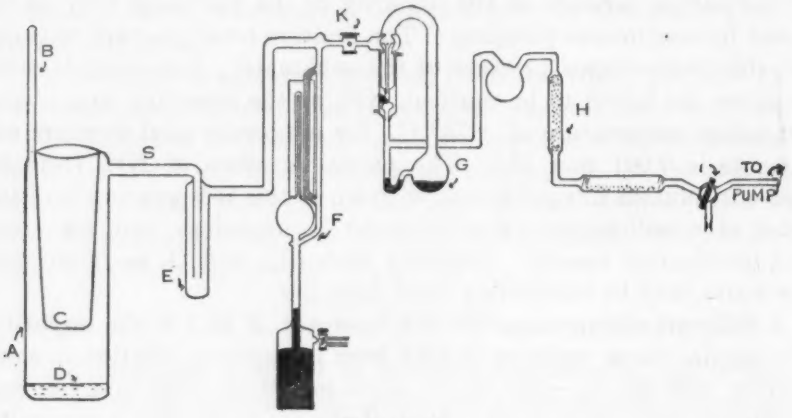

FIGURE 1

side arm *B*. Care is taken to allow no drops from the end of the pipette to touch the walls of either the inside or outside tubes. The side arm is then sealed off at the top. The entire apparatus is subsequently evacuated until the pressure is somewhat above that of the vapor pressure of the liquid to be purified. A cooling agent is then introduced into tube *C*.

If the temperature gradient between the liquid at *D* and tube *C* is great, and the vapor pressure of the liquid relatively high, the rate of evaporation will be excessive, and some of the impure liquid will be carried up in the vapor stream. The temperature, and, consequently, the vapor pressure, of the liquid must be adjusted by means of a suitable bath so that sublimation takes place at a reasonable rate. In the case of liquids of high vapor pressure, it is necessary to freeze them. After the temperatures of the liquid and of the condensing tube are correctly adjusted, the evacuating pumps are started and run continuously. In actual practice with water as the impure liquid; for example, the temperature of condensation is maintained

at about −78° C. by means of CO_2—snow and ether. The vapor pressure of water at this temperature is 0.001 mm. No significant loss occurs. The water is initially cooled with an ice pack and the reduction in pressure carried out very slowly. Because of the cooling effect from the vaporization, the water in *D* rapidly freezes. The rate of sublimation is so rapid, even under these conditions, that the ice is rapidly cooled. It is necessary, then, to warm the ice by a water jacket. This jacket may be maintained at a temperature between 50° and 80° C. without melting the ice. Without this external heat the sublimation is too slow.

When the sublimation is complete, the tube *C* is warmed, and the sublimate melts and drops to the bottom. The apparatus is still kept evacuated during this process. The liquid on the bottom is then frozen and cooled so that any traces of liquid remaining on the tube *C* distill to the bottom. A stopcock may be introduced at *S* between the sublimation tube and the mercury trap to prevent the distillation of the water into the trap during this operation. The process of sublimation may then be repeated if necessary. In case the impurity to be removed is other than the atmospheric gases, the stopcock may be omitted and the apparatus filled with purified air during the melting process.

V. EXPERIMENTAL RESULTS

1. PURIFICATION OF WATER, PART I, AMMONIA AS THE IMPURITY

EXPERIMENT 1.—The results of experiment 1 are given in the following table:

TABLE 1.—*Change in ammonia concentration with sublimation*

Number of sublimations	Ammonia concentration (in mg per ml)
0	1.1
1	.16
2	.025
3	.0075

The NH_3 concentration was estimated colorimetrically by means of Nessler's reagent. The temperature of condensation was approximately −78° C.

Only three-quarters of the original sample of 20 ml was sublimed in the last case. The residue was tested for NH_3 and showed an increase from 0.025 to 0.040 mg NH_3 per ml—that is, a total of 0.07 mg of the NH_3 in the residue was present as the carbonate. After the second sublimation the actual free NH_3 was, therefore, 0.021 mg

per ml. The residual NH_3 after several sublimations would approach 0.0036 mg NH_3 per ml. By sublimation of the greater fraction and rejection of the small remaining residue the ultimate limit of purification would be considerably extended.

EXPERIMENT II.—This experiment was undertaken to compare the relative effectiveness of freezing alone as compared with freezing followed by sublimation. The 25 ml sample was frozen in vacuum with pumping, as in the preceding experiments. After two freezings the initial ammonia concentration of 1.0 mg per ml was reduced to 0.5 mg per ml. With two more freezings this became 0.30 mg per ml.

Between the second and third freezings enough NaOH was added to correspond to about one-half of the NH_3 left. This was to fix the CO_2 possibly present. Following the fourth freezing the solution was sublimed as in the preceding experiments. The first sublimation gave immediately a change from 0.3 to 0.05 mg per ml.

The efficiency of the sublimation process is much greater than that of the freezing alone in this case.

2. PURIFICATION OF WATER, PART II, HYDROCHLORIC ACID AS THE IMPURITY

The method devised for the purification of the water-ammonia solution was then applied to dilute solutions of HCl. The concentration of the acid was determined in the following manner: 1 ml of the HCl solution of unknown concentration was added to 7 ml of saturated potassium iodate solution containing 30 g of KI in 200 ml. To this five drops of starch solution were added. The iodine, freed by the reaction of HCl with KIO_3, colors the starch in the usual manner. This colored solution was then colorimetrically compared with a solution which had been treated with a known amount of HCl.

The sublimation procedure was the same as that previously described.

In the first experiment the concentration of HCl changed from 1.0 to 0.95 mg per ml after one sublimation. A second sublimation reduced the concentration only to 0.70 mg per ml. The volume of the sample was 25 ml.

In a second experiment the HCl concentration in mg per ml changed from 1.0 to 0.90 after one sublimation. In this case 23 ml was sublimed. The remaining 2 ml was withdrawn and titrated with $AgNO_3$ solution. The concentration was slightly less than 2.5 mg per ml. The decrease in concentration caused by sublimation is offset by an increase in HCl concentration in the residue.

In a third experiment the HCl concentration changed from 1.0 to 0.88 mg per ml after one sublimation. The sample was 10 ml. All but 4 ml was sublimed. The residue contained 1.25 mg per ml. As in the second experiment, therefore, the decrease in concentration of HCl in the sublimate is accompanied by an increase in concentra-

tion of HCl in the residue. There is no actual removal of HCl in the process. The HCl concentration could be diminished by repeated fractional sublimation in this manner. It is evident that condition (*c*) 1)) under theory occurs.

3. PURIFICATION OF WATER, PART III, OXYGEN AS THE IMPURITY

The apparatus used in this case was similar to that used for the purification of water from ammonia or HCl, with the modification that a McLeod gauge was installed in the evacuating system. The oxygen-saturated water was placed in the sublimation system and there frozen during constant evacuation. The system was then closed off from the evacuating pumps leaving the gauge connected to the sublimation apparatus. The ice was then sublimed. During this process the pressure was measured at intervals. From the final pressure and the volume of the system, the residual oxygen at NTP may be calculated. Liquid air was used as the cooling agent in this experiment.

In the first experiment the oxygen concentration was 1.0 ml per ml in a sample of 25 ml. After one freezing, with no purification by sublimation, the oxygen concentration became 0.00048 ml per ml.

4. PURIFICATION OF WATER, PART IV, CARBON DIOXIDE AS THE IMPURITY

EXPERIMENT 1.—The CO_2 saturated water was treated in precisely the same manner as in the oxygen experiment. CO_2—snow, however, was used as the cooling agent. The saturated solution was evacuated while freezing. Pumping extended over a period of about 15 minutes to remove all the gas liberated from the freezing process alone. The system was then closed and the ice sublimed. The results are given in Table 2:

TABLE 2.—*The amount of carbon dioxide evolved on sublimation after one freezing*

Duration of sublimation (in minutes)	Pressure of CO_2 in mm Hg
0	0.001
20	.01
105	.13
165	.163
	.170

The original sample of 25 ml contained 22.5 ml CO_2 (NTP) per ml liquid. The final pressure of 0.170 mm Hg obtained after sublimation corresponded to a concentration of 0.135 ml CO_2 per ml liquid or a reduction to 0.6 per cent of the original concentration by one freezing.

The foregoing data under Parts III and IV represent the degree of purification due to freezing alone. If, however, the process of evacu-

ation is maintained during the initial sublimation, then after a second sublimation without evacuation the partial pressure of the dissolved gases remaining is not measureable even when the total volume of the system is reduced to 100 ml. Within the sensitivity of the pressure-measuring device, this means, for example, that the concentration of oxygen may be reduced by only one sublimation to less than one ten-thousandth of 1 per cent.

The author wishes to express his appreciation of the advice and criticisms given during this research by Dr. E. W. Washburn, and his indebtedness to him for the suggestion of this problem.

VI. SUMMARY

A method of removing dissolved gases from liquids has been devised which permits the complete recovery of both the dissolved gas and the liquid. Gas-free liquids may be prepared by this method for use in the determination of those physical constants of the liquids wherein extreme purity is prerequisite.

The theoretical and experimental limitations of the system have been discussed.

WASHINGTON, September 21, 1928.

SOME ABSORPTION PROPERTIES OF CLAY BRICKS

By L. A. Palmer

ABSTRACT

A study of the absorption properties of 10 manufacturers' bricks has been made. This investigation included a study of the extent of absorption during total immersion of the bricks in water both at boiling and at room temperatures, as well as the various rates of absorption during partial immersion of the specimens. Two empirical equations, one relating to total and the other to partial immersion, have been found to apply reasonably well to the data obtained.

CONTENTS

	Page
I. Introduction	105
1. Purpose of the investigation	105
2. Materials	106
II. Absorption during total immersion	107
1. Method of Procedure	107
2. Results	107
3. Discussion of results	113
III. Rate of absorption during partial immersion	117
1. Method of procedure	118
2. Results	118
3. Discussion of results	122
IV. General discussion	124
V. General summary	126
VI. Acknowledgments	127

I. INTRODUCTION

1. PURPOSE OF THE INVESTIGATION

The results of the investigation presented and discussed in this paper constitute the first step of an investigation, "Wet wall interiors," sponsored by the American Face Brick Association and being conducted at the National Bureau of Standards.

The data and discussion presented in this paper concern marketable bricks. The study has been restricted to the absorption properties of such bricks, taking into account not only the various degrees of water absorption under definite conditions but also the various rates of such absorption. Obviously these data are necessary if the various factors involved in the transmission of moisture through brick masonry are to be capable of a true analysis.

Frequent mention is being made of Kreüger's [1] ratio, or as he terms it, "coefficient of water saturation." This is the ratio of the pore

[1] H. Kreüger, "Utredning rorande klimatisk inverkan pä bjggnadsfasader" Ingeniörs Ventenspaka Akademien, No. 24, p. 73; 1923.

space (within a building unit) that is filled with water during a definite period of partial and total immersion of the specimen to the total pore space (including sealed pores) of the specimen. H. G. Schurecht [2] has used a ratio differing from that of Kreüger in that the apparent rather than the total porosity is considered. This "pore ratio," as used by Schurecht, is the percentage absorption (computed on the basis of the dry weight of the specimen) during 48 hours of total immersion of the specimen in water at room temperature divided by the percentage absorption during immersion of the specimen for five hours in boiling water. Essentially the Schurecht ratio alone (designated in this paper as X) has been evaluated from the data here presented. The procedure used by the author in the tests described herein was to continue total immersion of the brick in water at room temperature for a time such that the rate of gain in weight of the specimen was less than a gram during 24 hours. In no instance was this time less than 48 hours. In many cases it was 72 and 96 hours. A 7 rather than a 5 hour boiling period was another departure from Schurecht's procedure.

2. MATERIALS

Ten different manufacturers' bricks were studied. About 300 to 500 bricks were received from each of the 10 manufacturers. This number of bricks in each case, according to the manufacturer's statement, represented his "range"; that is, they were so selected from the kiln of bricks as to represent a vertical "cross section" of the kiln and included a number of the relatively soft-burned bricks in the kiln, a number of the hardest burned, and many that were distributed at various points between these two extreme conditions. In Table 1 are presented data showing the character of clays from which the bricks were made and how they were molded.

TABLE 1

Manufacturer's No.	Types of clays used	Method of forming
1	Surface clay	Dry-press.
2	do	Do.
3	Shale	Stiff-mud, side-cut.
4	Fire clay	Dry-press.
5	Shale	Do.
6	Shale (same as No. 5)	Stiff-mud, side-cut.
7	Shale	Do.
8	Surface clay	Soft-mud.
9	Shale	Stiff-mud, side-cut.
10	Fire clay	Do.

The fire clays used were not the typical high-grade fire clays used in the manufacture of refractory bricks.

[2] Senior fellow, National Terra Cotta Society research fellowship, National Bureau of Standards, Washington, D. C. Unpublished data.

II. ABSORPTION DURING TOTAL IMMERSION

1. METHOD OF PROCEDURE

Each brick was first dried in a gas-fired oven (temperature 110° to 160° C.) for a time such that during an additional 24 hours in the oven any further loss in weight was less than 1 g. They were then weighed on a balance sensitive to ± 1 g. The dried bricks were then kept in a dry atmosphere until they were cooled to room temperature. This required at least 24 hours. They were then completely immersed in water at room temperature and for a time such that the gain in weight became less than 1 g during 24 hours.

Upon removing a brick from the water and prior to weighing it, four minutes' time was allowed during which the brick rested on its edge in a dry pan. It was then wiped quickly with a damp (neither dry nor saturated) towel and weighed. If the amount of moisture gained by the brick during its period of immersion was relatively small, it was put back into water after the first weighing and, after an elapse of a few minutes, was removed, wiped, and weighed again. If the two weighings differed by more than 2 g an average of several weighings was made following several repetitions of this procedure.

From a hundred or more of bricks of one type so tested there were selected a representative number of such for further tests. This number included those lowest and those highest in absorption as determined by the cold-absorption test, as well as several which absorbed amounts of water to an intermediate extent.

These selected bricks were then quickly transferred to boiling water and kept in such for a period of seven hours. By admitting warm water slowly and fairly constantly during this period loss from evaporation was replenished and the vigorous boiling was seldom interrupted. The bricks were then cooled, while still immersed, to room temperature and were weighed in the air. They were then weighed again while immersed in water at room temperature. The weight of each brick (saturated with water) minus its weight while suspended in water represented the bulk volume in milliliters of that brick. This was converted to cubic inches, and the brick volumes so recorded. The absorption during the cold immersion and that during boiling were expressed in grams of water per 65 cubic inches [3] bulk volume of brick.

2. RESULTS

In the first column of Table 2 are given the numbers of individual bricks. In the second column, Y denotes grams of water absorbed per 65 cubic inches of bulk volume of brick during the period of

[3] 65 cubic inches is about the volume of a brick of average size. In specifications brick dimensions are expressed in inches.

cold immersion. This period ranged from 48 to 120 hours, depending upon the rate of absorption of the brick. As has already been mentioned, this test was terminated when it was found that the rate of gain in weight was less than 1 g during 24 hours. In the third column are given the number of grams of water absorbed per 65 cubic inches of bulk volume of brick following the 7-hour boiling period. Z (fourth column) denotes the difference between the $Y+Z$ value and the corresponding Y value. Z is then also computed on the basis of the volume, 65 cubic inches. Since 1 g of water occupies approximately a volume of 1 ml, all of the numbers under Y, $Y+Z$, and Z may be considered as ml. On this basis, Y represents the ml of open pore space per 65 cubic inches of bulk volume of brick that can be entered by cold water during a certain time interval, $Y+Z$ represents the volume in ml, of the pore space that was filled during the boiling tests, and Z is the pore space that can be entered by boiling water, but which can not be entered by cold water. In the fifth column, X is obtained by dividing the Y value by the corresponding $Y+Z$ value. In the last column are recorded the results obtained by dividing each Y value by the cube of X. The reason for so computing the data will be fully explained in the discussion following Table 2. The value, K, will hereafter be referred to as the "absorption constant."

TABLE 2.—*Grams of water absorbed per 65 cubic inches bulk volume of brick during total immersion*

BRICK NO. 1

Specimen No.	Grams of water absorbed during cold immersion (Y)	Grams of water contained after 7 hours' boiling ($Y+Z$)	Difference, grams of water contained after boiling—that absorbed during cold immersion (Z)	Ratio of Y to $Y+Z$ (X)	Values of $K=Y/X^3$
1	372	456	84	0.816	686
2	362	444	82	.815	669
3	339	435	96	.780	714
4	355	438	83	.810	668
5	338	423	85	.800	660
6	337	427	90	.790	686
7	335	422	87	.794	669
8	321	412	91	.779	679
9	318	403	85	.789	648
10	313	405	92	.772	680
11	313	404	91	.775	672
12	312	409	97	.760	710
13	310	405	95	.765	692
14	304	400	96	.763	684
15	298	389	91	.766	663
16	290	380	90	.763	653
17	280	379	99	.739	694
18	271	372	101	.728	702
19	264	365	101	.723	698
20	238	344	106	.692	718

TABLE 2.—*Grams of water absorbed per 65 cubic inches bulk volume of brick during total immersion*—Continued

BRICK NO. 2

Specimen No.	Grams of water absorbed during cold immersion (Y)	Grams of water contained after 7 hours' boiling ($Y+Z$)	Difference, grams of water contained after boiling—that absorbed during cold immersion (Z)	Ratio of Y to $Y+Z$ (X)	Values of $K=Y/X^3$
1	271	319	48	0.850	441
2	268	316	48	.846	440
3	276	327	51	.845	456
4	257	302	45	.850	417
5	251	305	54	.823	448
6	224	280	56	.800	437
7	219	273	54	.802	427
8	209	263	54	.795	416
9	208	267	59	.779	440
10	206	265	59	.777	439
11	205	256	51	.801	401
12	202	257	55	.785	418
13	165	223	58	.740	407
14	143	201	58	.711	400
15	137	200	63	.685	426

BRICK NO. 3

1	191	237	46	0.806	365
2	180	224	44	.804	345
3	173	221	48	.783	360
4	170	211	41	.806	325
5	165	214	49	.771	360
6	158	206	48	.767	350
7	157	205	48	.766	349
8	166	214	48	.776	355
9	139	186	47	.746	335
10	118	170	52	.694	353
11	118	168	50	.702	341
12	115	165	50	.700	335
13	103	155	52	.665	350
14	102	153	51	.667	344
15	101	153	52	.660	351
16	93	146	53	.637	359
17	91	140	49	.650	331
18	91	141	50	.645	339
19	86	134	48	.642	325
20	70	119	49	.588	344
21	62	102	40	.608	276
22	61	106	45	.575	321
23	58	107	49	.542	364

BRICK NO. 4

1	233	275	42	0.847	381
2	226	268	42	.843	377
3	224	265	41	.845	371
4	200	237	37	.844	333
5	194	240	46	.808	368
6	189	234	45	.808	358
7	184	227	43	.810	346
8	176	223	47	.790	357
9	174	214	40	.813	324
10	174	216	42	.805	334

TABLE 2.—*Grams of water absorbed per 65 cubic inches bulk volume of brick during total immersion*—Continued

BRICK NO. 4—Continued

Specimen No.	Grams of water absorbed during cold immersion (Y)	Grams of water contained after 7 hours' boiling ($Y+Z$)	Difference, grams of water contained after boiling—that absorbed during cold immersion (Z)	Ratio of Y to $Y+Z$ (X)	Values of $K=Y/X^2$
11	169	214	45	0.789	344
12	162	205	43	.790	329
13	162	203	41	.800	316
14	154	201	47	.766	343
15	153	197	44	.776	327
16	148	192	44	.770	326
18	142	183	41	.776	304
19	137	182	45	.755	318
20	131	179	48	.732	338
21	122	168	46	.726	319
22	102	153	51	.667	344
23	101	154	53	.658	355
24	100	152	52	.658	351
25	96	147	51	.653	345
26	90	141	51	.638	346

BRICK NO. 5

1	287	339	52	0.847	472
2	289	340	51	.850	476
3	283	333	50	.850	461
4	281	334	53	.842	471
5	282	336	54	.839	477
6	277	329	52	.842	464
7	277	334	57	.829	486
8	272	328	56	.829	477
9	271	327	56	.829	476
10	269	321	52	.838	457
11	269	322	53	.835	462
12	252	309	57	.816	464
13	252	308	56	.817	462
14	239	295	56	.810	450
15	232	294	62	.789	472
16	230	288	58	.800	450
17	229	282	53	.812	428
18	222	289	67	.767	492
19	221	284	63	.778	469
20	221	277	56	.800	432
21	220	282	62	.781	462
22	218	276	58	.790	442
23	197	264	67	.746	474

BRICK NO. 6

1	324	421	97	0.770	710
2	305	403	98	.757	703
3	302	387	85	.780	636
4	287	382	95	.751	678
5	280	378	98	.741	688
6	277	376	99	.737	693
7	277	371	94	.747	665
8	247	352	105	.702	714
9	241	345	104	.699	706
10	240	344	104	.698	706
11	215	321	106	.670	715
12	191	285	94	.670	635

TABLE 2.—*Grams of water absorbed per 65 cubic inches bulk volume of brick during total immersion*—Continued

BRICK NO. 7

Specimen No.	Grams of water absorbed during cold immersion (Y)	Grams of water contained after 7 hours' boiling ($Y+Z$)	Difference, grams of water contained after boiling—that absorbed during cold immersion (Z)	Ratio of Y to $Y+Z$ (X)	Values of $K=Y/X^3$
1	58	109	51	0.532	385
2	48	97	49	.500	384
3	35	76	41	.461	357
4	35	79	44	.443	403
5	41	87	46	.471	392
6	34	75	42	.445	386
7	34	75	41	.453	366
8	33	76	44	.434	404
9	32	70	38	.457	336
10	32	75	43	.427	411
11	30	71	41	.423	396
12	30	69	39	.435	364
13	25	58	33	.431	313
14	25	62	37	.403	382
15	24	61	37	.393	395
16	23	58	35	.400	360
17	20	54	34	.370	395
18	19	50	31	.380	346
19	19	52	33	.365	391
20	18	51	33	.353	409
21	18	50	32	.360	385
22	17	49	32	.347	407
23	16	48	32	.333	432
24	16	45	29	.356	354
25	15	45	30	.333	405
26	15	45	30	.333	405
27	13	40	27	.325	379
28	7	27	20	.260	400

BRICK NO. 8

1	249	303	54	0.822	449
2	247	303	56	.815	456
3	231	297	66	.778	491
4	230	294	64	.782	481
5	227	285	58	.793	455
6	179	240	61	.729	462
7	172	239	67	.720	461
8	152	220	68	.690	462
9	144	212	68	.679	462
10	132	203	71	.650	480
11	101	165	64	.612	436
12	95	151	56	.629	392
13	91	154	63	.591	441
14	90	152	62	.592	434
15	80	137	57	.584	402
16	73	124	51	.588	360
17	44	93	49	.473	416

TABLE 2.—*Grams of water absorbed per 65 cubic inches bulk volume of brick during total immersion*—Continued

BRICK NO. 9

Specimen No.	Grams of water absorbed during cold immersion (Y)	Grams of water contained after 7 hours' boiling ($Y+Z$)	Difference, grams of water contained after boiling—that absorbed during cold immersion (Z)	Ratio of Y to $Y+Z$ (X)	Values of $K=Y/X$
1	165	209	44	0.790	335
2	135	182	47	.742	330
3	133	178	45	.747	319
4	130	180	50	.722	345
5	131	178	47	.736	328
6	130	176	46	.735	328
7	125	175	50	.717	339
8	124	173	49	.716	338
9	122	173	51	.705	348
10	118	168	50	.702	341
11	115	164	49	.701	335
12	112	162	50	.690	341
13	107	160	53	.671	354
14	107	158	51	.677	345
15	107	161	54	.665	367
16	105	156	51	.673	344
17	104	155	51	.671	344
18	95	146	51	.651	344
19	92	145	53	.634	361
20	92	143	51	.643	346
21	88	138	50	.638	338
22	83	134	51	.619	350
23	80	127	47	.623	331
24	75	125	50	.597	352
25	70	119	49	.588	344
26	64	109	45	.583	323
27	63	111	48	.566	348
28	60	107	47	.561	339

BRICK NO. 10

1	154	243	89	0.634	604
2	141	228	87	.617	600
3	138	226	88	.610	608
4	125	211	86	.592	602
5	123	209	86	.584	618
6	113	193	80	.585	564
7	111	196	85	.566	612
8	110	192	82	.573	585
9	100	181	81	.552	595
10	100	178	78	.562	563
11	97	177	80	.548	589
12	94	174	80	.540	597
13	83	161	78	.516	604
14	72	145	73	.497	586
15	71	149	78	.477	654
16	63	132	69	.476	584
17	62	133	71	.465	617
18	59	124	65	.475	550
19	50	114	64	.440	587
20	47	112	65	.419	639
21	44	105	61	.418	602

3. DISCUSSION OF RESULTS

The various Y values of 8 of the 10 types of bricks are plotted against their corresponding X ratios on a logarithmic scale in Figures 1 and 2. The data for bricks Nos. 4 and 5, if plotted, would coincide with those of Nos. 3 and 2, respectively. By so plotting these data, it is noted that straight lines which are practically parallel to one another are obtained; that is, the slope is about the same and very nearly equal to 3 in all cases. The intercepts of any of these lines

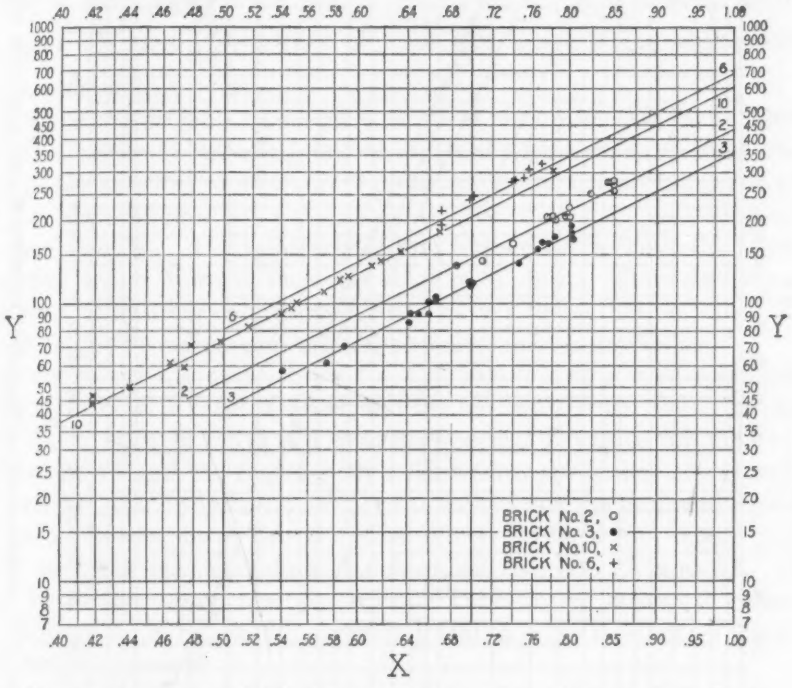

FIGURE 1.—*Values of Y plotted against corresponding values of X, on logarithmic scale*

on the ordinate axis ($X=1$) denote the absorption constants (K values) as obtained graphically. Starting with the equation

$$Y = KX^3 \tag{1}$$

since $X=\frac{Y}{Y+Z}$, or $Y(1-X)=XZ$, and $Y=\frac{XZ}{(1-X)}$, there results by substitution in equation (1)

$$Z = K(X^2 - X^3) \tag{2}$$

It is obvious that X can not have negative values, and it is further evident that all of the values of X will be greater than zero and less

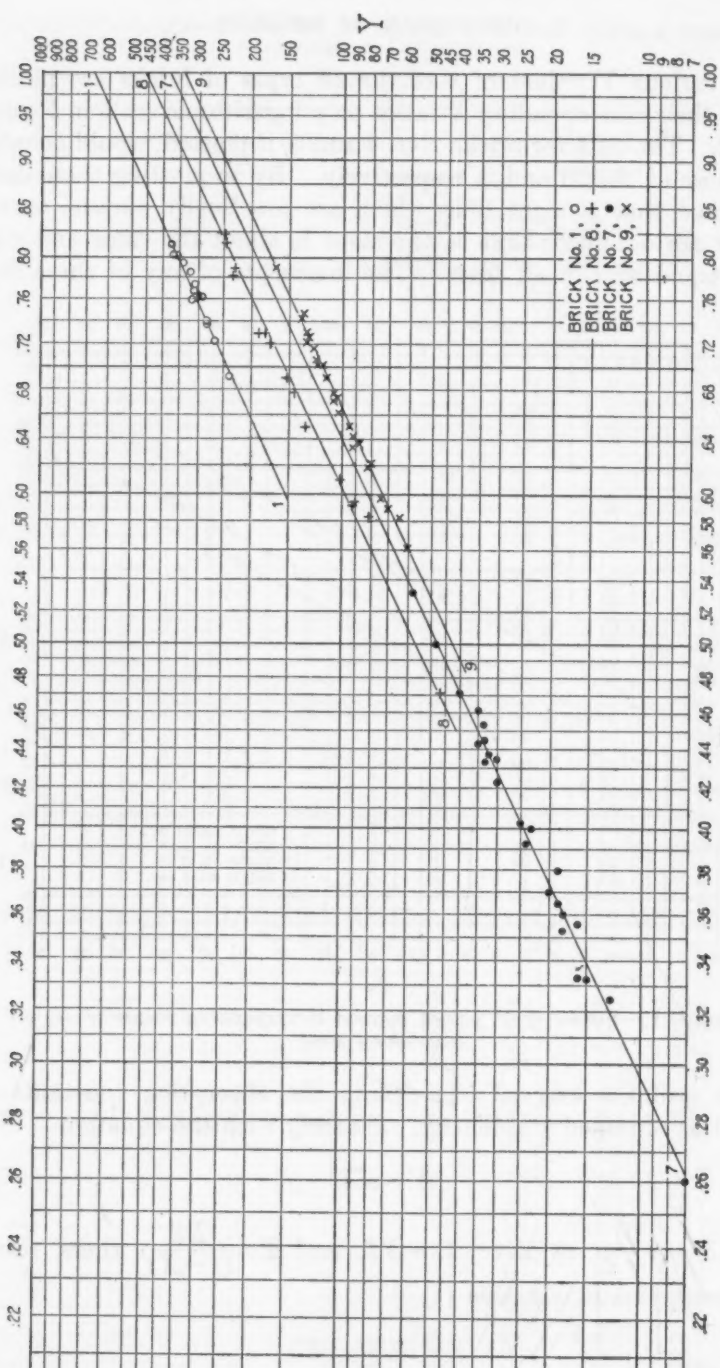

FIGURE 2.—*Values of Y plotted against corresponding values of X, on logarithmic scale*

than unity for the type of material studied. From equation (2) when X is zero, Z also is zero, and when X is unity, Z is zero. Since X can not be greater than one, Z can have no negative values. Z must, therefore, have a maximum value, since the curve from $X=0$ to $X=1$ is continuous. When Z is a maximum, $\frac{dZ}{dX}$ is zero. Differentiating equation (2) with respect to X gives

$$\frac{dZ}{dX} = KX(2-3X) \qquad (3)$$

Between the limits, $X=0$ and $X=1$, therefore, it is evident from equation (3) that $\frac{dZ}{dX}=0$ when $X=2/3$, and hence Z has its greatest magnitude at this point.

It would be difficult to assign a physical reason for this fact. One thing, however, is indicated, and this is that with increasing temperature in the kiln the pore structure of an individual brick changes more or less according to some fundamental law that may be expressed mathematically. The relatively harder burned bricks have the lower and the softer burned ones the higher X ratio. Between these extremes of burning conditions X may have a value, 2/3, at which Z, which might be called the residual porosity, is at a maximum.

As an example, consider brick No. 3. The softest-burned specimen is No. 1 with an X ratio of 0.806, and the hardest-burned one is No. 23 with an X ratio of 0.542. The corresponding Z values for the two bricks are 46 and 49, respectively. However, specimens 10, 11, 12, 13, and 14, which represent neither the softest nor the hardest burned of the 23 bricks, have the X ratios, 0.694, 0.702, 0.700, 0.665, and 0.667 and the corresponding Z values, 52, 50, 50, 52, and 51. It may be further noted that throughout Table 2 the various Z values are highest for X ratios ranging from 0.600 to 0.700 in all cases where this range is covered.

Certain corollaries follow from equations (1) and (2). These are—

1. Z reaches a maximum when $X=⅔$ as shown above.
2. From equation (1), $Y=Y+Z=K$ when $X=1$.
3. When Z is a maximum, $Y=$twice maximum Z. For since $Y=\frac{XZ}{1-X}$, and since Z is at a maximum when $X=⅔$, then $Y=\frac{(⅔)\ Z\ \text{maximum}}{1-⅔}=2Z_{max.}$
4. $K=6¾$ times $Z_{max.}$ From equation (1), $Y=(⅔)^3K$ when $X=⅔$, and since $Y=2Z_{max.}$ at this point, then $2Z_{max.}=(⅔)^3K$, or $K=6¾$ times $Z_{max.}$

These corollaries may now be applied to the data of Table 2. A few typical cases may be noted. In the following brief recapitulation

of a few of the results, figures in the fifth column are obtained by multiplying the Z value corresponding to an X ratio of ⅔ (characteristic of a particular specimen) by 6¾. The result may be compared with the corresponding K (sixth column), which is the average value for the type of brick considered.

TABLE 3

Brick No.	Specimen No.	X	$Z_{max.}$	$(6\frac{3}{4})$ $Z_{max.}$	K (average)	$2Z_{max.}$	Y corresponding to $Z_{max.}$
3	14	0.667	51	344	342	102	102
4	22	.667	51	344	336	102	102
6	11	.670	106	716	687	212	215
9	(1)	.669	53	358	341	106	106

[1] Average of Nos. 13, 15, and 17.

The figures in the seventh column compare favorably with the corresponding figures of the eighth, illustrating the applicability of corollary 3 to the data of Table 2.

The values of Z in the data for the other six types of bricks, not listed above, are seen to increase in every case as X approaches more and more closely to 0.667.

It is apparent also from a study of Table 2 that one manufacturer's single brick made from a certain clay or shale and molded by a particular process may have the same X ratio as that of another individual brick made by a different manufacturer from a different clay or shale, yet the degree of absorption of the two bricks differ markedly. A few examples will serve to illustrate this point.

TABLE 4

Brick No.	Specimen No.	X	Y	K (average)
1	20	0.692	238	682
2	15	.685	137	428
3	10	.694	118	342
6	10	.698	240	687
8	8	.690	152	444
9	12	.690	112	341

In this connection, note that sample 20, type No. 1, is a brick made from surface clay, molded by the dry-press process, whereas sample 12 of type No. 9 is a brick made from shale aud molded by the stiff-mud process. The absorption constant, K, of No. 1 is approximately equal to that of No. 6.

Since K in any case equals $(6\frac{3}{4})$ $Z_{max.}$, it is evident that the greater is K for any manufacturer's brick, the greater also (relatively) is $Z_{max.}$ Also, since the Y corresponding to $Z_{max.}$ is equal to twice $Z_{max.}$ it follows that for a given Schurecht ratio, X, types of bricks

having the relatively larger absorption constants are relatively more absorbent than are the types of bricks having the lower constants.

Whatever K for a particular type of brick may be dependent upon, it is apparently independent of the heat treatment which the brick received over a certain range of temperature at least. The bricks of any of the 10 types of Table 2 having the five largest Y and $Y+Z$ values are numbered from 1 to 5 in each case. These bricks were taken by the manufacturer from the lower portions of the down-draft kiln where the temperature during firing is usually lowest. The bricks of any of the 10 types designated by numbers higher than 10 are harder burned. These were selected from the tops of the kilns. They have lower Y and $Y+Z$ values, are darker in color, and are slightly smaller than are the softer burned bricks, yet both the relatively soft and the relatively hard burned bricks of any one type have the same absorption constant, K. The value, K, is apparently characteristic of a type of brick over a comparatively wide range of firing temperature.

Nothing has been done as yet to determine the limits in degree of burning beyond which the relation, $Y=KX^3$, ceases to hold. It was found to obtain among the 10 types of bricks over a relatively wide range of burning, but yet for marketable bricks only. None of these bricks have the appearance of being distinctly underburned or overburned. All of the water which any of the bricks absorbed during boiling was lost upon drying them at 100° to 110° C., and when placed in a chamber of 95 to 100 per cent relative humidity, none of these bricks, initially dry, gained as much as a gram of water during a week's time, thus indicating that there was no appreciable hydration or adsorption. It is possible that a brick that is distinctly underburned may hydrate and adsorb moisture. This is indicated in the results obtained by Washburn.[4] It has been further shown by McBain and Ferguson [5] that bricks burned at relatively high temperatures adsorb little or no moisture when kept in an atmosphere of high relative humidity. When there is an appreciable amount of hydration and adsorption together with absorption, it does not seem likely that the symmetrical relation, $Y=KX^3$, would apply.

III. RATE OF ABSORPTION DURING PARTIAL IMMERSION

In the study of the various factors involved in the transmission of water through brick masonry it is necessary to know the rate as well as the total extent of water absorption.

Aside from noting the approximate time required for water to wet the total length, breadth, or thickness of the brick, no attempt was

[4] Edward W. Washburn and Frank F. Footitt, J. Am. Cer. Soc., **4** (12), p. 974; 1921.
[5] McBain and Ferguson, J. Phys. Chem., **31** (4), pp. 562-594; 1927.

made to study rates of water penetration from the standpoint of any other distance versus time relationship. It was found to be exceedingly difficult to know in many cases when water "struck through"; that is, appeared on that face, end, or flat side opposite to the corresponding surface in contact with water. It was observed, also, that the upward flow of water by capillarity proceeded at markedly different rates through the various parts of some of the specimens tested.

1. METHOD OF PROCEDURE

The bricks were first dried to constant weight. If the bricks absorbed very rapidly (this was always characteristic of the dry-press bricks) so that the tests could be completed within less than 30 minutes with comparatively slight loss from evaporation, the tests were conducted in the air of the laboratory. In case the absorption proceeded more slowly and the error introduced by evaporation from the brick surface above the water became thereby appreciable, the tests were conducted in a chamber, the relative humidity of which was greater than 95 per cent.

The bricks were weighed when completely dry and cool and then set on thin wires in pans containing a measured volume of water at room temperature. This amount of water was so measured that the bricks were each immersed to a depth of ⅛-inch when they were set on end, on face, or flatwise in the pans. At the end of definite time intervals, the bricks were removed from the pan and the wetted portions were wiped with a damp towel, following which the samples were weighed. They were then returned to the pan. A half minute was taken for this complete operation in all cases.

2. RESULTS

In Table 5 are given some of the calculated results of these tests made with some of the 10 types of bricks described in Section II. Absorptions were noted, and the values of C were computed for minute intervals in the case of the dry-press bricks and at hour intervals for the more impervious stiff-mud bricks. In order to reduce the size of this table, instead of giving the actual gain in grams during partial immersion (⅛ inch) through the edge, end, or flat side of the brick at the end of definite time intervals, there is given for each single brick of a type a value, C, at the end of a time interval, T. If W equals the gain in grams of water in the brick at the end of a time interval, T, $C=\frac{W}{T^{1/3}}-BT$. C and B are constants.

As an example, consider the individual specimen No. 3 among brick No. 2 of Table 5. When No. 3 rested on edge in water to a depth of ⅛ inch, the actual gain in weight was as follows:

	1 min.	2 min.	3 min.	4 min.	5 min.	6 min.	7 min.	8 min.
gain (g)	110	152	174	197	217	237	256	274

This was one of a type of brick that was characterized by a very high rate of absorption. If these numbers are each divided by the cube root of the corresponding time interval, they become—

$$\frac{110}{1^{1/3}}=110, \quad \frac{197}{4^{1/3}}=124, \quad \frac{256}{7^{1/3}}=133,$$

$$\frac{152}{2^{1/3}}=117, \quad \frac{217}{5^{1/3}}=127, \text{ and } \frac{274}{8^{1/3}}=137.$$

$$\frac{174}{3^{1/3}}=121, \quad \frac{237}{6^{1/3}}=130,$$

It is seen that the rate of change of $\frac{W}{T^{1/3}}$ with respect to T is fairly constant; that is, $\frac{d}{dT}\left(\frac{W}{T^{1/3}}\right)=$ a constant, B. Proceeding from the first-minute interval to the eighth the difference between the respective $\frac{W}{T^{1/3}}$ values are 7, 4, 3, 3, 3, 3, and 4. Taking B or $\frac{d}{dT}\left(\frac{W}{T^{1/3}}\right)$ as 3 the average of these values obtained graphically, C at the first-minute interval equals $\frac{W_1}{T_1^{1/3}}-BT_1=110-3=107$. C at the end of the second-minute interval equals $\frac{W_2}{T_2^{1/3}}-BT_2=117-6=111$, and so on.

It was found to be generally true that $\frac{d}{dT}\left(\frac{W}{T^{1/3}}\right)=$ a constant B (within experimental error) under constant conditions and with a definite surface area of brick in contact with water. Performing the indicated operation, $\frac{d}{dT}\left(\frac{W}{T^{1/3}}\right)=\frac{T^{1/3}\,\frac{dW}{dT}-\frac{WT^{-2/3}}{3}}{T^{2/3}}=B$, this equation reduces to $\frac{dW}{dT}=\frac{W}{3T}+BT^{1/3}$, which is an expression for the actual rate of absorption. Integration of this simple linear differential equation, yields the equation, $C=\frac{W}{T^{1/3}}-BT$, where C is a constant of integration.

In the last column throughout Table 5, Y has the same meaning as assigned to it in Table 2. It denotes the total absorption of the individual brick when immersed in water at normal room temperature.

TABLE 5.—*Rate of absorption of water by partial immersion (depth of one-eighth inch) of brick*

BRICK NO. 2 (SET ON EDGE)

Sample No.	B	$C=\frac{W}{T^{1/2}}-BT$									Total grams of water absorbed Y
		1 minute	2 minutes	3 minutes	4 minutes	5 minutes	6 minutes	7 minutes	8 minutes	10 minutes	
3	3.0	107	114	112	112	112	112	112	113	----	282
208	3.0	102	104	104	103	103	102	101	101	----	295
175	4.0	104	108	109	109	107	106	105	104	----	296
214	2.3	120	121	122	118	122	122	122	122	----	296
144	1.0	102	104	103	103	104	104	103	104	----	274
74	2.0	92	94	95	95	95	95	95	93	----	242
155	2.7	85	86	87	86	86	85	84	84	----	222
24	2.3	85	85	87	88	87	86	85	85	----	217
127	2.6	49	52	51	54	53	51	50	49	----	210
12	2.3	69	69	70	70	70	73	70	69	----	203
210	2.0	79	81	83	83	82	81	81	80	----	202
111	2.3	57	60	60	60	60	59	58	57	----	196
171	1.0	53	47	49	50	50	51	51	51	48	171
4	0	47	50	42	44	43	44	46	46	46	156

BRICK NO. 3 (SET ON EDGE)

Sample No.	B	$C=\frac{W}{T^{1/2}}-BT$								Total grams of water absorbed Y
		1 hour	2 hours	3 hours	4 hours	5 hours	6 hours	7 hours	8 hours	
18	2.0	80	81	79	79	81	80	----	----	191
15	3.0	70	72	71	70	72	72	----	----	180
6	2.5	64	68	66	67	66	65	----	----	172
44	2.7	60	62	62	64	62	62	----	----	164
54	2.4	54	55	54	56	53	53	----	----	153
110	2.5	47	49	48	48	49	47	----	----	140
68	2.2	48	47	49	50	47	47	----	----	138
111	2.0	42	44	44	43	42	44	----	----	132
32	1.8	40	42	41	42	40	38	----	----	123
101	2.1	33	34	34	34	33	35	----	----	115
73	1.6	26	28	28	29	26	28	----	----	96
38	1.5	23	26	25	25	26	26	----	----	90
81	2.3	22	24	25	24	26	24	----	----	88
74	0.8	18	20	19	20	20	21	21	----	73
30	0.0	14	14	13	14	14	12	14	12	62
84	0.3	9	11	11	13	11	10	13	11	49

BRICK NO. 4 (SET ON END)

Sample No.	B	$C=\frac{W}{T^{1/2}}-BT$								Total grams of water absorbed Y
		1 minute	2 minutes	3 minutes	4 minutes	5 minutse	6 minutes	7 minutes	8 minutes	
108	1.0	39	39	39	39	39	39	39	39	130
95	0.0	38	37	37	38	38	38	38	39	98
110	1.0	46	47	47	47	47	47	47	47	129
147	1.0	35	35	36	36	37	37	37	37	123
146	1.4	33	33	33	33	34	34	33	33	117
100	0.4	31	32	32	31	31	33	32	33	98

TABLE 5.—*Rate of absorption of water by partial immersion (depth of one-eighth inch) of brick*—Continued

BRICK NO. 9 (SET ON END)

Sample No.	B	$C=\frac{W}{T^{1/2}}-BT$					Total grams of water absorbed Y
		1 hour	2 hours	3 hours	4 hours	5 hours	
213	3.1	28	30	30	29	28	135
48	1.4	28	30	29	28	29	131
214	2.4	24	25	24	24	24	125
168	2.3	20	22	22	20	20	124
169	2.3	28	28	28	28	28	122
201	1.8	23	25	24	24	23	118
142	0.1	5	4	4	5	5	64
62	0.5	6	5	5	4	5	60

BRICK NO. 9 (SET ON FLAT SIDE)

209	2.4	24	23	23	24		104
214	6.0	42	45	44	42		125
45	3.8	30	31	31	32	31	123
196	3.8	26	27	27	27	26	107
5	3.2	27	27	27	27	27	98
204	0.0	17	17	18	17	18	81
4	2.0	41	45	47	44	41	115
210	0.3	13	12	12	12	13	97
20	1.8	43	44	46	45	43	111
12	0.6	17	18	17	18	17	105

BRICK NO. 5 (SET ON END)

Sample No.	B	$C=\frac{W}{T^{1/2}}-BT$												Total grams of water absorbed Y
		1 minute	2 minutes	3 minutes	4 minutes	5 minutes	6 minutes	7 minutes	8 minutes	10 minutes	12 minutes	15 minutes	30 minutes	
142	0.4	23	22	22	23	23	24	23	23	23	23	22	22	211
135	0.3	20	21	22	22	23	22	23	23	23	23	24	22	270

BRICK NO. 5 (SET ON EDGE)

138	1.6	58	58	59	61	62	60	60	60	57				255
139	1.2	56	56	57	56	57	56	57	55	56				241
140	0.9	57	58	58	60	59	58	58	57	56				247
141	0.9	47	49	49	49	49	49	50	50	49				189
142	1.1	44	44	44	45	45	46	46	47	45				217
118	1.0	48	48	49	50	49	49	49	49	49				199
119	1.0	55	55	56	56	57	57	56	56	57				197
120	2.0	50	51	52	52	50	49	48	48	47				202
120	1.3	43	43	42	43	44	43	43	43	43				198
121	1.0	48	48	49	50	49	48	49	49					199

TABLE 5.—*Rate of absorption of water by partial immersion (depth of one-eighth inch) of brick*—Continued

BRICK NO. 10 (SET ON EDGE)

Sample No.	B	$C=\frac{W}{T^{1/3}}-BT$							Total grams of water absorbed
		1 hour	2 hours	3 hours	4 hours	5 hours	8 hours	16 hours	Y
151	2.1	47	49	49	50	49	47		154
100	3.0	42	42	40	40	42	42		141
53	2.5	31	33	33	32	31	33		125
32	2.0	25	26	27	27	26	27		119
25	2.1	23	23	23	24	23	24		100
52	1.9	19	20	21	21	20	20		94
133	2.0	16	17	17	18	17	17		83
146	1.6	14	15	15	15	14	14		73
138	1.0	12	14	14	13	13	13		71
204	0.7	12	12	13	12	12	12	12	63
205	0.0	8	9	9	9	8	9	8	50
143	0.3	7	8	8	8	7	9	8	47

3. DISCUSSION OF RESULTS

The relation, $C=\frac{W}{T^{1/3}}-BT$, where C and B are constants and W is the gain in weight at the end of any time interval, T, is characteristic of individual bricks studied. The values of the constants B and C were different for different bricks, and different values for these constants were evaluated from the data obtained by exposing the different surfaces (end, face, or flat side) of any one brick to water. This relation may not be applicable to the absorption rate of a clay body that is distinctly underburned or overburned.

Since $B=\frac{d}{dT}\left(\frac{W}{T^{1/3}}\right)$ and since $\frac{W}{T^{1/3}}=T^{2/3}\times W/T=T^{2/3}$ times the average rate of absorption during the time interval, T, it is seen that B equals the rate of change with respect to time of $T^{2/3}\times$ average rate. $C=T^{2/3}\times W/T-BT=T^{2/3}\times$ the average rate of absorption during the time interval, T, minus a constant times the time. C is fairly constant over a more or less definite time interval. The relation ceases to apply after water strikes through. After water has traveled through the entire length, breadth, or thickness of the clay brick, the rate of absorption decreases markedly. It is also seen from Table 5 that the magnitude of C for any single brick of one type is usually greater, the greater the magnitude of Y, the total apparent cold absorption. This relation between C and Y is illustrated in Figure 3. While it is seen that in Table 5 the magnitude of C generally increases as that of Y increases, it may also be noted that there are many exceptions to this rule. This rule applies best to bricks Nos. 3 and 10. No. 24 of brick 2 having a C of 51 has a Y of 210, whereas Nos. 12 and 210, each having a smaller Y than No. 24, have larger C's.

There are many other exceptions to be noted. These differences are due mainly to differences of permeability of surface; for example, the surface of No. 24 is apparently more flashed than the surfaces of Nos. 12 and 210. By grinding off the exterior surfaces it is possible to reduce these differences to a considerable extent. However, it was necessary to study the absorption rates of the bricks as they are made and not as modified in the laboratory.

The statement that the magnitude of C usually decreases as the magnitude of Y decreases might have more meaning were it restated as follows: Among bricks made from the same clay or shale and by

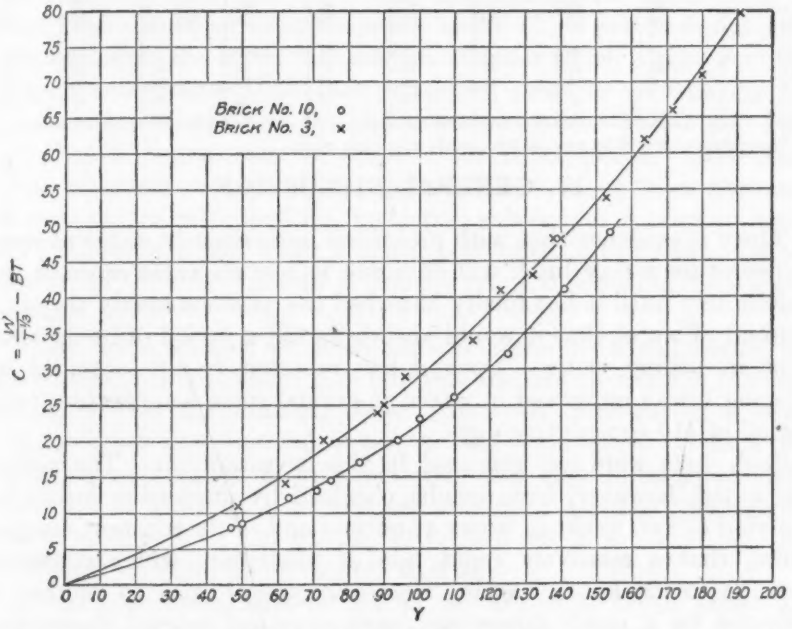

FIGURE 3.—*The more highly absorbent brick of a type have usually higher C values*

the same process of manufacture, the more highly absorbent bricks usually absorb relatively more rapidly and the less absorbent bricks, of course, usually absorb relatively more slowly. The reader is warned not to interpret this as applying to bricks in general. If the 10 different manufacturers' bricks were all mixed together in one pile, this rule would not apply to the pile. It would apply to all of any particular manufacturer's bricks in that pile.

In the belief that this point has some importance from the standpoint of transmission of water into a wall of bricks, the actual data concerning the rates of absorption of the individual bricks of brick No. 10 are given in Table 6. Computations of these data were given in Table 5.

TABLE 6.—*Absorption of water (grams) by partial immersion (depth of one-eighth inch) of brick set on edge*

BRICK NO. 10

Sample No.	1 hour	2 hours	3 hours	4 hours	5 hours	8 hours	16 hours	Total grams absorbed, *Y*	Per cent of *Y* gained in 8 hours
151	50	71	84	99	110	143	(1)	154	92.9
100	45	61	74	83	97	132	(1)	142	93.0
53	33	48	58	67	74	106	(1)	125	84.8
32	27	38	48	56	62	86	(1)	110	78.2
25	25	34	42	51	57	82	(1)	100	82.0
52	21	30	39	45	50	70	(1)	94	74.4
133	18	26	33	41	46	64	(1)	83	77.1
146	16	23	29	34	38	54	(1)	75	72.0
138	13	20	25	27	31	42	(1)	71	59.2
204	13	17	22	23	27	35	58	63	55.6
205	8	11	13	14	14	18	20	50	36.0
143	7	11	13	15	15	23	32	47	49.0

[1] Water struck through to opposite face shortly after eight hours.

IV. GENERAL DISCUSSION

There is evidence that with prolonged immersion in water at room temperature a clay brick will continue to absorb water more or less indefinitely until it has finally absorbed the same or nearly the same amount of water that it would absorb during a period of hours when kept in boiling water. Douty [6] has reported results obtained by keeping bricks immersed in water at normal room temperature for a period of 110 consecutive days.

Such tests were not repeated in this investigation. The author has noted, however, from results obtained by immersing bricks for a period of two weeks in water at normal and fairly constant temperature, that a relatively rapid rate of absorption which continues from 24 to 120 hours, varying from one type of brick to another, is followed by a much slower and more constant rate of absorption. The following explanation for this behavior is offered. Water enters the voids of the burned-clay body rapidly at first, then at a diminishing rate until the resultant of the forces, hydrostatic pressure, surface tension, etc., is balanced by the opposed pressure of entrapped air in the voids. Further absorption then proceeds very, very slowly, if the temperature of the water remains constant, through the gradual diffusion of this entrapped air. Under these conditions the brick absorbs less than a gram of additional water during 24 hours. As soon as this slow rate of absorption is attained it is conceivable that a condition of apparent or "pseudo" equilibrium exists.

It is difficult to account for this diffusion of air unless it is assumed that it dissolves in the water which partially fills the voids and so

[6] D. E. Douty and L. L. Beebe, Proc. Am. Soc. Testing Materials, **11**, p. 767; 1911.

makes its escape. However, the water is probably already saturated with air. It must be realized that this is only a theory.

An increase in the temperature of the water would result in a lower solubility of air in water and a decrease in the surface tension of that liquid. The apparent equilibrium would, therefore, be displaced. The viscosity of the water would also be reduced, and the frictional-wall resistance opposing its flow into the voids would be decreased. The following is an experimental fact: If a brick is immersed in water at 25° C. for a period of time such that the rate of gain in weight by absorption becomes less than 1 g during 24 hours and if it is then transferred to water at 75° C. and held therein for a half hour or more, then placed again in the water at 25° C., it will be found that, after cooling in the latter, the amount of water which it then contains is appreciably more than that contained prior to transferring the specimen to the water at the higher temperature. This would indicate that a displacement of some of the entrapped air takes place when immersed in the warmer water. Water vapor takes the place of some of the entrapped air, and upon subsequent cooling in water at 25° C. some of this water vapor is condensed in the voids, and the pressure of the entrapped air is thereby reduced, allowing more water to enter.

There are a number of mathematical equations pertaining to the time-distance relationships that apply to the flow of water in material already wetted or containing water. However, penetration of water into perfectly dry material is not so well understood. This is the condition that exists when a perfectly dry clay brick is partially immersed in water at a definite temperature. Capillary attraction, rate of viscous flow, and wetting of surface are all involved, and the problem is an exceedingly complicated one.

It has been noted that certain of the dry-press bricks tested absorbed water far more rapidly than did bricks molded by the stiff-mud process from the same clay or shale used in making the dry-press bricks. It would be expected that the pores of dry-press bricks would tend to be larger than those in bricks molded by the stiff-mud process from the same clay or shale, were the conditions of drying and burning of the two types of bricks identical.

During this investigation no attempt has been made to deduce from any theory these simple empirical equations that within the limits of experimental error apply to the data. It might, of course, be assumed that the pores in a clay brick are cylindrical and open at both ends or that they are conical in shape and closed at one end, or it may be assumed that the solid particles are spherical, packed, and more or less sintered together. On the basis of such assumptions a variety of equations may be deduced which may or may not be a

true picture of the mechanics of the process, absorption. In this investigation no such assumptions were made, but absorption measurements were made and the data analyzed. Certain simple empirical equations were seen to fit these data rather nicely.

It should be mentioned that in conducting such tests as the above and in the application of such methods of computation of the data obtained it will be found that the more a brick is laminated, checked, cracked, and filled with pebbles, etc., the more it will deviate from this somewhat symmetrical behavior. Deviations from the absorption constant, K, on the part of individual bricks of a type are considerably less if the burned-clay bodies are as nearly "homogeneous" as may be expected of such material. It is also probable that deviations may result from the addition of grog, fluxes, etc., to the clay.

V. GENERAL SUMMARY

1. The absorption properties of 10 different types of clay bricks have been studied.

2. Certain simple empirical equations fit these absorption data within the limits of experimental error.

3. Three constants have been evaluated. Two of these, B and C, are derived by a method of computation of the data obtained in the study of rate of absorption by partially immersing bricks in water. The third, the absorption constant, K, is obtained by immersing the brick in water at normal room temperature for a more or less definite period of time and following this by immersion in boiling water for a period of seven hours. The Schurecht ratio, slightly modified, is used in evaluating K for any type of brick.

4. It is indicated that the constants, B, C, and K, are more characteristic of a given clay or shale from which a type of brick is made than they are of any other single thing.

5. The absorption constant, K, is independent of the heat treatment that the clay body has received over a certain limited range in the burning temperature.

6. It may be possible to relate the absorption constant, K, characteristic of a manufacturer's brick, to the weather resistance of that material, and this constant and the others, B and C, may furthermore be of use in differentiating between underburned and overburned bricks on the one hand and well burned on the other. However, in the absence of any actual data, this is a matter of conjecture only. These constants will be studied in any future work here involving weather resistance or differentiating between degrees of burning. It is believed they will be of particular value in the study now under way of the process of water penetration through brick masonry.

VI. ACKNOWLEDGMENTS

The writer wishes to extend his thanks to Messrs. Bates, Parsons, and McBurney for many helpful suggestions and criticisms given by them during the course of this study. Gratitude is especially due William C. Koch, president of the American Face Brick Association, for many valuable suggestions and particularly for advising the author to compute all absorption data on the basis of volume alone. The cooperation of the various members of the face and common brick associations who furnished the materials for the study is also deeply appreciated.

WASHINGTON, March 15, 1929.

53811°—29——9

THE FIRST SPECTRUM OF KRYPTON

By William F. Meggers, T. L. de Bruin, and C. J. Humphreys

ABSTRACT

The older data on the first spectrum of krypton being inadequate for an analysis, discharge tubes were prepared with krypton gas of high purity and operated to emit the spectrum of neutral Kr atoms. About 200 lines (3302.54 to 9751.77 A) characterizing the first spectrum of krypton were photographed with concave grating and quartz spectrographs. From these spectrograms a new list of estimated intensities and measured wave lengths was obtained.

Analysis of these new data led to the identification of the main spectral terms analogous to those of the similarly constructed neon and argon spectra. Practically all of the Kr I lines have been classified in series of various types. From the combinations and series limits absolute term values are derived, and the ionization potential of 13.940 volts is deduced for Kr. The general features of the Kr I spectrum are found to be closely analogous to those of the preceding rare gases Ne I and A I, and in excellent accord with the theoretical expectations.

The proposal that the krypton line 5649.56 A be substituted for the cadmium line 6438.4696 A as a primary standard of wave length is discussed. The proposed krypton standard has relatively low intensity, and it involves a metastable level. These objections do not apply to the stronger line 5870.92 A, but it can not be recommended as a standard until it has been reexamined for hyperfine structure.

CONTENTS

	Page
I. Introduction	129
II. Wave-length measurements	132
III. Analysis of the Kr I spectrum	135
1. Theoretical terms; coordination to series limits	135
2. Absolute term values; ionization potential of Kr	138
3. The principal series, $1s_i - mp_k$	141
4. The X and Y series	149
5. The subordinate series	150
6. The Kr I spectrum in the extreme ultra-violet	153
7. Identification of the experimental terms	154
8. List of Kr I lines	156
IV. The first spectrum of krypton as a source of standard wave lengths	160

I. INTRODUCTION

Ramsay and Travers [1] discovered a new constituent of atmospheric air in 1898. They called it krypton (Kr) and indicated that its spectrum was characterized by two brilliant lines for which the approximate wave lengths 5867.7 and 5568.8 A were reported. Runge [2] in 1899 pointed out that, spectroscopically, krypton bears a close analogy to argon. Like argon it emits two different line spectra, one without

[1] Ramsay and Travers, Proc. Roy. Soc., 63, p. 405; 1898.
[2] Runge, Astrophys. J. 10, p. 73; 1899.

Leyden jar and spark gap in the secondary circuit of an induction coil, the other with Leyden jar and spark gap. He published the wave lengths for 16 lines (4274.09 to 7601.47 A) in the first spectrum, and 31 lines (3654.11 to 5419.38 A) in the second. The analogy of the first spectrum of krypton to the red spectrum of argon was further borne out by the discovery that the wave numbers of several pairs of lines showed equal differences, three pairs of lines with the difference 945 being noted by Runge.

Lists of wave lengths were also given by Liveing and Dewar [3] but only approximate values were obtained. A more complete and accurate determination of wave lengths for both spectra of krypton was completed by Baly [4] in 1903. He gave 74 lines (3502.69 to 6456.65 A) for the first spectrum and 733 lines (2418.13 to 5871.12 A) for the second, but the stronger lines are common to both lists and some in each are identifiable with xenon. For a quarter of a century Baly's results have held first place as the most comprehensive and accurate description of the krypton spectra. An extension to the longer waves was made in 1919 by Merrill,[5] who published the wave lengths of 41 lines (6421.1 − 8928.72 A) characterizing the first spectrum of krypton. Approximate values for the wave lengths of 24 red lines (5994 to 7595) of the first spectrum of Kr were reported by Collie.[6] An attempt to measure more Kr I lines was made by Otsuka [7] in 1926, but he was able to observe only 55 lines (3665.32 to 8112.91 A) before his spectrum tubes became inoperative. Contributions to the spectra of krypton in the extreme ultra-violet have been made by Hertz and Abbink,[8] by Taylor,[9] and by Abbink and Dorgelo.[10]

The electrodeless discharge was employed by L. Bloch, E. Bloch, and Déjardin [11] to separate various stages of krypton spectra, but no new information was obtained for the first spectrum.

In addition to these general descriptions of the emission spectra of krypton, a number of investigations have been made with interferometers to determine the wave lengths of some of the stronger lines relative to the primary standard, the red radiation from Cd (6438.4696 A). The first of these was by Buisson and Fabry [12] who measured the wave lengths of the bright green and yellow lines as 5570.2908 and 5870.9172 A, respectively. Meggers [13] determined the wave lengths of 17 of the stronger lines (4273.9696 to 7601.544 A) and

[3] Liveing and Dewar, Proc. Roy. Soc., **68**, p. 389; 1901.
[4] Baly. Phil. Trans., **202**, p. 183; 1904.
[5] Merrill, B. S., Sci. Papers, **15**, No. 345, p. 251; 1919.
[6] Collie, Proc. Roy. Soc., **97**, p. 349; 1920.
[7] Otsuka, Zeit. f. Phys., **36**, p. 786; 1926.
[8] Hertz and Abbink, Naturw., **14**, p. 648; 1926.
[9] Taylor, Proc. Nat. Acad. Sci., **12**, p. 658; 1926.
[10] Abbink and Dorgelo, Zeit. f. Phys., **47**, p. 221; 1928.
[11] L. Bloch, E. Bloch, and Déjardin, Ann. de. Phys. (10), **2**, p. 461; 1924.
[12] Buisson and Fabry, Comptes Rendus, **156**, p. 945; 1913.
[13] Meggers, B. S. Sci. Papers, **17**, p. 193; 1921.

found 5570.2872 and 5870.9137 for the green and yellow lines. The latter lines were measured by Perard [14] who obtained 5570.2892 and 5870.9154 for their values. Finally Weber [15] measured three lines of Kr (5649.5924, 5870.9463, and 6456.3241) relative to Cd (6438.5033 A in air at 20° C., 760 mm Hg and 10 mm water vapor), and proposed the yellow-green line (5649.5924 A) as a primary standard to replace the red line of Cd.

Sixteen of the stronger krypton lines (4273 – 5870 A) were examined with Lummer-Gehrcke interferometer plates by Gehrcke and Janicki;[16] they report that all the lines are sharp, especially 5570 and 5870 A. According to Perard,[17] who studied the latter lines with a Michelson interferometer, each has two close satellites. It is our intention to examine the Kr lines with a Fabry-Perot etalon of Adam Hilger's construction and to determine the hyperfine structure of complex lines.

The International Conference of Weights and Measures [18] in 1927 provisionally adopted the red radiation from Cd (6438.4696 A) as the primary standard of wave length, but recommended that the krypton line (565 mμ) be investigated with a view of its eventual substitution for the red ray of Cd.

This action of the conference is responsible in part for the present investigation. Since certain properties of spectral lines (pressure effect, reversibility, Zeeman effect, relative intensity) are now known to be related to the spectral terms (atomic energy levels) it appeared desirable first to classify the spectrum lines so as to be able to draw upon theoretical considerations in a discussion of the suitability of a line as a standard wave length. Before the structure of the Kr I spectrum could be successfully analyzed it was necessary to make an entirely new description of the spectrum, since the older data are entirely inadequate for this purpose. The present paper, therefore, deals with a preliminary description and with the interpretation of the Kr I spectrum. In later publications, we expect to give other data on interferometer comparisons of wave lengths, studies of hyperfine structure, detection of fainter lines, and extensions of series to higher members.

As already stated, the first regularities among krypton lines were discovered by Runge in 1899. Additional constant differences between wave numbers were found by Paulson [19] in 1914 and by Merrill in 1919.

---

[14] Perard, Comptes Rendus, **176**, p. 1060; 1923.
[15] Weber, Physik. Zeit., **29**, p. 233; 1928.
[16] Gehrcke and Janicki, Ann. der Phys., **81**, p. 314; 1926.
[17] Perard, Comptes Rendus, **184**, p. 447; 1927.
[18] Seventh Conf. Gen. des Poids et Mesures, p. 52; 1927.
[19] Paulson, Ann. d. Phys., **45**, p. 428; 1914.

More recently, McLennan and Ruedy [20] undertook absorption experiments with excited krypton to assist in identifying the metastable levels. Seven infra-red lines were found to show absorption, but the terms which they involve were not identified. Ten lines of shorter wave length were reported to be associated with the separation of 4,930 cm^{-1}; only one pair appears to be real.

In a recent paper announcing the discovery of new lines in various rare gas spectra Gremmer [21] mentions having observed three new lines (5672.4, 5993.7, and 9751.7 A) in the Kr I spectrum, and he presents a table of $1s_1 - 2p_k$ combinations which involve mostly infra-red lines.

Two additional papers dealing with the structure of krypton spectra must be mentioned for the sake of completeness, although they contribute nothing of value to the subject. They are by Hicks [22] and by Williams.[23]

II. WAVE-LENGTH MEASUREMENTS

The sources of radiation were glass or fused quartz tubes of the "dumb-bell" type described by Nutting [24] or by Meggers.[25] The bulbs contained aluminum disk electrodes 1 inch (25 mm) diameter, and the capillary connecting the bulbs in the case of the glass tubes had a bore of about 2 mm while in the quartz tube it was less than 1 mm. These tubes were used "side-on," a three or four fold magnified image of the capillary being projected on the slit of the spectrograph. The tubes were filled in this laboratory with gas purchased from the Linde Gesellschaft für Eismaschinen in Höllriegelskreuth b. München. Samples of both Kr and Xe were obtained, the arc spectra of both were measured and compared throughout the entire range accessible to photography; they reveal the only impurities as traces of H and Hg in each, a trace of Xe in Kr and a minute trace of Kr in Xe. Comparison of the two spectra observed under similar conditions has made possible for the first time a perfect separation of the lines and proper assignment of each to the element it characterizes. The identification of Xe lines in the Kr spectra was greatly facilitated by the variable intensity of the impurity lines. Owing to the gradual adsorption of the heavier rare gases coincident with electrode evaporation, the Xe lines became progressively weaker in the Kr tubes as their time of service increased so that after 50 to 100 hours discharge the Xe lines practically disappeared while the Kr lines remained as intense as ever. In a similar manner, the Hg

[20] McLennan and Ruedy, Trans. Roy. Soc. Can. (3), **22**, p. 15; 1928.
[21] Gremmer, Zeit. f. Phys., **50**, p. 716; 1928.
[22] Hicks, Phil. Trans., **A 220**, p. 335; 1919.
[23] Williams, Ciencias Fisicas y Matemáticas (No. 82), p. 255; 1928.
[24] Nutting, B. S. Sci. Papers, **4**, p. 511; 1907.
[25] Meggers, B. S. Sci. Papers, **12**, p. 202; 1915.

lines decreased in intensity until they almost vanished in the older tubes.

Most investigators of Kr spectra have remarked upon the rapidity with which electrode sputtering usually takes place and the accompanying gradual disappearance of the gas. Under such conditions the tube gradually increases in resistance until the discharge shows spark lines (the second spectrum) and finally ceases altogether when the tube appears to have become vacuous. Sometimes a portion of the gas can be released by heating, but sooner or later it becomes necessary to fill the tubes with a fresh supply of gas. This adsorption of the gas occurs most readily and rapidly in tubes filled at a low pressure so that the dark space surrounding the electrodes reaches the walls of the tube; it is extremely slow when the pressure is high enough to constrict the dark space to 1 mm or less. We have filled our tubes with a gas pressure corresponding to about 10 mm Hg. Several of them have been operated from 100 to 200 hours each, and although metallic deposits from the electrodes have gradually accumulated on the walls the arc spectrum still appears to be as intense as it was originally.

To emit the arc spectrum the Kr tubes have been operated with a. c. transformers by connecting the electrodes directly to the secondary terminals without encumbering the circuit with extra inductances, condensers, or spark gaps. Two different transformers have been employed, one rated to give 10,000 volts and the other 40,000 volts, the former being used to excite the quartz tube illuminating a quartz spectrograph and the latter for the operation of glass tubes photographed with a diffraction grating spectrograph. The primaries in each case were connected to 110 volts, 60 cycles, the current being 3 to 4 amperes in the smaller transformer and 10 to 12 in the larger. With these discharges the tubes emitted almost perfectly pure arc spectra (Kr I), only a few of the most intense spark lines (Kr II) appearing very faintly.

Most of the spectrograms were made in the first (and second) order of a 6-inch Anderson grating with 7,500 lines per inch, giving a scale of 10.4 A in the first order. This grating has a radius of curvature of 21 feet and is illuminated with parallel light in a Wadsworth mounting which has been described in other papers.[26] These spectrograms were supplemented by others made with an E_1 Hilger autocollimating quartz-spectrograph especially to record faint lines in the ultra-violet where the principal series converge.

For the longer wave spectral regions, the photographic plates were sensitized with pinaflavol, pinaverdol and pinacyanol, dicyanin, rubrocyanin, and neocyanin. The exposure times ranged from 12 to

[26] Meggers and Burns, B. S. Sci. Papers, **18**, p. 191; 1922.

50 hours, but little or no advantage was gained by exposing longer than 20 or 24 hours.

Comparison spectra of iron were superposed before and after each of the long exposures to Kr, and wave-length determinations were made relative to the secondary standards in the spectrum of the iron arc. Acknowledgments are due to Bourden F. Scribner for making most of the wave-length computations. The majority of the lines were measured on four or more spectrograms, and the error of the mean in such cases is probably not more than one or two hundredths of an Angstrom unit. This accuracy of the wave lengths in relative value is attested by the combination principle and series relations presented below.

So far as we are aware, except for a colored drawing of 20 lines reproduced in a paper by Ramsay and Travers,[27] no map of the krypton arc spectrum has ever been published. To remedy this deficiency, we are reproducing in Figures 1, 2, 3, and 4 portions of our spectrograms showing the first spectrum of krypton from its limit in the ultra-violet near 3300 A to the longest wave length, 9751 A, which we have been able to photograph in the infra-red. In addition to the intense green and yellow lines which dominate the visible spectrum, the most striking feature of this spectrum is the group of intense lines in the blue-violet (4274 to 4502 A) and a similar group of even stronger lines in the infra-red. The plates made with the grating and glass tubes were remarkably free from continuous background, but the exposures made with the quartz spectrograph exhibited some special features deserving mention. The quartz tube used for these exposures has an extra fine capillary. It showed an intense Kr I spectrum, a small number of impurity lines of Xe, a few of the stronger Hg lines, one or two lines of the Balmer series of H, 2 Si lines and in addition a strong continuous background extending over the entire spectrum, superposed upon which was a peculiar distribution of fine lines suggesting band structure. It may be that the continuous background arises from some sort of fluorescence in the quartz capillary; we have been unable to identify the groups of fine lines. Suspecting that they might be parts of known band spectra, selected by unique conditions of the discharge, attempts were made to identify them with the secondary spectrum of hydrogen and with cyanogen bands, but no correspondence could be found with these or with any known band spectrum. They may be due to some silicon compound or unrecognized impurity. Although a band spectrum is ascribed to He, none has ever been mentioned for any of the other rare gases.

These fine lines appear mainly in two groups, one in the ultra-violet (3064 to 3270 A) and the other in the violet (4050 to 4250 A);

[27] Ramsay and Travers, Phil. Trans., **A 197**, p. 47; 1901.

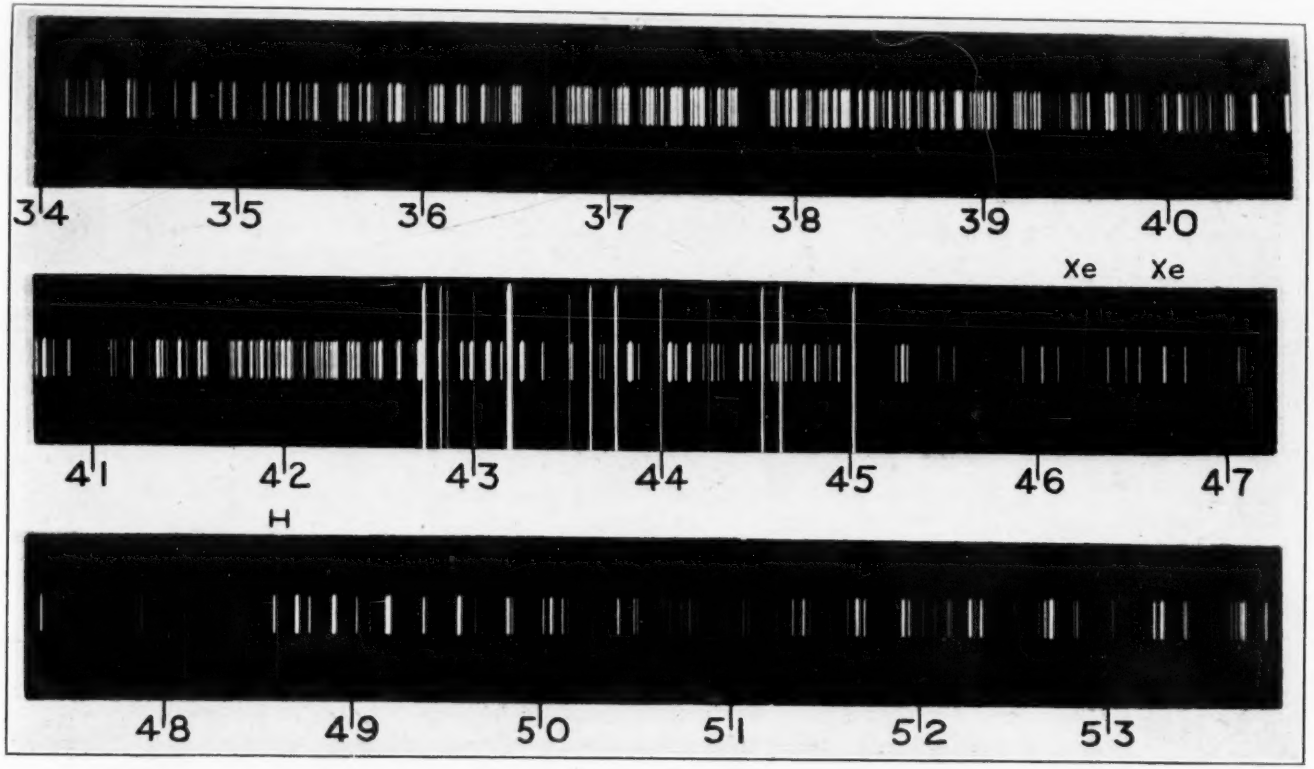

FIGURE 1.—*Arc spectrum of krypton (3400 A to 5400 A) with comparison spectrum of iron*

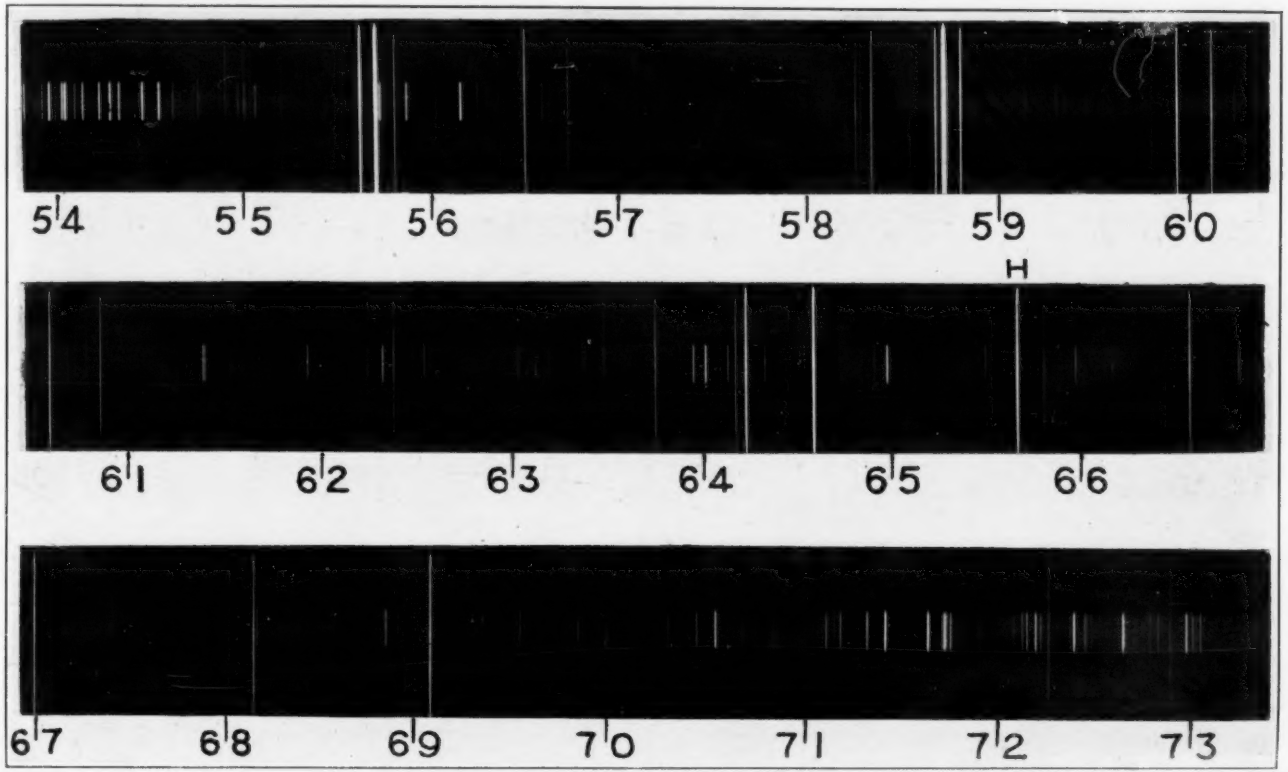

FIGURE 2.—*Arc spectrum of krypton (5400 A to 7340 A) with comparison spectrum of iron*

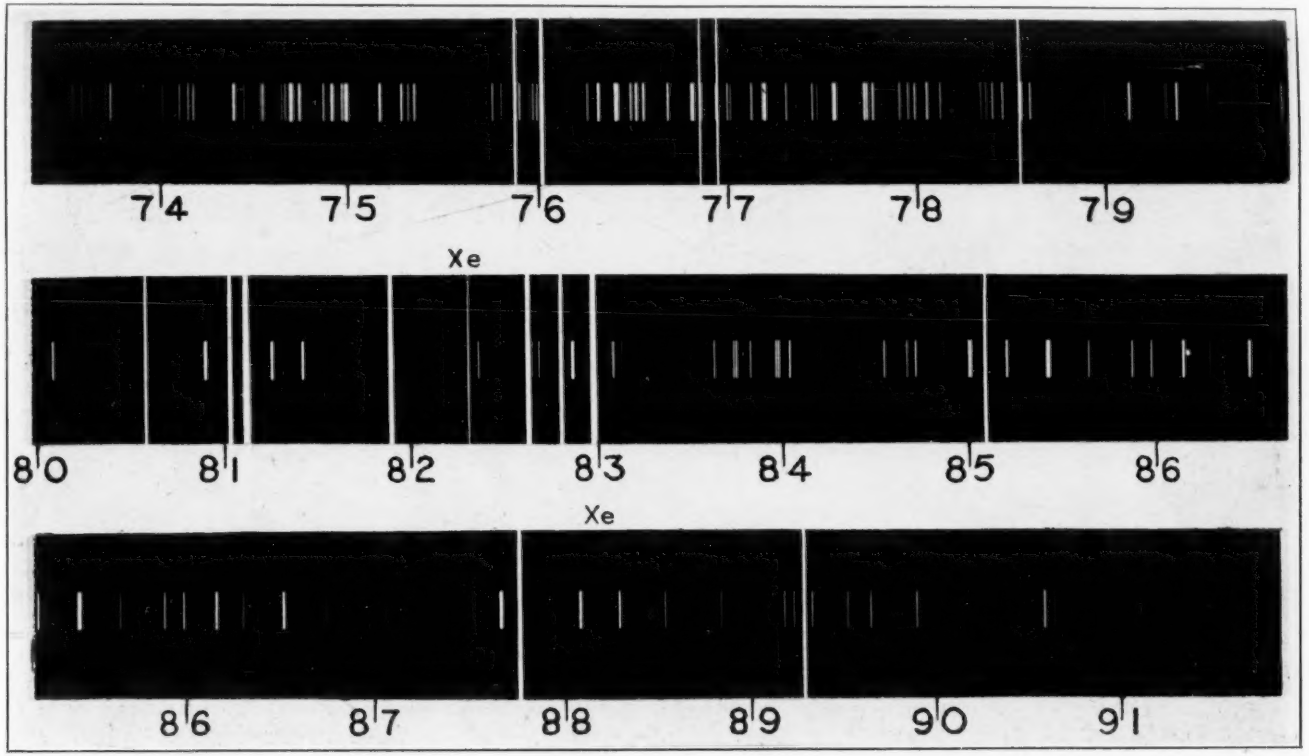

FIGURE 3.—*Arc spectrum of krypton (7340 A to 9200 A) with comparison spectrum of iron*

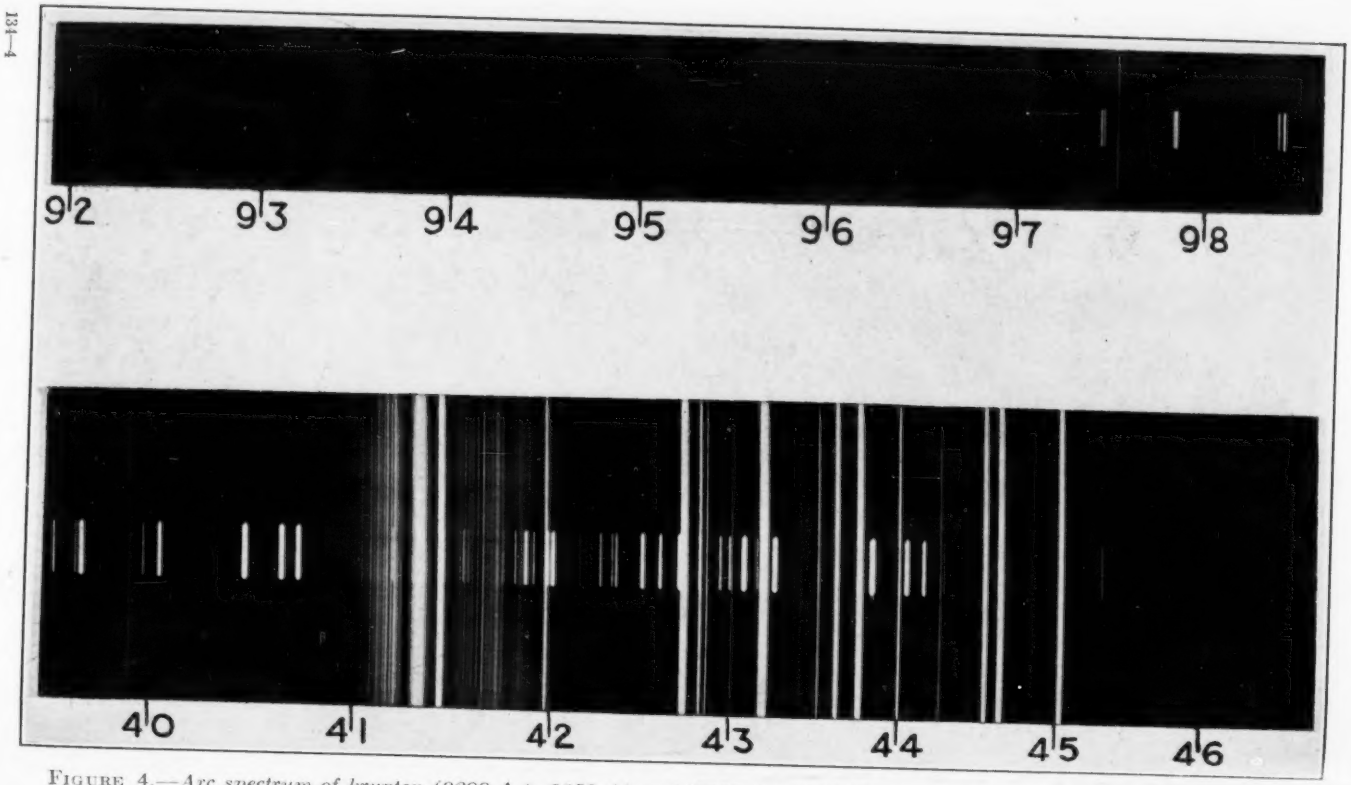

FIGURE 4.—*Arc spectrum of krypton (9200 A to 9850 A) and (3960 A to 4700 A), each with comparison spectrum of iron*

the former may be identifiable with H_2O. The latter group is the more prominent; it is reproduced in the last spectrogram in Figure 4, from an enlargement of a prismatic spectrogram which may be compared with a grating spectrogram of nearly the same scale in Figure 1, the grating spectrograms were made with glass tubes having capillary bore of 2 mm and only the strongest exposures with these tubes show the main lines of this band very faintly. We have not determined whether or not current density or applied potential accounts for this difference in the behavior of the quartz and glass tubes.

III. ANALYSIS OF THE Kr I SPECTRUM

1. THEORETICAL TERMS; COORDINATION TO SERIES LIMITS

In the unexcited state of neutral krypton (Z=36) the atomic configuration has a closed shell with two $4s$ and six $4p$ electrons symbolized by $4s^2\ 4p^6$. According to Hund's [28] theory the spectral term which characterizes the normal state is a single level, $^1S_0$. The terms which represent the excited states of the atom result from the interaction of the series electron with the electron group $s^2\ p^5$ which characterizes the unexcited state of the ion, Kr^+. The term arising from the configuration $s^2\ p^5$ is an inverted $^2P_{2,\ 1}$.[29] This term has already been established for Kr II by Kichlu;[30] the levels have a separation of 5,371 cm^{-1}. We may, therefore, derive the terms representing the excited states of the neutral atom by finding the resultant obtained by adding in turn the electrons ns, np, nd, etc., to the term ^2P. In the following table are given the theoretical terms which may be expected to account for the first spectrum of krypton.

TABLE 1.—*Electron configurations and theoretical terms of the Kr I spectrum*

Electron configuration	Theoretical terms based on $^2P_{2,1}$ of Kr II					
$(s^2\ p^6)$		$^1S_0$				
$(s^2\ p^5)\cdot s$		$^1P_1$			$^3P_{2,1,0}$	
$(s^2\ p^5)\cdot p$	$^1S^1$	$^1P_1$	$^1D_2$	$^3S_1$	$^3P_{2,1,0}$	$^3D_{3,2,1}$
$(s^2\ p^5)\cdot d$	$_1P^1$	$^1D_2$	$^1F_3$	$^3P_{2,1,0}$	$^3D_{3,2,1}$	$^3F_{4,3,2}$

The binding of an s-electron thus gives 4 levels, a p-electron 10, and a d-electron a set of 12 levels. In the analogous spectra of the other rare gases, Ne I and A I, these energy levels have been established, respectively, by Paschen [31] and by Meissner.[32] In the nota-

[28] Hund, Linienspektren und periodisches system des Elemente, p. 144; Julius Springer; Berlin, 1927.
[29] For convenience in printing and reading, the inner quantum numbers of levels belonging to even multiplicities are increased by one-half.
[30] Kichlu, Proc. Roy. Soc., **A 120**, p. 643; 1928.
[31] Paschen, Ann d. Phys., **60**, p. 405; 1919; **63**, p. 201; 1920.
[32] Meissner, Zeit. f. Phys., **37**, p. 238; 1926; **39**, p. 172; 1926; **40**, p. 839; 1927.

tion introduced by Paschen, and used also by Meissner to facilitate comparison of the argon analysis with the neon data, the set of four levels was designated "s-terms," s_2, s_3, s_4, s_5 in the order of increasing magnitude. The set of 10 levels was referred to as "p-terms," $p_{1, 2, 3, \ldots 10}$, and the 12 levels as d and s' terms.

In order that the structure of the Kr I spectrum may be conveniently compared with Ne I and A I the Paschen notation will be retained in the present paper and a translation into the modern notation is added. In all three cases the designation of the 4 s-terms is the same but if the 10 p-terms are numbered in order of magnitude they must be rearranged to compare levels with the same inner quantum numbers in the different spectra. The notation for the corresponding terms in the Ne I, A I, and Kr I spectra is compared in Table 2 in Paschen's notation.

TABLE 2.—*Corresponding terms in Ne I, A I, and Kr I spectra*

j	0	1	0	2	1	2	1	2	3	1	1	0	1	2
Ne I	p_1	p_2	p_3	p_4	p_5	p_6	p_7	p_8	p_9	p_{10}	s_2	s_3	s_4	s_5
A I	p_1	p_2	p_5	p_3	p_4	p_6	p_7	p_8	p_9	p_{10}	s_2	s_3	s_4	s_5
Kr I	p_1	p_3	p_5	p_2	p_4	p_6	p_7	p_8	p_9	p_{10}	s_2	s_3	s_4	s_5

In the analyses of the Ne I and A I spectra, it was found that the terms converge to two limits, separated by a displacement constant A. These two limits are related to the ground levels $^2P_2$ and $^2P_1$ of the ion. Thus of the 10 p-terms, $p_{1, 2, 3, 4}$, are coordinated to $^2P_1$, while $p_{5, 6 \ldots 10}$ converge to $^2P_2$. The latter are called Ritzian terms because they follow the Ritz series formula, whereas the former, the non-Ritzian terms, require the addition of a constant to the term value. Similarly 8 of the d-terms go to $^2P_2$ and the other 4 to $^2P_1$ as limits. The coordination of the various terms to the series limits [33] is summarized in Table 3. We are confident that this identification of the experimental terms (in Paschen notation) with the theoretical terms is mainly correct, although it must be admitted that it is open to question in a few particulars and lacks verification of Zeeman-effect data in the case of krypton.

On the basis of Zeeman effects for neon, Goudsmit and Uhlenbeck (Zeit. f. Phys., **35**, p. 618; 1926) give the following identification of the 10 p-terms as the most probable:

$$p_1\ p_2\ p_3\ p_4\ p_5\ p_6\ p_7\ p_8\ p_9\ p_{10}\ {}^1S_0\ {}^3P_1\ {}^3P_0\ {}^3P_2\ {}^1P_1\ {}^3D_2\ {}^3D_1\ {}^1D_2\ {}^3D_3\ {}^3S_1$$

The analogous interpretation for the krypton terms is as follows:

$$p_1\ p_2\ p_3\ p_4\ p_5\ p_6\ p_7\ p_8\ p_9\ p_{10}\ {}^1S_0\ {}^3P_2\ {}^3P_1\ {}^1P_1\ {}^3P_0\ {}^3D_2\ {}^3D_1\ {}^1D_2\ {}^3D_3\ {}^3S_1$$

[33] Hund, Zeit. f. Phys., **52**, p. 601; 1928.

It does not appear possible at the present time to harmonize the deductions from Zeeman-effects and the theory of coordination to limits; in the meantime a certain amount of arbitrariness must exist in the translation of the Paschen notation into the quantum notation.

TABLE 3.—*Coordination of terms in Kr spectra*

Limits	$^2P_2$				$^2P_1$	
s-terms	$^3P_2$ s_5	$^3P_1$ s_4			$^3P_0$ s_3	$^1P_1$ s_2
p-terms	$^3D_1$ p_{10}	$^3D_3$ p_9	$^3D_2$ p_8		$^3S_1$ p_4	$^1P_1$ p_3
	$^3P_1$ p_7	$^3P_2$ p_6	$^3P_0$ p_5		$^1D_2$ p_2	$^1S_0$ p_1
d-terms	$^3P_0$ d_6	$^3P_1$ d_5	$^3F_4$ d'_4	$^3F_3$ d_4	$^3P_2$ s''_1	$^1D_2$ s''''_1
	$^3F_2$ d_3	$^3D_2$ d''_1	$^3D_3$ d'_1	$^3D_1$ d_2	$^1F_3$ s'''_1	$^1P_1$ s'_1

For the 10 *p*-terms the Russell-Saunders coupling

$$(l_1\, l_2)\ (s_1\, s_2) = (ls) = j$$

gives the following arrangement of inner quantum numbers:[34]

321, 210, 1, 2, 1, 0

The intermediate coupling

$$(\ (l_2\, s_2)\ s_1)\ l_1 = (\ (j_2 s_1)\ l_1) = j$$

or

$$(\ (\ (s_1\, s_2)\ l_2)\ l_1) = (\ (sl_2)\ l_1) = j$$

gives

321, 210, 210, 1

and the coupling

$$(\ (l_1\, s_1)\ (l_2\, s_2)\ ) = (j_1\, j_2) = j$$

gives

3210, 21, 21, 10

In neon the observed grouping of terms is

1, 3212, 1201, 0

In argon it is

1, 3212, 0121, 0

and in krypton, we find the grouping

132120, 1120

[34] Mack, Laporte, and Lang, Phys. Rev., **31**, p. 748; 1928.

The displacement constants, A, found by Paschen and by Meissner for the limits of the Ritzian and non-Ritzian series, are related to the coordination of arc spectrum levels to the two levels $^2P_{2,1}$ of the ions. This constant is, however, not exactly equal to the $^2P_{2,1}$ separation, as is shown in Table 4, where also the data for krypton have been added.

TABLE 4.—*Level separations in Ne I, A I, and Kr I*

	Neon	Argon	Krypton
$1s_5-1s_3$ $^3P_2-^3P_0$	776. 90	1, 409. 92	5, 219. 90
A	780. 0	1, 423. 20	5, 330±
$^2P_{2\ 1}$	782	1, 431	5, 371
Centers of gravity of $3p$-term groups	788	1, 451	5, 353

Since the ground doublet of Kr II has a relatively large separation ($\triangle \nu = 5{,}371\ \text{cm}^{-1}$) it was expected that the two groups in the 10 p-terms and in the 12 d-terms would be clearly separated; this has, indeed, been found to be the case.

2. ABSOLUTE TERM VALUES; IONIZATION POTENTIAL OF Kr

In both neon and argon it was found that the mathematical representation of certain series showed irregularities which appeared as discontinuities in the graphs plotted with effective quantum numbers as ordinates and order numbers as abscissas. In both cases, however, the series $2p_9-md'_4$ gave a smooth curve indicating that it fits a Ritz formula very closely. The krypton series behave very similarly to their neon and argon analogues, but it is a striking fact that with the krypton sources used for our observations the series are relatively short and the intensity decrement is very large so that for the most part each series is traced only through 2, 3, 4, or 5 members.

For the determination of the absolute term values, it is best to extrapolate a long series following a Ritz formula without discontinuities. The series $2p_9-md'_4$ mentioned above is the most regular as well as the longest; in neon, 11 members were observed, in argon 14, and in krypton 8, omitting the first line which lies in the unobserved infra-red at 1.9 μ. We have followed the example of Meissner in basing all term values upon the limit derived from this series. The $2p_9-md'_4$ series fixes the $2p_9$ level at 20,620.87. Adding the wave number of the line $1s_5-2p_9=12{,}322.60$ places the $1s_5$ level at 32,943.47. It must be remarked that this line has been interpreted as $2p_9-3d'_4$ and $1s_5-2p_9$; it may be an unresolved doublet.

The $1s_5$ level can, however, also be calculated from other series; for example, $1s_5-mp_9$ and $1s_5-mp_6$. Furthermore, it can be calcu-

lated from the series $1s_4 - mp_6$ and $1s_4 - mp_7$ because the $1s_5 - 1s_4$ difference ($\Delta\nu = 945.00$ cm^{-1}) is known. The results of these various methods of obtaining $1s_5$ are as follows:

1. Series $2p_9 - md'_4$

$$1s_5 = 32{,}943.47$$

and $\nu = 1s_5 - 2p_9$

2. Series $1s_5 - mp_9$

$$1s_5 = 32{,}941.54$$

3. Series $1s_5 - mp_6$

$$1s_5 = 32{,}943.65$$

4. Series $1s_4 = mp_7$

$$1s_5 = 32{,}944.87$$

and $\Delta\nu = 1s_5 - 1s_4$

5. Series $1s_4 - mp_6$

$$1s_5 = 32{,}943.94$$

and $\Delta\nu = 1s_5 - 1s_4$

The mean of the five values is 32,943.49, practically identical with the first one, which is chosen as the basic value to which all remaining term values are referred. Any error in the level $1s_5 = 32{,}943.47$ is therefore the same for all the other terms.

The data for the five series mentioned above are presented in Table 5.

From the established terms, $1s_4 = 31{,}998.47$, $1s_2 = 27{,}068.57$, and the known resonance lines of krypton

$$p_0 - 1s_4 = 1{,}235.85\text{A};\ \nu = 80{,}916$$
$$p_0 - 1s_2 = 1{,}164.88\text{A};\ \nu = 85{,}846$$

the term value representing the normal state $^1S_0$ of the neutral krypton atom is calculated to be

$$^1S_0 = 112{,}914.50$$

corresponding to an ionization potential of 13.940 volts. This value is in good agreement with the estimation of Abbink and Dorgelo[35] on the absorption of spark lines (ca. 13.9 volts) but somewhat higher than the value obtained by Hertz and Kloppers[36] from critical potential measurements (ca. 13.3 volts).

---

[35] Abbink and Dorgelo, Zeit. f. Phys., **47**, p. 232; 1928.
[36] Hertz and Kloppers: Zeit. f. Phys., **31**, p. 463; 1925.

TABLE 5.—*Determination of absolute term values*

Series $2p_9 - m\ d'_4$ $(5p^3D_3 - 5d^3F_4)$

$$\nu = A - \frac{R}{[m+\mu+\alpha(A-\nu)]^2}$$

$R = 109{,}736.36.$
$A = 20{,}620.868.$
$\mu = +0.5980788914.$
$\alpha = +0.000004693149215.$

m.	Int.	$\lambda_{obs.}$	$\nu_{obs.}$	$\nu_{calc.}$	$\Delta\nu_{calc.-obs.}$
2				5, 231. 214	
3	300	8, 112. 94	12, 322. 60	12, 325. 017	+2. 42
4	50	6, 456. 29	15, 484. 50	15, 484. 500	00
5	10	5, 832. 84	17, 139. 57	17, 139. 570	00
6	4	5, 520. 45	18, 109. 45	18, 109. 180	−. 27
7	3	5, 339. 07	18, 724. 65	18, 724. 483	−. 17
8	1	5, 223. 53	19, 138. 83	19, 138. 877	+. 05
9	−1	5, 144. 97	19, 431. 06	19, 431. 060	. 00
10	−1	5, 089. 02	19, 644. 69	19, 644. 708	+. 02

$\nu = 12{,}322.60 = 1s_5 - {}^2p_9.$
$1s_5 = 20{,}620.87 + 12{,}322.60 = 32{,}943.47.$

Series $1s_5 - mp_9$. $(5s^3P_2 - 5p^3D_3.)$

$A = 32{,}941.544.$
$\mu = +0.379381302 \pm 10^{-10}.$
$\alpha = -0.00000333814841.$

m.	Int.	$\lambda_{obs.}$	$\nu_{obs.}$	$\nu_{calc.}$	$\Delta\nu_{calc.-obs.}$
2	300	8, 112. 94	12, 322. 60	12, 390. 266	+67. 67
3	150	4, 319. 58	23, 143. 86	23, 143. 860	. 00
4	10	3, 679. 60	27, 169. 16	27, 169. 160	. 00
5	2	3, 431. 68	29, 131. 92	29, 131. 395	−. 53
6	1	3, 306. 21	30, 237. 44	30, 237. 440	. 00

$1s_5 = 32{,}941.54.$

Series $1s_5 - mp_6$.

$A = 32{,}943.646.$
$\mu = +0.4149578862 \pm 10^{-10}.$
$\alpha = -0.000002684173300.$

m.	Int.	$\lambda_{obs.}$	$\nu_{obs.}$	$\nu_{calc.}$	$\Delta\nu_{calc.-obs.}$
2	100	7, 601. 55	13, 151. 60	13, 276. 972	+125. 37
3	100	4, 273. 96	23, 390. 94	23, 390. 940	. 00
4	8	3, 665. 35	27, 274. 78	27, 274. 780	. 00
5	2	3, 424. 90	29, 189. 59	29, 187. 182	−2. 41
6	1	3, 302. 54	30, 271. 04	30, 271. 040	. 00

$1s_5 = 32{,}943.65.$

TABLE 5.—*Determination of absolute term values*—Continued

Series $1s_4 - mp_7$

$A = 31{,}999.868.$
$\mu = 0.4024498806.$
$a = -0.000002295749196.$

m	Int.	$\lambda_{obs.}$	$\nu_{obs.}$	$\nu_{calc.}$	$\Delta\nu_{calc-obs.}$
2	300	8, 298. 12	12, 047. 53	12, 248. 58	+200. 95
3	80	4, 463. 69	22, 396. 72	22, 396. 72	. 00
4	5	3, 800. 00	26, 304. 19	26, 304. 19	. 00
5	1	3, 540. 96	28, 232. 89	28, 227. 95	−4. 94
6	1--	3, 409. 94	29, 317. 65	29, 317. 65	. 00

$1s_4 = 31{,}999.87.$
$1s_5 - 1s_4 = \quad 945.00.$
$1s_5 = 32{,}944.87.$

Series $1s_4 - mp_6$.

$A = 31{,}998.942.$
$\mu = 0.4145597886.$
$a = -0.000002649589035.$

m	Int.	$\lambda_{obs.}$	$\nu_{obs.}$	$\nu_{calc.}$	$\Delta\nu_{calc-obs.}$
2	150	8, 190. 10	12, 206. 51	12, 337. 28	+130. 77
3	50	4, 453. 92	22, 445. 85	22, 445. 85	. 00
4	4	3, 796. 94	26, 329. 55	26, 329. 55	. 00
5	1	3, 539. 52	28, 244. 37	28, 242. 10	−2. 27
6	1—	3, 408. 96	29, 326. 08	29, 326. 08	. 00

$1s_4 = 31{,}998.94.$
$1s_5 - 1s_4 = \quad 945.00.$
$1s_5 = 32{,}943.94.$

3. THE PRINCIPAL SERIES, $1s_i - mp_k$

The data for 10 series of the type $1s_i - mp_k$ are presented in Table 6 where the observational data are represented by estimated intensity of the spectral line (in parentheses) followed by the wave length λ. The corresponding wave number in vacuum, ν, was computed with the aid of Kayser's "Tabelle der Schwingungszahlen," except for lines in the unobserved infra-red region which are represented by term differences. Values of m_p have been calculated from each combination, and finally the mean value of each term and the effective quantum number $\sqrt{\frac{R}{m_p}}$, associated with it, are given.

TABLE 6.—*Kr I principal series* $1s_1 - mp_k$

Principal series mp_1

Limit: $1s_2 = 27{,}068.57$

Comb.	m	2	3
s_2p_1	λ	(20)7, 685. 25	(10)4, 351. 36
	ν	13, 008. 37	22, 974. 88
	mp_1	14, 060. 10	4, 093. 69
s_4p_1	λ		
	ν	(17, 938. 27)	(27, 904. 78)
	mp_1		
		14, 060. 20	4, 093. 69
	$\sqrt{\frac{R}{mp_1+A}}$	2. 3789	3. 4124

$A = 5{,}330.$

Principal series, mp_2

Limits: $1s_2 = 27{,}068.57$
$1s_4 = 31{,}998.47$
$1s_5 = 32{,}943.47$

Comb.	m	2	3
s_2p_2	λ	(200)8. 263. 29	(20)4, 399. 97
	ν	12, 098. 39	22, 721. 07
	mp_2	14, 970. 18	4, 347. 50
s_4p_2	λ	(300)5, 870. 92	(4)3, 615. 47
	ν	17, 028. 40	27, 651. 06
	mp_2	14, 970. 07	4, 347. 41
s_5p_2	λ	(50)5, 562. 22	(1)3, 495. 95
	ν	17, 973. 46	28, 596. 37
	mp_2	14, 970. 01	4, 347. 08
Mean	mp_2	14, 970. 09	4, 347. 34
	$\sqrt{\frac{R}{mp_2+A}}$	2. 3250	3. 3674

$A = 5{,}330.$

TABLE 6.—*Kr I principal series*—Continued

Principal series, mp_3
Limits: $1s_2=27{,}068.57$
$1s_3=27{,}723.57$
$1s_4=31{,}998.47$
$1s_5=32{,}943.47$

Comb.	m	2	3
s_2p_3	λ	(100)8, 281. 11	(6)4, 410. 34
	ν	12, 072. 36	22, 667. 64
	mp_3	14, 996. 21	4, 400. 93
s_3p_3	λ	(40)7, 854. 82	(10)4, 286. 45
	ν	12, 727. 53	23, 322. 79
	mp_3	14, 996. 04	4, 400. 78
s_4p_3	λ	(25)5, 879. 88	
	ν	17, 002. 45	
	mp_3	14, 996. 02	
s_5p_3	λ	(200)5, 570. 30	(3)3, 502. 53
	ν	17, 947. 38	28, 542. 65
	mp_3	14, 996. 09	4, 400. 84
Mean	mp_3	14, 996. 09	4, 400. 84
	$\sqrt{\frac{R}{mp_3+A}}$	2. 3235	3. 3581

$A=5{,}330.$

Principal series: mp_4
Limits: $1s_2=27{,}068.57$
$1s_3=27{,}723.57$
$1s_4=31{,}998.47$
$1s_5=32{,}943.47$

Comb.	m	2	3
s_2p_4	λ	(100)8, 508. 92	(10)4, 425. 18
	ν	11, 749. 15	22, 591. 63
	mp_4	15, 319. 42	4, 476. 94
s_3p_4	λ	(50)8, 059. 51	(8)4, 300. 47
	ν	12, 404. 30	23, 246. 75
	mp_4	15, 319. 27	4, 476. 82
s_4p_4	λ	(25)5, 993. 83	(1)3, 632. 46
	ν	16, 679. 21	27, 521. 66
	mp_4	15, 319. 26	4, 476. 81
s_5p_4	λ	(6)5, 672. 40	(1)3, 511. 86
	ν	17, 624. 34	28, 466. 83
	mp_4	15, 319. 13	4, 476. 64
Mean	mp_4	15, 319. 27	4, 476. 80
	$\sqrt{\frac{R}{mp_4+A}}$	2. 3053	3. 3451

$A=5{,}330.$

TABLE 6.—*Kr I principal series*—Continued

Principal series: mp_5

Limits: $1s_3 = 27{,}068.57$

$1s_4 = 31{,}998.47$

Comb.	m	2	3	4	5	6
s_2p_5	λ		(10)5, 580. 33	(2)4, 736. 06	(3)4, 263. 65	(1)4, 086. 91
	ν	8, 246. 23	17, 915. 12	21, 564. 02	23, 449. 65	24, 461. 48
	mp_5		9, 153. 45	5, 504. 55	3, 618. 92	2, 607. 09
s_4p_5	λ	(50)7, 587. 40	(70)4, 376. 13	(6)3, 773. 47	(2)3, 522. 65	(1)3, 401. 40
	ν	13, 176. 13	22, 844. 84	26, 493. 31	28, 379. 63	29, 391. 26
	mp_5	18, 822. 34	9, 153. 63	5, 505. 16	3, 618. 84	2, 607. 21
Mean	mp_5	18, 822. 34	9, 153. 54	5, 504. 86	3, 618. 88	2, 607. 15
	$\sqrt{\frac{R}{mp_5}}$	2. 4145	3. 4624	4. 4646	5. 5067	6. 4876

Principal series: mp_6

Limits: $1s_2 = 27{,}068.57$

$1s_4 = 31{,}998.47$

$1s_5 = 32{,}943.47$

Comb.	m	2	3	4	5	6
s_2p_6	λ		(4)5,707.47			
	ν	7,276.65	17,516.05			
	mp_6		9,552.52			
s_4p_6	λ	(150)8,190.10	(50)4,453.92	(4)3,796.94	(1)3,539.52	(1−)3,408.96
	ν	12,206.51	22,445.85	26,329.55	28,244.37	29,326.08
	mp_6	19,791.96	9,552.62	5,668.92	3,754.10	2,672.39
s_5p_6	λ	(100)7,601.55	(100)4,273.96	(8)3,665.35	(2)3,424.90	(1)3,302.54
	ν	13,151.60	23,390.94	27,274.78	29,189.59	30,271.04
	mp_6	19,791.87	9,552.51	5,668.69	3,753.88	2,672.43
Mean	mp_6	19,791.92	9,552.56	5,668.85	3,753.99	2,672.41
	$\sqrt{\frac{R}{mp_6}}$	2.3546	3.3893	4.3997	5.4067	6.4080

TABLE 6.—*Kr I principal series*—Continued

Principal series: mp_7

Limits: 1 s_2=27,068.57
1 s_3=27,723.57
1 s_4=31,998.47
1 s_5=32,943.47

Comb.	m	2	3	4	5	6
s_2p_7	λ		(2) 5,723.50			
	ν	7,117.77	17,466.99			
	mp_7		9,601.58			
s_3p_7	λ		(3) 5,516.56		(1) 4,172.75	(1) 3,992.01
	ν	7,772.77	18,122.22		23,958.27	25,042.98
	mp_7		9,601.35		3,765.83	2,680.59
s_4p_7	λ	(300) 8,298.12	(80) 4,463.69	(5) 3,800.60	(1) 3,540.96	(1) 3,409.94
	ν	12,047.63	22,396.72	26,304.19	28,232.89	29,317.65
	mp_7	19,950.84	9,601.75	5,694.28	3,765,58	2,680.82
s_5p_7	λ	(30) 7,694.52	(20) 4,282.94	(2) 3,668.76		
	ν	12,992.71	23,341.90	27,249.43		
	mp_7	19,950.76	9,601.57	5,694.03		
Mean	mp_7	19,950.80	9,601.56	5,694.16	3,765.58	2,680.70
	$\sqrt{\frac{R}{mp_7}}$	2.3453	3.3807	4.3899	5.3984	6.3980

Principal series: mp_8

Limits: 1 s_2=27,068.57
1 s_4=31,998.47
1 s_5=32,943.47

Comb.	m	2	3	4
s_2p_8	λ		(1) 5,787.13	
	ν	6,460.69	17,274.94	
	mp_8		9,793.63	
s_4p_8	λ	(150) 8,776.80	(60) 4,502.35	(3) 3,812.24
	ν	11,390.55	22,204.42	26,223.88
	mp_8	20,607.92	9,794.05	5,774.59
s_5p_8	λ	(100) 8,104.37	(50) 4,318.57	(10) 3,679.60
	ν	12,335.63	23,149.32	27,169.16
	mp_8	20,607.84	9,794.15	5,774.31
Mean	mp_8	20,607.88	9,793.94	5,774.45
	$\sqrt{\frac{R}{mp_8}}$	2.3075	3.3474	4.3593

TABLE 6.—*Kr I principal series*—Continued

Principal series: mp_9

Limit: $1s_5 = 32{,}943.47$

Comb.	m	2	3	4	5	6
s_5p_9	λ	(300)8, 112. 94	(150)4, 319. 58	(10)3, 679. 60	(2)3, 431. 68	(1)3, 306. 24
	ν	12, 322. 60	23, 143. 86	27, 169. 16	29, 131. 92	30, 237. 17
	mp_9	20, 620. 87	9, 799. 61	5, 774. 31	3, 811. 55	2, 706. 30
	$\sqrt{\frac{R}{mp_9}}$	2. 3069	3. 3463	4. 3593	5. 3657	6. 3678

Principal series: mp_{10}

Limits: $1s_2 = 27{,}068.57$
$1s_3 = 27{,}723.57$
$1s_4 = 31{,}998.47$
$1s_5 = 32{,}943.47$

Comb.	m	2	3	4	5
s_2p_{10}	λ		(20)5, 866. 75	(2)4, 724. 84	(2)4, 302. 41
	ν	5, 321. 85	17, 040. 50	21, 158. 84	23, 236. 27
	mp_{10}		10, 028. 07	5, 909. 73	3, 832. 30
s_3p_{10}	λ		(15)5, 649. 54	(3)4, 582. 80	(3)4, 184. 46
	ν	5, 976. 85	17, 695. 66	21, 814. 63	23, 891. 24
	mp_{10}		10, 027. 91	5, 908. 94	3, 832. 33
s_4p_{10}	λ	(3)9, 751. 77	(5)4, 550. 30		
	ν	10, 251. 75	21, 970. 43		
	mp_{10}	21, 746. 72	10, 028. 04		
s_5p_{10}	λ	(100)8, 928. 73	(50)4, 362. 64	(1)3, 698. 01	(1)3, 434. 10
	ν	11, 196. 75	22, 915. 48	27, 033. 90	29, 111. 40
	mp_{10}	21, 746. 72	10, 027. 99	5, 909. 57	3, 832. 07
Mean	mp_{10}	21, 746. 72	10, 028. 00	5, 909. 65	3, 832. 23
	$\sqrt{\frac{R}{mp_{10}}}$	2. 2463	3. 3079	4. 3092	5. 3512

Table 6 verifies the statement made before that the ten $1s_i$-mp_k series are separated into two groups, $p_{1,\,2,\,3,\,4}$ going to the higher level ($^2P_1$) of the ion, and $p_{5,\,6\,\ldots\,10}$ to the lower level ($^2P_2$). Since the $1s - mp_{1,\,2,\,3,\,4}$ series are short, having only two members each, it is not possible to determine the displacement constant A accurately. Assuming that the change in quantum defects for the $2p_{1,\,2,\,3,\,4}$ and $3p_{1,\,2,\,3,\,4}$ terms is of the same order as for the terms $mp_{5,\,6\,\ldots\,10}$ following the Ritz formula the displacement constant turns out to be about 5,330.

Another approximation can be obtained with the aid of Landé's center-of-gravity rule. It has been shown by Landé [37] that for neon

[37] Back-Landé, Zeemaneffekt u. Multipletstruktur, Julius Springer, Berlin, 1925, p. 58.

the separation of the center of gravity of the 2-term groups ($p_{1,\ 2,\ 5,\ 4}$) and ($p_{3,\ 7,\ 10,\ 6,\ 8,\ 9}$) has nearly the same value as the displacement constant A, and with higher order number approaches this magnitude. The analogous groups in krypton are ($p_{1,\ 3,\ 4,\ 2}$) and ($p_{5,\ 7,\ 10,\ 6,\ 8,\ 9}$). The separation of the centers of gravity of these two groups amounts to 5,420 for the $2p$ terms, and 5,353 for the $3p$ terms.

Both approximations, 5,330 from the series limits and 5,353 from the center-of-gravity calculation, are in close agreement with the separation of the $^2P_{2,\ 1}$ levels of Kr^+ which is 5,371 cm^{-1}. From the term table, it is seen that the center of gravity of the $3p_{1,\ 2,\ 3,\ 4}$ term group will have the value of about 420 so that these terms are already very high and would be expected to give only very faint lines. Thus it is apparent that the large separation of the $^2P_{2,\ 1}$ levels of the Kr ion is partly responsible for the relative simplicity of the observed Kr I spectrum.

It may be questioned whether the p_1 term is correctly identified since the combinations with the $1s_4$ level are not present. After ordering the lines in the sp and pd series only the strong line at 7685.25 A remained. Assuming that this is the lacking $1s_2-2p_1$ combination puts the $2p_1$ term in the region where it must be expected, and the effective quantum number also supports this interpretation. The absence of other expected combinations can not be explained, but similar cases occur in other spectra; for example, $1s_2-2p_5$, $1s_5-4p_{10}$, $1s_5-5p_{10}$, and $1s_5-4p_4$, which are expected to be relatively strong are entirely absent in argon.

No lines of the principal series can be expected shorter than 3034 A, and between this limit and the resonance line at 1236 A no krypton arc lines can be present. Above this limit some additional faint lines may be observable; further investigation of these with a brighter source will be important for the extension of some of the relatively short series.

The corresponding terms in Ne I, A I, and Kr I spectra and their coordination to limits are compared in Table 7.

TABLE 7.—*Corresponding terms in Ne I, A I, and Kr I spectra, and their coordination to limits in Ne II, A II, and Kr II spectra*

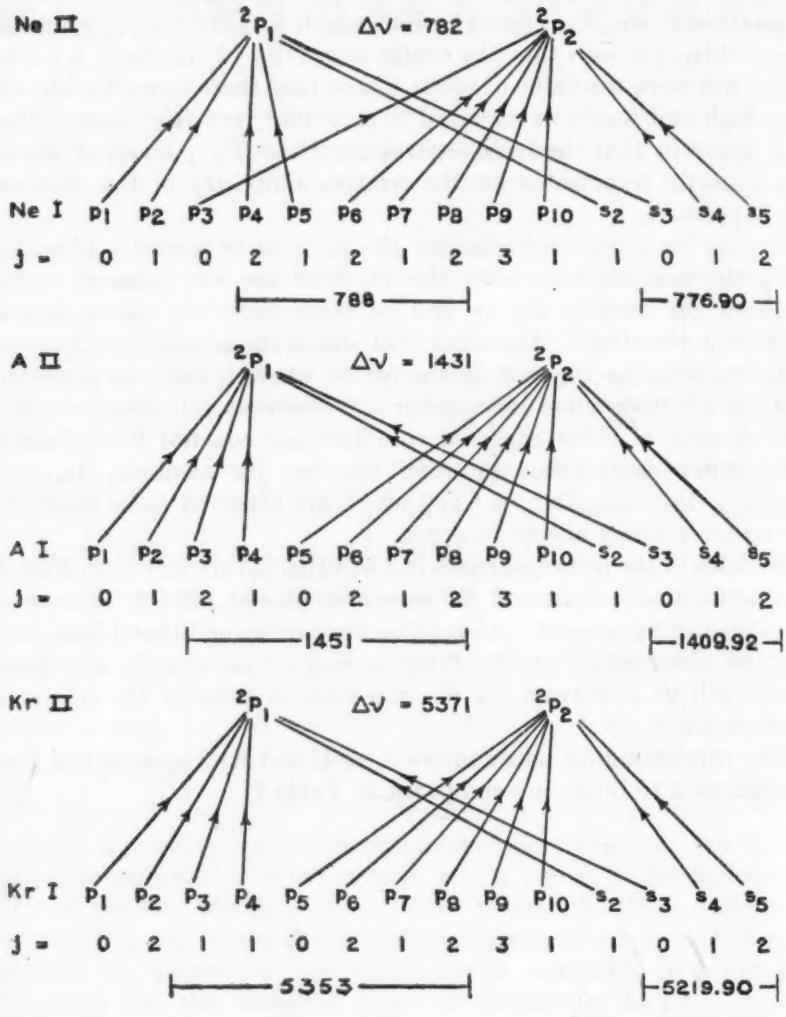

4. THE X AND Y SERIES

Paschen found in the Ne I spectrum some terms which he could not identify, so he labeled them x and y terms. In the A I spectrum Meissner found similar terms which he called X, Y, and Z terms. Important characteristics of these unidentified terms are that they begin with order No. 4 and are hydrogenlike; thus in neon, these terms have effective quantum numbers 3.9937 and 3.9939, in argon 3.9813, 3.9932, and 3.9937. In krypton four such terms have been found; their effective quantum numbers are 3.9726, 4.9746, 3.9896, and 4.9693.

Judging from the effective quantum numbers, Meissner suspected that these terms came from an f-electron. The addition of an f-electron to the $(s^2\ p^5)$ configuration of krypton would give rise to the term group

$$^1D_2,\ ^1F_3,\ ^1G_4,\ ^3D_{1,\ 2,\ 3},\ ^3F_{2,\ 3,\ 4},\ ^3G_{3,\ 4,\ 5}.$$

Only one level, $^3D_1$ can combine with the four s-levels, and it is possible that this is the correct interpretation of our mX terms. For the mY terms there remains a choice between $^3D_2$, $^3F_2$, $^1D_2$, but it seems most likely that they should be identified as $^3D_2$ since the separation between the mX and mY terms is relatively small.

Data for the X and Y series of krypton are collected in Table 8 which is arranged in the same way as Table 6.

TABLE 8.—*The X and Y series*

Series mX

Limits: $1s_2$=27,068.57
$1s_3$=27,723.57
$1s_4$=31,998.47
$1s_5$=32,943.47

Comb.	m	4	5	6
s_2X	λ	(5d) 4, 969. 17	(3) 4, 416. 84	(1−) 4, 167. 26
	ν	20, 118. 49	22, 634. 28	23, 989. 84
	mX	6, 950. 08	4, 434. 29	3, 078. 73
s_3X	λ	(6) 4, 812. 61	(1) 4, 292. 64	(1−) 4, 056. 39
	ν	20, 772. 96	23, 289. 16	24, 645. 53
	mX	6, 950. 61	4, 434. 41	3, 078. 04
s_4X	λ	(5) 3, 991.13		(1−) 3, 456. 80
	ν	25, 048. 50		28, 920. 23
	mX	6, 949. 97		3, 078. 21
s_5X	λ	(3) 3,846. 06	(1) 3, 506. 67	
	ν	25, 993. 29	28, 508. 96	
	mX	6, 950. 18	4, 434. 51	
Mean	mX	6, 950. 21	4, 434. 40	3, 078. 40
	$\sqrt{\frac{R}{mpX}}$	3. 9726	4. 9746	5. 9705

TABLE 8.—*The X and Y series*

Series mY

Limits: 1 s_2=27,068.57
1 s_4=31,998.47
1 s_5=32,943.47

Comb.	m	4	5
s_2Y	λ	(3) 4, 955. 22	(5) 4, 418. 74
	ν	20, 175. 12	22, 624. 35
	mY	6, 893. 45	4, 444. 22
s_4Y	λ	(1) 3, 982. 26	(2) 3, 628. 12
	ν	25, 104. 29	27, 554. 66
	mY	6, 894. 18	4, 443. 81
s_5Y	λ	(5) 3, 837. 87	(1) 3, 507. 87
	ν	26, 048. 75	28, 499. 21
	mY	6, 894. 72	4, 444. 26
Mean	mY	6, 893. 68	4, 444. 10
	$\sqrt{\frac{R}{mY}}$	3. 9896	4. 9693

5. THE SUBORDINATE SERIES

All the observed combinations of md_1 and ms_1 levels with the mp_1 terms are collected in Table 9. It is seen from this table that numerous combinations which can be expected on the basis of the assigned inner quantum numbers have not been observed, some on account of faintness and others because they lie in the unexplored infra-red. Further efforts to record fainter lines will be necessary to test some of the tentatively assigned inner quantum numbers.

The combinations with the non-Ritzian term group, $2p_{1,\ 2,\ 3,\ 4}$ are expected in the far infra-red. Strong combinations, both ps and pd, are expected in the spectral region between 1 μ and 2 μ; the wave lengths can be calculated from the terms with considerable precision.

Table 9 also shows that the group of four d-terms coordinated to $^2P_1$ is not yet found. First, it was supposed that some of the terms now interpreted as higher d-terms represented this group, but since these terms were later found to be in series with the lower d-terms the earlier point of view was discarded. It is further seen from Table 9 that the non-Ritzian terms are already high even with relatively low order number. This is no doubt the reason that the observed spectrum is mainly due to combinations with terms coordinated to the lower $^2P_2$ level of the Kr ion. One may expect that this feature will be still further developed in the arc spectrum of xenon.

TABLE 9.—*The subordinate series*

			18,822.34	19,791.92	19,950.80	20,607.88	20,620.87	21,746.72	112,914.50
				969.58	158.88	657.08	12.99	1,125.85	
j	Term value	Term symbol	$^2p_5$	$^2p_6$	$^2p_7$	$^2p_8$	$^2p_9$	$^2p_{10}$	p_0
3	9, 213. 84	$4d'_1$				(1)11, 393. 99	(2)11, 407. 08		
1	9, 113. 43	$4d_5$				(1)11, 494. 47		(5)12, 633. 27	(2)103, 803
0	8, 393. 70	$4d_6$						(5)13, 353. 02	
4	8, 298. 27	$4d'_4$					(100)12,322.60		
3	7, 998. 83	$4d_4$				(4)12, 609. 08	(1)12, 622. 00		
2	7, 907. 97	$4d_3$		(2)11, 883. 95				(5)13, 838. 74	
2	7, 751. 72	$4d''_1$			(2)12, 199. 06	(1)12, 856. 17			
1	7, 267. 46	$3s$		(2)12, 524. 22		(1)13, 340. 88	(5)13, 353. 02+	(10)14, 479. 03	(4)105, 645
1	7, 144. 49	$4d_2$	(1)11, 677. 93		(1)12, 806. 24	(3)13, 463. 35		(3)14, 602. 24	(3)105, 772
	6, 452. 01	x		(1)13, 340. 17				(3)15, 294. 44	
0	5, 311. 57	$5d_6$			(1)14, 639. 4			(10)16, 435. 15	
1	5, 238. 90	$5d_5$		(4)14, 552. 94	(1)14, 712. 15	(3)15, 368. 95		(20)16, 507. 69	
4	5, 136. 37	$5d'_4$					(50)15, 484. 50		
2	5, 118. 27	$5d_3$		(8)14, 673. 65	(4)14, 832. 62		(4)15, 502. 58	(20)16, 628. 47+	
3	5, 038. 30	$5d_4$				(30)15, 569. 53	(8)15, 582. 61		
2	4, 922. 37	$5d''_1$		(1)14, 869. 8	(10)15, 028. 45	(8)15, 685. 49	(1)15, 698. 52		
3	4, 868. 83	$5d'_1$		(15)14, 923. 09		(3)15, 739. 08	(5)15, 752. 02		
2	4, 590. 11	$4s$		(5)15, 201. 77	(1)15, 360. 76	(3)16, 017. 80	(10)16, 030. 72	(6)17, 156. 57	
1	4, 541. 94	$5d_2$	(1)14, 280. 3	(3)15, 249. 90	(5)15, 408. 82	(6)16, 065. 88		(2)17, 204. 98	
0	3, 584. 02	$6d_6$			(1)16, 366. 49			(4d)18, 162. 98	

TABLE 9.—*The subordinate series*—Continued

j	Term value	Term symbol	$^2p_5$	$^2p_6$	$^2p_7$	$^2p_8$	$^2p_9$	$^2p_{10}$	p_0
1	3, 572. 26	$6d_5$	(3)15, 249. 90+	(3)16, 219. 70				(6)18, 174. 60	
2	3, 539. 84	$6d_3$		(5)16, 252. 13	(1)16, 411. 06		(1)17, 080. 97	(5)18, 206. 87	
4	3, 481. 30	$6d'_4$					(10)17, 139. 57		
3	3, 443. 72	$6d_4$			(20)16, 507. 69+	(8)17, 164. 14	(4)17, 177. 17		
2	3, 387. 57	$6d''_1$			(4)16, 563. 26	(3)17, 220. 28			
3	3, 336. 02	$6d'_1$		(5)16, 455. 82		(1)17, 271. 89	(2)17, 284. 83		
2	3, 163. 03	$5s$		(20)16, 628. 47+		(1)17, 444. 90	(3)17, 457. 72	(2)18, 583. 76	
1	3, 135. 82	$6d_2$			(2)16, 814. 96	(2)17, 472. 18			
1	2, 811. 72			(1)16, 980. 2	(10)17, 139. 57+			(1)18, 935. 00	
1	2, 579. 47	$7d_5$		(1)17, 212. 34				(2)19, 167. 38	
4	2, 511. 42	$7d'_4$					(4)18, 109. 45		
3	2, 406. 97	$7d'_1$		(2)17, 384. 68			(1)18, 214. 2		
2	2, 402. 13	$7d_3$		(1)17, 389. 58				(1)19, 344. 85	
2	2, 306. 71	$6s$					(1h)18, 313. 73	(7)19, 440. 01	
3	1, 867. 90					(2)18, 740. 17		(1)19, 878. 63	

6. THE Kr I SPECTRUM IN THE EXTREME ULTRA-VIOLET

The following krypton arc lines in the extreme ultra-violet have been reported (Table 10) by Abbink and Dorgelo.[38]

TABLE 10.—*First spectrum of Kr in the extreme ultra-violet*

Line No.	Int.	λ	(Obs.)	(Calc.)	Combination
1	30	1, 235. 85	80, 916. 0		$p_0 - 1s_4$
2	20	1, 164. 88	85, 846. 0		$p_0 - 1s_2$
3	(3)	1, 134. 89	88, 114. 3		
4	(3)	1, 134. 15	88, 171. 8		
5	5	1, 003. 54	99, 647. 3		$p_0 - 3d_3$
6	7	1, 001. 09	99, 891. 1		$p_0 - 2s_4$
7	2	963. 36	103, 803	103, 801. 07	$p_0 - 4d_5$
8	(3)	953. 42	104, 886	104, 886. 60	$p_0 - 2s_2$
9	4	946. 57	105, 645	105, 647. 04	$p_0 - 3s_2$
10	3	945. 43	105, 772	105, 770. 01	$p_0 - 4d_2$

The adherence of lines 3, 4, and 8 to the first spectrum of krypton is admitted to be doubtful. The first pair (1,235.85 and 1,164.88 A) are the resonance lines which we have used in connection with our terms to calculate the ionization potential of krypton. (See p. 139.) Lines 5, 6, 7, 9, and 10, respectively, fix the following levels: 13,267, 13,023, 9,111, 7,269, and 7,142.

Comparison with our term table (Table 9, p. 151) shows that the last three are identifiable with our levels 9,113.96, 7,267.46, and 7,144.49. In argon, a group of five strong lines on the short wavelength side of the resonance lines is explained by combinations of p_0 with $3d_5$, $2s_4$, $3d_2$, $2s_2$, and $3s_1'$ which are the levels with the inner quantum number $j=1$. Five lines have also been observed in krypton, but it is doubtful if these lines involve the same levels as in argon.

On account of the large displacement constant A for krypton, we interpret the 13,267 level as $3d_5$, the lowest of the group, in analogy with argon. The 13,023 level is probably $2s_4$; its effective quantum number is 2.9024, in agreement with the effective quantum number of $1s_4$, viz, 1,8519.

The doubtful doublet at 1134 A would give levels in a region where no terms can be expected; these lines can not belong to the first spectrum of krypton. The remaining line at 953 A was also doubtful, but it appears to be real; it involves a level at 8,028 identifiable with our level 8,027.90 separated 4,995 cm $^{-1}$ from the $2s_4$ level at 13,023, the former being identified as $2s_2$ since the separation $s_4 - s_2$ which is 4,930 cm $^{-1}$ in the $1s$ group must approach the $^2P_{2,1}$ separation (5,371 cm $^{-1}$), of the ion.

[38] Abbink and Dorgelo, Zeit. f. Phys. **47**, p. 221; 1928.

An interpretation is thus given of all the lines ascribed to the first spectrum of krypton in the extreme ultra-violet. From analogy with argon more krypton lines may be expected in this region, and further attempts to record fainter lines will be important for the identification of certain levels which still remain doubtful.

7. IDENTIFICATION OF THE EXPERIMENTAL TERMS

In Table 11 we give a complete list of the Kr I terms. The first column contains the added electron.

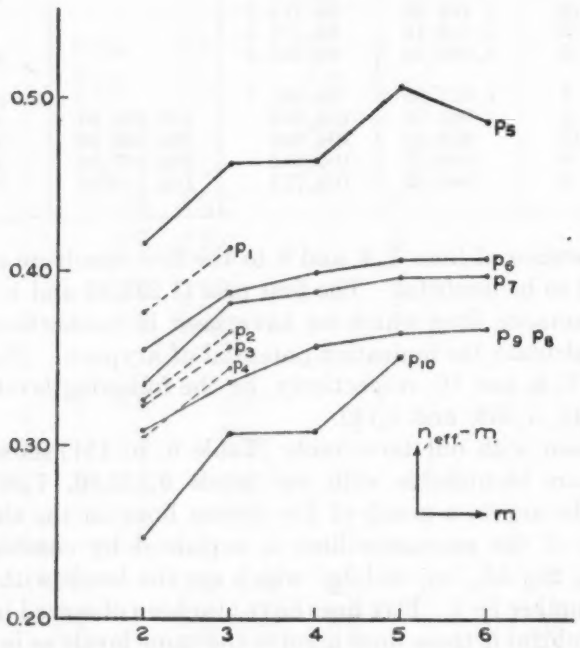

FIGURE 5.—*Effective quantum numbers for p-terms*

The inner quantum numbers are given in column 2. The Paschen notation is presented in the third column, and the remaining columns contain alternately the term values and the corresponding effective quantum numbers. The latter are an excellent criterion for the arrangement of terms in series, and when they are plotted as a function of the order number they present some interesting facts and relations. Such plots are shown in Figures 5 and 6, *p* terms in the former, *d* and *s* terms in the latter. Comparison with similar diagrams published for argon reveal further analogies between the Kr I spectrum and the A I spectrum.

Thus, Figure 5 compared with argon shows that in both cases the series converging to the upper limit $^2P_1$ are shorter than those coordi-

TABLE 11.—*Terms and effective quantum num*

Electron	j	Term Paschen notation		1		2		3		4		5		
p	0	p_0	112, 914. 50 =13. 940 volts											
s	2	s_5		32, 943. 47	1. 8251	(13, 500±)								
	1	s_4		31, 998. 47	1. 8519	13, 023	2. 9024	7, 267. 46	3. 8857					
	0	s_3		27, 723. 57	1. 8220	(8, 300±)								
	1	s_2		27, 068. 57	1. 8404	8, 027. 90	2. 8662							
p	1	p_{10}				21, 746. 72	2. 2463	10, 028. 00	3. 3079	5, 909. 65	4. 3092	3, 832. 18	5. 3512	
	3	p_9				20, 620. 87	2. 3069	9, 799. 61	3. 3463	5, 774. 31	4. 3593	3, 811. 55	5. 3657	2, 7
	2	p_8				20, 607. 88	2. 3075	9, 793. 94	3. 3474	5, 774. 45	4. 3593	3, 809. 29	5. 3672	
	1	p_7				19, 950. 80	2. 3453	9, 601. 56	3. 3807	5, 694. 16	4. 3899	3, 765. 58	5. 3984	2, 6
	2	p_6				19, 791. 92	2. 3546	9, 552. 56	3. 3893	5, 668. 85	4. 3997	3, 753. 99	5. 4067	2, 6
	0	p_5				18, 822. 34	2. 4145	9, 153. 54	3. 4624	5, 504. 86	4. 4648	3, 618. 88	5. 5067	2, 6
	1	p_4				15, 319. 27	2. 3053	4, 476. 80	3. 3451					
	1	p_3				14, 996. 09	2. 3235	4, 400. 84	3. 3581					
	2	p_2				14, 970. 09	2. 3250	4, 347. 34	3. 3674					
	0	p_1				14, 060. 20	2. 3789	4, 098. 69	3. 4124					
f	1	X								6, 950. 21	3. 9726	4, 434. 40	4. 9746	3, 0
	2	Y								6, 893. 68	3. 9896	4, 441. 10	4. 9693	
d	0	d_6								8, 393. 70	3. 6157	5, 311. 57	4. 5453	3, 5
	1	d_5						13, 267	2. 8760	9, 113. 43	3. 4700	5, 238. 90	4. 5766	3, 5
	4	d'_4								8, 298. 27	3. 6364	5, 136. 37	4. 6222	3, 4
	2	d_3								7, 907. 97	3. 7254	5, 118. 27	4. 6304	3, 5
	3	d_4								7, 998. 83	3. 7039	5, 038. 30	4. 6670	3, 4
	2	d''_1								7, 751. 72	3. 7625	4, 922. 37	4. 7215	3, 3
	3	d'_1								9, 213. 84	3. 4511	4, 868. 83	4. 7480	3, 3
	1	d_2								7, 144. 49	3. 9191	4, 541. 94	4. 9154	3, 1
	2(1)	s								7, 267. 46	3. 8857	4, 590. 11	4. 8895	3, 1

ntum numbers of Kr I

	$m=$											
	6		**7**		**8**		**9**		**10**		**11**	
3512												
3657	2, 706. 30	6. 3678										
3672												
3984	2, 680. 82	6. 3980										
4067	2, 672. 43	6. 4080										
5067	2, 607. 43	6. 4876										
9746	3, 078. 40	5. 9705										
9693												
5453	3, 584. 02	5. 5335	2, 624. 77	6. 4659	1, 981. 07	7. 4370						
5766	3, 572. 26	5. 5426	2, 579. 47	6. 5226	1, 911. 99	7. 5759						
6222	3, 481. 30	5. 6144	2, 511. 42	6. 6102	1, 896. 22	7. 6073	1, 482. 04	8. 6049	1, 189. 81	9. 6033	976. 18	10. 6025
6304	3, 539. 84	5. 5679	2, 402. 10	6. 7590								
6670	3, 443. 72	5. 6450	2, 444. 62	6. 6977	1, 867. 71	7. 6651	1, 464. 47	8. 6564				
7215	3, 387. 57	5. 6912	2, 418. 41	6. 7361								
7480	3, 336. 02	5. 7353	2, 406. 97	6. 7518								
9154	3, 135. 82	5. 9157										
8895	3, 163. 03	5. 8901	2, 306. 71	6. 8907								

nated to $^2P_2$. The plots of $n_{eff} - m$ for p_6 and p_7 series run parallel. This is also true for the p_8 and p_9 series; in krypton they are practically identical and so could not be separated in the diagram. The term sequences p_5 and p_{10} are most irregular, but the discontinuities are of the same type for both series in krypton as well as in argon.

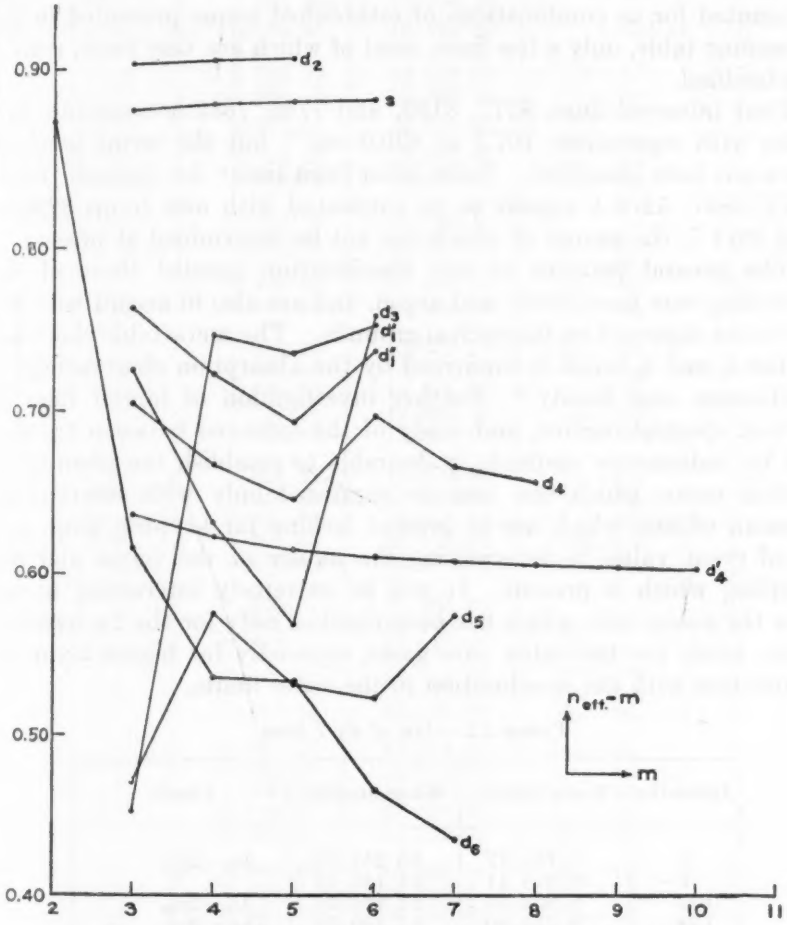

FIGURE 6.—*Effective quantum numbers for d- and s- terms*

Comparison of Figure 6 with the corresponding diagram for argon attracts attention to the following analogies. In both cases the d'_4 series gives the most perfect smooth curve; the curves for d''_1 and d_4 are irregular, but of the same type; the d_2 series is well separated from the others; most of the remaining series are very irregular and dissimilar.

8. LIST OF Kr I LINES

A complete list of the observed lines characteristic of the first spectrum of krypton is presented in Table 12, in which the estimated intensities appear in the first column, the wave lengths (international scale) in the second, wave numbers (vacuum) in the third, and level combinations in the fourth. Almost all of the 205 observed lines are accounted for as combinations of established terms presented in the preceding table, only a few lines, most of which are very faint, remain unclassified.

Four infra-red lines, 8272, 8199, and 7746, 7682 A constitute two pairs with separations 107.7 or 820.0 cm^{-1}, but the terms involved have not been identified. Some other faint lines; for example, 6410, 5977, 5887, 5279 A appear to be connected with new terms 3226.84 and 2811.7, the nature of which can not be determined at present.

The general features of this classification parallel those of the preceding rare gases, neon and argon, and are also in accord with the structure expected on theoretical grounds. The metastable character of the s_3 and s_5 levels is confirmed by the absorption observations of McLennan and Ruedy.[39] Further investigation of fainter lines in certain spectral regions, and study of the infra-red between 1 μ and 2 μ by radiometric methods, is desirable to establish the identity of certain terms which can now be suggested only with reservation. Zeeman effects, which are at present lacking for krypton lines, will be of great value in determining the nature of the terms and the coupling which is present. It will be extremely interesting to see how the g-sum rule, which has been checked only for the $2p$ terms of neon, holds for the other rare gases, especially for higher terms in connection with the coordination to the series limits.

TABLE 12.—*List of Kr I lines*

Intensity	Wave length	Wave number	Comb.
3	9, 751. 77	10, 251. 75	$1s_4-2p_{10}$
1−	8, 978. 11	11, 135. 15	
100	8, 928. 73	11, 196. 75	$1s_5-2p_{10}$
150	8, 776. 80	11, 390. 55	$1s_4-2p_9$
1	8, 774. 15	11, 393. 99	$2p_8-4d'_1$
2	8, 764. 08	11, 407. 08	$2p_9-4d'_1$
1−	8, 697. 45	11, 494. 47	$2p_8-4d_5$
1	8, 560. 81	11, 677. 93	$2p_5-4d_2$
1	8, 548. 44	11, 694. 83	
100	8, 508. 92	11, 749. 15	$1s_2-2p_4$
1−	8, 498. 15	11, 764. 02	$2p_6-2s_2$
2	8, 412. 40	11, 883. 95	$2p_6-4d_3$
1−	8, 386 62	11, 920. 48	
1−	8, 351. 22	11, 971. 01	
300	8, 298. 12	12, 047. 53	$1s_4-2p_7$

[39] McLennan and Ruedy, Trans. Roy. Soc. Can., 22 (3), p. 15; 1928.

TABLE 12.—*List of Kr I lines*—Continued

Intensity	Wave length	Wave number	Comb.
100	8, 281. 11	12, 072. 36	$1s_2-2p_3$
3	8, 272. 41	12, 085. 06	+819. 90
200	8, 263. 29	12, 098. 39	$1s_2-2p_2$
1—	8, 209. 67	12, 177. 42	
1	8, 199. 41	12, 192. 66	+820. 11
2	8, 195. 10	12, 199. 06	$2p_7-4d''_1$
150	8, 190. 10	12, 206. 51	$1s_4-2p_6$
300	8, 112. 94	12, 322. 60	$1s_5-2p_9$, $2p_9-4d_4$
100	8, 104. 37	12, 335. 63	$1s_5-2p_8$
50	8, 059. 51	12, 404. 30	$1s_3-2p_4$
1	8, 026. 36	12, 455. 53	
2	7, 982. 34	12, 524. 22	$2p_6-3s$
1—	7, 946. 99	12, 579. 93	$2p_3-2s_2$
4	7, 928. 61	12, 609. 08	$2p_8-4d_4$
1	7, 920. 50	12, 622. 00	$2p_9-4d_4$
5	7, 913. 43	12, 633. 27	$2p_{10}-4d_5$
40	7, 854. 82	12, 727. 53	$1s_3-2p_3$
1	7, 806. 55	12, 806. 24	$2p_7-4d_2$
1	7, 776. 23	12, 856. 17	$2p_8-4d''_1$
4	7, 746. 83	12, 904. 96	−819. 90
30	7, 694. 52	12, 992. 71	$1s_5-2p_7$
20	7, 685. 25	13, 008. 37	$1s_2-2p_1$
1	7, 682. 65	13, 012. 77	−820. 11
100	7, 601. 55	13, 151. 60	$1s_5-2p_6$
50	7, 587. 40	13, 176. 13	$1s_4-2p_5$
1	7, 520. 51	13, 293. 32	
1	7, 494. 01	13, 340. 17	$2p_8-x_3$
1	7, 493. 70	13, 340. 88	$2p_8-3s_2$
5	7, 486. 87	13, 353. 02	$2p_{10}-4d_6$, $2p_9-3s$
3	7, 425. 53	13, 463. 35	$2p_8-4d_2$
4	7, 287. 25	13, 718. 82	$2p_{10}-2s_2$
5	7, 224. 10	13, 838. 74	$2p_{10}-4d_3$
1	7, 000. 73	14, 280. 3	$2p_5-5d_2$
10	6, 904. 64	14, 479. 03	$2p_{10}-3s$
4	6, 869. 57	14, 552. 94	$2p_6-5d_5$
3	6, 846. 38	14, 602. 24	$2p_{10}-4d_2$
1	6, 829. 0	14, 639. 4	$2p_7-5d_6$
8	6, 813. 06	14, 673. 65	$2p_8-5d_3$
1	6, 795. 23	14, 712. 15	$2p_7-5d_5$
4	6, 740. 04	14, 832. 62	$2p_7-5d_3$
1	6, 723. 2	14, 869. 8	$2p_8-5d''_1$
15	6, 699. 18	14, 923. 09	$2p_6-5d'_1$
10	6, 652. 21	15, 028. 45	$2p_7-5d''_1$
5	6, 576. 37	15, 201. 77	$2p_7-4s$
3	6, 555. 61	15, 249. 90	$2p_6-5d_2$, $2p_5-5d_5$
3	6, 536. 52	15, 294. 44	$2p_{10}-x$
1	6, 508. 30	15, 360. 76	$2p_7-4s$
3	6, 504. 83	15, 368. 95	$2p_8-5d_5$
5	6, 488. 00	15, 408. 82	$2p_7-5d_2$
50	6, 456. 29	15, 484. 50	$2p_6-5d'_4$

TABLE 12.—*List of Kr I lines*—Continued

Intensity	Wave length	Wave number	Comb.
4	6, 448. 76	15, 502. 58	$2p_9-5d_3$
30	6, 421. 03	15, 569. 53	$2p_8-5d_4$
8	6, 415. 64	15, 582. 61	$2p_9-5d_4$
2	6, 410. 12	15, 596. 03	$2p_5-3226.33$
8	6, 373. 56	15, 685. 49	$2p_8-5d''_1$
1	6, 368. 27	15, 698. 52	$2p_9-5d''_1$
3	6, 351. 86	15, 739. 08	$2p_8-5d'_1$
5	6, 346. 64	15, 752. 02	$2p_9-5d'_1$
3	6, 241. 33	16, 017. 80	$2p_8-4s$
10	6, 236. 30	16, 030. 72	$2p_9-4s$
6	6, 222. 65	16, 065. 88	$2p_8-5d_2$
3	6, 163. 64	16, 219. 70	$2p_6-6d_5$
5	6, 151. 34	16, 252. 13	$2p_6-6d_3$
1	6, 108. 36	16, 366. 49	$2p_7-6d_6$
1	6, 091. 77	16, 411. 06	$2p_7-6d_3$
10	6, 082. 84	16, 435. 15	$2p_{10}-5d_6$
5	6, 075. 20	16, 455. 82	$2p_6-6d'_1$
20	6, 056. 11	16, 507. 69	$2p_{10}-5d_5$
4	6, 035. 79	16, 563. 26	$2p_8-6d''_1$
20	6, 012. 12	16, 628. 47	$2p_{10}-5d_3$ $2p_6-5s$
25	5, 993. 83	16, 679. 21	$1s_4-2p_4$
1	5, 977. 6	16, 724. 5	$2p_7-3, 226.3$
2	5, 945. 42	16, 814. 96	$2p_7-6d_2$
1	5, 933. 53	16, 848. 72	
1	5, 887. 6	16, 980. 2	$2p_6-2, 811.72$
25	5, 879. 88	17, 002. 45	$1s_4-2p_3$
300	5, 870. 92	17, 028. 40	$1s_4-2p_2$
20	5, 866. 75	17, 040. 50	$1s_2-3p_{10}$
1	5, 852. 85	17, 080. 97	$2p_9-6d_3$
10	5, 832. 84	17, 139. 57	$2p_9-6d'_4$
6	5, 827. 06	17, 156. 57	$2p_{10}-4s$
8	5, 824. 49	17, 164. 14	$2p_9-6d_4$
4	5, 820. 07	17, 177. 17	$2p_9-6d_4$
2	5, 810. 73	17, 204. 78	$2p_{10}-5d_2$
1	5, 808. 18	17, 212. 34	$2p_6-7d_5$
3	5, 805. 50	17, 220. 28	$2p_8-6d''_1$
1	5, 788. 15	17, 271. 89	$2p_8-6d'_1$
1	5, 787. 13	17, 274. 94	$1s_2-3p_8$
2	5, 783. 82	17, 284. 83	$2p_9-6d'_1$
2	5, 750. 60	17, 384. 68	$2p_6-7d'_1$
1	5, 748. 98	17, 389. 58	$2p_8-7d_3$
1	5, 730. 75	17, 444. 90	$2p_8-6s$
3	5, 726. 54	17, 457. 72	$2p_9-5s$
2	5, 723. 50	17, 466. 99	$1s_2-3p_7$
2	5, 721. 80	17, 472. 18	$2p_8-6d_2$
4	5, 707. 47	17, 516. 05	$1s_2-3p_6$
1	5, 702. 15	17, 532. 39	$2p_7-7d''_1$
6	5, 672. 40	17, 624. 34	$1s_3-2p_4$
15	5, 649. 54	17, 695. 66	$1s_3-3p_{10}$
1	5, 629. 64	17, 758. 21	

TABLE 12.—*List of Kr I lines*—Continued

Intensity	Wave length	Wave number	Comb.
10	5, 580. 33	17, 915. 21	$1s_2-3p_5$
2	5, 575. 56	17, 930. 45	$1s_3-3p_8$
200	5, 570. 30	17, 947. 38	$1s_5-2p_3$
50	5, 562. 22	17, 973. 46	$1s_5-2p_2$
4	5, 520. 45	18, 109. 45	$2p_9-7d'_4$
3	5, 516. 56	18, 122. 22	$1s_3-3p_7$
4*d*	5, 504. 18	18, 162. 98	$2p_8-7d_4$ $2p_{10}-6d_6$
6	5, 500. 66	18, 174. 60	$2p_{10}-6d_5$
5	5, 490. 91	18, 206. 87	$2p_{10}-6d_3$
1	5, 488. 7	18, 214. 2	$2p_9-7d'_1$
1*h*	5, 458. 87	18, 313. 73	$2p_9-6s$
2	5, 379. 55	18, 583. 76	$2p_{10}-5s$
3	5, 339. 07	18, 724. 65	$2p_9-8d'_4$
2	5, 334. 65	18, 740. 17	$2p_8-8d_4$
1	5, 279. 76	18, 935. 00	$2p_{10}-2$, 811. 72
3	5, 228. 14	19, 121. 95	$2p_{10}-7d_6$
1	5, 223. 53	19, 138. 83	$2p_9-9d'_4$
1	5, 222. 28	19, 143. 41	$2p_8-9d_4$
2	5, 215. 75	19, 167. 38	$2p_{10}-7d_5$
1	5, 167. 90	19, 344. 85	$2p_{10}-7d_3$
1—	5, 144. 97	19, 431. 06	$2p_9-10d'_4$
1—	5, 142. 60	19, 440. 01	$2p_{10}-6s$
1	5, 057. 90	19, 765. 65	$2p_{10}-8d_6$
1	5, 040. 26	19, 834. 73	$2p_{10}-8d_5$
1	5, 029. 13	19, 878. 63	$2p_{10}-8d_4$
5*d*	4, 967. 17	20, 118. 49	$1s_2-4X$
3	4, 955. 22	20, 175. 12	$1s_2-4Y$
6	4, 812. 61	20, 772. 96	$1s_3-4X$
2	4, 724. 84	21, 158. 84	$1s_2-4p_{10}$
2	4, 636. 06	21, 564. 02	$1s_2-4p_5$
5	4, 550. 30	21, 970. 43	$1s_4-3p_{10}$
60	4, 502. 35	22, 204. 42	$1s_4-3p_8$
80	4, 463. 69	22, 396. 72	$1s_4-3p_7$
50	4, 453. 92	22, 445. 85	$1s_4-3p_6$
10	4, 425. 18	22, 591. 63	$1s_2-3p_4$
5	4, 418. 74	22, 624. 55	$1s_2-5Y$
3	4, 416. 84	22, 634. 28	$1s_2-5X$
6	4, 410. 34	22, 667. 64	$1s_2-3p_3$
20	4, 399. 97	22, 721. 07	$1s_2-3p_2$
1	4, 383. 85	22, 804. 61	
70	4, 376. 13	22, 844. 84	$1s_4-3p_5$
50	4, 362. 64	22, 915. 48	$1s_5-3p_{10}$
10	4, 351. 36	22, 974. 88	$1s_2-3p_1$
150	4, 319. 58	23, 143. 86	$1s_5-3p_9$
50	4, 318. 57	23, 149. 32	$1s_5-3p_8$
2	4, 302. 41	23, 236. 27	$1s_2-5p_{10}$
8	4, 300. 47	23, 246. 75	$1s_3-3p_4$
1	4, 292. 64	23, 189. 16	$1s_3-5X$
10	4, 286. 45	23, 322. 79	$1s_3-3p_3$
20	4, 282. 94	23, 341. 90	$1s_5-3p_7$

TABLE 12.—*List of Kr I lines*—Continued

Intensity	Wave length	Wave number	Comb.
100	4, 273. 96	23, 390. 94	$1s_5-3p_6$
3	4, 263. 26	23, 449. 65	$1s_2-5p_5$
3	4, 184. 46	23, 891. 24	$1s_3-5p_{10}$
1	4, 172. 75	23, 950. 27	$1s_3-5p_7$
1—	3, 992. 01	25, 042. 98	$1s_3-6p_7$
5	3, 991. 13	25, 048. 50	$1s_4-4X$
1	3, 982. 26	25, 104. 29	$1s_4-4Y$
3	3, 846. 06	25, 993. 29	$1s_5-4X$
5	3, 837. 87	26, 048. 75	$1s_5-4Y$
3	3, 812. 24	26, 223. 88	$1s_4-4p_8$
5	3, 800. 60	26, 304. 19	$1s_4-4p_7$
4	3, 796. 94	26, 329. 55	$1s_4-4p_6$
6	3, 773. 47	26, 493. 31	$1s_4-4p_5$
1	3, 698. 01	27, 033. 90	$1s_5-4p_{10}$
10	3, 679. 60	27, 169. 16	$1s_5-4p_9$
2	3, 668. 76	27, 249. 43	$1s_5-4p_7$
8	3, 665. 35	27, 274. 78	$1s_5-4p_6$
1	3, 632. 46	27, 521. 66	$1s_4-3p_4$
2	3, 628. 12	27, 554. 66	$1s_4-5Y$
4	3, 615. 47	27, 651. 06	$1s_4-3p_3$
1	3, 546. 45	28, 189. 18	$1s_4-5p_8$
1	3, 540. 96	28, 232. 89	$1s_4-5p_7$
1	3, 539. 52	28, 244. 37	$1s_4-5p_6$
2	3, 522. 65	28, 379. 63	$1s_4-5p_5$
1	3, 511. 86	28, 466. 83	$1s_5-3p_4$
1	3, 507. 87	28, 499. 21	$1s_5-5Y$
1	3, 506. 67	28, 508. 96	$1s_5-5X$
1	3, 503. 87	28, 531. 74	
3	3, 502. 53	28, 542. 65	$1s_5-3p_3$
1	3, 495. 95	28, 596. 37	$1s_5-3p_2$
1	3, 456. 80	28, 920. 23	$1s_4-6X$
1	3, 434. 10	29, 111. 40	$1s_5-5p_{10}$
2	3, 431. 68	29, 131. 92	$1s_5-5p_9$
2	3, 424. 90	29, 189. 59	$1s_5-5p_8$
1	3, 409. 94	29, 317. 65	$1s_4-6p_7$
1	3, 408. 96	29, 326. 08	$1s_4-6p_6$
1	3, 401. 40	29, 391. 26	$1s_4-6p_5$
1	3, 345. 67	29, 880. 82	
1	3, 306. 24	30, 237. 17	$1s_5-6p_5$
1	3, 302. 54	30, 271. 04	$1s_5-6p_6$

IV. THE FIRST SPECTRUM OF KRYPTON AS A SOURCE OF STANDARD WAVE LENGTHS

It has been suggested that some line from the krypton spectrum might be more suitable as a primary standard of wave length than the red line (6438.4696 A) of cadmium which has been provisionally adopted as the fundamental standard, and a proposal has been made to substitute a yellow-green krypton line (5649.56 A) for the latter.

The cadmium line was selected by Michelson by empirical methods many years before any theoretical considerations based upon an analysis of the spectrum were possible. It was found experimentally that the Cd red line was very narrow, capable of a high order of interference, free from satellites or hyperfine structure, not easily reversed or absorbed. Later investigations have shown it to be only moderately sensitive to pressure and quite free from Stark effect (splitting in electric fields). Most of these properties of the Cd line can be accounted for by the methods of spectral structure analysis developed in recent years.

A theoretical consideration which favors the krypton lines is that a Kr source can be operated at a lower temperature than Cd; the Doppler motions of the radiating particles will, therefore, be smaller, the line narrower, and capable of a higher order of interference. The Doppler widening is a function of $\sqrt{\frac{T}{m}}$ where T is the absolute temperature and m is the atomic weight. On this basis xenon is the most favorable radiator.

In investigating the possibility of krypton and xenon spectra as sources of length standards of superior quality, we have begun with preliminary descriptions of the entire range of spectra which is accessible to photographic observation. As in the present case, these descriptions permit identification of the atomic energy states and classification of practically all of the spectral lines. The relative values of the energy levels and the quantum numbers associated with them give information about the individual lines and enable one to discuss their relative merits as wave-length standards. Thus the relative intensities can be derived theoretically, the susceptibility of the line to reversal or to pressure can be estimated, and the lines best qualifying as standards may then be selected for practical tests.

Analysis of the first spectrum of krypton shows that theoretical objections can be raised against the Kr green line (5649.56 A) proposed as a primary standard. First of all, the line is not sufficiently intense for general practical use. It originates with the term combination $1s_3 - 3p_{10}$ $(^3P_0 - {}^3D_1)$, thus arising from a transition between levels with small inner quantum numbers 0 and 1.

Furthermore, the final state $1s_3$ is a metastable level and lines involving such metastable levels are the first to show absorption or reversal. The yellow line of krypton (5870.92 A; 300) is estimated to be at least twenty times as intense photographically as the proposed yellow-green line (5649.56 A; 15); it arises from the term combination $1s_4 - 2p_2$ $(^3P_1 - {}^1D_2)$, thus involving stable levels with larger inner quantum numbers 1 and 2. It may be added that the relative intensities of the analogous lines in neon (6096 and 7438 A) have been measured by Dorgelo;[40] the ratio is found to be 20.5 to 1. The strong-

[40] Dorgelo, Physica, **5**, p. 90; 1925.

est line of the Kr I spectrum is undoubtedly 8112.94 A, which has been classified as $2p_9-4d'_4$ ($^3D_3-{}^3F_4$) and $1s_5-2p_9$ ($^3P_2-{}^3D_3$). It is unsuited as a practical standard because it is invisible and because it is probably a blend of two lines, one of which involves the metastable level $1s_5$. The relative intensities of the neon lines analogous to $1s_3-3p_{10}$ and $1s_5-2p_9$ of krypton have been measured as 1:100.

Now that the energy diagrams are known for both krypton and cadmium it is possible to compare the relative positions of the atomic energy levels concerned in the production of standard wave lengths in the two spectra. The largest term [41] (lowest energy, normal state) of neutral cadmium is $^1S=72{,}538.8$. The primary standard (6438.4696 A) arises from the term combination $^1P_2-{}^1D_3$; in absolute value $^1P_2=28{,}846.6$ and $^1D_2=13{,}319.2$. These terms are well above the middle of the energy diagram, thus guaranteeing that the line will not be easily absorbed or reversed, and still far enough from the highest levels to protect it from large pressure or "Stark" effects. Assuming that the depression of terms observed by Babcock [42] in the iron spectrum applies also to cadmium we may estimate a depression of about 0.013 cm $^{-1}$ for $^1P_2$ and 0.033 cm $^{-1}$ for $^1D_3$ as the pressure changes from 0 to 1 atmosphere. The vapor pressure in a standard Cd tube is usually very small, but even if it should reach 0.1 atmosphere, it would increase the wave length only about 1 part in 8,000,000 or 10,000,000.

Now it is interesting to note that the krypton lines which have been suggested as standards involve the four s-terms (ca 30,000) and ten p-terms (ca 18,000) which occupy roughly the same relative position in the krypton diagram as the above-mentioned cadmium terms in the cadmium diagram. Excepting the lines connected with the long-lived metastable levels s_3 and s_5, the remaining combinations may be expected to be no more sensitive to reversal and pressure effects than the cadmium standard itself.

Other things being equal the yellow line appears to be the best krypton standard.

Unfortunately the theory of hyperfine structure has not been developed far enough to predict what may be expected for krypton lines, and since the existing data which bear on this point are contradictory, it will be necessary to investigate this phase more carefully.

The cooperation of the authors has been made possible in this investigation through the grant of a research fellowship to one of them (T. L. de B) by the International Education Board.

WASHINGTON, March 16, 1929.

[41] Fowler, Report on Series in Line Spectra, Fleetway Press, London; 1922.
[42] Babcock, Astrophys. J., 67, p. 240; 1928.

A COMPARISON OF THE FORMULAS FOR THE CALCULATION OF THE INDUCTANCE OF COILS AND SPIRALS WOUND WITH WIRE OF LARGE CROSS SECTION

By Frederick W. Grover

ABSTRACT

Two methods have been used for the calculation of the inductance of coils of wire having a relatively large cross section. Of these, the summation method gives the inductance of the coil as the sum of the self-inductances of the turns and the mutual inductances of all the pairs of turns. The Rosa method calculates the inductance of the equivalent current sheet as a first approximation to the inductance of the coil, and obtains the correction which must be applied by calculating (*a*) the differences between the self-inductance of the turns of wire and of the current sheet and (*b*) the differences of the mutual inductances of pairs of turns of wire and of the corresponding turns of the current sheet.

It is here shown that, contrary to previous opinions, the two methods give identical results, when terms of the same degree are retained in the series expressions.

The accurate formula of Snow for the inductance of a helix is written so as to include the Rosa correction terms, and it is proved that the error of the Rosa method may be neglected in all except the most precise work.

It is recommended that, lacking precision formulas, the Rosa method be used as giving a general solution of the problem in such cases where the current sheet formula is known. Certain important cases are reviewed briefly.

CONTENTS

		Page
I.	Introduction	164
II.	Equivalence of the summation method and the Rosa method for solenoids of round wire	165
III.	Summation formulas for the inductance of polygonal solenoids and spirals and their generalization	170
IV.	Current sheet formulas for polygonal solenoids and spirals and the Rosa correction terms	172
V.	Recalculation of the table of the Rosa B correction	174
VI.	Limitations of the summation method and the Rosa method	176
VII.	Calculation of the inductance of a helix of round wire by Rosa's method compared with the calculation by Snow's formula	180
VIII.	Generalization of the Rosa method for solenoids wound with wire of any cross section	182
IX.	Comparison of the Rosa method with Snow's formula for the inductance of a helix of wire of rectangular cross section	183
X.	Conclusion	187
XI.	Bibliography	188
XII.	Appendix	190

I. INTRODUCTION

In a recent paper Doctor Snow (1) [1] has derived a formula for the calculation of the inductance of a helical coil wound with wire of any desired cross section, and has illustrated its use both for round wires and for wires of rectangular cross section. Snow's formula is very accurate, since no terms greater than those of the fourth power in the ratio of pitch of the winding to the radius of the winding form have been neglected. It also takes into account the helical shape of the winding, and thus allows for the effect of the axial component of the current in contributing to the magnetic field. This is true of no other existing formula, so that Snow's formula is able to serve as a standard in investigating the accuracy of other formulas for the inductance of a solenoid.

To a first approximation, the inductance of a single-layer coil or solenoid may be calculated by one of the numerous formulas for the inductance of a cylindrical current sheet (2). These give the value for the current sheet with great accuracy, and for coils wound closely with fine wire the difference in the inductance of coil and current sheet is not important. For wire of larger cross section, and for coils where the diameter of the wire is small compared with the pitch of the winding, the error due to the assumption that the coil and the cylindrical current sheet are equivalent is too large to be neglected in the light of the modern requirements of accuracy.

To obtain more accurate formulas, two general methods have been used, which may also be applied in other cases, such as, for example, polygonal single-layer coils and circular and polygonal spirals. For convenience these may be designated as (*a*) the summation method, and (*b*) the differential or Rosa method. In the former the inductance is found by summing the self-inductances of all the turns and the mutual inductances of all the pairs of turns of which the coil is composed. By this method, in 1905, Strasser (3) obtained a formula for the inductance of a circular single-layer coil of round wire. In more recent years Esau (4), by the use of the same method has obtained expressions for the inductance of circular flat spirals, of single-layer coils wound on square forms, and of flat spirals with square turns, and Koga (5) has extended the method to triangular, hexagonal, and octagonal coils and spirals of round wire.

The second method was developed in 1906 by Rosa (6), who employed it to calculate the inductance of a single-layer circular coil wound with round wire, and published tables to aid in the calculations. In Rosa's method the difference is calculated between the inductance of the coil and that of a cylindrical current sheet having the same

[1] The figures given in parentheses here and throughout the text relate to the reference numbers in the bibliography given in Section XI of this paper.

mean radius, the same number of turns, and an axial length equal to the product of the number of turns and the pitch of the winding. The difference of inductance in the two cases is expressed as the sum of two terms, one of which takes into account the difference in the self-inductance of a turn of wire and that of a turn of the current sheet, while the other depends on the difference in the mutual inductance of corresponding pairs of turns of the coil and of the current sheet. These correction terms are added to the inductance of the current sheet to find the inductance of the coil. The inductance of the current sheet may be calculated by that one of the known formulas which is most suitable for the case in question.

The Rosa method is evidently capable of extension to other cases, provided that the expressions for the correction terms can be obtained. Its use for single-layer coils of round wire wound on square or rectangular forms has been treated by Niwa (7) in a very complete paper devoted principally to the derivation of current sheet formulas for these and many other related cases and to aids in their calculation.

Esau (8) has found differences between the values of the inductances of coils wound on square forms, found by Niwa's method and by the summation method, and has claimed a greater accuracy for the summation method. In commenting on Esau's criticism, Niwa (7) has pointed out numerical errors in Esau's calculations, but has failed to draw notice to the fact that Esau has incorrectly taken the dimensions of the current sheet to which the corrections given by the Rosa method are to be applied.

It is the purpose of the present paper (*a*) to show that the Rosa method and the summation method lead to exactly the same formula if terms of the same order be retained in each, (*b*) to discuss the approximations made in deriving the formulas in the two methods, (*c*) to compare the Rosa method with Snow's formula for the inductance of a helical coil, for both round wire and rectangular wire, and to derive the expression for the error of the Rosa method in these two cases, and (*d*) to recommend the generalized Rosa method as giving the most simple and accurate method available in certain other cases, such as polygonal coils and spirals.

II. EQUIVALENCE OF THE SUMMATION METHOD AND THE ROSA METHOD FOR CIRCULAR SOLENOIDS OF ROUND WIRE

The summation method assumes the solenoid to be composed of n coaxial circular rings of equal radii, spaced uniformly at a distance apart which is the pitch of the winding g. Thus, the axial length of the coil is ng. The current is assumed to get from one ring to the next by means of connections of negligible inductance; that is,

the helicity of the actual winding is neglected, the current being assumed to flow in planes perpendicular to the axis of the coil.

The inductance of the coil is then

$$L = nL_1 + 2\sum_{1}^{n-1} M_p \tag{1}$$

where L_1 is the inductance of a turn, and M_p is the mutual inductance of two turns separated by a distance pg. Strasser used for L_1 a formula which is only approximate. Using the accurate formula for the inductance of a circular ring (9) of mean radius a having a cross section of radius ρ,

$$nL_1 = 4\pi na\left[\left(1+\frac{\rho^2}{8a^2}\right)\log_e\frac{8a}{\rho} - \frac{\rho^2}{24a^2} - \frac{7}{4}\right] \tag{2}$$

The mutual inductance M_p is obtained by the Maxwell series formula (10) for the mutual inductance of coaxial circular filaments near together.

$$M_p = 4\pi a\left[\left(1+\frac{3}{16}\frac{p^2g_2}{a^2}+\cdots\right)\log_e\frac{8a}{pg} - \left(2+\frac{p^2g^2}{16a^2}+\cdots\right)\right] \tag{3}$$

and summing this over all the pairs of turns of the coil, we have to find

$$2[(n-1)M_1 + (n-2)M_2 + \cdots + (n-p)M_p + \cdots + M_{n-1}] \tag{4}$$

The resulting formula for the inductance of the coil is, neglecting terms in $\frac{\rho^2}{a^2}$,

$$\begin{aligned} L = 4\pi a\Big[& n\left(\log_e\frac{8a}{\rho} - 1.75\right) + n(n-1)\left(\log_e\frac{8a}{g} - 2\right) - A_1 \\ & + \frac{1}{8}\frac{g^2}{a^2}\left\{\left(3\log_e\frac{8a}{g} - 1\right)\frac{n^2(n^2-1)}{12} - B_1\right\}\Big] \end{aligned} \tag{5}$$

which is slightly more accurate than that given by Strasser, on account of the greater accuracy in the formula used for L_1. In this

$$\begin{aligned} A_1 &= 2[\log_e(n-1)! + \log_e(n-2)! + \cdots + \log 2!] \\ B_1 &= 3[(n-1)1^2\log_e 1 + (n-2)2^2\log_e 2 + \cdots + (n-p)p^2\log_e p \\ &\quad + \cdots + (n-1)^2\log_e(n-1)] \end{aligned} \tag{6}$$

Tables of the values of A_1 and B_1 were given by Strasser (3), including $n=30$. These were apparently calculated directly from the defining formulas (6), a tedious process.

To calculate the inductance by the Rosa method the inductance L_s of a cylindrical current sheet of n turns of radius a and having a length $b=ng$ is calculated. To this is to be added the difference between the inductance of the coil and the current sheet. To obtain this difference the inductance l_w of a turn of the round wire is cal-

culated by formula (2), divided by n. The inductance l_t of a turn of the current sheet is obtained by placing $b=g$ in the Rayleigh and Niven expression (11) for the inductance of a short cylindrical current sheet. (See Formula (15) below.) Subtracting l_t from l_w and multiplying by n, the difference in inductance of coil and current sheet due to the fact that the individual turns of wire have a different

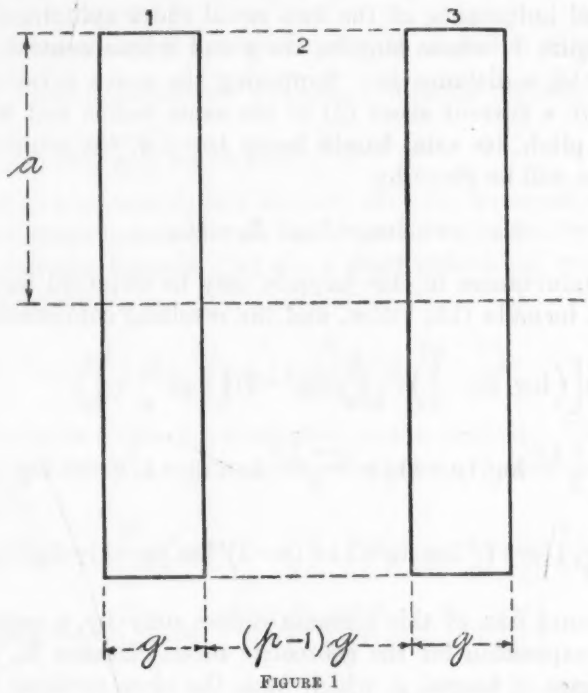

FIGURE 1

inductance than the turns of the current sheet is obtained. The result is, neglecting terms in ρ^2/a^2,

$$n(l_w-l_t)=4\pi a\left[n\left(\log_e\frac{g}{\rho}-\frac{5}{4}\right)-\frac{ng^2}{32a^2}\left(\log_e\frac{8a}{g}+\frac{1}{4}\right)\right]=-4\pi naA \quad (7)$$

The principal term of this is the constant A of Rosa, only with opposite sign. It will be convenient to speak of this type of correction as the "A correction."

Designating by M_p the mutual inductance of any pair of turns of the wire separated by a distance of pg, and by m_p the mutual inductance of the corresponding turns of the current sheet, then the total correction to the inductance of the current sheet due to all the pairs of wire is

$$2[(n-1)(M_1-m_1)+(n-2)(M_2-m_2)+\cdots+(n-p)(M_p-m_p)+\cdots \\ +(M_{n-1}-m_{n-1})]=-4\pi naB \quad (8)$$

For convenience this will be referred to as the "B correction." The inductance of the coil is then

$$L = L_s - 4\pi n a\,(A+B) \tag{9}$$

The values of M_p are to be calculated by the Maxwell expression for circular filaments, formula (3). To obtain m_p we have to find the mutual inductance of the two equal short cylindrical sheets, 1 and 3, Figure 1, whose lengths are g and whose central planes are separated by a distance pg. Supposing the space between them to be filled by a current sheet (2) of the same radius and wound with the same pitch, its axial length being $(p-1)g$, the required mutual inductance will be given by

$$2m_p = L_{123} + L_2 - 2L_{12} \tag{10}$$

The self-inductances in this formula may be obtained from the current sheet formula (15) below, and the resulting expression is

$$\begin{aligned} m_p = 4\pi a\Bigg[&\left(\log_e 8a - \frac{1}{2}\right) + \frac{g^2}{32a^2}(6p^2-1)\left(\log_e \frac{8a}{g} + \frac{1}{4}\right) \\ &- \left\{\frac{(p+1)^2}{2}\log_e (p+1)g + \frac{(p-1)^2}{2}\log_e (p-1)g - p^2 \log_e pg\right\} \\ &- \frac{g^2}{64a^2}\left\{(p+1)^4 \log_e (p+1) + (p-1)^4 \log_e (p-1) - 2p^4 \log_e p\right\}\Bigg] \end{aligned} \tag{11}$$

The second line of this formula differs only by a constant term from the expression for the geometric mean distance R_p of the two straight lines of length, g, which form the cross sections of the two turns of the current sheet (13). Writing $-Y$ for the last line of equation (11), and subtracting equation (11) from equation (3) there is found the general relation

$$\begin{aligned} M_p - m_p = 4\pi a\Bigg[&\log_e \frac{R_p}{pg} - \frac{3}{16}\frac{p^2 g^2}{a^2}\log_e p - \frac{g^2}{32a^2}\log_e \frac{8a}{g} \\ &- \frac{7}{64}\frac{p^2 g^2}{a^2} - \frac{g^2}{128a^2} + Y\Bigg] \end{aligned} \tag{12}$$

which is to be summed over the coil according to equation (8).

Writing for $\log \frac{R_p}{g}$ its value (12)

$$\log_e \frac{R_p}{g} = \frac{(p+1)^2}{2}\log_e (p+1) + \frac{(p-1)^2}{2}\log_e (p-1) - p^2 \log_e p - \frac{3}{2} \tag{13}$$

and summing over the coil there is found $n^2 \log_e n - \frac{3}{2} n\,(n-1)$, while

the summation of $\log p$ gives the constant A_1 of Strasser, defined in equation (6). Thus we may identify the constant B of Rosa with the expression

$$n \log_e n - \frac{3}{2}(n-1) - \frac{A_1}{n} = -\overline{B} \tag{14}$$

in which $\overline{B}$ has been put for the Rosa constant, which is the principal term of B in equation (8).

The summation of the second term in equation (12) leads to $-\frac{1}{8}\frac{g^2}{a^2}B_1$, where B_1 is Strasser's constant, formula (6), while the summation of Y yields $\frac{n^4g^2}{32a^2}\log_e n$ only.

In order to compare Rosa's method with the summation method, the current sheet inductance L_s will here be expressed by the Rayleigh and Niven's formula (11) for a short cylindrical current sheet of radius a, length b,

$$L = 4\pi a n^2\left[\left(\log_e \frac{8a}{b} - \frac{1}{2}\right) + \frac{b^2}{32a^2}\left(\log_e \frac{8a}{b} + \frac{1}{4}\right) - \cdots\right] \tag{15}$$

although no such limitation is inherent in the method. Thus writing ng for b in equation (15) the terms in equation (9) may be collected and we have

$$\begin{aligned}
L_s &= 4\pi a\left[n^2\left(\log_e \frac{8a}{ng} - \frac{1}{2}\right) + \frac{n^4g^2}{32a^2}\left(\log_e \frac{8a}{ng} + \frac{1}{4}\right)\right] \\
-4\pi naA &= 4\pi a\left[n\left(\log_e \frac{g}{\rho} - \frac{5}{4}\right) - \frac{ng^2}{32a^2}\left(\log_e \frac{8a}{g} + \frac{1}{4}\right)\right] \\
-4\pi naB &= 4\pi a\left[n^2 \log_e n - \frac{3}{2}n(n-1) - A_1 - \frac{1}{8}\frac{g^2}{a^2}B_1 - \frac{n(n-1)}{128}\frac{g^2}{a^2}\right. \\
&\left. - \frac{n(n-1)}{32}\frac{g^2}{a^2}\log_e \frac{8a}{g} - \frac{7}{384}\frac{n^2(n^2-1)g^2}{a^2} + \frac{n^4g^2}{32a^2}\log_e n\right]
\end{aligned} \tag{16}$$

Adding and simplifying

$$\begin{aligned}
L = 4\pi a\Big[&n^2\left(\log_e \frac{8a}{g} - 2\right) + n\left(\log_e \frac{g}{\rho} + \frac{1}{4}\right) - A_1 - \frac{1}{8}\frac{g^2}{a^2}B_1 \\
&+ \frac{n^2(n^2-1)}{32}\frac{g^2}{a^2}\log_e \frac{8a}{g} - \frac{n^2(n^2-1)}{96}\frac{g^2}{a^2}\Big]
\end{aligned} \tag{17}$$

and if we add and subtract $\left(n \log_e \frac{8a}{g} + 2n\right)$, the expression goes over into Strasser's formula (5) exactly.

This result was to have been expected, since the methods should agree if correct inductance formulas are used, and if, in both methods, terms of the same order are retained.

In the correction constants A and B, as given by Rosa, terms in $\frac{g^2}{a^2}$ were neglected as of small effect, compared with the main or geometric mean distance terms. This was justified by Rosa by numerical examples, but it may be shown more generally that the terms in $\frac{g^2}{a^2}$ in equation (17) are very small. To accomplish this, the Strasser constant B_1 may be expanded in the asymptotic series

$$B_1=\frac{1}{4}\left(n^4-n^2+\frac{1}{10}\right)\log_e n-\frac{7}{48}n^4+\frac{n}{12}\left(1+\frac{1}{10}-\cdot\cdot\right)+\frac{1}{16}+\frac{1}{1008n^2}+\cdot\cdot \quad (18)$$

and substituting this in the last two equations of (16) it is found that the combined terms in $\frac{g^2}{a^2}$ are $-\frac{n^2g^2}{32a^2}\left(\log_e\frac{8a}{ng}-\frac{1}{3}\right)-\frac{1}{96}\frac{ng^2}{a^2}-$ smaller terms. For the case $n=30$, $g=0.1$, $a=15$, these terms amount to only 8 parts in 10,000 of the total correction, and the latter is only 18 parts in 10,000 of the whole inductance of the coil, so that the neglected terms here are of the order of only a part in a million of the whole inductance. A further discussion of this point will be made in Section VI.

III. SUMMATION FORMULAS FOR THE INDUCTANCE OF POLYGONAL SOLENOIDS AND SPIRALS AND THEIR GENERALIZATION

Formulas for the inductance of polygonal solenoids and spirals have been obtained by Esau (4) and by Koga (5). Esau treated the case of square coils, making use of the known formulas for the inductance of a square of round wire and for the mutual inductance of equal parallel coaxial square filaments.

Koga extended the method to triangular, hexagonal, and octagonal coils and spirals, and derived for this purpose the basic formulas which had to be summed over the coil. Thus he gives formulas for the mutual inductance of concentric coplanar polygons with their sides parallel. His formulas for the inductance of polygons of round wire and for the mutual inductance of equal parallel coaxial polygons check those of the author of the present paper which were published a little earlier (13).

Both Esau and Koga in their use of the summation method first expanded the basic formulas in terms of the ratio of the pitch to the length of a side of the polygon. Tables are given for different numbers of turns up to 30, and for different sizes of wire and pitch of winding. Since powers no higher than the square of the ratio of pitch to side of polygon are retained, the formulas converge well only for relatively short coils or for spirals of small axial width.

An inspection of these summation formulas has made clear that they may all be written in the same form, only with different numerical coefficients depending upon the number of sides of the polygon. After checking all the coefficients and correcting errors in two instances,[2] the writer finds the following results, the constants being collected in Tables 1 and 2.

Inductance of a polygon of round wire.

$$L=2Na\left[\log_e\frac{a}{\rho}+q\right] \tag{19}$$

in which

N = the number of sides of the polygon,
a = the length of a side of the polygon,
ρ = the radius of cross section of the wire.

Mutual inductance of equal parallel coaxial polygons.

$$M=2Na\left[\log_e\frac{a}{d}-r+s\frac{d}{a}+t\frac{d^2}{a^2}\right] \tag{20}$$

where d = the distance between their planes.

Inductance of polygonal solenoids.

Letting n be the number of turns, g the pitch of winding

$$L=2Nan\left[\left(\log_e\frac{a}{\rho}+q\right)+(n-1)\left(\log_e\frac{a}{g}-r\right)+\frac{n^2-1}{3}\cdot s\frac{g}{a}+\frac{n(n^2-1)}{6}\cdot t\frac{g^2}{a^2}-\frac{A_1}{n}\right] \tag{21}$$

A_1 is Strasser's constant, formula (6).

TABLE 1.—*Values of numerical constants in formulas (19), (20), (21), and (22)*

	q	r	s	t
Triangles	−1.1555	1.4055	2.2092	$-1\frac{1}{12}$
Squares	−.52401	.77401	1	−0.0420
Hexagons	+.098476	.15152	.3954	+.1160
Octagons	+.46198	−.21198	.2146	+.1052

Mutual inductance of parallel concentric coplanar polygons.

Putting here a for the mean length of a side of the polygon

$$M=2Na\left[\log_e\frac{a}{d}-r+s'\frac{d}{a}+t'\frac{d^2}{a^2}\right] \tag{22}$$

the constants being given in Table 2, excepting r which is the same as in the preceding formulas

[2] Koga gives S^1 for the octagon as $-(\sqrt{2}-1)\times 8.5509=-0.3452$ and T for the triangle as $\frac{13}{12}$.

Inductance of a polygonal flat spiral.

If a represents the mean length of a side of the polygonal turns of the spiral, g the (axial) pitch of the winding, n the number of turns

$$L=2Nan\left[\left(\log_e\frac{a}{\rho}+q\right)+(n-1)\left(\log_e\frac{a}{g}-r\right)+\frac{n^2-1}{3}s'\frac{g}{a}+\frac{n(n^2-1)}{6}\frac{Tg^2}{a^2}-\frac{A_1}{n}\right] \tag{23}$$

Between the coefficient T and t' there exists the relation $T=t'-\frac{v^2}{2}$. The constants of the last two formulas are collected in Table 2.

TABLE 2.—*Values of numerical constants in formulas (22) and (23)*

	s'	T	t'	v
Triangles	1.2396	$\frac{23}{12}$	$\frac{5}{12}$	$\sqrt{3}$
Squares	.53284	$\frac{3}{4}$	$\frac{3}{4}$	1
Hexagons	.20328	0.2947	0.1280	$1/\sqrt{3}$
Octagons	.10898	.1662	.0804	$(\sqrt{2}-1)$

IV. CURRENT SHEET FORMULAS FOR POLYGONAL SOLENOIDS AND SPIRALS AND THE ROSA CORRECTION TERMS

The formula for the inductance for a solenoidal current sheet on a square form was derived by Niwa (14), and independently, at about the same time, by the writer (13), who also derived series formulas for short triangular, hexagonal, and octagonal current sheets.

To obtain the formula for the inductance of a polygonal solenoid by the Rosa method, it is necessary to start with the formula for the corresponding current sheet. Putting, as before, a for the mean side of the polygon, and supposing that the n turns have an axial length of ng, the generalized formula (13) for the inductance of the current sheet is

$$L_s=2Nan^2\left[\log_e\frac{a}{ng}+\left(\frac{3}{2}-r\right)+\frac{s}{3}\frac{ng}{a}+\frac{t}{6}\frac{n^2g^2}{a^2}\right] \tag{24}$$

which holds for cases where the ratio of the axial length to the side of the polygon is small. The numerical coefficients have the values given in Table 1.

The Rosa corrections for the cross section of an actual winding of round wire may be obtained by the method already outlined for a circular solenoid in Section II. The A correction is obtained from equation (24), putting g in place of ng. This gives the inductance of a turn of the current sheet. Formula (19) gives the inductance of a turn of the round wire. The B correction is obtained by summing over the coil an equation corresponding to equation (8), the values

of the mutual inductances for two turns of the current sheet being obtained from differences of self-inductances, as in equation (10), using equation (24), while the values for pairs of turns of the round wire are given by equation (20) for polygonal filaments.

The results may be summarized as follows:

$$\begin{aligned} L_s &= 2Nan^2\left[\log_e\frac{a}{ng}+\left(\frac{3}{2}-r\right)+\frac{s}{3}\frac{ng}{a}+\frac{t}{6}\frac{n^2g^2}{a^2}\right] \\ -2NanA &= 2Nan\left[\log_e\frac{g}{\rho}-\left(\frac{3}{2}-r\right)+q-\frac{s}{3}\frac{g}{a}-\frac{t}{6}\frac{g^2}{a^2}\right] \\ -2NanB &= 2Nan\left[n\log_e n-\frac{3}{2}(n-1)-\frac{A_1}{n}-\frac{t}{6}(n-1)\frac{g^2}{a^2}\right] \end{aligned} \tag{25}$$

and adding these, the inductance of the polygonal solenoid is

$$L=2Nan\left[\left(\log_e\frac{a}{\rho}+q\right)+(n-1)\left(\log_e\frac{a}{g}-r\right)-\frac{A_1}{n}+\frac{n^2-1}{3}\frac{sg}{a}+\frac{n(n^2-1)}{6}\frac{tg^2}{a^2}\right]$$

which is, exactly, the formula (21) obtained by the summation method for this case.

Niwa (7) calculated the correction for cross section as equal to twice the total length of wire in the coil, times the sum of the two constants tabulated by Rosa for circular solenoids, and applied it to his current sheet formulas for square and rectangular solenoids. This procedure is justified, if we neglect terms in $\frac{g}{a}$ and $\frac{g^2}{a^2}$, since it will be found that, using the values of Table 1, the quantity $-\left(\frac{3}{2}-r\right)+q$ is always equal to $-\frac{5}{4}$, whatever the number of sides of the polygon. Thus, comparing with equation (16) the principal terms of the correction are $-2Nan(A+B)$, the constants A and B being the same as for a circular solenoid.

To treat the polygonal spiral by the same method requires a current sheet formula for a polygonal disk or ring, and no formula for this case has been published. It may readily be derived by the method of geometric mean distance and arithmetical mean distances by substituting in formula (22) for coplanar polygons, $\log ng-\frac{3}{2}$ for $\log d$, $\frac{1}{3}ng$ for d (15), and $\frac{1}{6}n^2g^2$ for d^2. This result was checked by integrating equation (22) twice over the current sheet. This yields a formula which differs from that obtained by the simpler method only in the coefficient of $\frac{n^2g^2}{a^2}$, the simpler method giving t' instead of T.

The value by integration, which is the more accurate result, may be written in the general form

$$L_s = 2Nn^2a\left[\log_e \frac{a}{ng} + \left(\frac{3}{2} - r\right) + q + \frac{s'}{3}\frac{ng}{a} + \frac{T}{6}\frac{n^2g^2}{a^2}\right] \tag{26}$$

in which a is the side of the mean polygonal filament. The coefficients have already been given in Tables 1 and 2.

The derivation of the Rosa corrections for cross section follows the course already illustrated in Section II, although the process of summation is more involved, on account of the varying sizes of the turns of the spiral.

The resulting correction terms are

$$-2NanA = 2Nan\left[\log_e \frac{g}{\rho} + q - \left(\frac{3}{2} - r\right) - \frac{s'}{3}\frac{g}{a} - \frac{T}{6}\frac{g^2}{a^2}\right] \tag{27}$$

$$-2NanB = 2Nan\left[n\log_e n - \frac{3}{2}(n-1) - \frac{A_1}{n} - \frac{T}{6}(n-1)\frac{g^2}{a^2}\right]$$

and adding these to the current sheet value in equation (26), the final formula for the polygonal spiral is exactly the same as formula (23), which was derived by the summation method. Here also as in the previous case the principal terms of the correction have the same value, and may be calculated from the same table of constants as for circular solenoids.

It has been proved that the Rosa method and the summation method agree, if terms of the same degree are retained in both, not only in the case of circular solenoids but also with polygonal solenoids and spirals. It may be shown by the same methods that this result is likewise true for circular flat spirals. As already intimated, these results were to have been expected, and that they are found to be true gives a check on the various inductance formulas employed. It also shows that Esau's criticism is without ground.

V. RECALCULATION OF THE TABLE OF THE B CORRECTION OF ROSA

The quantity B tabulated by Rosa for wire of round cross section was defined by the relation (6)

$$B = \frac{2}{n}\left[(n-1)\log_e \frac{R_1}{g} + (n-2)\log_e \frac{R_2}{2g} + \cdots + (n-p)\log_e \frac{R_p}{pg} + \cdots + \log_e \frac{R_{n-1}}{(n-1)g}\right] \tag{28}$$

in which $\frac{R_p}{pg}$ represents the ratio of the geometric mean distance of two straight lines (cross sections of a pair of the turns of the current

sheet) whose centers are separated by a distance pg, to the distance between them. This quantity may be calculated by formula (130) of Bureau of Standards Scientific Paper No. 169, and for more distant turns by the very convergent series formula (131) of the same paper. Thus the direct calculation of B by formula (28) offers no difficulty, except that the calculation for large values of n becomes very tedious. Furthermore, in the calculation of a table for different values of n, the fact that the calculation for a given value of n rests upon the calculation for smaller values of n, although seemingly an advantage, works to the end that any error made with a smaller value of n is carried through into the calculation for the larger values of n. Thus, it is difficult to obtain values of B for the larger values of n, which shall be free from error.

From equations (8) and (12) (the first term), it has already been noted that the correction B may be written in the form shown in equation (14). This equation, which does not seem to have been previously noticed, gives a means for checking the values found by the formula (28). For this purpose the table of values of A_1, given by Strasser and, corrected for small errors, in Table 5, Bureau of Standards Scientific Paper No. 169, should be useful. Beyond $n=30$, the range of this table, the quantity A_1, as may be seen from equation (6), labors under the same disadvantage for purposes of calculation as does equation (28).

This difficulty may be very completely avoided by using for A_1 a development in an asymptotic series, as was done by Rolf (16) and by Koga (5). Since, however, the expressions used by these two authors differ slightly, it was necessary to investigate the cause for the discrepancy. The two expressions are as follows:

$$\frac{A_1}{n}=n\left(\log_e n-\frac{3}{2}\right)+\log_e 2\pi-\frac{1}{6n}\log_e n-\frac{0.3312}{n}-\frac{1}{120n^3}+\frac{7}{2160n^4} \quad \text{(Rolf)}$$

$$\frac{A_1}{n}=n\left(\log_e n-\frac{3}{2}\right)+\log_e 2\pi-\frac{1}{6n}\log_e n-\frac{0.33084}{n}-\frac{1}{120n^3}+\frac{1}{270n^4} \quad \text{(Koga)}$$

Koga explains that his expression was derived by applying the Euler (17) summation formula to the Stirling asymptotic formula for $\log m!$, making use, of course, of the defining equation for A_1, formula (6). The Stirling formula is (17)

$$\log_e m!=\left(m+\frac{1}{2}\right)\log_e m-m+\frac{1}{2}\log_e 2\pi+\frac{1}{12m}-\frac{1}{360m^3}+\frac{1}{1260m^5} \quad (29)$$

This may be summed directly by formula (6) for integral values of m from 1 to $(n-1)$, inclusive, the series which enter being made to depend upon known series, or it may be summed by applying the

Euler summation formula to each term. The result is an asymptotic series in which the term in $\frac{1}{n}$ is given by an asymptotic series, while the coefficients of the terms in higher powers of $\frac{1}{n}$ begin to increase after that of $\frac{1}{n^5}$. The numerical coefficient of $\frac{1}{n}$ was found to be about -0.33086, but, by making use of the exact formula for A_1, it is found that, for all values of n greater than 3, the value -0.330842 is indicated as correct. Adopting this value the resulting expansion is

$$\frac{A}{n}=n\left(\log_e n-\frac{3}{2}\right)+\log_e 2\pi-\frac{1}{6n}\log_e n-\frac{0.330842}{n}-\frac{1}{120n^3}+\frac{1}{504n^5} \quad (30)$$

which differ from Koga's expression only in the last term. This difference is of no consequence for all except the smallest values of n. (Evidence will be given later of the correctness of the last term of equation (30).)

Substituting equation (30) in equation (14) there results

$$B=0.337877-\frac{1}{6n}\log_e n-\frac{0.330842}{n}-\frac{1}{120n^3}+\frac{1}{504n^5} \quad (31)$$

The first term $\left(\log 2\pi-\frac{3}{2}\right)$ shows what is the limiting value of B, as n increases indefinitely, a value which has hitherto been lacking. Formula (31) has been checked for values of n up to 30, by calculating A_1 directly from equation (6), and also by making use of Strasser's values. For all values of n greater than 3, it is found that equation (31) gives a 6-figure accuracy or better. The error is evidently smaller, the greater the value of n; that is, the formula is most accurate in just those cases where the exact formula is most difficult to calculate.

By these means Table 8, Bureau of Standards Scientific Paper No. 169, has been recalculated. The values of B were found to be correct up to $n=15$, but beyond that point the values of Table 8 are too large by amounts which vary from a few units up to 12 units in the fourth place. The revised table is given as Table 3 in the Appendix.

VI. LIMITATIONS OF THE SUMMATION METHOD AND THE ROSA METHOD

In the preceding sections it has been proved that the summation method and the Rosa method lead to exactly the same expressions for the inductance of solenoids and spirals, when terms of the same order are retained in both. The proof has included second degree terms only, but there is no reason to doubt that the agreement would

be found for higher degree terms in the series expansions. The agreement is, in fact, only a check on the basic inductance formulas which have been employed in the two methods. This agreement of the two methods does not signify, however, that the Rosa method and summation method are of equal accuracy in all cases.

Since in order to be able to carry out the summations with any degree of simplicity, it is necessary in the summation method to use series expansions for the basic formulas which are to be summed, it follows that the summation method gives series formulas which converge well only for short coils or narrow spirals. Thus the tables of Strasser, Esau, and Koga cover a range up to only 30 turns of wire.

This limitation is not inherent in the Rosa method. It is true that in the comparison of the Rosa method with the summation method the current sheet formulas used were series expansions, subject to the same limitations as the summation formulas, but these were used merely for the purpose of proving the identity of the final results by both methods. Current sheet formulas are, however, available for circular solenoidal current sheets, and for circular disks which fit all cases and give an accuracy greater than is necessary in practice, and to the suitable current sheet formula in any given case the Rosa correction may be applied. It remains only to show that the Rosa correction may be calculated with an accuracy sufficient to cause no appreciable error in the final result.

Since the correction to the current sheet value of the inductance to take into account the cross section of the actual winding is usually no greater than about 1 per cent of the whole inductance, the correction does not need to be calculated with great accuracy in order to give a suitable accuracy in the total inductance. As originally developed by Rosa, only the principal or geometric mean distance terms were included, and it will be shown that these terms, which we may conveniently designate as the "simple Rosa corrections," are, in general, sufficient.

Consider, for example, two turns of a circular solenoid of round wire and the corresponding two turns of the current sheet, which has the same radius and pitch of winding. The mutual inductance of the two turns of wire may be calculated by formula (3) in which the terms in $\frac{p^2g^2}{a^2}$, which become zero for circles of very great radius a, may be regarded as corrections for the curvature of the turns. Likewise for the turns of the current sheet, curvature terms enter, as is shown by equation (11). In both cases the curvature terms are not negligible, but in the difference of the two mutual inductances, which is the quantity which enters into the Rosa correction, the curvature terms must nearly cancel, unless the dimensions of the cross sections

are large in comparison with the radius of the turns. It has already been shown that these differences of curvature terms are, for a short coil, of very small effect on the Rosa correction terms. (See p. 170.)

For a long coil the total effect of the curvature terms is not so easy to evaluate, since they are expressed by a series which converges only for relatively short coils. It is evident also that, for the more distant turns of wire, the curvature terms are relatively more important compared with the principal terms. However, the mutual inductances of the distant turns, and still more so their differences, are very small, so that the curvature effect for such turns should contribute, absolutely, very little to the total correction.

The following detailed examination of a practical problem will make some of these points clearer, in that it will give a more quantitative measure of the importance of the terms neglected. The coil considered has 400 turns, wound on a form of 15 cm radius with a winding pitch of 0.1 cm, so that the coil has an axial length of 40 cm. The contribution to the Rosa B correction of all the turns which are separated by a distance of pg is $-4\pi a\left[2(n-p)\log_e\frac{R_p}{pg}\right]$ The contributions to the correction for pairs of turns of all distances up to $p=10$ are as follows:

p	Correction	p	Correction	p	Correction
1	$-4\pi a(90.741)$	4	$-4\pi a(4.178)$	7	$-4\pi a(1.342)$
2	(17.496)	5	(2.655)	8	(1.024)
3	(7.522)	6	(1.834)	9	(0.806)

giving a total of $-4\pi a(127.598)$. The total sum of the principal terms may be obtained from Table 3 for $n=400$. It is $-4\pi a[400\times 0.33455]=-4\pi a(133.820)$; that is, the contributions of all the pairs of turns separated by more than nine times the pitch is only about 5 per cent of the whole B correction. It may be shown that turns for which p is greater than 20 contribute only 2.2 per cent, those at distances greater than 50 g only 0.6 of 1 per cent, while those for which the separation is greater than 250 g account for only 1 part in 6,500 of the whole.

For separations as great as 3 g the contribution of all the pairs of turns with a separation pg may be calculated from Rosa's (19) formula (49), Bureau of Standards Scientific Paper No. 169, which reads:

$$\Delta M_p=-4\pi a\cdot 2(n-p)\left[\frac{1}{12}\frac{1^2}{p^2}\left\{1+\frac{3}{8}\frac{p^2g^2}{a^2}\left(\log_e\frac{8a}{pg}-\frac{11}{6}\right)-\frac{45}{256}\frac{p^4g^4}{a^4}\left(\log_e\frac{8a}{pg}-\frac{97}{60}\right)+\cdots\right\}+\frac{1}{60}\frac{1}{p^4}\left\{1+\frac{1}{16}\frac{p^2g^2}{a^2}\right\}+\frac{1}{168}\frac{1}{p^6}+\cdots\right] \tag{32}$$

In this formula the series in powers of $\frac{1}{p^2}$ is the expansion of the

geometric mean distance ratio; the other terms give, therefore, the curvature terms. For cases where formula (32) converges, the summation of these terms can be performed, and their effect evaluated, as was done for a winding of 30 turns on the same form, page 170. For the long coil here considered, formula (32) is not sufficiently convergent in the case of turns which are separated by distances much greater than the radius of the coil. In such cases the Rosa-Weinstein (19) formula (50) of Bureau of Standards Scientific Paper No. 169 may be used in place of formula (32) to obtain the contributions of chosen pairs of wires. Thus, for the extreme turns, for which $p=399$, the true value of ΔM_p is $-4\pi a[2.3\times10^{-7}]$, while the principal terms of formula (32) give a value which is numerically more than twice as great. The 150 different pairs of turns separated by a distance of 25 cm contribute $\Delta M_p=-4\pi a[0.000331]$, while the g, m, d terms are about 20 per cent greater. Unfortunately, since the Rosa-Weinstein formula involves elliptical integrals, it is impracticable to obtain its summation over the coil. It is, however, evident that, for the more distant turns of the coil, the curvature effect is of opposite sign to what it is for the nearer turns, so that, proportionately, the curvature effect should be smaller rather than greater than for a short coil on the same form, and it has already been shown that in the latter case its effect on the whole inductance is very small.

The summation method of Strasser assumes that the current flows in circular turns whose planes are perpendicular to the axis of the solenoid. Thus the effect of the axial component of the current, which is present when the current flows in the actual helical winding, is neglected. The effect of the axial component has also been neglected in obtaining the correction for cross section by the Rosa method, but if a current sheet formula for a true continuous helix without insulation be available, the neglect of helicity in getting the correction for cross section is of second order in its effect on the total inductance. In a recent paper Snow (1) has given a very accurate formula for the inductance of a helix of wire, which enables the correction to be calculated which must be applied to the formula for a cylindrical current sheet to obtain the true inductance of the helix. He gives also the formula for the inductance of a true continuous helical current sheet. Thus, it is now possible to evaluate the error from neglecting the helicity of the winding, and also to calculate what is the error of the simple Rosa method when applied to the calculation of the inductance of a helical winding of wire of round or rectangular cross section.

VII. CALCULATION OF THE INDUCTANCE OF A HELIX OF ROUND WIRE BY ROSA'S METHOD COMPARED WITH THE CALCULATION BY SNOW'S FORMULA

The formula for the inductance of a helix of round wire is given as equation (114), page 466, in Snow's article.[3] In the nomenclature of the present paper this reads

$$L=L_o+4\pi na\left[-\left(0.89473-\log_e\frac{g}{2\rho}\right)+\frac{1}{6n}\log_e\frac{2\pi a}{g}+\frac{A_2(k)}{2n}+\frac{1}{4n}\left(\frac{E}{k}-1\right)\left(\frac{2\rho}{g}\right)^2\right] \tag{33}$$

In this L_o is the inductance of a cylindrical current sheet (helicity neglected) whose length is ng and whose mean radius is a, $k=\frac{2a}{\sqrt{4a^2+n^2g^2}}$ is the modulus of the elliptic integral of second kind E, and $A_2(k)$ is a complicated function of k, to be obtained from the curve of page 475. It is the principal term in the correction for the effect of the axial component of the current.

If we notice that $0.89473=\log\pi-\frac{1}{4}$, and substitute for $\log 2\pi-\frac{3}{2}$ its value in terms of B from equation (31), we find, making use of equation (7), that Snow's formula may be written for uniform current distribution

$$L=L_o+4\pi na\left[-(A+B)-\frac{1}{6n}\log_e\frac{ng}{a}-\frac{0.02458}{n}+\frac{A_2(k)}{2n}+\frac{1}{4n}\left(\frac{E}{k}-1\right)\left(\frac{2\rho}{g}\right)^2-\frac{1}{120n^3}+\frac{1}{504n^5}\right] \tag{34}$$

Here the Snow formula for the difference between the inductance of a helix of round wire and cylindrical current sheet is expressed in terms of the simple Rosa correction constants A and B (curvature terms omitted). Thus the error of the Rosa correction may be calculated for any desired case.

For the example solved by Snow on page 476, $n=400$, $g=0.1$, $a=15$, $\alpha=0.05$. The value of A (see principal term of formula (7)) is -0.13629, and from Table 3, for $n=400$, $B=0.33455$. Thus the simple Rosa correction is $4\pi na[0.13629-0.33455]=-14949$ mμh (millimicrohenrys), whereas Snow's equation (114) and formula (34) both give -14883. Since the value of L is 26,568,401, this difference of 66 mμh amounts to about 2.5 parts in 1,000,000 of the whole

[3] The first term of the second line of this equation should read $-\frac{1}{3}\log_e\frac{a}{\rho}$, instead of $-\frac{1}{3}\log_e\frac{a}{\rho}$. The correct reading is employed in the example of p. 476.

[4] The difference of 4 parts in 1,000,000 found by Snow in the solution of the same problem is explained by the use of the value 0.3351 for B, as given in Table 8, B. S. Sci. Paper No. 169. This table has been found to be in error at this and other points as explained in Section V.

inductance, the Rosa method giving too small a value.[4] This difference is mainly due to the neglect of the axial component of the current. The formula for a continuous helical current sheet is given in Snow's formula (129). In the nomenclature of the present paper it reads

$$L_s = L_o + 4\pi na\left[\frac{A_2(k)}{2n} - \frac{0.03775}{n} + \frac{1}{6n}\left[2\left(\frac{K-E}{k}\right) - kK\right]\right] \qquad (35)$$

K and E being the complete elliptical integrals of first and second kind to the modulus, k, defined for the preceding equation. The quantity in the brackets of the last term of equation (35) is tabulated in Table I, Bureau of Standards Scientific Paper No. 169, or may also be obtained as $\frac{1000f}{4\pi}$, using the values of f given in Table 1, Scientific Paper No. 498.

Subtracting equation (35) from equation (34) there results

$$L - L_s = 4\pi na\left[-(A+B) - \frac{1}{6n}\log_e\frac{ng}{a} + \frac{0.01322}{n} + \frac{1}{4n}\left(\frac{E}{k}-1\right)\left(\frac{2\rho}{g}\right)^2 - \frac{1}{6n}\left\{2\left(\frac{K-E}{k}\right) - kK\right\} - \frac{1}{120n^3} + \frac{1}{504n^5}\right] \qquad (36)$$

which gives the correction for cross section which has to be applied to the formula for a continuous helical current sheet of tape with negligible insulation to obtain the inductance of a helix of round wire of the same radius, pitch, and number of turns. The error of the simple Rosa correction is given by the terms in equation (36) exclusive of $-4\pi na(A+B)$. For the previous example these extra terms are, in order, $4\pi na[-0.000409+0.000033+0.000213-0.000024] = -14.1$ mμh; that is, the error of the simple Rosa correction when applied to the true helical current sheet (the logical current sheet formula), is only about one-half of 1 part in 1,000,000 of the total inductance of the coil. If this error be attributed mainly to the neglect of the curvature terms in the Rosa correction (and the algebraic sign is what would be expected), its value shows that the curvature terms are proportionately smaller for the long coil than for the shorter wound on the same form. For example, for a coil of only 30 turns wound with the same pitch on the same form, the correction to the Rosa correction in equation (36) is -0.55 mμh in a total of 540,845; that is, about 1 part in 1,000,000. In this case, where the convergence of the formula for the summation of the curvature terms is satisfactory, their calculated value by equations (16) and (18) is -0.79 mμh.

Before testing the use of the Rosa method for a helix of rectangular wire, it is convenient to generalize the method for a solenoid wound with wire of any cross section.

VIII. GENERALIZATION OF THE ROSA METHOD FOR A SOLENOID WOUND WITH WIRE OF ANY CROSS SECTION

If we put

R_w = the geometric mean distance of the cross section of the wire from itself,

R_t = the geometric mean distance of a turn of the current sheet (straight line),

r_{wp} = the geometric mean distance of the cross sections of a pair of wires separated by a distance pg,

r_{tp} = the geometric mean distance of the sections of the corresponding turns of the current sheet,

L_s = inductance of the equivalent current sheet,

then the general expressions for the Rosa corrections are

$$-4\pi naA = -4\pi na\ (\log_e R_w - \log_e R_t)$$

$$-4\pi naB = 4\pi na\left[\frac{2}{n}\left\{(n-1)\log_e\frac{r_{t1}}{r_{w1}} + (n-2)\log_e\frac{r_{t2}}{r_{w2}} + \cdots + (n-p)\log_e\frac{r_{tp}}{r_{wp}} + \cdots + \log_e\frac{r_{t(n-1)}}{r_{w(n-1)}}\right\}\right] \quad (37)$$

and

$$L = L_s - 4\pi na(A+B)$$

If the cross section of the wire is not circular, it is convenient to write the second of these equations in the form

$$-4\pi naB = 4\pi na\left[\frac{2}{n}\sum_{p=1}^{n-1}(n-p)\log_e\frac{r_{tp}}{pg} - \frac{2}{n}\sum_{p=1}^{n-1}(n-p)\log_e\frac{r_{wp}}{pg}\right] \quad (38)$$

The first series of terms gives the B correction for circular wire and is tabulated in Table 3. The second series depends upon the differences of the geometric mean distances of the actual cross sections of the wire and those of circular turns wound with the same pitch and number of turns. In general, formulas for the geometric mean distance are not known, except in the important case of a rectangular cross section. The comparison of the Rosa correction with Snow's formula for wire of rectangular cross section is therefore of special interest. The author has in preparation tables for aiding in numerical computations for this case.

IX. COMPARISON OF THE ROSA METHOD WITH SNOW'S FORMULA FOR THE INDUCTANCE OF A HELIX OF WIRE OF RECTANGULAR CROSS SECTION

Snow's formula (126) for the inductance of a helix of wire of rectangular cross section of axial dimension β and radial thickness a is as follows for uniform current density over the cross section:

$$L=L_o+2\pi a\left\{A_2(k)+\frac{1}{3}\left[1+\frac{\alpha^2-\beta^2}{g^2}\right]\log_e\frac{2\pi a}{g}\right.$$

$$-2n\left[-\log_e\frac{g}{p}-4.41212+\frac{1}{6}(\tan^2\theta\log_e\sin\theta+\cot^2\theta\log_e\cos\theta)\right.$$

$$+\frac{2}{3}\left(\left(\frac{\pi}{2}-\theta\right)\tan\theta+\theta\cot\theta\right)$$

$$-\frac{f\left(\frac{\alpha}{g},\frac{\beta}{g}\right)-f\left(\frac{\alpha}{g},o\right)-f\left(o,\frac{\beta}{g}\right)}{6\left(\frac{\alpha}{g}\right)^2\left(\frac{\beta}{g}\right)^2}$$

$$\left.-\frac{8}{\sin^2\theta\cos^2\theta}\sum_{m=1}^{\infty}\frac{\left(\frac{\rho}{g}\right)^{2m}(\cos^{2m+4}\theta+(-1)^m\sin^{2m+4}\theta-\cos(2m+4)\theta)}{2m(2m+1)(2m+2)(2m+3)(2m+4)}(S_{2m}-1)\right] \tag{39}$$

$$\frac{2}{3}\left(\frac{E}{k}-1\right)\left(\frac{\alpha}{g}\right)^2+\frac{1}{3}\left[1.18123+2\left(\frac{K-E}{k}\right)-kK\right]\frac{\beta^2-\alpha^2}{g^2}$$

$$-\frac{25}{3}-\frac{f\left(\frac{\alpha}{g},\frac{\beta}{g}\right)-f\left(\frac{\alpha}{g},o\right)-f\left(o,\frac{\beta}{g}\right)}{3\left(\frac{\alpha}{g}\right)^2\left(\frac{\beta}{g}\right)^2}$$

$$\left.-\frac{16}{\sin^2\theta\cos^2\theta}\sum_{m=2}^{\infty}\frac{\left(\frac{\rho}{g}\right)^{2m}(\cos^{2m+4}\theta+(-1)^m\sin^{2m+4}\theta-\cos(2m+4)\theta)}{2m(2m+1)(2m+2)(2m+3)(2m+4)}(S_{2m-1}-1)\right\}$$

In this equation $\theta=\tan^{-1}\frac{\alpha}{\beta}$, $S_m=\sum_{k=1}^{\infty}\frac{1}{k^m}$ and the f's are functions of the ratios $\frac{\alpha}{g}$ and $\frac{\beta}{g}$, defined in Snow's formulas (123), (124), and (125). For the rest the equation has been written in terms of quantities already defined.

Making use of the definition of the geometric mean distance of a rectangle in terms of θ, Snow's equation (118), and the known expression for the geometric mean distance of a straight line $R_t=\log g-\frac{3}{2}$, and the defining equation for A in equation (37), the second and third lines of equation (39) may be written

$$4\pi na\left[-A+\left(\frac{3}{2}-\log_e 2\pi\right)+\frac{25}{6}\right] \tag{40}$$

Comparing the defining equations for the f functions with the formula for the geometric mean distance of two equal parallel rectangles (12) it is seen that the fourth line of equation (39) is

$$4\pi na\left[-2n\log_e\frac{r_{w1}}{g}-\frac{25}{6}n\right] \tag{41}$$

while the next to last line of equation (39) is

$$4\pi a\left[2\log_e\frac{r_{w1}}{g}\right] \tag{42}$$

so that together they give the first term of the last series of terms in equation (38).

The geometric mean distance of two equal parallel rectangles may be expanded in a series which holds for separations, pg, which are greater than the dimensions of the rectangle. The series is

$$\begin{aligned}\log_e\frac{r_{wp}}{pg}=&-\frac{1}{12}\left(\frac{\beta}{pg}\right)^2-\frac{1}{60}\left(\frac{\beta}{pg}\right)^4-\frac{1}{168}\left(\frac{\beta}{pg}\right)^6-\frac{1}{360}\left(\frac{\beta}{pg}\right)^8-\cdots\\&+\frac{1}{12}\left(\frac{\alpha}{pg}\right)^2\left[1+\frac{1}{2}\left(\frac{\beta}{pg}\right)^2+\frac{1}{3}\left(\frac{\beta}{pg}\right)^4+\frac{1}{4}\left(\frac{\beta}{pg}\right)^6+\cdots\right]\\&-\frac{1}{60}\left(\frac{\alpha}{pg}\right)^4\left[1+\frac{5}{3}\left(\frac{\beta}{pg}\right)^2+\frac{7}{3}\left(\frac{\beta}{pg}\right)^4+\cdots\right]+\frac{1}{168}\left(\frac{\alpha}{pg}\right)^6\left[1\right.\\&\left.+\frac{7}{2}\left(\frac{\beta}{pg}\right)^2+\cdots\right]-\frac{1}{360}\left(\frac{\alpha}{pg}\right)^8+\cdots\end{aligned} \tag{43}$$

Expanding the summation in the fifth line of Snow's equation and comparing the result with equation (43), it is seen that the Snow series is identical with the terms $\sum_2^{n-1} n\log_e\frac{r_{wp}}{pg}$ in equation (38), except that the series S_{2m} are taken to infinity, whereas in the summation of the geometric mean distances it ends with $(n-1)$. The difference, that is, the sum between $(n-1)$ and infinity may, however, readily be expressed in a series involving powers of $\frac{1}{n}$. The series in the last line of equation (39) is identical with the terms $\sum_2^{n-1} p\log_e\frac{r_{wp}}{pg}$, except that the second degree terms in α and β are lacking and that here again the summations S_{2m-1} are carried to infinity instead of $(n-1)$, and it will be necessary to expand the difference in a series in powers of $\frac{1}{n}$.

The remaining terms in $\sum_{2}^{n-1} p \log_e \frac{r_{wp}}{pg}$ in the B (rectangle) correction of equation (38) may be identified with the last term in the first line of equation (39) (that in $(\alpha^2-\beta^2)$), by writing it to involve $\log ng$ and substituting for $\log n$ its value in terms of the series $\sum_{2}^{n-1} \frac{1}{k}$ which arises when the series of equation (43) is used for $\log \frac{r_{wp}}{pg}$.

The remaining term in $\log \frac{2\pi a}{g}$ in the first line of equation (39) may be expressed in terms of the Rosa B correction for circles, as was done in Section VII.

The results of collecting all the transformed terms is that Snow's equation (39) may be written in the form

$$L=L_0+4\pi na\left[-(A+B)-\frac{1}{6n}\log_e\frac{ng}{a}-\frac{0.02453}{n}-\frac{1}{120n^3}+\frac{1}{504n^5}\right.$$
$$+\frac{A_2}{2n}+\frac{1}{3n}\left(\frac{E}{k}-1\right)\left(1+\frac{2au_z}{u}\right)\left(\frac{\alpha}{g}\right)^2 \qquad (44)$$
$$+\frac{1}{6n}\frac{(\beta^2-\alpha^2)}{g^2}\left\{\log_e\frac{ng}{a}-0.07943+2\frac{(K-E)}{k}-kK+\frac{1}{12n^2}-\frac{1}{40n^4}\right\}$$
$$-\frac{1}{3n^3}\left(1-\frac{1}{2n^2}\right)\left(\frac{1}{60}\frac{\beta^4}{g^4}-\frac{1}{24}\frac{\beta^2\alpha^2}{g^4}+\frac{1}{60}\frac{\alpha^4}{g^4}\right)$$
$$\left.-\frac{1}{10n^5}\left(\frac{1}{168}\frac{\beta^6}{g^6}-\frac{1}{36}\frac{\beta^4\alpha^2}{g^6}+\frac{1}{36}\frac{\beta^2\alpha^4}{g^6}-\frac{1}{168}\frac{\alpha^6}{g^6}\right)+\cdots\right]$$

where A and B are defined in equations (37) and (38).

For square wire, the second and sixth degree terms in $\frac{\alpha}{g}$ and $\frac{\beta}{g}$ drop out, and the fourth degree terms become $\frac{1}{360n^3}\left(1-\frac{1}{2n^2}\right)\frac{\beta^4}{g^4}$. For the special case $\alpha=o$ and $\beta=g$, equation (44) goes over into Snow's formula for a continuous helical current sheet, as it should. It is of interest to note that in that case the terms in powers of $\frac{1}{n}$ all cancel, thus giving a check on the coefficients in the series expansions, and especially furnishing evidence that the term in $\frac{1}{n^5}$ in formula (31) is correct.

Making use of the formula (44) the difference may be evaluated between the accurate formula of Snow for square wire and the solution by Rosa's method in the case of the example treated by Snow

on page 477 of his article. In this the coil is supposed to be wound with square wire, instead of round, the side of the section being taken as $\alpha=\beta=0.05$ cm. The radius, number of turns, and pitch of the winding are taken the same as in the preceding problem for round wire. The distribution of the current over the cross section being assumed to be uniform, the value of u_z in equation (44) is zero.

For the calculation of the A correction, we have $\log R_t=\log g-\frac{3}{2}$, and $R_w=0.44705\alpha$. Thus from equation (37), $-A=\log\frac{R_t}{R_w}=-0.001773$. The B correction for the circle is 0.33455 as before. For the value of $\log\frac{r_{w1}}{g}$ the exact formula gives 0.0005109, which multiplied by $\frac{2}{n}(n-1)$ amounts to 0.001019. For the more distant wires, the formula (43) may be used, and only a few terms have to be included. These bring up the total of the value of B for the rectangles to 0.001104. Thus the Rosa terms in equation (44) amount to

$$-0.001773-0.334554-0.001104=-0.337431$$

which, multiplied by $4\pi na$, gives for the Rosa correction -25442 mμh. The correction terms in equation (44) are found to be

$$\frac{A_2}{2n}= \quad 0.001125$$

$$-\frac{1}{6n}\log_e\frac{ng}{a}=-0.000409$$

$$-\frac{0.02453}{n}=-0.000061$$

$$\frac{1}{3n}\left(\frac{E}{k}-1\right)\left(\frac{\alpha}{g}\right)^2= \quad \underline{0.000284}$$

$$\text{sum}= \quad 0.000939$$

which, multiplied by $4\pi na$, show that the error of the Rosa correction is 70.8 mμh. This amounts to about 2.7 parts in 1,000,000 of the whole inductance. Thus, the true correction for cross section to be applied to the inductance of the cylindrical current sheet, in order to find the inductance of the helical coil of square wire, is $-25442+71=-25371$ mμh. This value, found by equation (44), should agree with the value found directly from Snow's equation (126). The value calculated by Snow is -25345. The source of the discrepancy lies in an error in the value of the term multiplied by $\frac{8}{3}$ in the last equation of the calculation on page 477. The true value is 1.56288 instead

of 1.56268, as given by Snow. Making this change, Snow's equation gives −25372.

The error of the Rosa method quoted in Snow's paper for this problem is 6 parts in 1,000,000. This is affected by both the error in the value of B used for the circle (already discussed in Section V) and by the numerical error in Snow's calculation just noted.

If the Rosa corrections were applied to the formula of Snow for a continuous helical current sheet we use the result from equation (35), that the inductance L_s of the helical current sheet is related to L_o, that of the cylindrical current sheet, by the relation $L_s = L_o + 79.5$ mμh, and the calculated inductance of the coil is

$$L = L_o + 79.5 - 25442 = L_o - 25362 \text{ mμh.}$$

which is in error by only 0.4 of 1 part in 1,000,000. This is in line with the calculation on page 181, which showed that the error of the Rosa correction as ordinarily applied to the cylindrical sheet formula is principally due to neglect of the helicity. The residual error of the Rosa method is practically the same for both round and square cross section, as would be expected.

X. CONCLUSION

In the preceding sections it has been shown that the simple Rosa method of correction for the effect of cross section gives results for circular solenoids of round or rectangular wire which are amply accurate for all practical cases. Indeed, for the examples given, the Rosa method gives results of high precision, when applied to the logical current sheet formula—that in which the axial component of magnetic field is taken into account. The numerical proof of this degree of accuracy in the Rosa method is made possible by the existence of the accurate formulas of Snow.

Unfortunately, formulas corresponding to those of Snow for other cases, circular flat spirals, polygonal solenoids, and polygonal spirals, are not available, and it would seem to be a work of great difficulty to derive them. Lacking them, the Rosa method applied to the available current sheet formulas offers the simplest and most accurate general method of calculation. It has been shown that for short windings the summation method and the Rosa method are in agreement, but the Rosa method applies to any case where the current sheet formula is available. It remains to note the use of the method in the cases already cited.

It is easy to show that for a circular flat spiral the curvature terms in the Rosa correction are of second degree in $\frac{g^2}{a^2}$ and may, therefore, be neglected as of less importance than the effect of the radial component of the current. The current sheet formula for a disk-shaped or annular current sheet of negligible axial thickness is known, as

well as series expansions holding for the case where the axial width of the current sheet is small compared with the mean radius (18). In all of these the radial component of the current is neglected. Thus the inductance of a flat circular spiral wound with wire of round or rectangular cross section may best be found by applying the simple Rosa correction, calculated by the methods and formulas already fully treated, to the inductance of a current sheet having the same mean radius as the spiral coil and a radial width equal to the product of the pitch by the number of turns.

The case of a short polygonal solenoid has already been fully treated and the inductance formula given as equation (25). In this it is to be noted that the principal terms in the correction equations here are the Rosa constants; that is, for round wire the simple Rosa constants are the same for polygonal solenoids as for circular. In both cases they are multiplied by twice the length of wire in the winding. No formula is available for long polygonal solenoids, except in the case of the square solenoids (14). It would be possible, though a great deal of work, to derive the formulas for the other cases, but it is sufficient in practical cases to make use of the formula for the equivalent circular cylindrical current sheet as was described (13) in Bureau of Standards Scientific Paper No. 468, and to apply to this the simple Rosa correction.

The calculation of the inductance of a polygonal spiral is covered by formulas (26) and (27). These apply most accurately to spirals where the radial width is small compared with the side of the polygon, but this will cover many practical cases. No general formula is known for a disk of polygonal shape. A good approximation to it can be obtained by calculating the inductance of a circular disk current sheet whose mean element incloses the same area as the mean element of the polygonal disk. It is to be noticed that in equation (27) the principal Rosa constants are the same as those which hold for circular and polygonal solenoids of round wire.

XI. BIBLIOGRAPHY

1. Chester Snow, Formula for the Inductance of a Helix Made with Wire of Any Section, B. S. Sci. Paper No. 537. In this, formula (114) gives the inductance of a helix of round wire, formula (126) that of a helix of wire of rectangular cross section, and formula (129) the inductance of a continuous helical current sheet.
2. F. W. Grover, Methods for the Derivation and Expansion of Formulas for the Mutual Inductance of Coaxial Circles and for the Inductance of Single-Layer Solenoids, B. S. Jour. Research, **1** (RP16), p. 487; October, 1928.
3. Strasser, A Formula for the Inductance of a Single-Layer Coil of Round Wire by the Summation Method, Wied. Ann., **17**, p. 763; 1905. A somewhat more accurate form of Strasser's formula is given in B. S. Sci. Paper No. 169, p. 124; 1912; formula (82), and a table of Strasser's constants in Table 5, p. 195. Note that in the present paper A_1 and B_1 correspond to A and B in Strasser's notation.

4. A. Esau, A Summation Formula for the Inductance of a Flat Circular Spiral, Jahrb. der drahtl. Tel., **5,** p. 212; 1911. This is modeled on Strasser's formula for the solenoid. Ueber die Berechnung des Selbstinduktionskoefficienten von Spulen mit rechteckigem bzw. quadratischem Querschnitt. I. Nebeneinander liegende Windungen, Jahrb. der drahtl, Tel., **14,** p. 271; 1919. II. Spulen mit uebereinander liegenden Windungen (Flachspulen), Jahrb. der drahtl. Tel., **14,** p. 386; 1919.
5. I. Koga, Inductance of Polygonal Coils, J. Inst. of E. E. of Japan; October, 1924. Formulas for triangular, hexagonal, and octagonal solenoids and spirals. Gives an asymptotic formula for A_1 on page 7.
6. E. B. Rosa, Calculation of the Self-Inductance of Single-Layer Coils, B. S. Bulletin, **2,** p. 161; 1906. Rosa's formula is also given in B. S. Sci. Paper No. 169, p. 122, as formula (80) and Tables 7 and 8, pp. 197–199, give his tables of constants A and B.
7. Yasujiro Niwa, A study of Coils Wound on Rectangular Frames with Special Reference to the Calculation of the Inductance, Researches of the Electrotechnical Laboratory, Tokyo, No. 141, April, 1924. A very full collection of formulas for the self and mutual inductance of various rectangular current sheets, together with tables of constants and curves. On page 56 is given the Rosa correction for a square solenoid of round wire.
8. A. Esau, Criticism of Niwa's Formula for the Inductance of Square Solenoids, Jahrb. der drahtl. Tel., **18,** p. 453; 1921. This is answered by Niwa, pp. 51–55 of the reference in No. 7.
9. M. Wien, The Inductance of a Circular Ring of Wire of Circular Cross Section, Wied. Ann., **53,** p. 935; 1894. Given as formula (61) of B. S. Sci. Paper No. 169, p. 110.
10. Maxwell, Series Formula for the Mutual Inductance of Equal Coaxial Circular Filaments, Elect. and Mag., **II,** sec. 705. Also appears as formula (12), p. 13 of B. S. Sci. Paper No. 169.
11. Rayleigh and Niven, Inductance of a Short Cylindrical Current Sheet, Proc. Roy. Soc., **32,** pp. 104–141; 1881. Rayleigh's Collected Papers, **2**, p. 15. This also appears as formula (69) of B. S. Sci. Paper No. 169.
12. Formulas for the calculation of the geometric mean distance of certain figures were given by Maxwell, Elect. and Mag., **II,** secs. 691 and 692; Gray, Absolute Measurements, **II,** pt. 1, pp. 288–306; Rosa, On the Geometric Mean Distances of Rectangular Areas and the Calculation of Self-Inductance, B. S. Bulletin, **3,** p. 1; 1907. The more important of these are collected in B. S. Sci. Paper No. 169, pp. 167–170, formulas (123) to (131), inclusive.
13. F. W. Grover, Formulas and Tables for the Calculation of the Inductance of Coils of Polygonal Form, B. S. Sci. Paper No. 468; 1923. Triangular square, hexagonal, and octagonal solenoids. Exact formula for square solenoid on p. 742. Radius of equivalent circular solenoid, p. 753 and Table 1, p. 761.
14. Y. Niwa, On the Solenoid with Rectangular Cross Section, Researches of the Electrotechnical Laboratory, Tokyo, No. 73; November, 1918; and J. Elect. Soc. Japan, pp. 535–564; 1919.
15. Formulas for Arithmetic Mean Distances and for Arithmetic Mean Square Distances were Given by Rosa, B. S. Bulletin, **4,** p. 326; 1907. These are collected pp. 171–172, B. S. Sci. Paper No. 169. Of these formulas (137) and (138) refer to straight lines.
16. Bruno Rolf, Zur Frage der Berechnung des Selbstinduktionskoefficienten von Spulen mit quadratischem Windungsquerschnitt, Jahrb. der drahtl. Tel., **19,** p. 127, 1922. He gives an asymptotic formula for A_1 and simplifies Esau's formula for the inductance of a square solenoid so as to admit of

tabulation for any number of turns. This does not take into account that Esau's formula, like other summation formulas, converges only for short coils.

17. Stirling's formula, Smithsonian Math. Tables, p. 28. Euler summation formula, Smithsonian Math. Tables, p. 25.

18. Spielrein, Arch. für Elektrotech., **3,** p. 187, 1915; gives a formula for the inductance of an annular disk current sheet. See also B. S. Sci. Paper No. 320, p. 555; 1918; formula (24A). A series formula for the same case is given by T. Lyle, Phil. Trans., **213A,** pp. 421–435; 1914; and B. S. Sci. Paper No. 320, p. 557; 1918; and Tables C and D, pp. 569–570. In a paper On the Inductance of Single-Layer Flat Coils, S. Butterworth, Proc. Lond. Phys. Soc., **32,** pt. 1, p. 31; December, 1919; are derived formulas which check those of Lyle and Spielrein.

19. Revision of the Formulae of Weinstein and Stefan for the Mutual Inductance of Coaxial Coils, B. S. Bulletin, **2,** p. 331; 1906. The revised Stefan formula appears as equation (48) and the revised Weinstein formula as equation (50) in B. S. Sci. Paper No. 169.

XII. APPENDIX

TABLE 3.—*Values of the Rosa constant B, calculated by formula (31)*

n	B	n	B	n	B
1	0	31	0.30874	100	0.32689
2	.11371	32	.30949	110	.32775
3	.16626	33	.31019	120	.32847
4	.19728	34	.31086	130	.32909
5	.21800	35	.31149	140	.32963
6	.23293	36	.31210	150	.33010
7	.24426	37	.31267	160	.33062
8	.25318	38	.31322	170	.33090
9	.26042	39	.31374	180	.33123
10	.26641	40	.31424	190	.33153
11	.27146	41	.31471	200	.33181
12	.27579	42	.31517	220	.33229
13	.27954	43	.31561	240	.33269
14	.28282	44	.31602	260	.33304
15	.28573	45	.31643	280	.33334
16	.28832	46	.31681	300	.33360
17	.29064	47	.31718	350	.33414
18	.29273	48	.31754	400	.33455
19	.29464	49	.31789	450	.33488
20	.29637	50	.31822	500	.33514
21	.29796	55	.31972	550	.33536
22	.29942	60	.32099	600	.33555
23	.30077	65	.32208	650	.33571
24	.30202	70	.32304	700	.33584
25	.30318	75	.32387	750	.33596
26	.30427	80	.32461	800	.33607
27	.30528	85	.32527	850	.33616
28	.30623	90	.32587	900	.33625
29	.30712	95	.32640	950	.33633
30	.30795	100	.32689	1000	.33640
				∞	.33788

Values not found in the table may be calculated by the formula

$$B = 0.337877 - \frac{1}{6n}\log_e n - \frac{0.330842}{n} - \frac{1}{120n^3} + \frac{1}{504n^5}$$

WASHINGTON, January 25, 1929.